UNIVERSITÀ
DEGLI STUDI
FIRENZE

DOTTORATO DI RICERCA TOSCANO IN NEUROSCIENZE

CICLO XXXII

COORDINATORE Prof. Renato Corradetti

"Direct pharmacological effects of the multimodal antidepressant trazodone on the serotonergic neuron activity in the dorsal raphe nucleus."

Settore Scientifico Disciplinare BIO/14

Dottorando
Dott. Bonfiglio Francesco

Tutore
Prof. Corradetti Renato

Coordinatore
Prof. Corradetti Renato

Anni 2016/2019

Index:

Abbreviations:

5-CT	5-carboxamidotryptamine maleate
5-HT	5-hydroxytryptamine
5-HT1A	5- hydroxytryptamine1A receptors (general term)
5-HT1AARs	5- hydroxytryptamine1A autoreceptors (receptors located on somatodendrites of serotonergic neurons)
5-HTP	5-hydroxytryptophan
5-HTP decarboxylase	aromatic amino acid decarboxylase
8-OH-DPAT	(±)8-hydroxy-2-(di-n-dipropylamino) tetralinhydrobromide
ACSF	Artificial CerebroSpinal Fluid
AHP	After-HyperPolarization
BUSP	buspirone
CA1	Cornus Ammonis 1
C.I.	confidence interval
cAMP	3',5'-cyclic adenosine monophosphate
CGP-55845	3-N[1-(S)-(3,4-dichlorophenyl)ethyl]amino-2-(S)-hydroxypropyl-P-benzyl-phosphinic acid hydrochloride
DAG	diacylglycerol
d-AP5	d-(-)-2-amino-5-phosphonopentanoic acid
DPCPX	8-cyclopentyl-1,3-dipropylxanthine
DRC	Dose Response Curve
DRN	Dorsal Raphe Nucleus
DSM	Diagnostic and Statistical manual for Mental Disorders
fEPSP	field excitatory postsynaptic potential
GIRK	G-protein coupled inward rectifying K+ channel
GM	geometric mean
HHW	Half-Height Width
IL	InfraLimbic
IP3	Inositol Trisphosphate
IQR	interquartile range
ISI	interspike interval
LSCAT	loose-seal cell-attached patch-clamp
LTP	Long-Term Potentitiation
MAOI	monoamine oxidase inhibitor
MDS	Major Depression Syndrome
mPFC	medial PreFrontal Cortex
MRN	Medial Raphe Nucleus

NA	noradrenaline
NBQX	2,3-dioxo-6-nitro-1,2,3,4-tetrahydrobenzo[f]quinoxaline-7-sulfonamide disodium salt
PE	PhenylEphrine
PKC	protein kinase C
PL	PreLimbic
PLC	protein phospholipase C
PV	Parvalbumin
Racc	access resistance
Rin	input resistance
Rleak	leak resistance
Rm	cell resistance
Rpipette	resistance of the pipette
Rs	series resistance
Rtot	total resistance
SD	standard deviation
SEM	standard error of mean
SERT	sodium-dependent serotonin transporter
SNRI	Selective serotonin-Noradrenaline Reuptake Inhibitor
SRC	stimulus-response curve
SR-95531	6-imino-3-(4-methoxyphenyl)-1(6H)-pyridazinebutanoic acid hydrobromide
SSRI	Selective Serotonin Reuptake Inhibitor
TBS	theta burst stimulation
TPH	tryptophan hydroxylase
TZD	trazodone
UDHD	Upstroke-Downstroke Half Distance

Abstract:

"Direct pharmacological effects of the multimodal antidepressant trazodone on the serotonergic neuron activity in the dorsal raphe nucleus"

The principal research activity that characterized my PhD studies was the investigation of the electrophysiological and pharmacological *direct* effects of trazodone at somatodendritic 5-HT_{1A} receptors (5-HT_{1A}ARs) of serotonergic neurons of dorsal raphe nucleus (DRN).

INTRODUCTION: Multimodal antidepressant drugs form a class of heterogeneous substances that, in addition to SERT inhibition, exert a variety of receptor actions believed to participate in the therapeutic action of these medicines. Trazodone, in addition to its inhibitory activity at cell membrane serotonin transporter (SERT), displays considerable affinity for 5-HT_{1A} 5-HT_{2A}, 5-HT_{2C} receptors and α_1-adrenoceptors. Although these pharmacological properties have been suggested to contribute to trazodone a profile of antidepressant and sleep facilitator, the direct effects of trazodone on serotoninergic neuron activity are still not adequately known for modelling the possible pharmacological mechanisms underlying the therapeutic action(s) of the drug. Indeed, the interplay between the 5-HT_{1A} receptor agonist activity and α_1-adrenoceptor antagonist activity of trazodone at the level of serotonergic neurons likely plays a crucial role in regulating the firing of serotonergic neurons, hence the release of serotonin in projection areas during acute and chronic administration of the drug.

METHODOLOGY: We designed *in vitro* experiments directed to quantify the agonist efficacy of trazodone at 5-HT_{1A}ARs of DRN serotonergic neurons and to establish the possible effect of α_1-adrenoceptor antagonism. The activity of serotonergic neurons was recorded with *loose-seal cell-attached patch-clamp* (LSCAT) in brainstem slices. To reproduce in slices the noradrenergic drive which *in vivo* facilitates serotonergic neuron firing, ACSF was supplemented with the selective α_1-adrenoceptor agonist phenylephrine (PE 10 µM, unless otherwise indicated). To quantify the intrinsic activity of trazodone, we investigated the potency and the functional effect of the drug at 5-HT_{1A}ARs using *whole-cell* recordings. To this purpose, we measured the changes in slope conductance of 5-HT_{1A} receptor-coupled GIRK channels, which provided a direct measure of 5-HT_{1A} receptor activation produced by the application of trazodone.

RESULTS: In LSCAT recording of serotonergic neuron activity facilitated by 10 µM PE, the firing rate of neurons was concentration-dependently inhibited by trazodone (1 - 30 µM). The selective 5-HT_{1A} receptor antagonist Way-100635 partially antagonized the effect of the antidepressant indicating that the inhibitory effect exerted by trazodone comprised an additional action of the drug. Both effects of the antidepressant drug were also observed in slices from $Tph2^{-/-}$ mice that lack synthesis

of brain serotonin, showing that the activation of 5-HT_{1A}ARs and the unknown additional effect were not mediated by endogenous serotonin.

As trazodone binds with relatively high affinity to α_1-adrenoceptors for which it is antagonist, in conditions of α_1-adrenoceptor stimulation, as those we applied *in vitro*, the non 5-HT_{1A} receptor-mediated inhibitory effect of trazodone on serotonergic neuron activity could have been produced by α_1-adrenoceptor block. Consistent with this hypothesis, in the absence of phenylephrine, trazodone (1 - 10 µM) concentration-dependently silenced neurons through activation of 5-HT_{1A}ARs, as the effect was fully antagonized by Way-100635.

In experiments in which the 5-HT_{1A} receptor-mediated component of trazodone action was blocked by the presence of Way-100635, trazodone (1 - 10 µM) concentration-dependently inhibited neuron firing facilitated by 1 µM phenylephrine. Parallel rightward shift of dose-response curves for trazodone recorded in higher phenylephrine concentrations (10 and 100 µM) indicated competitive antagonism at α_1-adrenoceptors. On the other hand, in the presence of a high concentration of PE (100 µM, Way-100635 absent) to minimize the α_1-adrenoceptor-dependent effect of trazodone, the drug dose-dependently inhibited serotonergic neuron activity. The effect was variable and often did not silence the neuron firing, indicating the possibility that trazodone is a partial agonist at 5-HT_{1A}ARs.

To confirm this property, in whole-cell recordings we measured the 5-HT_{1A}AR-coupled GIRK conductance activated by the drug. These recordings confirmed the weak partial agonism of trazodone at 5-HT_{1A} receptors, with an efficacy of ~35 % when compared to the 5-HT_{1A} receptor full agonist 5-carboxamidotryptamine (5-CT) in the same neurons. Consistent with its weak partial agonist activity, trazodone was able to partially antagonize the effect of 5-CT at 5-HT_{1A}ARs.

CONCLUSIONS: Our data show that trazodone, at concentrations relevant to its clinical effects, exerts weak partial agonism at 5-HT_{1A}ARs and disfacilitation of firing through α_1-adrenoceptor antagonism. These two actions converge in inhibiting dorsal raphe serotonergic neuron activity, albeit with varying contribution depending on the intensity of α_1-adrenoceptor stimulation. These two *direct* effects on serotonergic neuron activity are likely to be implicated in the in the therapeutic action of trazodone. Indeed, it has been suggested that antidepressant drugs endowed of 5-HT_{1A} receptor partial agonist property could hasten the therapeutic response during the treatment. Furthermore, antagonism at α_1-adrenoceptor is likely to dampen the effects of noradrenergic system reactivation that occurs during sleep and prevent insomnia-related microarousals, which may underlie the sleep facilitating property of trazodone.

Introduction:

Mood disorders: major depression syndrome and the role of monoaminergic systems.

Major depression syndrome (MDS) is a complex low-mood state characterized by the inability to experience pleasure (anhedonia) towards events in life (Hyman, 2010) and could possibly lead to suicide, if not treated.
MDS is the leading cause of disability worldwide with ~ 350 million people around the world suffering from this disorder, and the disease burden of depression has been estimated to represent the second highest among all diseases by 2020 (World Health Organization, 2016).
The symptomatology that accompanies the "low mood" experienced by the patients is heterogeneous and the diagnosis is often imprecise despite the possible symptoms listed in the *Diagnostic and Statistical Manual for Mental Disorders* (DSM-5; APA, 2013). The symptomatology varies from body weight changes (loss or gain), to sleep disorders as insomnia, fatigue and psychomotor retardation and difficulty in concentration. Today we know that most of symptoms involve an altered transmission of monoamines as 5-hydroxytryptamine (5-HT, serotonin) and noradrenaline.
The pathogenesis of this complex disorder still remains unclear and clinical diagnosis of depression suffers from lack of objective diagnostic biomarker (Jentsch et al., 2015). Furthermore, great difficulties in the identification of the most appropriate treatment for each patient persist, which also causes that the overall remission rate of MDS following antidepressant treatments still remains below 70% (Rush et al., 2006).
In addition, the first-line drugs recommended in MDS guidelines, including selective serotonin reuptake inhibitors (SSRIs) and selective serotonin-noradrenaline reuptake inhibitors (SNRIs), display delayed onset of clinical effects. Namely, it takes longer than 3-4 weeks on average for these drugs to show initial, clinically measurable, therapeutic effects.
Historically, depressed patients were treated with drugs that could inhibit the mitochondrial monoamine oxidases enzyme, involving the catecholamine metabolism and compensating the "naturally occurring abnormalities" of the progression of depression. On the basis on these clinical studies, the *catecholamine hypothesis of affective disorders* or *monoaminergic hypothesis* was postulated (Schildkraut, 1965).
Few years later it was observed that depressed patients treated with tryptophan, the precursor of serotonin, had a potentiated antidepressant response to the administration of monoamine oxidase inhibitors. On the other hand, the response measured using the precursor of noradrenaline did not change, suggesting serotonin as one of the most important neurotransmitters participating in the symptomatology of MDS and introducing the *low serotonin hypothesis* (Coppen, 1967). The basis for this hypothesis is that a progressive functional impairment of serotonergic neuron

terminals and a reduction in serotonergic transmission occurs in projection areas, altering the functional homeostasis of these regions.

The hypothesis that the sole decrease in brain serotonin level could account for depression was challenged by the failure to induce a depression-like state in non-depressed patients by acutely reducing the biosynthesis of serotonin through a diet poor in tryptophan (*see in*: Ruhé et al., 2007).

This conclusion is in agreement with the long standing evidence that acute modifications of brain serotonin and/or noradrenaline levels are not sufficient to recover patients from their depressive state and that long-term treatment is required for a therapeutical effect of antidepressant drugs.

More recently, new theories about the pathophysiology of depression and the action of antidepressant medications have been proposed and offer new potential targets for therapies. Observations conducted in depressed patients with magnetic resonance imaging showed a reduction in the grey matter volume occurring in the striatum, prefrontal cortex and hippocampus. This reduction occurs because of atrophy, apoptosis or altered regulation of neurotrophic factors as Brain-derived neurotrophic factor and neurotrophines. In the hippocampus, dendrites of CA3 region incur into atrophy while in the dentate gyrus there is a decrease in adult neurogenesis (*see in*: Fossati et al., 2004). Similarly a reduction of the dendritic tree is observed also in prefrontal cortex (*see in*: Pittenger and Duman, 2008).

These structural changes are only partially responsible for depression and altered neuroplasticity occurring in the hippocampus, prefrontal cortex and amygdala and have been suggested to participate in depression and in the cognitive impairment that often accompanies the more severe forms of MDS. Supporting evidences that depression and altered neuroplasticity are linked, come from studies conducted on depressed patients after pharmacological treatment with monoamine oxidase inhibitors (MAOIs) or fluoxetine. These patients exhibited an improvement in memory tasks and attention (Allain et al., 1992; Vythilingam et al., 2004; both reviewed in: Pittenger and Duman, 2008). Moreover, electron microscopy measures of synapse number in the hippocampal region after chronic treatment with antidepressant drugs revealed increased number of synapses in the CA1 and CA3 pyramidal cell layer (Hajszan et al., 2005), suggesting that the long-term administration of antidepressants has a neuroprotective effect on the brain (*see in*: Manji et al., 2003).

Recently, intravenous administation of the dissociative anaesthetic ketamine has been proposed for treatment-resistant forms of depression. Ketamine has a fast antidepressant effect, established within hours (Berman et al., 2000) and the pharmacological effects of this compound are ascribed to antagonism of NMDA receptors with subsequent reduction in the production of nitric oxide and increase in the release of glutamate (*see in*: Pereira and Hiroaki-Sato, 2018).

Antidepressant drugs in the treatment of Major Depressive Syndrome.

Notwithstanding the possible role of noradrenaline in depression, from the studies of Coppen in 1967 it was already clear that serotonin was a crucial neurotransmitter participating in the complex symptomatology of MDS. Therefore, the leading hypothesis ascribed the development of major depression to the impairment in serotonin system homeostasis and turnover, with subsequent decrease in serotonin content and release in raphe nuclei projection areas. Thus, the main focus on the treatment of MDS was the development of drugs that could increase the extracellular levels of serotonin by inhibiting its catabolism and/or its reuptake.
At present, antidepressant drugs represent a heterogeneous class of medicines and many of them are endowed of multiple pharmacological actions that encompass antagonist or agonist action at neurotransmitter receptors in addition to their inhibitory effect on neurotransmitter membrane transporters, notably those specific for serotonin and/or noradrenaline.
These multiple characteristics of antidepressant drugs have originated a complex classification in subclasses of drugs (Stahl, 1998; *see in*: Stahl and Felker, 2008; Stahl, 2009a; APA 2013), grouped on the basis of their pharmacological action(s) and their possible rational indication in different clinical manifestations of depression.

In the following, the principal classes of antidepressant drugs are briefly summarized to highlight the multiplicity of pharmacological actions and mechanisms that may concur in the therapeutic effects of different compounds.

Monoamine oxidase inhibitors.
Monoamine oxidase inhibitors (MAOIs) block the mitochondrial enzyme monoamine oxidase and their therapeutic activity is correlated with a substantial slowing of brain serotonin degradation, which allows a more persistent stimulation of serotonergic receptors.
At present, the use of MAOIs is very limited and restricted to selected patients. MAOIs are still used as antidepressant drugs for their positive effects in the treatment of "atypical depression" (Liebowitz et al., 1984; Jarrett et al., 1999).
This limitation in the use of MAOIs is due to the potentially lethal effects when administered with other serotonergic drugs (Bleumink et al., 2003), but also by diet restrictions because assumption of tiramine containing food (e.g. cheese, wine) could produce severe hypertension.

Tricyclic antidepressants.
This class of antidepressants are named after their chemical structure composed of three rings and include amitryptiline and imipramine that were introduced in the clinical use more than 60 years ago. The recognized mechanism of action of these compounds is the unselective inhibition of the membrane transporters for

noradrenaline and serotonin expressed at level of synaptic terminals of the respective monoamine system. The therapeutic efficacy of tricyclic antidepressants is generally good and higher than other antidepressant drugs in the treatment of melancholic depression (Mitchell and Mitchell, 1994). At present they are considered second line antidepressants and are prescribed when newer compounds (e.g. the Selective Serotonin Reuptake Inhibitors – SSRIs – *see below*) fail their therapeutical action. Indeed, the use of tricyclic antidepressants is limited by a number of adverse effects caused by multiple pharmacological actions exerted through the block of several receptors (histamine H_1 receptor, acetylcholine muscarinic receptors and α_1-adrenoceptor) in addition to the block of ion channels at cardiac level.

Selective and non-selective serotonin reuptake inhibitors.

Although tricyclic antidepressants and, in lesser extent, MAOIs remain in use for their therapeutic effectiveness in selected patients (e.g. non responders to newer antidepressants), nowadays the most widely used antidepressant drugs belong to the classes of SSRIs. Acute administration of SSRIs has been shown to effectively inhibit SERT activity, leading to the increase in extracellular serotonin both in dorsal raphe nucleus (DRN) and in projection areas (Fuller, 1994; *see in*: Piñeyro and Blier, 1999).

The use of these newer antidepressant drugs is clinically favoured because of their better tolerability and much lower acute toxicity compared to tricyclic compounds (Anderson and Tomeson, 1994; Burke et al., 1997; Stahl, 1998; Celada et al., 2004; Stahl, 2009a). Yet, they can induce dry mouth, weight gain, lack of sex drive with episodes of erectile dysfunction, anhedonia and emotional blunting.

As the therapeutic effect of SSRIs appeared limited in comparison with that of tricyclic antidepressants that inhibit both serotonin and noradrenaline reuptake, a newer class of serotonin and noradrenaline reuptake inhibitors has been developed. These drugs are not endowed with the multiple pharmacological actions that determine the most common and typical adverse effects of tricyclic antidepressants.

Multimodal antidepressants.

This class of antidepressants includes a number of heterogeneous substances that, in addition to SERT inhibition, exert a variety of receptor actions that are believed to participate in the therapeutic action of these drugs. This class comprises new compounds (e.g. vortioxetine) but also older medicines (e.g. trazodone, nefazodone) for which some of the pharmacological actions that in the past were dismissed or considered of minor therapeutic impact, have recently been reinterpreted as favourable for the overall therapeutic action and/or reduction of side/adverse effects.

Thus, each multimodal antidepressant presents a specific pharmacological profile according to its binding to one or more serotonergic receptor subtypes and/or other receptors. For example, trazodone, nefazodone and vortioxetine bind to 5-HT_{1A} and 5-HT_{2A} receptors (Ghanbari et al., 2012), but trazodone also binds to α_1-adrenoceptors (Owens et al., 1997; Giannangeli et al., 1999; Krege et al., 2000; Betti et al., 2002),

while vortioxetine exerts additional effects through 5-HT_3 receptors (Gonda et al., 2018).
These multiple pharmacological properties have been implicated in the therapeutic effects of multimodal compounds providing new interpretations on the mechanism of action and suggesting therapeutic targets that new antidepressant drugs should have to represent an advancement beyond SSRIs (Stahl 2009a; Artigas, 2013; Sanchez et al., 2015; Artigas et al 2018).
It should be noted that despite the number of antidepressant drugs and the variety of pharmacological actions known to play favourable effects in depression, none of the compounds available at present is effective in all patients and/or all forms of depression.

Monoamine systems in depression.

The pathophysiological mechanisms leading to depression remain largely elusive and certainly involve complex interplay of different neurotransmitter systems both during the depressive episode and in the process of recovery activated by antidepressant drugs. Under this perspective to restrict the interpretation of the causes of depression to impairment of serotonergic and noradrenergic systems is clearly simplistic, nevertheless a more accurate knowledge of the pharmacological actions that antidepressant drugs have on these two systems becomes instrumental to understand their therapeutic mechanism of action and to reveal possible pharmacological targets to improve their effectiveness.

In the following I present a brief overview of the noradrenergic and serotonergic systems focussing on their mutual anatomical connections and functional interplay in behavioural responses relevant to the effects of antidepressant drugs.

The noradrenergic system: neurons, nuclei and projections.

Noradrenaline is released in almost all brain regions by terminals originating from small nuclei of noradrenergic neurons located in the brainstem.
The main source of noradrenergic innervation in the brain is the locus coeruleus, a cluster of neurons located near the wall of the fourth ventricle (Swanson and Hartman, 1975; Swanson, 1976; Foote et al., 1983). The noradrenergic neurons in this nucleus, have a great arborization with dendrites extending out of the boundaries of the nucleus and converging to afferents coming from the pontine reticular formation (Swanson, 1976). Noradrenergic projections innervate dorsal raphe, ventrolateral periaqueductal gray, pontine reticular formation and other brain regions (Clavier, 1979; Foote et al., 1983). Thus locus coeruleus neurons project to the dentate gyrus of the hippocampus and the posterior portion of the entorhinal cortex (Beckstead, 1978) and diffusely innervate the cortical layer VI. The dorsolateral neocortex receives innervation from the locus coeruleus via a continuous group of fibres crossing the medial forebrain

bundle, frontal pole and caudal layers of cortex (Morrison et al., 1981). On the other hand, noradrenergic nuclei receive projections from dorsal raphe as well as pontine formation and hypothalamus (Saper et al., 1976; Krieger et al., 1979; Foote et al., 1983).
Functionally, noradrenergic system is implicated in the sleep-waking cycle mediating arousal (Aston-Jones and Bloom, 1981) with locus coeruleus neurons changing their firing pattern from tonic to phasic when behavioural activity requires a certain focus and attention (Aston-Jones and Waterhouse, 2016). The anatomical connections between noradrenergic and raphe nuclei suggests functional interplay between the two systems. Indeed, the firing of serotonergic neurons in the DRN appears regulated by the activity of the noradrenergic system and becomes maximal during wake due to the activation of α_1-adrenoceptors by noradrenaline (Levine and Jacobs, 1992).

Noradrenergic receptors.

Noradrenergic receptors are divided into two families: α and β. The first classification was initially made in 1948 by Ahlquist following the effects elicited by different catecholamines (Ahlquist, 1948; Berthelsen and Pettinger, 1977). On the basis of their molecular structure, noradrenergic receptors are further divided into α_1- and α_2-adrenoceptors and β_1-, β_2- and β_3-adrenoceptors (Box 1).
Activation of α_1-adrenoceptors mediate excitatory activities in different brain regions. As previously mentioned, the stimulation of these receptors by the selective agonist phenylephrine (PE), increases the activity of serotonergic neurons in the DRN of awake cats (Levine and Jacobs, 1992). This excitatory activity may be mediated by the activation of G_q protein, as proposed from pharmacological essays on isolated cells (Theroux et al., 1996; Cotecchia, 2010). Differently from α_1-adrenoceptors, the α_2-adrenoceptors are inhibitory and coupled to a $G_{i/o}$ protein (Qin et al., 2008). They are located at the pre-synaptic cleft to induce a feedback control on the release of noradrenaline but also other neurotransmitters including serotonin. In the brain, β_1 and β_2 adrenoceptors are coupled to G_s proteins and activate adenylate cyclase producing excitatory effects on target neurons. β_3-adrenoceptors are mainly expressed in periphery in the adipose tissue where they are involved in the regulation of lipolysis and thermogenesis (see in: Lowell and Flier, 1997).

Box 1.

Adrenergic receptors: classification and signal pathways.

Receptor	Sub-types	G-protein	Main Signal Pathways
α_1	α_{1A}	G_q	↑IP3/DAG
	α_{1B}	G_q	↑IP3/DAG
	α_{1D}	G_q	↑IP3/DAG
α_2	α_{2A}	G/G_0	↓cAMP
			↓Ca^{2+} permeability
			↑K^+ permeability
	α_{2B}	G_i/G_0	↓cAMP
			↓Ca^{2+} permeability
	α_{2C}	G_i/G_0	cAMP
β	β_1	G_s	↑cAMP
	β_2	G_s	↑cAMP
	β_3	G_s	↑cAMP

cAMP, 3',5'-cyclic adenosine monophosphate; IP3, Inositol trisphosphate; DAG, diacylglycerol. From Govoni et al., 2014.

The serotonergic system: neurons, nuclei and projections.

Serotonergic system plays an important role in the modulation of autonomic nervous system functioning (e.g. respiratory and cardiovascular responses to hypercapnia and stress; Guyenet et al., 1985; Hodges and Richerson, 2008; see in: Guyenet et al., 2010; Cummings and Hodges, 2019) and in several higher brain functions including circadian rhythms, appetite, memory and learning and mood state behaviour (Young, 2007, Cools et al., 2008, Lesch et al., 2012, Saper et al., 2010).

The biosynthesis of serotonin in the brain, requires the amino acid tryptophan and the rate-limiting enzyme 5-hydroxytryptophan decarboxylase Type 2 (Tph2, Mössner et al., 2006; Gutknecht et al, 2012), whereas at peripheral level the synthesis of serotonin is under the control of the 5-hydroxytryptophan decarboxylase Type 1 rate-limiting enzyme.
Once serotonin is released from the neuron, the exceeding external concentration is degraded by monoamine oxidase B activity into 5-hydroxyindolealdehyde. The last

step in the process of degradation will be the conversion of 5-hydroxyindolealdehyde into 5-hydroxyindoleacetic acid by aldehyde dehydrogenase type II enzyme.

First studies to identify brain serotonergic neurons were made in the DRN with histochemistry fluorescence detection on rat slices (Dahlstrom and Fuxe, 1964). Later studies showed the presence of serotonergic neurons near the midline, in more rostral regions below the aqueduct of Sylvius and the fasciculi longitudinalis medialis. Caudally the population of serotonergic neurons can be found at the periaqueductal grey expanding also to the lateral and ventral part of DRN. On the IVth ventricle, the population of serotonergic neurons decreases and disappears (Steinbusch, 1981; Descarries et al., 1982; *see in*: Hornung, 2003).
The most populated clusters of serotonergic neurons are located partially in the midbrain and rostral pons (caudal linear nucleus, dorsal and median raphe) and partially in the caudal pons and medulla (raphe magnus, raphe obscurus and raphe pallidus). The neurons located in the midbrain and rostral pons, show projections extending to forebrain structures modulating behaviour, sleep-wake cycle, memory and emotions. Those located in the caudal pons and medulla project to the spinal cord's ventral, intermediate and dorsal columns and modulate movement and nociception (*see in*: Mohammad-Zadeh et al., 2008; Walker and Tadi, 2019).
These anatomical characteristics of the serotonergic system, first described in rodents, have been confirmed also in primates (Azmitia and Gannon, 1986; *see in*: Jacobs and Azmitia, 1992).
Within the Raphe, serotonergic neuron bodies of the midbrain are clustered to form a dorsal nucleus (the DRN) and a median nucleus (medial raphe nucleus, MRN).
A large part of serotonergic neurons contained in mammals' brain, is located in the DRN (Descarries et al., 1982; Daszuta and Portalier, 1985; Ishimura et al., 1988) which extends from the rostral Edingher Westphal Nucleus III to the caudal fourth ventricle and cerebral aqueduct (Steinbusch, 1981).
Connection to the DRN have long been studied and at present we know that a substantial part of input afferents to serotonergic neurons come from within the DRN itself either from collaterals of serotonergic neuron axons or from interneurons (e.g. GABAergic neurons, Aghajanian et al., 1977; Mosko et al., 1977; Clemett et al., 2000; López-Giménez et al., 2001; Serrats et al., 2005).

The main efferent connections are ascending and project to telencephalon and diencephalon (Fuxe, 1965; Azmitia and Segal, 1978) forming bundles (Schofield and Everitt, 1981; Azmitia and Gannon, 1986). The dorsal bundle comprises connection from the DRN lateral wings and ventromedial DRN. The ventral bundle collects projections originating from the midline of the DRN. The efferent projections appear to be organized also along the rostro-caudal axis, with the rostral DRN connected with cortical areas as motor cortex (Waterhouse et al., 1986) whereas the caudal DRN

connected with hippocampus (Jacobs et al., 1978) receives serotonergic afferents also from median raphe nuclei (see in Jacobs and Azmitia, 1992).
The organization of these efferent projections into clusters allows a finer control of all the inputs going out of the DRN, giving selectivity to the connected area in regards to the specific neuron group activated.
Among the excitatory inputs noradrenergic afferents mediate a tonic activation of serotonergic neurons via stimulation of α_1-adrenergic receptors, as shown by previous studies in anaesthetized and awake animals with α_1-adrenoceptor antagonists and agonists (Baraban and Aghajanian, 1980, 1981; Vandermaelen and Aghajanian, 1983; Levine and Jacobs, 1992).
Furthermore, different brain nuclei project to the DRN and the neurotransmitters involved provide both excitatory and inhibitory inputs to the serotonergic neurons. GABAergic pathways from the lateral habenula (Aghajanian et al., 1977) are either mono- or polysynaptic and provide a negative control on the serotonergic neurons activity. The habenular connections constitute the "dorsal pathway", responsible to transfer information from forebrain limbic structures to the "midbrain limbic areas".
Moreover, anterograde and retrograde tracing studies have reported an interconnection between the infralimbic (IL) and prelimbic (PL) areas of the medial prefrontal cortex (mPFC) and different regions of the raphe nucleus (Peyron et al., 1998). The role of these projections is to be found on the mPFC regions involved. Where the IL projections are consistent with visceral and autonomic activities, the PL projections assume cognitive functions (Vertes, 2004). These connections can then activate either serotonergic or GABAergic neurons, with a higher predominance for the latter (Hajós et al., 1998; Jankowski and Sesack, 2004). However, it has been reported that an increase in glutamatergic transmission can possibly override the feedback inhibition provided by 5-HT_{1A} autoreceptors (5-HT_{1A}ARs; *see infra*), during treatment with SSRIs (Geddes et al., 2015; Commons and Linnros, 2019).

Serotonergic receptors.

The serotonergic receptors are divided in seven families and comprise 22 types of serotonergic receptors of which 17 different types are seven-fold transmembrane receptors whereas the rest (5-HT_3 receptor type) are ligand-operated ion channels (Barnes and Sharp, 1999; Malenka et al., 2009; Box 2).
Each family is classified on the basis of the degree of amino acid similarity of the transmembrane region which contains the binding site (Strader et al., 1994). In fact, receptors of the same family show similar pharmacological profile, displaying similar affinities for different compounds (*see in*: Hartig et al., 1992).

Box 2.

Serotonergic receptors: classification and signal pathways.

Receptor		Major signal pathway	Other G-proteins	Main signal pathways
5-HT_1	5-HT_{1A}, 5-HT_{1B}, 5-HT_{1D}, 5-HT_{1E}, 5-HT_{1F}	Gi/o	Gz	↓ cAMP
5-HT_2	5-HT_{2A}, 5-HT_{2B}, 5-HT_{2C}	Gq/11	Gi/o, G12, and G13	PLC, Ca^{2+}, and PKC (+)*
5-HT_3	5-HT_{3A}, 5-HT_{3B}, 5-HT_{3C}, 5-HT_{3D}, 5-HT_{3E}	Ion channel	–	Depolarization
5-HT_4	5-HT_{4A} - 5-HT_{4H}, 5-HT_{4HB}	Gs	G13	↑ cAMP
5-HT_5	5-HT_{5A}, 5-HT_{5B}	Gi/o	NT	↓ cAMP
5-HT_6	–	Gs	NT	↑ cAMP
5-HT_7	5-HT_{7A}, 5-HT_{7B}, 5-HT_{7C}, 5-HT_{7D}	Gs	G12	↑ cAMP

cAMP, cyclic adenosine monophosphate; PLC, phospholipase C; PKC, protein kinase C; NT, not tested. Adapted from Yun and Rhim, 2011.

The multiplicity of receptor subtypes may account for the fine tuning exerted by serotonin on the activity of a variety of neurons in different regions of the central nervous system and in periphery (Albert et al., 1996; Barnes and Sharp, 1999; Albert and Tiberi, 2001; *see in*: Albert and Lemonde, 2004; Yun and Rhim, 2011; *see in*: Albert et al., 2014; *see in*: Albert and Vahid-Ansari, 2019).

In the brain, the regulation of serotonergic neuron activity is of primary relevance to the functioning of the whole serotonergic system, as changes in serotonergic neuron firing immediately translate in parallel changes in the amount of serotonin released at level of projection areas.

In my thesis the electrophysiological recordings have been conducted in DRN slices *in vitro*, and the afferents belonging to long-loop feedback and feed-forward pathways mentioned above (*see in*: Sharp et al., 2007; Sharp, 2010) have been severed. On the other hand, within the raphe nuclei serotonin itself can directly influence serotonergic neuron activity by stimulating 5-HT_{1A}ARs or, indirectly, by activating GABAergic interneurons through stimulation of 5-HT_{2A} and/or 5-HT_{2C} receptors (Shen and Andrade, 1998; Millan et al., 1998; Gobert and Millan, 1999; Abi-Saab et al., 1999).

Therefore, here I will only highlight the principal characteristics of the serotonergic receptors that play a major role in regulating the activity of serotonergic and GABAergic neurons in the DRN nucleus and could be implicated in the action of the

drugs investigated in the present work (e.g. trazodone, buspirone, serotonin itself). For a review of the relevance of serotonergic receptors in the neurobiology of depression see in Köhler et al. (2016).

5-HT$_{1A}$ receptors.

This class of receptors are mainly located in raphe nuclei, amygdala, septum and hippocampus, as observed from mRNA detection (Albert et al., 1990) and binding studies (Hoyer et al., 1994). Raphe serotonergic neurons express 5-HT$_{1A}$ARs at somatodendritic level (Riad et al., 2000) and therefore the activation of these autoreceptors inhibits the activity of serotonergic neurons. However, in projection areas as the hippocampus and cortex, the 5-HT$_{1A}$ receptor assumes the classical post-synaptic role. The activity of this receptor produces the inhibition of the neuron excitability negatively modulating adenylate cyclase (Pauwels et al., 1993) and activating a G-protein coupled inward rectifying K^+ channel (GIRK, Andrade et al., 1986). The activation of GIRK depends on the βγ subunit binding to the regulatory domain of the K^+ channel (*see in*: Raymond et al., 1999). Moreover, the activity of this receptor weakly couples to protein phospholipase C (PLC) activating it with the $G_{\beta\gamma}$ subunit resulting in a second messenger signalling mediated by two components: IP3 and DAG. Whereas the IP3 regulates the increase in intracellular Ca^{2+} levels, DAG activates the protein kinase C (PKC; *see in*: Raymond et al., 1999; Albert and Vahid-Ansari, 2019). The repeated exposure to an agonist induces a process of decrease in the signalling efficacy that is called desensitization. This is mediated by a group of kinases that phosphorylate 5-HT$_{1A}$ receptors, thereby reducing their coupling with G proteins or the affinity towards the agonist according to the neuron type expressing the receptor (*see in*: Raymond et al., 1999). Desensitization can also occur with an autoregulatory mechanism after prolonged treatment with serotonin. In particular, the receptor will mediate the uncoupling from the G protein depending on PKC and/or phospholipase A2 activity and Ca^{2+} levels (Harrington et al., 1994).

5-HT$_{1B}$ and 5-HT$_{1D}$ receptors.

5-HT$_{1B}$ receptors are mainly located in the caudate nucleus, putamen, nucleus accumbens, central gray, hippocampal formation, subiculum and in Purkinje cells of the cerebellum, as observed from mRNA detection and receptor binding techniques (Voigt et al., 1991; Bonaventure et al., 1997). This receptor subtype is mainly expressed presynaptically on serotonergic terminals (Riad et al., 2000). Its stimulation inhibits adenylate cyclase activity and regulates intracellular Ca^{2+} levels (Zgombick et al., 1993) thereby decreasing the release of serotonin by serotonergic terminals.

Detection of RNA transcript for 5-HT$_{1D}$ receptors has been reported for nucleus accumbens, caudate and raphe nuclei (Hoyer et al., 1994). These receptors display functional properties and molecular binding affinities similar to those of 5-HT$_{1B}$ receptors (Hartig et al., 1992).

5-HT$_{2A}$ and 5-HT$_{2C}$ receptors.

5-HT$_{2A}$ receptors are widely distributed in the brain and play an important role in higher brain functions with specific implications in the regulation of prefrontal cortex connectivity (*see in*: Celada et al., 2013; *see in*: Mengod et al., 2015; Santana and Artigas, 2017a). The finding that 5-HT$_{2A}$ receptors have the ability to dimerize with glutamate metabotropic mGlu2 receptors has suggested that this property could account for the functional cross-talk between these two receptors in the prefrontal cortex (*see in*: Delille et al., 2013) and that this could be involved in therapeutic action of antipsychotics and antidepressants. Indeed, 5-HT$_{2A}$ receptors are considered a therapeutic target in the action of second-generation (atypical) antipsychotics (Bymaster et al., 1996; *see in*: Arnt and Skarsfeldt, 1998; *see in*: Meltzer, 2012). The multimodal antidepressant trazodone also binds to 5-HT$_{2A}$ receptors and this property has been suggested to participate in the antidepressant and/or hypnotic effect of the drug (Stahl, 2009b).

The 5-HT$_{2C}$ receptor has high genomic sequence similarity with the 5-HT$_{2A}$ receptor and is also expressed in the prefrontal cortex (Santana and Artigas, 2017b). 5-HT$_{2C}$ receptors have been implicated in weight control (Sargent et al., 1997) and their blockade likely contributes in the weight gain associated with the atypical antipsychotic drugs show high affinity (Bymaster et al., 1996; *see in*: Arnt and Skarsfeldt, 1998).

The presence of 5-HT$_{2C}$ receptors in prefrontal cortex and anatomically related brain areas, suggests that the may participate in cognitive and affective functions (Heisler et al., 2007; Pennanen et al., 2013) as well as the tonic inhibition of the ascending dopaminergic pathways (Gobert et al., 2000; *see in*: Di Giovanni et al., 2006) exerted by midbrain 5-HT$_{2C}$ receptors.

Both 5-HT$_{2A}$ and 5-HT$_{2C}$ receptors are expressed by raphe GABA neurons, and their stimulation activates GABAergic neurons producing a negative feedback control of serotonergic activity (Serrats et al., 2005).

Other serotonergic receptors.

The other families and subtypes of serotonergic receptors are responsible for a wide panel of different actions across the whole nervous system.

As summarized in box 2, most of receptors activate (i.e. 5-HT$_4$, 5-HT$_6$, and 5-HT$_7$) or inhibit (5-HT$_5$) adenylate cyclase activity. 5-HT$_4$, 5-HT$_6$, 5-HT$_7$ receptors have been implicated in cognitive functions and drugs directed to these receptors have been proposed as cognition enhancers in Alzheimer disease and dementia (Quiedeville et al., 2014; also *see in*: Mitchell and Neumaier, 2005; Ramirez et al., 2014; Meneses, 2014; *see in*: Gasbarri and Pompili, 2014; Stiedl et al., 2015; Zareifopoulos and Papatheodoropoulos, 2016; Hagena and Manahan-Vaughan, 2017; *see in*: Rebholz et al., 2018; *see in*: Khoury et al., 2018). Together with 5-HT$_3$ receptors some of these receptors (e.g. 5-HT$_7$ receptors) have been suggested to participate in the therapeutic

effect of multimodal antidepressant drugs (Sanchez et al., 2015; Gonda et al., 2019). However, the direct role of these receptors in the regulation of raphe serotonergic neuron activity is minor or indirect through activation of long-loop feedback circuitries to raphe nuclei. Comprehensive illustration of the implication of these receptors in brain functioning and brain disorders are reviewed in Köhler et al. (2016) and Rebholz et al. (2018).

Electrophysiological properties of serotonergic neurons in Dorsal Raphe.

Serotonergic neurons of the DRN have distinct electrical properties that allow for recognition of the serotonergic neuron while performing electrophysiological experiments.
Serotonergic neurons are relatively large as indicated by their membrane capacitance of ~40 pF in rats (Marinelli et al., 2004) and in mice (Montalbano et al., 2015a).
The action potential shows a characteristic shoulder in the descending phase (typical high-threshold Ca^{2+} channel conductance of monoaminergic neurons; Penington and Kelly, 1990) with a half-height width (HHW) around 2.4 ms in mice (Montalbano et al., 2015a, Figure 1) and 1.2 ms in rats (Li et al., 2001).

The influx of Ca^{2+} into the neuron caused by the action potential, triggers a Ca^{2+}-activated K^+ out-ward current responsible of the after-hyperpolarization (AHP; Vandermaelen and Aghajanian, 1983; Aghajanian, 1985; *see in*: Piñeyro and Blier 1999) The AHP induces a long refractory period that allows voltage-activated sodium and calcium channels to deinactivate and be available for the successive action potential.

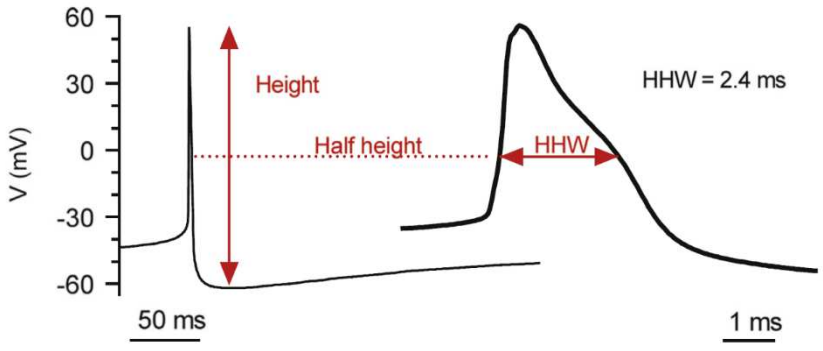

Figure 1. Serotonergic neuron action potentials.
Example of an action potential in a DRN serotonergic neuron. Trace is average of 20 individual action potentials, evoked with minimal constant current injection of 10 pA sufficient to evoke repetitive a firing of 0.8 Hz. On the right the same trace in an expanded timescale displays shoulder in the descending phase, characteristic of monoaminergic neurons. HHW = half height width. Adapted from Montalbano et al., 2015a.

Regulatory activity of serotonergic neuron firing rate.

The alternating activity of these voltage-activated conductances induces a regular, spontaneous and low-frequency firing rate for serotonergic neurons. The activity of serotonergic neurons changes during the sleep-wake cycle, being maximal when the animal is awake and slowly decreasing with the sleep progression to result almost silent during REM sleep (McGinty and Harper 1976, Jacobs and Fornal 1993). This pattern of activity depends on the activation of serotonergic neurons by noradrenergic input, since firing of serotonergic neurons is maximally facilitated by α_1-adrenoceptor stimulation (Baraban and Aghajanian, 1980, 1981, Levine and Jacobs 1992, Mlinar et al., 2016).
Under these conditions, the firing of serotonergic neurons is tonically limited via the stimulation of somatodendritic 5-HT_{1A} autoreceptors (5-HT_{1A}ARs) exerted by the endogenous serotonin present in the extracellular space surrounding serotonergic neurons (Fornal et al., 1996, Corradetti et al., 1996b; Mlinar et al., 2005; Mlinar et al., 2015a). The extracellular pool of serotonin is shared between the serotonergic neurons, meaning that serotonin released by one of the serotonergic neurons can bind to the 5-HT_{1A}AR on another neuron (Mlinar et al., 2015a) thereby activating a G-protein Inward Rectifying K^+ conductance (Williams et al., 1988, Montalbano et al., 2015b).
Studies conducted with Way-100635, a 5-HT_{1A} receptor competitive and selective antagonist (Corradetti et al., 1996a, 1996b, 1998, Mlinar et al., 2005; Mlinar et al., 2015a), support the idea that firing rate of serotonergic neurons is tonically regulated by the activation of 5-HT_{1A}ARs exerted by extracellular serotonin.
Importantly, the major regulator of external serotonin concentration is the activity of SERT that transports serotonin from the synaptic cleft back to the presynaptic neuron at the axon terminals (Mlinar et al., 2015a).
Taken together, SERT, 5-HT_{1A} receptor and α_1-adrenoceptor, constitute a complex regulatory mechanism for serotonergic neuron activity and serotonin release in DRN and projection areas.

Importance of 5-HT_{1A} autoreceptors in the functioning of antidepressant drugs.
The complex regulatory activity on the firing rate of serotonergic neurons produced by the rise in extracellular serotonin, caused by SERT inhibition, and the stimulation of 5-HT_{1A}ARs is believed to play an important role in the delay in onset of therapeutical action of most antidepressant drugs.

It appears fairly well established that the increase in extracellular level of serotonin produced by inhibition of SERT in projection areas contributes to the therapeutic action of SSRIs. However, the firing activity of serotonergic neurons is under (auto)inhibitory control exerted by extracellular serotonin through stimulation of somatodendritic 5-HT_{1A}ARs, opening G protein-activated inwardly rectifying

potassium (GIRK) channels and neuron membrane hyperpolarization (Llamosas et al., 2015; Mlinar et al., 2015a; Penington et al., 1993; Williams et al., 1988). Thus, increased extracellular serotonin in raphe nuclei results in hyperpolarization of serotonergic neurons, inhibition of their activity and reduction of serotonin release in projection brain areas (de Montigny et al., 1984; Sprouse and Aghajanian, 1987; Sharp et al., 1989) that is believed to limit the therapeutic effectiveness of SSRIs.
However, with chronic treatment the sustained stimulation of 5-HT_{1A}ARs by elevated serotonin concentration induces adaptive subsensitivity of these receptors (*see in:* Raymond, 1999) and weakens the autoinhibitory feedback producing the recovery of serotonergic neuron activity to higher firing rates, even in the presence of increasd extracellular serotonin. In terminal projection areas, the recovery of activity of serotonergic neurons to normal firing rate, combined with the inhibition of SERT, will result in higher availability of serotonin in the synaptic cleft per impulse received. As the subsensitivity of 5-HT_{1A}ARs requires several days to develop, this phenomenon has been proposed to underlye the delay in the onset of therapeutic effect displayed by SSRIs (Blier and de Montigny, 1994).
On the basis of this notion it has also been proposed that the association of 5 HT_{1A} receptor antagonists could hasten the response to monoamine uptake blockers (*see in*: Artigas et al., 1996; Piñeyro and Blier, 1999; Portella et al., 2011) and, more recently, that antidepressant drugs with partial agonist property at 5 HT_{1A} receptors could display faster onset of therapeutic response (Artigas et al., 2018).
The advantage of compounds endowed of 5-HT_{1A} receptor weak partial agonist properties in comparison with SSRIs is that the activity of these drugs depends on the levels of external serotonin. In fact, when serotonin external concentrations are low, these drugs directly activate 5-HT_{1A}ARs, albeit with a weaker efficacy compared to the endogenous agonist, thereby producing a moderate inhibition of serotonergic neuron activity. When the level of extracellular serotonin is greatly enhanced by SERT inhibition the partial antagonism exerted by the drug against the full agonism of serotonin at 5-HT_{1A}ARs effectively decreases the autoinhibitory response of serotonergic neurons to elevated serotonin (*see in:* Artigas, 2013; Artigas et al., 2018).

Trazodone as a multimodal antidepressant drug.

Trazodone is a multimodal antidepressant that, in addition to its inhibitory activity at SERT displays a considerable affinity for a variety of 5-HT receptors, including 5-HT_{2A}, 5-HT_{2C} and 5-HT_{1A} receptors, and α_1-adrenoceptors blocking effect on hippocampus (Cusack et al., 1994; Owens et al., 1997; Ghanbari et al., 2012).
In vivo recording of serotonergic neuron activity in anaesthetized rats showed that acute administration of trazodone inhibits DRN serotonergic neuron firing (Scuvée-Moreau and Dresse, 1982) an action mediated by activation of somatodendritic 5-HT_{1A}ARs which desensitize after chronic treatment with the antidepressant drug (Ghanbari et al., 2010a). Nevertheless, the direct functional effects of trazodone on 5-

HT_{1A}ARs are still insufficiently characterized to establish whether the drug exerts full or partial agonism at 5-HT_{1A}ARs. In the rat, in a functional assay *in vitro* trazodone was found to activate [^{35}S]GTPγS binding with weak efficacy (Odagaki et al., 2005), while *in vivo* its action on serotonergic neuron firing appeared consistent with stronger agonism at 5-HT_{1A}ARs (Ghanbari et al., 2012).

The interplay between the 5-HT_{1A} receptor agonist activity and α_1-adrenoceptor antagonist activity of trazodone at the level of serotonergic neurons likely plays a crucial role in regulating the firing of serotonergic neurons, hence the release of serotonin in projection areas during acute and chronic administration of the drug. In fact, since the noradrenergic input to raphe nuclei tonically activates serotonergic neurons via α_1-adrenoceptors, the α_1-adrenoceptor antagonist properties of trazodone could participate to the inhibiton of DRN serotonergic neuron firing by reducing the noradrenergic drive. However, *in vivo* experiments were unable to quantify this action in the DRN in conditions in which trazodone appeared to have α_1-adrenoceptor blocking effects in the hippocampus (Ghanbari et al., 2012).

In the present work we designed *in vitro* experiments directed to accurately quantify the agonist efficacy of trazodone at 5-HT_{1A}ARs of DRN serotonergic neurons and to establish the possible effect of α_1-adrenoceptor antagonism.

Aim of the study.

The major aim of the present research was to characterize the *direct* effects exertedby the antidepressant drug trazodone on the activity of serotonergic neurons of the dorsal raphe nucleus (DRN) through its binding to5-HT_{1A} receptors and α_1-adrenoceptors.
As mentioned in the introduction, trazodone has a relatively high affinity for these receptors which suggests that, at therapeutic brain concentrations of the drug, the action at somatodendritic 5-HT_{1A} (auto)receptors (5-HT_{1A}ARs) of serotonergic neurons and the concomitant effects exerted through α_1-adrenoceptors produces responses that could be relevant to the overall antidepressant action and/or to the specific pharmacological profile of this multimodal antidepressant drug. The knowledge of the pharmacological *direct* effects of trazodone on serotonergic neuron activity is of particular importance because changes in the activity of DRN serotonergic neurons directly translate in parallel changes in the release of serotonin by terminals and, accordingly, modify the serotonergic tone in projection areas. Qualitatively, from the published data it was to be expected that trazodone exerts an agonist action at 5-HT_{1A}ARs and an antagonist effect at α_1-adrenoceptors. Nevertheless, only scattered and contradictory data on the possible *direct* effects exerted by trazodone through 5-HT_{1A}ARs and α_1-adrenoceptors on serotonergic neurons were available in the scientific literature.
To characterize the action of trazodone at these receptors, we have applied electrophysiological recording techniques in brainstem slices containing DRN. Namely, we used loose-seal cell-attached patch-clamp recording, often combined with pharmacological tools, to investigate the activity response of serotonergic neurons to the application of trazodone, which provides the principal parameter of interest for interpreting the possible functional effects of the drug on serotonergic system *in vivo*.
Furthermore, the efficacy of trazodone in activating 5-HT_{1A}ARs was insufficiently characterized and it remained to be elucidated whether the drug is a full agonist or a partial agonist at these receptors. To this purpose we have quantified the activation of GIRK channels produced by trazodone through the stimulation of 5-HT_{1A}ARs in DRN serotonergic neurons. Since the amount of activated GIRK channels is proportional to the number of stimulated 5-HT_{1A} receptors, GIRK conductance reliably reports the concentration-dependent effect of the agonist and the response of serotonergic neurons to maximal 5-HT_{1A} receptors stimulation. Thus, this experimental approach allows an accurate quantitative study of the potency and the intrinsic efficacy of trazodone at 5-HT_{1A}ARs.
Finally, as the antidepressant effect of trazodoneis mainly due to SERT inhibition and this action increases the level of extracellular serotonin in DRN with subsequent activation of 5-HT_{1A}ARs, we calculated how the agonist efficacy of trazodone at therapeutic concentrations could modify the total stimulation of 5-HT_{1A}ARs by endogenous serotonin *in vivo*.

Materials and Methods:

Animals and animal care.

Animal care and experimental procedures strictly complied with the European Communities Council Directive (2010/63/UE) and were approved by the Italian Ministry of Health (Aut: 224/2017-PR and 938/2017-PR). Every effort was made to reduce the number of animals used. Male Wistar rats were purchased from Envigo Italy (Milan, Italy). Tryptophan hydroxylase-2 knock-out ($Tph2^{-/-}$) mice were obtained from Prof. K.P. Lesch (University of Würzburg, Würzburg, Germany). Animals were housed on a 12:12h day-night cycle with food and water *ad libitum*.
Procedures for tissue isolation, slice superfusion and electrophysiological recording from DRN serotonergic neurons of rat and mouse have been previously described in detail (Araragi et al., 2013, Mlinar et al., 2015a, Montalbano et al., 2015a, Montalbano et al., 2015b).

Preparation of brain slices.

Slices were prepared from animals aged 4-10 weeks (4-5 weeks for whole-cell patch-clamp recordings). Animals were deeply anesthetized with isoflurane and decapitated. Brains were rapidly removed and dissected in ice-cold gassed (95% O_2 and 5% CO_2) artificial cerebrospinal fluid (ACSF) composed of: 124 mM NaCl, 2.75 mM KCl, 1.25 mM NaH_2PO_4, 1.3 mM $MgCl_2$, 2 mM $CaCl_2$, 26 mM $NaHCO_3$, 11 mM D-glucose. The brainstem was sliced coronally into 200 µm thick slices with a vibratome (DSK, T1000, Dosaka, Japan). After recovery for at least 90 min at room temperature, the slices were individually transferred to the recording chamber and superfused continuously, at a rate of 2 ml * min^{-1}, with warmed ACSF (Warner Instruments in-line heater TC324-C). Slices were allowed to equilibrate for at least 15 min before the beginning of the recording. Drugs were bath-applied through a peristaltic pump-driven perfusion system and a complete exchange of the recording chamber volume occurred in approximately 1 min. Neurons within dorsal raphe nucleus were visualized by infrared differential interference contrast (IR-DIC) video microscopy with a Newicon camera (C2400-07; Hamamatsu, Hamamatsu City, Japan) mounted on an upright microscope (Axioskop; Zeiss, Göttingen, Germany). Recordings were made using an EPC-10 amplifier (HEKA Elektronic, Lamberecht, Germany). Patch pipettes were prepared from thick-walled borosilicate glass on a P-97 Brown-Flaming electrode puller (Sutter Instruments, Novato, CA, USA). Data were analyzed using Patchmaster 2 (HEKA Elektronic), Clampfit 9.2 (Molecular Devices, Sunnyvale, CA, USA) and Prism 7 software (GraphPad Software, San Diego, CA, USA).

Electrophysiology.

Loose-seal cell-attached recordings.

Advantages of loose-seal configuration.

Loose-seal configuration is obtained by approaching the pipette to the neuron without touching the membrane. Is a non-invasive patch clamp configuration particularly suitable to monitor neuron activity without introducing major perturbations or lesioning the cell. Differently from the classical tight cell attached configuration, this patch clamp technique preserves better the neuron membrane avoiding stretch conductances that will influence firing rate.

Neuron activity is recorded in voltage clamp to detect the firing pattern and allow measurement of the action current duration (e.g. Figure 2B).

When the pipette approaches the neuron, a gentle suction allows the establishment of a light seal that will isolate the pipette tip from the surrounding neuron network, without the neuron membrane. When sucking, the spike amplitude progressively increases without affecting the firing frequency (Figure 2A), spike duration (Figure 2B) or the interspike interval (Figure 2C). The firing frequency is the average number of spikes during the whole recording, the spike duration is the difference between the upstroke and the second downstroke peak ($UDHD_2$, Figure 2B) and the interspike interval is the time between a first spike and the following.

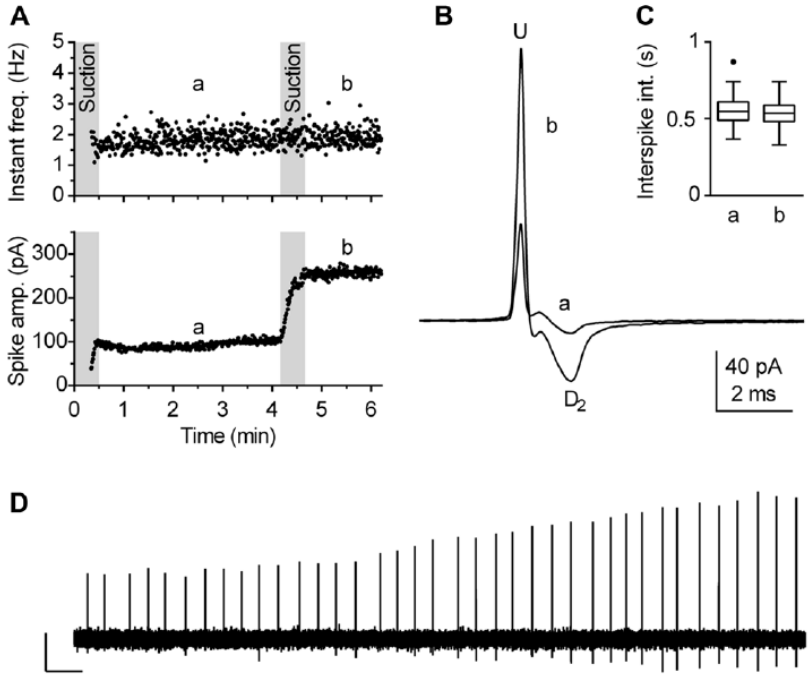

Figure 2. Validity of firing rate measurement by use of loose-seal cell-attached recordings.
(A – D) The procedure used to verify the lack of pipette interference with the measurement. **(A)** Time-course of a recording illustrating the procedure. During the first 30 s, gentle suction was applied to the pipette to establish loose-seal cell-attached recording configuration. The pressure was then released and after 30 s, left to allow relaxation of the patched cell membrane, a 3 min long segment (denoted a, from 1 to 4 min) was acquired for the measurement. Afterward, additional suction was slowly applied until the spike amplitude approximately doubled (lower panel) and the recording was prolonged for an additional 1.5 min (denoted b). Since the firing rate remained essentially the same after the test (second suction), the recording was considered reliable, i.e., free of pipette interference. **(B)** Superimposed average spike of the same experiment. Spike duration, measured as the interval from the upstroke peak (U) to the second dowstroke peak (D_2), was unchanged by the additional suction. **(C)** Box plot of the experiments show no changes in distribution of interspike intervals (ISI). Boxes represent median and interquartile range (IQR). Whiskers denote 1.5 IQR. **(D)** Trace shows a segment (4:10 – 4:30 min) of the original recording during which additional (test) suction was applied. Scale bars: 50 pA, 1 s. Figure adjusted from Mlinar et al., 2016.

Recording of serotonergic neuron firing activity.

Loose-seal technique was used to record action currents in serotonergic neurons (Figure 3) to calculate the firing activity at a temperature of 34 - 36 ˚C.

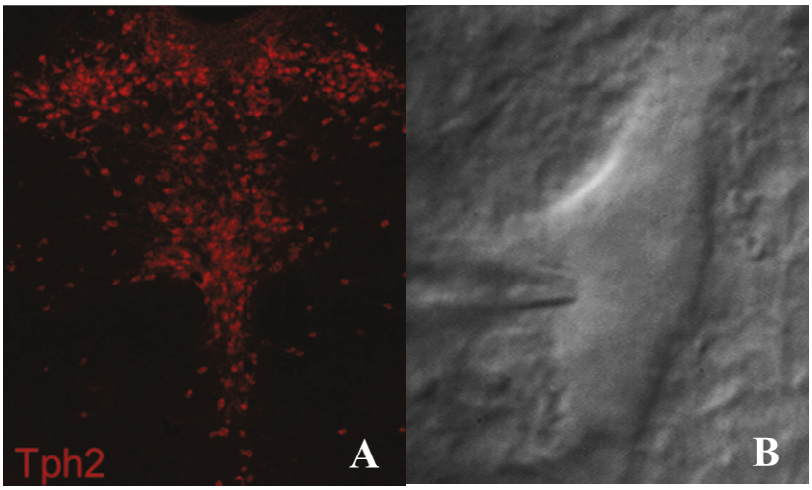

Figure 3. Typical recording arrangement of serotonergic neurons in DRN slice
(A) Obtained image with epifluorescence microscopy of rostral DRN (-4.6 mm from bregma) of Pet1-CreeGFP:Tph2$^{+/+}$ mice. Image adapted from Montalbano et al., 2015a. **(B)** Infrared image obtained from a DRN slice from a rat as seen through the 40x objective lens. A nylon net holds the slice down in the bath chamber, submerged with ACSF.

To reproduce in slices the noradrenergic drive which facilitates serotonergic neuron firing during wakefulness (Levine and Jacobs 1992), ACSF was supplemented with the α_1-adrenoceptor agonist phenylephrine (PE, 10 µM, unless otherwise stated). In a set of experiments neuron firing was facilitated using a modified ACSF containing 0.67 mM Ca^{2+} and 5.5 mM K^+. When appropriate, ACSF contained a "cocktail" of glutamate GABA/glycine and adenosine A1 receptor blockers consisting of: 10 µM NBQX (2,3-dioxo-6-nitro-1,2,3,4-tetrahydrobenzo[f]quinoxaline-7-sulfonamide disodium salt), 20 µM d-AP5 (d-(-)-2-amino-5-phosphonopentanoic acid), 10 µM SR-95531 (6-imino-3-(4-methoxyphenyl)-1(6H)-pyridazinebutanoic acid hydrobromide), 2 µM CGP-55845 (3-N[1-(S)-(3,4-dichlorophenyl)ethyl]amino-2-(S)-hydroxypropyl-P-benzyl-phosphinic acid hydrochloride) and 10 µM strychnine hydrochloride, 0.2 µM DPCPX (8-Cyclopentyl-1,3-dipropylxanthine) to functionally isolate the recorded neuron from major synaptic input. Patch pipettes were prepared from thick-walled borosilicate glass on a P-97 Brown-Flaming electrode puller (Sutter Instruments, Novato, CA, USA) and had resistances of 3-6 MΩ when filled with solution containing (in mM): 125 NaCl, 10 HEPES, 2.75 KCl, 2 $CaCl_2$, 1.3 $MgCl_2$ (pH 7.4 with NaOH). Loose-seal cell-attached recordings (5-20 MΩ seal resistance) were acquired continuously in the voltage-clamp mode (Figure 4A).

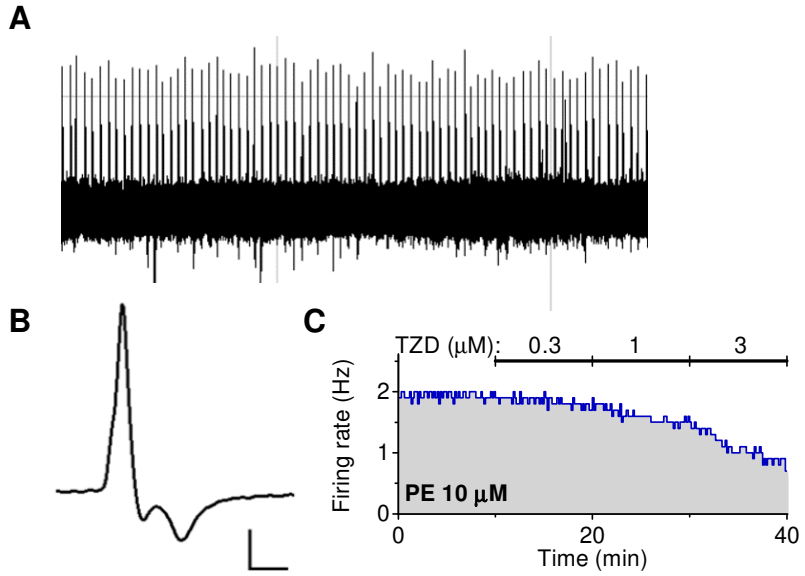

Figure 4. Example of loose-seal cell attached recording.
(A) Recording of firing rate from a serotonergic neuron in DRN. Each spike is an action current of the serotonergic neuron. Firing rate is determined by counting the number of spike peaks. Frequency of action potential discharge was facilitated *via* stimulation of α_1-adrenoceptors by phenylephrine (PE). **(B)** Average spike recorded from a serotonergic neuron. Scale bar: 15 pA, 1 ms. **(C)** Time-course of the firing rate changes produced by the application of trazodone . Note the decrease in firing rate with the increase in drug concentration. Firing rate reported in 10 s bins.

Signals were filtered at 3 kHz and digitized at 10 kHz. The firing rate was reported using 10 s bins. Data were analyzed using Clampfit 9.2 (Molecular Devices, Sunnyvale, CA, USA). Most recorded neurons were located in the dorsal and ventromedial part of the DRN. Neurons were identified following the criteria related to the spike frequency and duration of ~2 Hz and ~1.2 ms, respectively as already reported in (Mlinar et al., 2015a; 2016). Only neurons with a stable baseline firing rate were used. Neurons having a firing rate of less than 0.8 Hz in phenylephrine-supplemented ACSF were not used since they typically had unstable baseline activity and often ceased to discharge action potentials.

Whole-cell patch-clamp electrophysiology.

Principles of whole-cell configuration and passive properties of neuron.
Generally, a whole-cell configuration is obtained by disrupting the neuron membrane underneath the patch electrode with suction or a zap current. The internal solution of the pipette becomes then a continuum with the cytoplasm. In this configuration, macroscopic currents and potential changes such as action potentials and synaptic responses can be recorded and the cytoplasmic environment can be controlled by

changing the composition of the internal solution. For example, inhibitors can be intracellularly applied to block enzymes and intracellular transduction cascades in the recorded neuron. In addition, channel blockers (e.g. potassium channel blockers such as Cs^+) can be introduced to improve recordings, in particular the space clamp efficacy under voltage-clamp mode.

In electronic terms (Figure 5), the whole-cell configuration represents a complex circuit where the resistance of the pipette (Rpipette) is in series with the resistance established in the patch, the access resistance (Racc). This component is named series resistance (Rs) and is in parallel with the cell resistance (Rm). The figure below shows also another important component for the circuit: the leak resistance (Rleak). This defines the resistance of the patch seal through which there is a loss of signal and determines the quality of the patch.

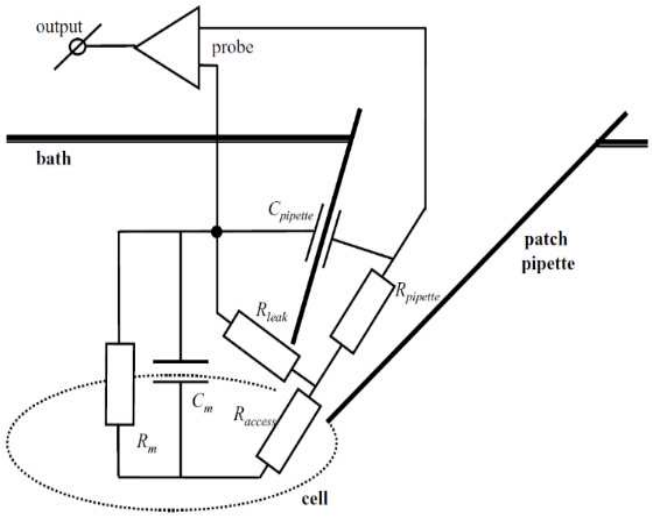

Figure 5. Equivalent circuit for whole-cell configuration.
The membrane under the patch is disrupted by suction. The pipette resistance (Rpipette) is controlled by the probe. When the seal breaks, the Rpipette is in series with the membrane resistance (Rm). In parallel, there is the leak resistance (Rleak) which determines the current lost during the recording and indicates the quality of the seal. Cm is the capacitance of the neuron membrane. Cpipette is the capacitance of the pipette and is compensated for before forming the seal. Adapted from Molleman, 2003.

To simplify and clarify the electronic terminology in real recording conditions, I refer to Rleak as seal resistance (Rseal), to Rm as input resistance (Rin) and to Rs + Rpipette as Racc since I cannot separate the two in my measurements.

An additional component of the circuit is the capacitance of the neuron. This is a passive property of the neuron and affects the time characteristics of voltage changes imposed by the amplifier. The cell membrane is a capacitor and together with the different resistances forms a RC circuit. Charging and discharging the RC circuit, will change the potential of the neuron with a certain time constant (tau or T) which is the time at which 63% of the maximal change in potential or current are reached along the exponential rise or decay curve.

Importance of patch seal quality in the measurement of neuron input resistance in whole-cell recordings.

One important parameter that influences the measurement of Rin is the goodness of the seal. For a good estimation of Rin the seal between the pipette and the neuron membrane should be theoretically impermeable to ions so that Rseal is very high. In practical terms, Rseal should be greater than 1-2 GΩ (see below). In fact, as shown in the Figure 5, Rseal (indicated in Figure by Rleak) is in parallel to Rin. Both resistances form a divider for the current flowing from the pipette to the neuron when the voltage command is imposed.

The general equation to describe the total resistance (Rtot) for this arrangement is the equation used to describe two resistances in parallel in an electrical circuit:

$$Rtot = \frac{Rin * Rseal}{Rin + Rseal}$$

A simple example can solve the equation where Rtot is the membrane total resistance as it will be read by the amplifier. If we calculate the Rtot measured from a neuron with actual membrane resistance of 300 MΩ and a recording with a seal resistance of 1 GΩ, Rtot will result 230 MΩ. On the other hand, if the recording Rseal is 10 GΩ, the calculated Rtot will result ~291 MΩ, i.e. closer to the actual total neuron resistance. Thus, the lower the seal resistance, the greater the error in determining the total membrane resistance of the neuron. As a general rule, for an accurate measurement of total Rin of the recorded neuron Rseal should be at least one order of magnitude greater than the neuron Rin.

Measurement of GIRK channel conductance.

Methods used for measuring GIRK channel conductance have been detailed previously (Mlinar et al., 2015a; Montalbano et al., 2015a). All experiments were performed in ACSF supplemented with a cocktail of neurotransmitter blockers (*see* above). ACSF contained 5.5 mM K^+ to increase the driving force for inward potassium current (the additional 2.75 mM by Na^+ substitution). Recording pipettes had a resistance of 2 - 5 MΩ. The pipette solution consisted of: 120 mM K-gluconate, 15 mM KCl, 2 mM $MgCl_2$, 10 mM HEPES, 0.1 mM EGTA, 10 mM Na_2phosphocreatine, 4 mM MgATP, 0.3 mM Na_3GTP (pH 7.35 with KOH). After establishing whole-cell recording configuration, serotonergic neurons were identified on the basis of electrophysiological properties displayed in current-clamp mode (action potential half-height width > 1.1 ms; absent or very small fast afterhyperpolarization; sustained repetitive firing in response to depolarizing current injection). In current-clamp recordings signals were filtered at 5 kHz and digitized at 25 kHz.

To monitor access resistance throughout the recording, hyperpolarizing pulses (10 mV; 100 ms duration; 16 kHz low-pass filter; 25 kHz sampling frequency; cell capacitance cancellation circuit switched off) were used (Figure 6).

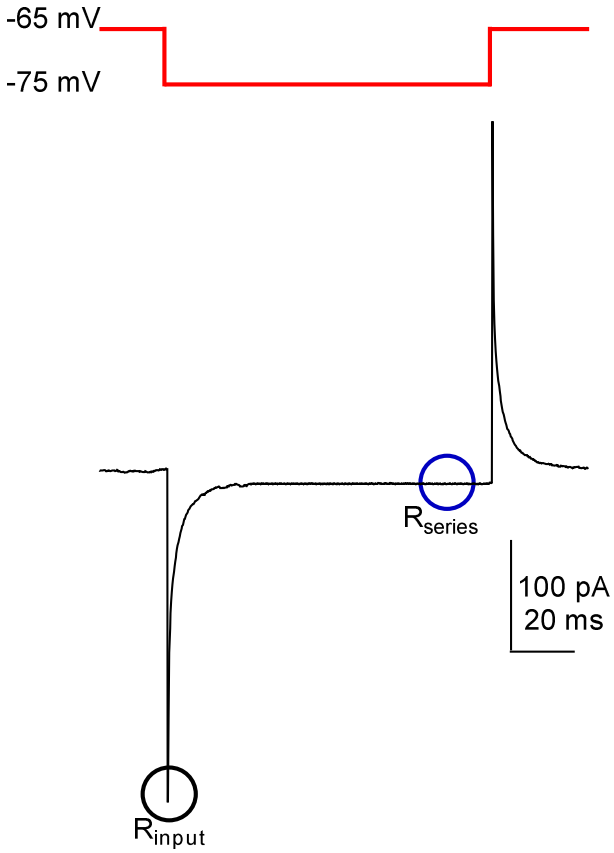

Figure 6. Protocol applied to monitor access resistance.
Top: Schematic representation of the test pulse protocol. The neuron membrane potential is held at -65 mV and hyperpolarized by a -10 mV step for 100 ms. Circles are the points where the Rin (black) and Rseries (blue) are calculated from the respective currents applying Ohm's law. *Bottom*: Average of 10 test pulse sweeps. Signals were sampled at 5 kHz after filtering with the amplifiers internal Bessel filter at 2 kHz. Scale bar: 100 pA; 20 ms.

Access resistance was not compensated and when it was higher than 25 MΩ recordings were discarded.
To estimate inwardly-rectifying K^+ conductance, we used hyperpolarizing voltage ramps from the holding potential of -65 mV (to -125 mV, every 10 s; 100 mV s^{-1}; 3 kHz cutoff frequency low-pass filter; 10 kHz sampling frequency) and measured the conductance from the slope of inward K^+ current in the range from -110 to -85 mV ($G_{-110/-85\ mV}$, Figure 7A).
When using the ramp protocol, we were able to monitor the current peak value at both -65 mV and -125 mV (I_{-65} and I_{-125} respectively, Figure 7A) and extract the single

pulse values to reconstruct a time course (Figure 7B). However, monitoring of the peak current was not as strong as monitoring the conductance. In fact, these current peaks were influenced by some mechanical artifacts that could sparely appear and ruin the recording (Figure 7B *top*, *middle*). The conductance, instead, was more stable and less influenced by artefactual changes (Figure 7B *bottom*) since the value obtained was from the detection of a bigger number of points compared to the single peak current value. Thus, in our experiments we decided to address changes to 5-HT_{1A} receptors-mediated GIRK activation by measuring the conductance of the channel.

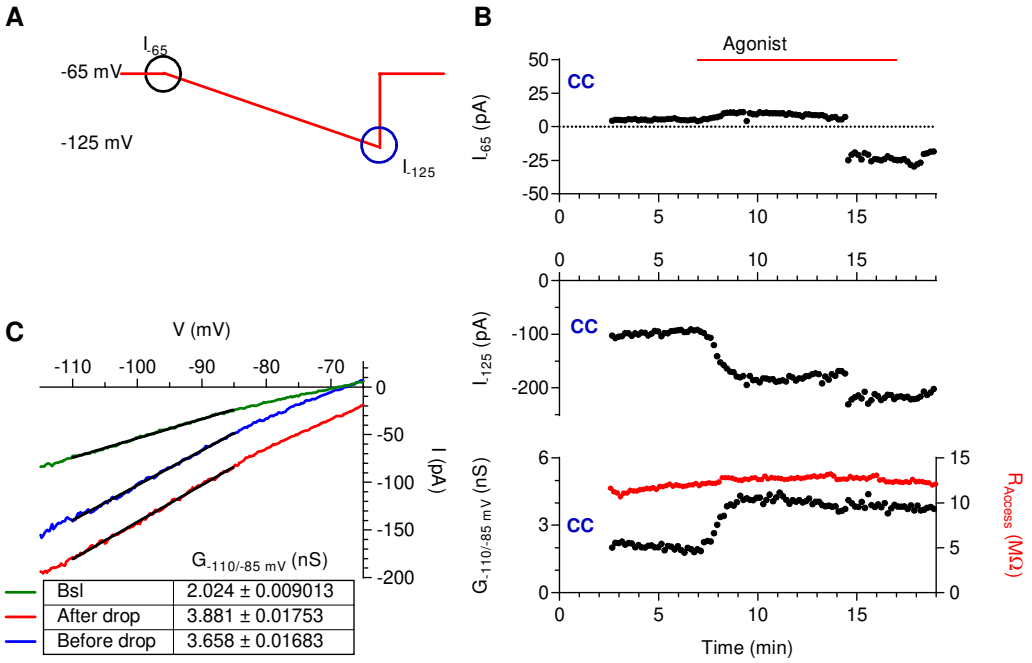

Figure 7. Importance of monitoring channel conductance instead of current peak.
(A) Schematic representation of the ramp protocol used. The neuron membrane potential is held at -65 mV and hyperpolarized to -125 ms every 10 s, 100 mV * s^{-1}. Circles are the points where the peak current at -65 mV (black circle, I_{-65}) and -125 mV (blue circle I_{-125}) were calculated. **(B)** Time course of I_{-65} current (*top*), I_{-125} current (*middle*) and conductance (*bottom*) in a serotonergic neuron. The first two minutes of recordings in current clamp (CC) are needed to let the cytoplasmic solution equilibrate with the pipette internal solution. Application of the Agonist produces the increase in peak currents and conductance. Note the drastic changes visible in the time course of peak currents (but not in the time course of the conductance). Since Raccess remains stable (red line in *bottom panel*), we assumed that the sudden change could have been caused by opening of K^+ channels that produced a "leak" current. While this change clearly compromised the quantification of agonist induced peak current, it was still possible to quantify the effect of the agonist by measuring the slope conductance. **(C)** Current-Voltage relationship of the conductance related to the opening of GIRK. Green, blue and red traces are the average of 7 consecutive individual ramps of events considered for Baseline (Bsl), before and after drop recorded in **(B)**. In this case, the drop occurring when measuring the slope between a membrane potential of -85 and -110 mV (black lines, best linear fit of the slope) is reflected by a 9% change in the slope, a value lower than those calculated for both I_{65} and I_{125} (-30% and -80% respectively). Note the inward rectification on GIRK shown form a voltage value of -80 mV.

Concentration–response curves for trazodone were obtained using a cumulative protocol in which increasing concentrations were applied in 7-10 min intervals as appropriate. Average of 7 consecutive individual ramps, corresponding to the segment with the maximal effect for the given trazodone concentration were used to obtain conductance values (Figure 8). To calculate net 5-HT_{1A}ARs activated GIRK current and conductance ($G_{5\text{-}HT1A}$) present during a recording, the 5-HT_{1A} receptor-insensitive current was measured at the end of a recording following application of the selective and competitive 5-HT_{1A} receptor antagonist Way-100635 (20 nM; 10 - 15 min) and subtracted from the total current (Figure 8B).

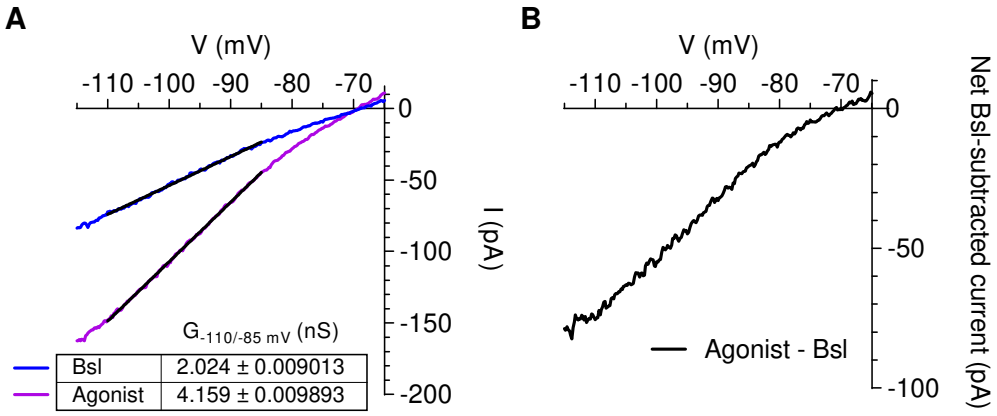

Figure 8. Example of 5-HT_{1A} receptor-mediated GIRK-conductance in a serotonergic neuron. **(A)** Current-Voltage relationship of the conductance related to the opening of GIRK. Blue and purple traces are the average of 7 consecutive individual ramps of baseline and agonist-mediated responses to change in the conductance of the activated GIRK channel. In this case, the agonist action is visible by the increase in the slope. Black lines are the best linear fit of the slope when the membrane potential is between -85 and -110 mV. Note the inward rectification on GIRK shown form a voltage value of -80 mV. **(B)** Net agonist induced current obtained by subtraction of baseline current from the current measured at the end of agonist application.

To activate 5-HT_{1A}ARs in comparative tests we used 5-carboxamidotryptamine (5-CT), a 5-HT_{1A} receptor agonist which is structurally similar to serotonin and shows full agonist coupling efficiency at 5-HT_{1A} receptors estimated by [^{35}S]-GTPγS binding assay (Pauwels et al., 2003; Heusler et al., 2005) and by electrophysiological recordings (Williams et al., 1988). Notably, under our experimental conditions, 5-CT behaves as a selective agonist because it was ineffective on serotonin neurons of 5-$HT_{1A}^{-/-}$ mice in concentrations up to 300 nM (Audero et al., 2013). In addition, serotonin is subject to metabolism and uptake which limits the accuracy in estimating the actual concentration in tissue.

Calculation of concentration-response relationships.

To create cumulative concentration-response curves for trazodone, the drug was applied for 10 - 30 min (as appropriate for the specific experimental objective) and mean firing rates were calculated from the last one-minute segment of each experimental epoch (e.g. baseline, trazodone 0.3 μM, 1 μM, etc.). Trazodone dose-response relationship for suppression of serotonergic neuron firing was computed by fitting data to the logistic equation $b + (a - b) / (1 + (EC_{50} / [\text{trazodone}])^{n}_{H})$, where EC_{50} is the half-maximally effective concentration, n_H is the Hill coefficient, a is the baseline firing rate and b is the fraction remaining at the maximal trazodone effect. Fitting of average dose-response relationship of normalized firing rate: for each experiment, firing rate was measured during the last 2 min of drug application for each concentration and normalized by taking the pre-drug baseline firing rate as unity. Then the relationship for suppression of serotonergic neuron firing was computed by fitting mean values (± SD) for each concentration to the logistic equation, $b + (1 - b) / (1 + (EC_{50} / [\text{trazodone}])^{n}_{H})$, where EC_{50} is the half-maximally effective concentration, n_H is the Hill coefficient and b is the fraction remaining at the maximal trazodone effect.
The respective fractional occupancy of 5-HT_{1A}ARs by trazodone and the full agonist, either 5-CT or serotonin, in the presence of trazodone was calculated using the Gaddum equation: $[AR]/Rt = [A]/([A]+K_a(1+[B]/K_b))$, where [AR]/Rt is the fractional occupancy by the full agonist, [A] is the concentration of the full agonist with K_a affinity constant and [B] and K_b are trazodone concentration and affinity, respectively. To allow comparison of theoretical values with the responses experimentally obtained in rat serotonergic neurons, we calculated the occupancies for 5-CT and trazodone by applying the K_i of the two agonists for the rodent 5-HT_{1A} receptor (5-CT: K_i = 0.325 nM, Waeber and Moskowitz, 1995; trazodone: K_i = 42 nM, Owens, 1997). For the action of trazodone on serotonin we used the K_i of the two agonists for the human 5-HT_{1A} receptor (serotonin: K_i = 3.98 nM, Boess and Martin, 1994: Sundaram et al., 1993; trazodone: K_i = 96 nM, Cusack et al., 1994) to allow inference on the effects of trazodone on responses to endogenous serotonin *in vivo*.
In both cases, the expected total activation of GIRK conductance was calculated from the respective occupancies of the two compounds by using the measured maximal efficacy of 0.35 for trazodone and 1.0 for the full agonist.

Drugs.

Trazodone was provided by A.C.R.A.F. (Santa Palomba, Rome). Serotonin (5-HT), SR-95531, *D*-AP5, NBQX were purchased from Ascent Scientific Ltd. (Bristol, UK). Way-100635 maleate, CGP-55845 hydrochloride, 5-CT and DPCPX were purchased from Tocris Bioscience (Bristol, UK). L-Phenylephrine and strychnine hydrochloride from Sigma-Aldrich S.r.l. (Milan, Italy).

Statistical analysis.

Data are presented as geometric mean and confidence interval (C.I.) or mean ± SD as appropriate. Statistical comparisons were performed by ANOVA followed by Tukey *post-hoc* test, paired or unpaired t-test (two tailed), as appropriate. Pearson test was used to assess for correlation between variables. All the statistical tests were performed by GraphPad Prism version 7. Throughout the analyses, statistical significance was taken as $p < 0.05$.

Results:

As mentioned in the introduction, trazodone has been reported to silence serotonergic neuron activity *in vivo*, an effect that has been ascribed to stimulation of 5-HT_{1A}ARs. However, *in vivo* experiments were unable to unravel whether the inhibitory effect of the antidepressant drug was due to partial or full agonist action at 5-HT_{1A}ARs and if other pharmacological direct actions of the drug on serotonergic neurons participate in the inhibitory effect.
As a first step we investigated the action of trazodone on the activity of DRN serotonergic neurons *in vitro* recorded using the loose-seal cell-attached patch-clamp technique. To reproduce the noradrenergic drive present *in vivo*, firing was facilitated by the presence of the selective α_1-adrenoceptor agonist phenylephrine (10 μM).

Trazodone inhibits the firing of serotonergic neurons in standard ACSF.

In dose-response curves (Figure 9A) obtained by cumulative application of increasing concentrations of trazodone, the concentration of drug that produced 50 % inhibition of firing rate (EC_{50} value) was 1.78 μM (Geometric mean, GM, 95% Confidence Interval, 95% C.I.: 1.165 - 2.713, n = 11, Figure 9B, C). To confirm the involvement of 5-HT_{1A}ARs in the action of trazodone, we applied the competitive and selective 5-HT_{1A} receptor antagonist Way-100635 (20 nM). As illustrated in Figure 9A and summarized in Figure 11, the firing rate recovered only partially (47.54 ± 21.41 %; n = 7).
This finding was in contrast with the full antagonism of trazodone effect by Way-100635 previously shown *in vivo* and suggested the possibility the antidepressant may inhibit neuronal firing through additional direct actions on serotonergic neurons or indirect action(s) via modification of the activity of surrounding neurons (e.g. GABA interneurons). Therefore, we designed a series of experiments directed to elucidate the nature of the additional inhibitory action exerted by trazodone.

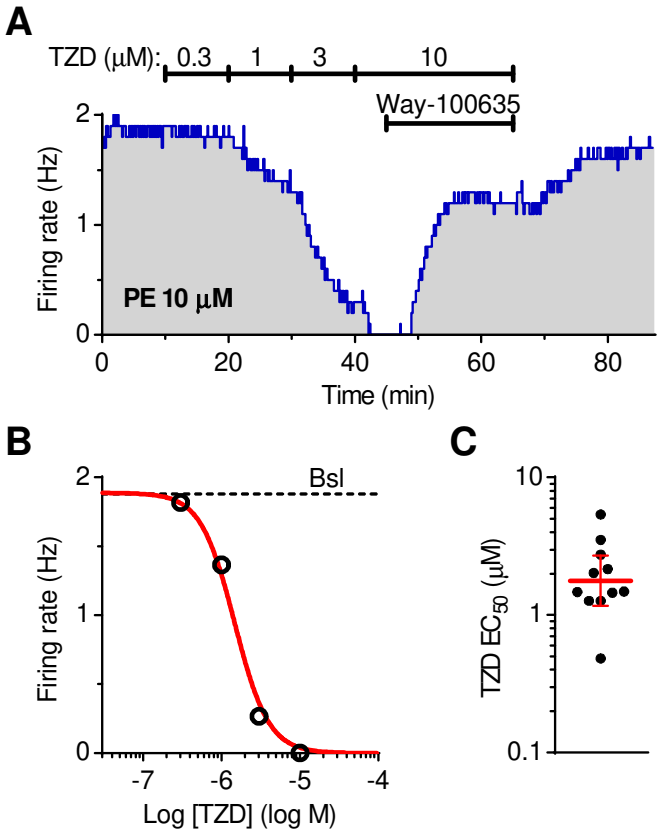

Figure 9. The inhibition of serotonergic neuron activity by trazodone in standard ACSF.
(A) Representative recording illustrating the time-course of the changes in firing frequency produced by increasing concentrations of trazodone (0.3 – 10 µM). TZD 10 µM produced the total inhibition (silencing) of serotonergic neuron firing rate before the competitive and selective 5-HT_{1A} receptor antagonist Way-100635 (20 nM) partially reversed it. **(B)** Dose-response curve (DRC) resulting from the experiment shown in **(A)**. Red line is the best least-squares fit to the logistic equation. TZD 0.3 µM does not produce an effect on serotonergic neuron firing rate and between 1 and 3 µM the least-square fit as maximal slope. Effect of 5-HT_{1A} receptor antagonist Way-100635 is not shown here. **(C)** Scatter plot of the individual EC_{50} values calculated from all experiments (n = 11).

Trazodone inhibits serotonergic neuron firing by more than one action.

To pharmacologically isolate the activity of serotonergic neurons from the action of the major neurotransmitters present in the raphe nuclei, in a second set of recordings we used ACSF supplemented with a "cocktail" of glutamate, GABA/glycine and adenosine A1 receptors blockers (*see methods*). In this set of experiments, trazodone still inhibited the activity of serotonergic neurons with an EC_{50} value of 1.77 µM (GM, 95% C.I.: 1.023 - 3.034, n = 11, Figure 10B, C). Interestingly, also in these experimental conditions Way-100635 (20 nM) only partially reversed inhibition of serotonergic neurons firing rate (45.93 ± 30.32 %; n = 6; Figure 10A and Figure 11B). These experiments excluded the possibility that modifications in the release of the

major neurotransmitters present in the raphe participate in the inhibitory effect of trazodone on the activity of recorded neurons.

Although we detected no obvious differences in the potency and efficacy of trazodone measured in standard ACSF and ACSF containing the mixture of antagonists, all the following experiments were performed using the "cocktail" ACSF.

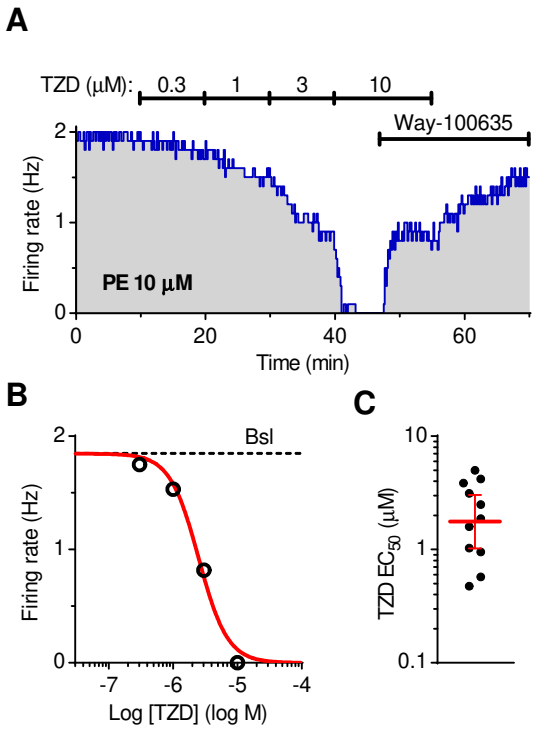

Figure 10. The inhibition of serotonergic neuron activity by trazodone in cocktail of synaptic blockers.

(A) Representative recording illustrating the time-course of the changes in firing frequency produced by increasing concentrations of trazodone (0.3 – 10 µM). TZD 10 µM produced the total inhibition (silencing) of serotonergic neuron firing rate before the competitive and selective 5-HT_{1A} receptor antagonist Way-100635 (20 nM) partially reversed it. Washout of TZD produced total recovery of serotonergic neuron firing rate. **(B)** Dose-response curve (DRC) resulting from the experiment shown in **(A)**. Red line is the best least-squares fit to the logistic equation. In cocktail, TZD 0.3 µM produces inhibition of serotonergic neuron firing rate higher, but not significantly different, then standard ACSF (data not shown). Between 1 and 3 µM the least-square fit as maximal slope. Effect of 5-HT_{1A} receptor antagonist Way-100635 is not shown here. **(C)** Scatter plot of the individual EC_{50} values calculated from all experiments (n = 11).

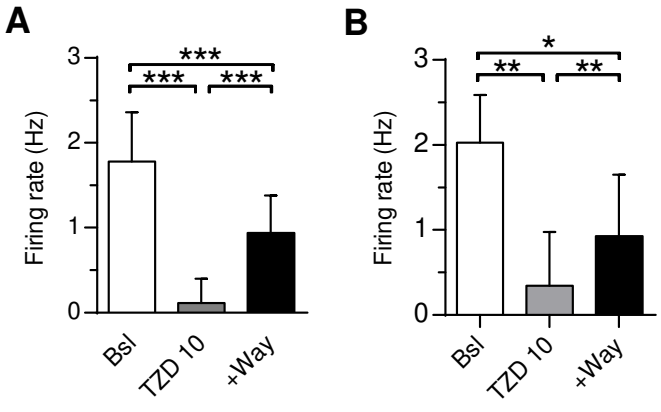

Figure 11. Antagonistic effect of Way-100635 on the inhibition of serotonergic neuron activity by trazodone in ACSF and ACSF-containing cocktail.
Antagonism of trazodone (10 µM) effect by Way-100635 (n = 6). In both ACSF **(A)** and ACSF-containing cocktail **(B)**, the activity of serotonergic neurons was facilitated by the presence of 10 µM phenylephrine. TZD produced significant inhibition of firing rate compared to Bsl, antagonized by Way-100635. Antagonism of Way-100635 was not complete. * $p < 0.05$; ** $p < 0.01$; *** $p < 0.005$; **** $p < 0.001$ (One-way RM ANOVA, followed by a Tukey *post-hoc* test).

Trazodone inhibits serotonergic neuron activity through stimulation of somatodendritic 5-HT$_{1A}$ autoreceptors.

The lack of full recovery of serotonergic neuron firing rate provided by Way-100635, could be explained by the inhibitory action on SERT exerted by trazodone. In fact, block of the serotonergic transporter provided by the antidepressant, could increase the extracellular concentration of endogenous serotonin, thus limiting Way-100635 antagonism of 5-HT$_{1A}$ARs. To investigate whether trazodone acted directly at 5-HT$_{1A}$ARs to inhibit firing rate or if the effect was indirectly mediated by the increase in extracellular serotonin, we designed a specific group of experiments in a mouse line lacking the gene for tryptophan-2-hydroxylase (Tph2$^{-/-}$ mice). As the Tph2$^{-/-}$ mice lack synthesis of brain serotonin, indirect effects of trazodone through a raise of extracellular serotonin would be prevented.
It should be noted that in this mouse line the sensitivity of 5-HT$_{1A}$ARs is higher than in wild-type mice and rats (Montalbano et al., 2015a; Montalbano et al., 2019).
In Tph2$^{-/-}$ mice, the dose-response curve for trazodone had an EC_{50} value of 0.66 µM (GM, 95% C.I.: 0.3157 – 1.364, n = 9; Figure 12C). When near maximal effect (96.1 ± 7.3 %) of trazodone was obtained with 1 µM concentration, the effect was fully antagonized by Way-100635. However, when higher concentration of trazodone were used (10 µM), the recovery of firing observed in the presence of Way-100635 was only partial (40.13 ± 6.74 %; n = 5, Figure 12B).

These experiments show that trazodone inhibits the firing of serotonergic neurons by direct activation of 5-HT_{1A}ARs and that an additional inhibitory effect of the drug contributes in silencing firing.

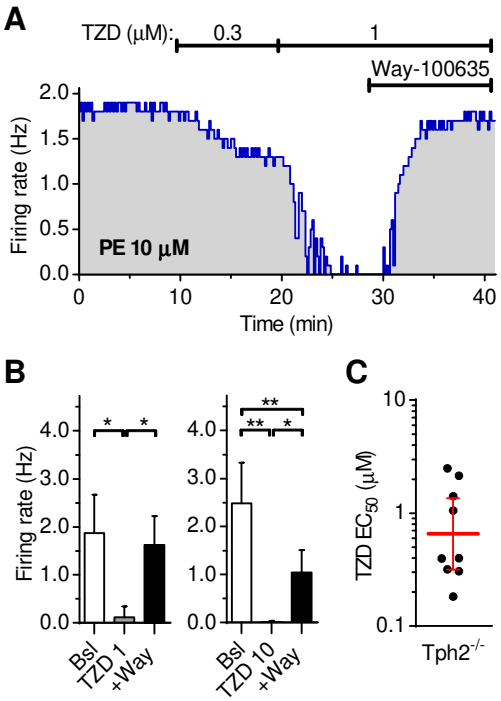

Figure 12.
Effect of trazodone in Tph2$^{-/-}$ mice.
(A) Representative recording of concentration-dependent effect of TZD facilitated by 10 μM PE. The effect was fully antagonized by 20 nM Way-100635. Note that concentrations used for TZD are only 0.3 and 1 μM compared to previous experiments in rats. The use of lower concentrations of TZD depends on higher sensitivity of 5-HT_{1A} receptors in Tph2$^{-/-}$ mice. In fact, compared to rats, TZD efficacy in inhibiting serotonergic neuron firing rate is higher. **(B)** Summary of the antagonism exerted by 20 nM Way-100635 (+Way) on responses to 1 μM (n = 4) and 10 μM (n = 5) trazodone. Note the partial antagonism of responses to 10 μM trazodone. **(C)** Scatter plot of the individual EC_{50} values calculated from all experiments (n = 9). Red line and error bars indicate the geometric mean and 95% C.I.* p < 0.05; ** p < 0.01 (One-way RM ANOVA, followed by a Tukey *post-hoc* test).

Trazodone acts as a α_1-adrenoceptor competitive antagonist.

It has been shown *in vivo* that trazodone may antagonize α_1-adrenoceptors in the hippocampus (Ghanbari et al., 2012). Since noradrenergic input to DRN facilitates the firing of serotonergic neurons, a decrease in the noradrenergic drive produced by α_1-adrenoceptor antagonism could account for the inhibition in the activity of serotonergic neurons produced by the antidepressant drug. Indeed, in our experiments the firing of serotonergic neurons was facilitated by the presence of 10 μM PE, and therefore the non 5-HT_{1A} receptor-mediated effect of trazodone could result from α_1-adrenoceptor antagonism with consequent disfacilitation of neuron firing and not from a direct inhibitory action of the drug on neuron rhythmicity.
Thus, in rat DRN slices we tested if the inhibitory effect of trazodone on serotonergic neuron activity could fully be antagonized by Way-100635 in the absence of α_1-adrenoceptor stimulation. As in the absence of PE serotonergic neurons are almost silent, in these experiments the basal firing was facilitated by lowering Ca^{2+} concentration in the ACSF (*see methods*). As shown in Figure 13, under these

conditions 20 nM Way-100635 fully antagonized the effect of trazodone concentrations (10 μM) indicating a possible interaction of trazodone with α_1-adrenoceptors.

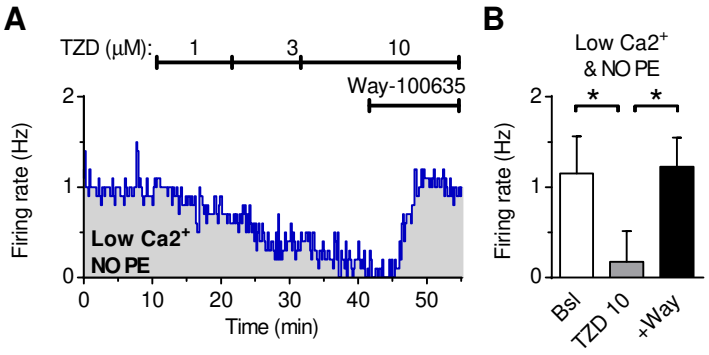

Figure 13. Antagonism at 5-HT$_{1A}$ARs by trazodone contributes in the inhibition of serotonergic neuron activity in the absence of phenylephrine.
(A) Representative recording of the concentration-dependent effect of trazodone on neuron activity facilitated by low calcium ACSF in the absence of PE. The lack of α_1-adrenoceptor activation, shows the inhibitory effect of TZD at 5-HT$_{1A}$ARs. The inhibition is fully antagonized by Way-100635 20 nM. **(B)** Summary of five experiments (mean ± SD). * p< 0.05 (One-Way RM ANOVA followed by Tukey post-hoc test).

To confirm the interaction of trazodone with α_1-adrenoceptors we tested the effects of the drug on neurons whose activity was facilitated by a low concentration of PE (1 μM) in the presence of Way-100635 to block the 5-HT$_{1A}$ receptor-mediated component of trazodone actions.
Under these conditions, trazodone 10 μM silenced serotonergic neuron firing rate and the effect was reversed and surmounted (Figure 14) by increasing the concentration of PE (100 μM), suggesting a competitive antagonism at α_1-adrenoceptors by trazodone.

To better characterize the contribution of α_1-adrenoceptor antagonism in the inhibition of serotonergic neuron firing by trazodone, we compared the concentration-dependent effect of trazodone in preparations where the firing was facilitated by different concentrations of PE (1, 10, 100 μM) in the presence of 20 nM Way-100635 to block the 5-HT$_{1A}$ receptor-mediated effect of trazodone (Figure 15A, D, G).

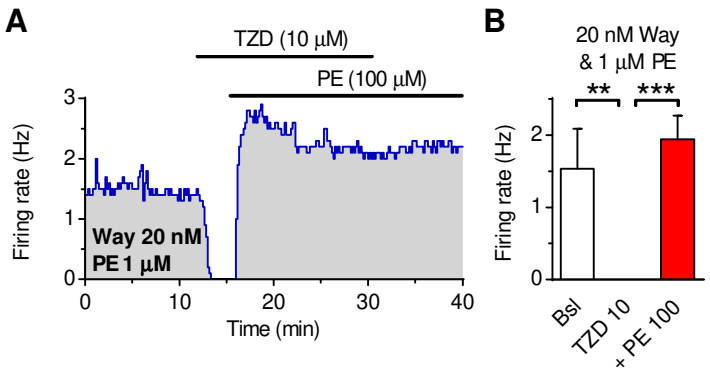

Figure 14. Antagonism at α_1-adrenoceptors by trazodone contributes in the inhibition of serotonergic neuron activity.

(A) Representative recording of neuron activity facilitated by 1 µM PE in the presence of Way-100635 (20 nM). The inhibitory effect of 10 µM trazodone is surmounted by addition of 100 µM PE, suggesting that TZD exerts a competitive antagonism on α_1-adrenoceptors compared to full agonist PE. This effect, together with the activation of 5-HT_{1A}ARs, is responsible of serotonergic neuron firing rate inhibition. **(B)** Summary of five experiments (mean ± SD). ** $p< 0.01$; *** $p< 0.005$(One-Way RM ANOVA followed by Tukey *post-hoc* test).

In PE 1 µM, trazodone concentration-dependently suppressed neuron firing with an average EC_{50} value of 1.985 µM (GM, 95% C.I.: 1.451 – 2.716, n = 15; Figure 15C). When neurons were activated by PE 10 µM the average EC_{50} value was increased to 9.881 µM (GM, 95% C.I.: 7.284 – 13.40, n = 11; Figure 15F) in PE 10 µM. In the experiments in which neuron activity was facilitated by 100 µM PE, we used only 10 and 30 µM trazodone to avoid aspecific effects of the drug. Thus, individual EC_{50} values could not be calculated from this set of experiments (n = 9) because of low number of points for fitting responses from single neurons. Nevertheless, the mean effects for these two drug concentrations were sufficient to obtain the EC_{50} value for trazodone effect in 100 µM PE (39.07 µM) from the calculated average concentration-response curve.

Figure 15H shows comparison of the concentration-response curves of the inhibitory effect of trazodone obtained in different concentrations of PE with 5-HT_{1A}ARs blocked. The rightward shift of the inhibitory effect of trazodone produced by increasing the concentration of the agonist phenylephrine confirmed that the action of trazodone was due to competitive antagonism at α_1-adrenoceptors of serotonergic neurons.

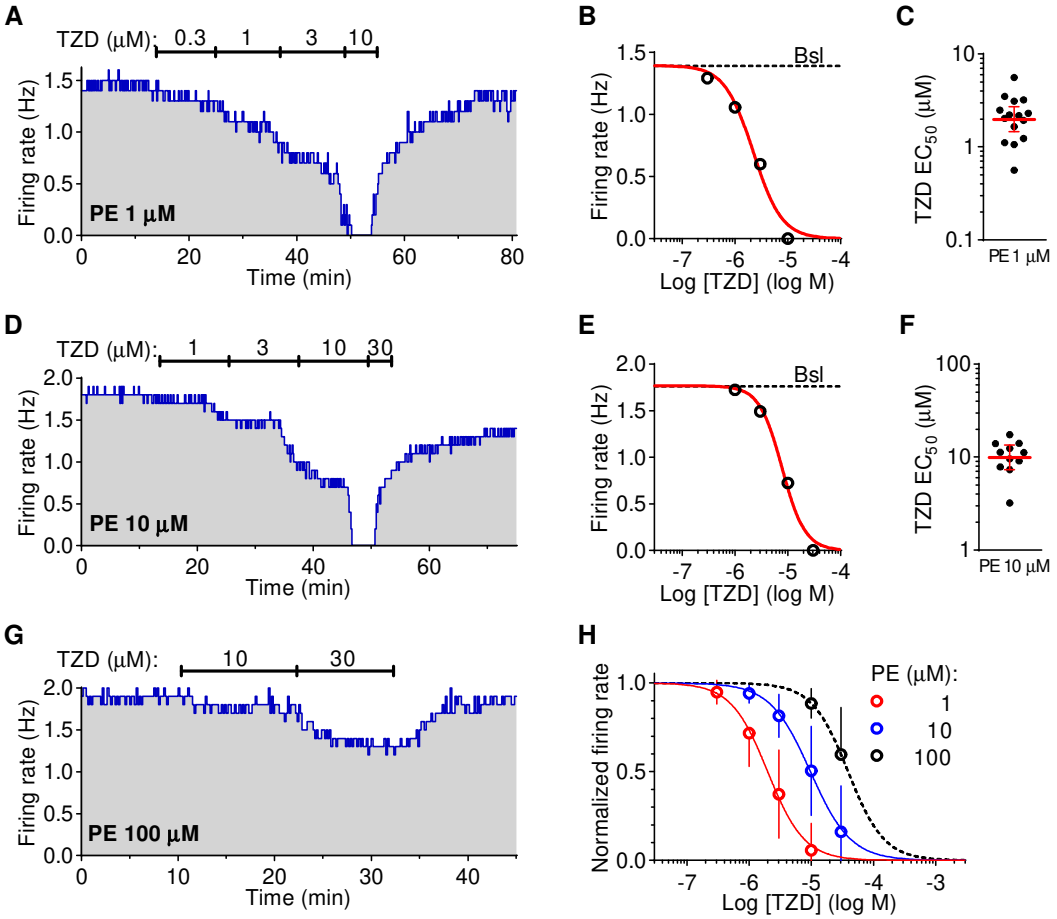

Figure 15. Block of 5-HT$_{1A}$ARs by Way-100635 uncovers the α_1-adrenoceptor- dependent effect of trazodone.

(A) Representative experiment showing the effect of TZD on neuron firing facilitated by 1 μM PE in the presence of Way-100635 (20 nM). **(B)** DRC resulting from the experiment shown in **(A)**. Red line is the best least-squares fit to the logistic equation. **(C)** Scatter plot of the individual EC_{50} values calculated from fifteen similar experiments. **(D)** Representative experiment showing the effect of trazodone on neuron firing facilitated by 10 μM PE **(E)** DRC resulting from the experiment shown in **(D)**. Red line is the best least-squares fit to the logistic equation. Note that 30 μM trazodone is required to silence the neuron. **(F)** Scatter plot of the individual EC_{50} values calculated from eleven experiments. **(G)** Representative recording from a set of experiments (n = 9) in which trazodone 10 μM and 30 μM was applied in the presence of 100 μM PE. In **(B)** and **(E)**, dotted line indicates the baseline (Bsl) firing rate before application of trazodone. In **(C)** and **(F)**, red line and error bars indicate the geometric mean and 95% C.I. **(H)** Average DRCs of trazodone inhibition of serotonergic neuron firing rate obtained from the experiments in PE 1 - 100 μM. The potency of TZD depends on the concentration of PE, underlying the competitive antagonist at α_1-adrenoceptors dependent from noradrenergic activation. Symbols and error bars correspond to the mean values ± SD obtained for each concentration in the corresponding set of experiments. Red line is the best least-squares fit to the logistic equation. Data are normalized on average baseline firing rates recorded before trazodone application. The baseline firing rates of neurons recorded in the three groups were (Hz, mean ± SD): 1.840 ± 0.5444 in PE 1 μM (n = 15), 1.766 ± 0.4040 in PE 10 μM (n = 11) and 1.970 ± 0.5559 in PE 100 μM (n = 9). These values were not significantly different ($F_{(2.32)}$ = 0.4046; p = 0.6706; One-Way ANOVA).

Effects of trazodone at 5-HT$_{1A}$ receptors when its action through α$_1$-adrenoceptors is minimized by the presence of high phenylephrine concentration.

Based on the experiments shown in Figure 15G, H, in the presence of PE 100 µM the contribution of α$_1$-adrenoceptor antagonism in the overall inhibitory effect at concentrations of trazodone up to 10 µM was small (12 ± 8% *see* Figure 15G). We therefore sought to evaluate the potency of trazodone in suppressing serotonergic neuron firing through 5-HT$_{1A}$AR stimulation in these conditions (i.e. in PE 100 µM) in which the α$_1$-adrenoceptor antagonism by the drug was minimized.
As shown in Figure 16A and 16B, trazodone inihibited the activity of neurons in a concentration-dependent manner and the effect was completely antagonized by the addition of Way-100635 (20 nM; Figure 16A and 16E).

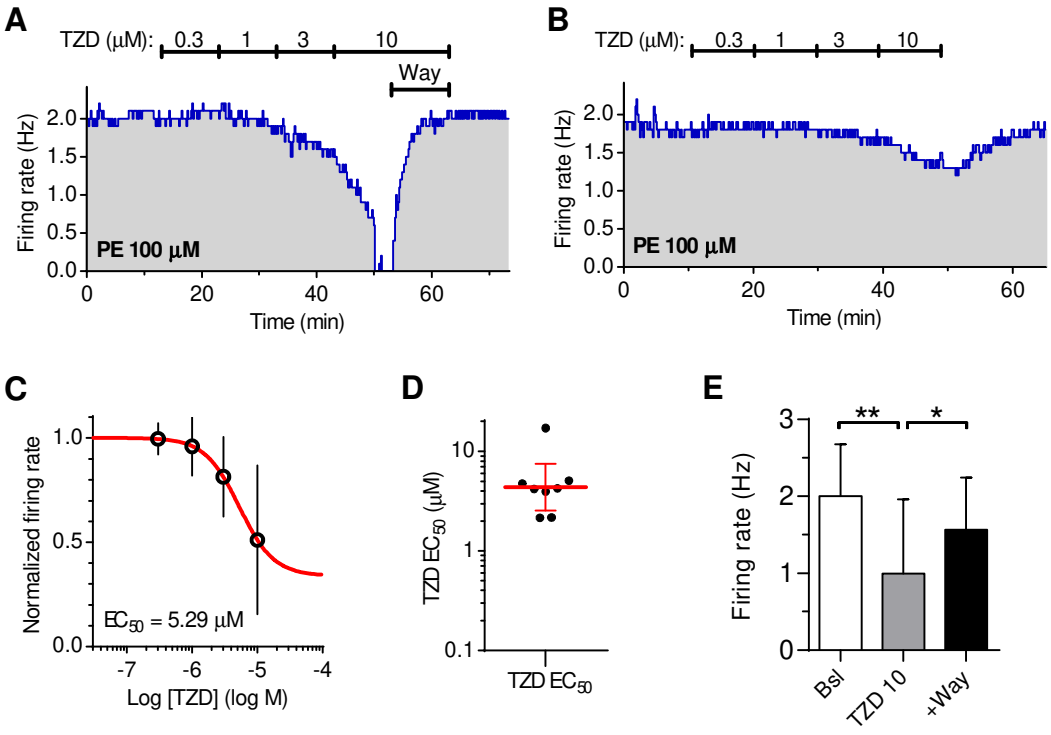

Figure 16. Activation of 5-HT$_{1A}$ARs by trazodone in high phenylephrine.
(A, B) Representative recordings of potent **(A)** and weak **(B)** trazodone effects on serotonergic neuron firing in the presence of 100 µM PE. Note that TZD effect in **(A)** was fully antagonized by 20 nM Way-100635 (Way), whereas in **(B)** the effect of TZD was very weak and did not require Way-100635. **(C)** Average DRC obtained from all the experiments (n = 11). **(D)** Summary scatter plot of individual EC$_{50}$ values from experiments in which complete DRC were obtained (n = 8). Data are normalized on Bsl firing rate. Red line is the best least-squares fit to the logistic equation. Symbols and error bars report the mean value ± SD. **(E)** Summary of the antagonism of Way-100635 on trazodone 10 µM (mean ± SD; n = 7). *p< 0.05, **p< 0.01 (One-Way RM ANOVA followed by a Tukey *post-hoc* test).

The average dose-response relationship calculated on the mean response of nine experiments, is reported in Figure 16C. In eight neurons in which individual EC_{50} could be calculated the average EC_{50} value was of 4.365 μM (GM, 95% C.I.: 2.553–7.466, n = 8; Figure 16D). Notably, the curve shown in Figure 16C suggested that the agonism of trazodone at 5-HT_{1A}ARs was partial. Nevertheless, due to the residual interference of α_1-adrenoceptor antagonism by trazodone at concentrations > 10 μM the efficacy of the drug at 5-HT1AARs was impossible to be reliably quantified.

Whole cell recordings of 5-HT_{1A} receptor-mediated GIRK activation.

To clarify whether trazodone was a partial agonist, we investigated the potency and the functional effect of trazodone at 5-HT_{1A}ARs of rat DRN serotonergic neurons recorded in whole-cell configuration. To this purpose, we measured the changes in slope conductance of 5-HT_{1A} receptor-coupled GIRK channels, which provided a direct measure of 5-HT_{1A} receptor activation produced by the application of trazodone. Notably, these experiments were performed in the absence of α_1-adrenoceptor activation by PE.

5-CT has the same efficacy of serotonin in activating 5-HT_{1A} autoreceptors.

In a first set of experiments we confirmed that the maximal response to 5-CT was similar to that of serotonin and greater than that of the prototypical 5-HT_{1A} receptor partial agonist buspirone (Figures 17, 18).
As shown in Figure 17A, application of serotonin (1 - 30 μM) produced a concentration-dependent increase in GIRK channel conductance that was maximal at 10 μM (EC_{50} value: 2.275 μM, Geometric mean, 95% C.I.: 1.8 – 2.875; Log EC_{50} = -5.66 ± 0.0397, log M ± SD; n = 4).
Comparison of the maximal GIRK channel activation by serotonin (10 μM) and 5-CT (30 nM, Montalbano et al., 2015a) in the same serotonergic neurons showed that 5-CT produced an effect similar to serotonin (106.8 ± 11.85 %, n = 5; P= 0.2717, one sample t test P = 0.4375; Figure 17C). The steady-state values of 5-HT_{1A} receptor-activated conductance (nS) produced by the two agonists in five neurons were not significantly different: serotonin 5.796 ± 1.586, 5-CT 6.251± 2.044 (Mean ± SD; n = 5; P = 0.1996, Paired t test, two-tailed P = 0.1875).

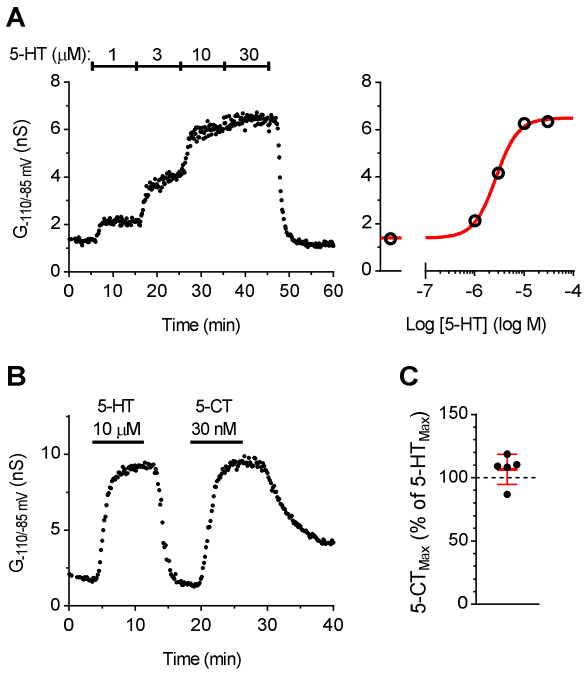

Figure 17. 5-CT is a full agonist at 5-HT$_{1A}$ARs.
(A) *Left panel*: Representative DRC of increasing concentrations of bath-applied 5-HT on GIRK conductance ($G_{-110/-85\ mV}$) in a dorsal raphe serotonergic neuron. The increasing extracellular concentration of 5-HT provides a higher activation of 5-HT$_{1A}$ARs directly correlated with GIRK activity. *Right panel*: 5-HT concentration-response relationship of the same experiment. The red line is the best least squares fit to four parameter logistic equation. **(B)** Time-course of a representative experiment performed to compare the efficacy of 30 nM 5-CT with that of 10 μM 5-HT on GIRK conductance ($G_{-110/-85\ mV}$) in a dorsal raphe serotonergic neuron. 5-CT is confirmed as a full agonist of 5-HT$_{1A}$ARs, with the same efficacy of 5-HT, although with different potency. **(C)** Scatter plot summarizing the comparison of maximal responses produced by 5-CT (5-CT$_{Max}$) with that by 5-HT (5-HT$_{Max}$) in the same neuron (n = 5). Bars correspond to mean ± SD.

After establishing that 5-CT is full agonist at 5-HT$_{1A}$ARs, we compared the efficacy of buspirone with that of the full agonist 5-CT to ensure that in our conditions the sensitivity of the method was able to discriminate between a full agonist and a partial agonist. We have chosen buspirone for this test because this compound is a prototypical partial agonist at the 5-HT$_{1A}$ receptors and, in addition, is therapeutically used as anxiolytic.

Buspirone (10 nM - 3 μM) produced a concentration-dependent response (Figure 18A, EC_{50} value: 56.67 ± 7.68 nM, mean ± SD; n = 3) reaching the maximal response at 300 nM. Then, the efficacy of buspirone was assessed by comparing its maximally effective concentration (300 nM) with that of the full agonist 5 CT (30 nM) on 5-HT$_{1A}$AR-mediated activation of GIRK channels in the same neuron (Figure 18B). From the peak effects produced by buspirone and 5-CT (3.490 ± 1.108 vs 5.218 ± 1.349 nS; mean ± SD, P= 0.0003, Paired t test, two-tailed P=0.0156, n = 7). the

calculated average efficacy of buspirone compared to 5-CT was 66.7 ± 9.0 % (mean ± SD; Figure 18C).

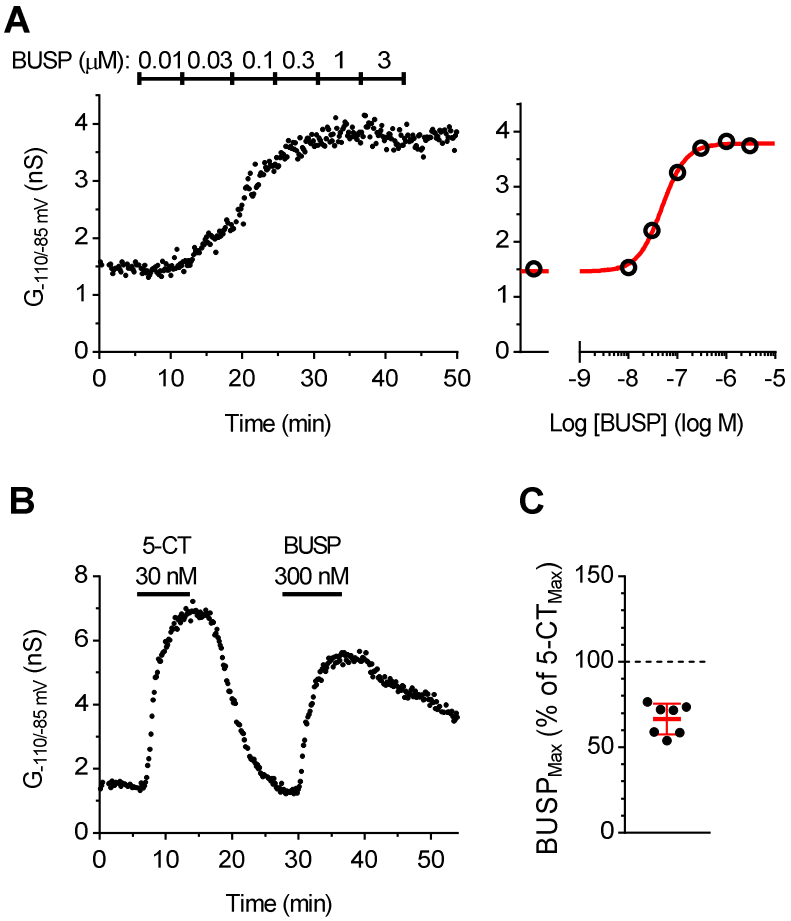

Figure 18. Buspirone is a partial agonist at 5-HT$_{1A}$ receptors.
(A) *Left panel*: Representative DRC of increasing concentrations of bath-applied 5-HT$_{1A}$ receptor partial agonist buspirone (BUSP) on GIRK conductance ($G_{-110/-85\ mV}$) in a dorsal raphe serotonergic neuron. The increasing extracellular concentration of BUSP (0.01 – 3 μM) provides a higher activation of 5-HT$_{1A}$ARs directly correlated with GIRK activity. The effect persisted also after wash. *Right panel*: 5-HT concentration-response relationship of the same experiment. The red line is the best least squares fit to four parameter logistic equation. Between 0.1 and 0.3 μM the least-square fit as maximal slope. **(B)** Time-course of a representative experiment performed to compare the efficacy of 300 nM BUSP with that of 30 nM 5-CT on GIRK conductance ($G_{-110/-85\ mV}$) in a dorsal raphe serotonergic neuron. BUSP is confirmed as a partial agonist of 5-HT$_{1A}$ARs, with lower efficacy than 5-CT. **(C)** Scatter plot summarizing the comparison of maximal responses produced by BUSP ($BUSP_{Max}$) with that by 5-CT ($5\text{-}CT_{Max}$) in the same neuron (66.56 ± 9.012, mean ± SD, n = 7). Bars correspond to mean ± SD.

These results show that 5 CT acts as full agonist at 5-HT$_{1A}$ARs and activates maximal GIRK conductance in serotonergic neurons confirming the reliability of 5-CT as a comparator for quantitative estimation of trazodone efficacy in our experimental conditions. Furthermore, the comparison between buspirone and 5-CT resulted in an

efficacy value for buspirone similar to that previously reported by Katayama and Colleagues (Katayama et al., 1997) and confirmed that our recordings were able to discriminate a full agonist from a partial agonis.

Trazodone activates 5-HT$_{1A}$ receptor-mediated GIRK conductance.

As illustrated in Figure 19A, the concentration-dependent effect of trazodone (1 - 30 μM; n = 12) was maximal at 30 μM and was reversed by the application of the selective 5-HT$_{1A}$ receptor antagonist Way-100635. In nine out of twelve recorded neurons, the magnitude of the concentration-dependent increases in GIRK channel conductance permitted reliable fitting of data in individual concentration-response curves. In the remaining three neurons the effect was too small to enable fitting (e.g. Figure 19B) and only the response to 30 μM trazodone was retained for analyses. Thus, the magnitude of responses to 30 μM trazodone ranged from 0.01 to 5.89 nS (1.67 ± 1.56; n = 12; Figure 19C). The average EC$_{50}$ value for GIRK channel opening by trazodone obtained from individual neurons was 3.34 μM (Geometric mean, 95% C.I.: 2.21 – 5.06; n = 9; Figure 19D). In Figure 19E, the standard deviation of the mean concentration-response curve obtained from fitting the values from all the experiments (n = 12) illustrates the variability of 5-HT$_{1A}$ receptor-mediated responses produced by trazodone over the range of concentrations tested.
In current clamp recordings, performed in the presence of 20 nM Way-100635 to mask the 5-HT$_{1A}$ receptor-mediated response, 30 μM trazodone did not significantly change resting membrane potential (66.8 ± 8.1 mV vs 70.1 ± 5.9 mV in control; n = 4; p = 0.061, paired t test; *data not shown*) and membrane input resistance (834.8 ± 280.9 MΩ vs 793.3 ± 285.2 MΩ in control; n = 4 p = 0.301, paired t test; *data not shown*). Altogether, these results show that trazodone is a competitive agonist at 5-HT$_{1A}$ARs, albeit with variable efficacy, and does not produce non-5-HT$_{1A}$ receptor-mediated additional direct changes in the excitability of serotonergic neurons.

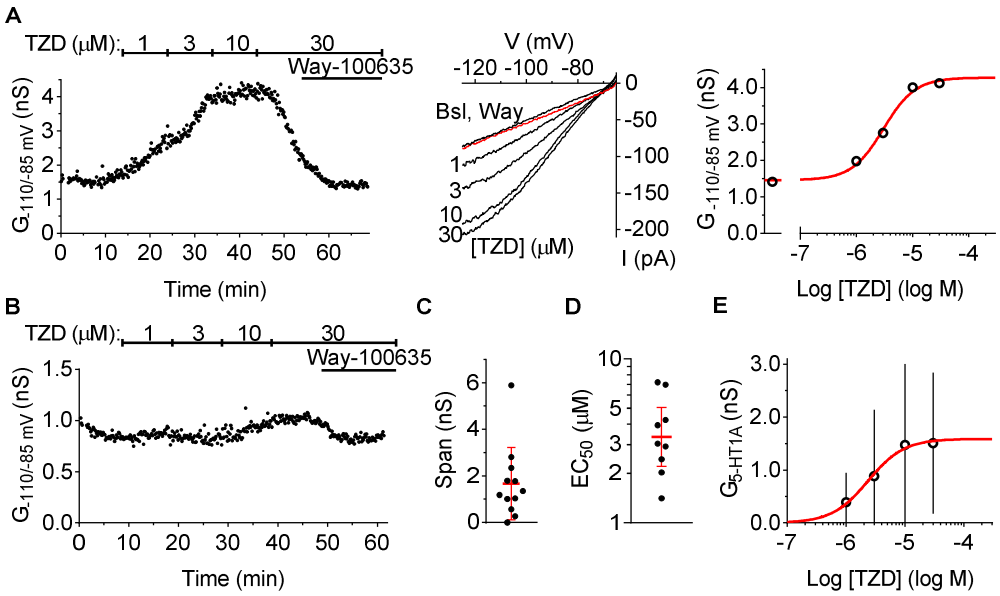

Figure 19. Concentration-response relationship for 5-HT$_{1A}$ receptor-mediated activation of GIRK conductance by trazodone.

(A) *Left panel*: Time-course of a representative experiment showing the effect of increasing concentrations of bath-applied TZD on GIRK conductance ($G_{-110/-85\ mV}$) in a dorsal raphe serotonergic neuron. $G_{-110/-85\ mV}$ was measured as the slope conductance activated in the range from -110 to -85 mV membrane potential by hyperpolarizing ramps under whole-cell voltage-clamp (see methods). Application of the selective 5-HT$_{1A}$ receptor antagonist Way-100635 (20 nM) reveals the 5-HT$_{1A}$ receptor-mediated component of the response. Time indicates duration of whole-cell configuration. *Middle panel*: Current-voltage plot of the same experiment. Traces are averages of the last 7 individual ramps recorded before trazodone application (Bsl); at the indicated trazodone concentrations and following the co-application of Way-100635 (20 nM; Way; red trace). *Right panel*: concentration-response relationship of the same experiment. The red line is the best least squares fit to four parameters (variable slope) logistic equation. **(B)** Time-course of an experiment illustrating a very weak effect of trazodone in a subset (3 out of 12) of neurons for which only maximal effect was determined. **(C)** Scatter plot showing the maximal trazodone effect in all 12 neurons. Bars correspond to mean ± SD. **(D)** Scatter plot of EC_{50} values of trazodone in individual neurons. Note the ordinate in logarithmic scale. Bars correspond to geometric mean ± 95% C.I. **(E)** Average concentration-response curve for activation of GIRK conductance by trazodone in all 12 neurons. Data are normalized such that baseline conductance equals zero and thus correspond to net 5-HT$_{1A}$ receptor-activated GIRK conductance ($G_{5\text{-}HT1A}$). The red line is the best least squares fit to four parameters (variable slope) logistic equation. Extracellular solution contained 5.5 mM K^+ and a mix of synaptic blockers (see methods). Error bars represent mean ± SD.

Trazodone is a weak partial agonist at 5-HT$_{1A}$ autoreceptors.

To quantify the efficacy of trazodone at 5-HT$_{1A}$ARs, we compared the effect of the maximally active concentration of trazodone with that of 5-CT.

In all recordings in which 5-CT (30 nM) and trazodone (10 μM) were applied in the same neurons the application of 5-CT produced an increase in GIRK channel conductance greater than that of trazodone (n = 14; Figure 20), which occasionally

was very small (n = 3). From the peak effects produced by trazodone and 5-CT (1.43 ± 1.29 nS and 3.85 ± 1.89 nS, respectively, n = 14; Figure 20B) the calculated average efficacy of trazodone compared to 5-CT was 35.3 %, Figure 20C). To confirm these findings in a larger number of neurons and to further ensure that the application of 5-CT in the same neuron did not change the sensitivity to trazodone action at 5-HT_{1A}ARs, we compared the response to single applications of 5-CT and trazodone in different neurons.

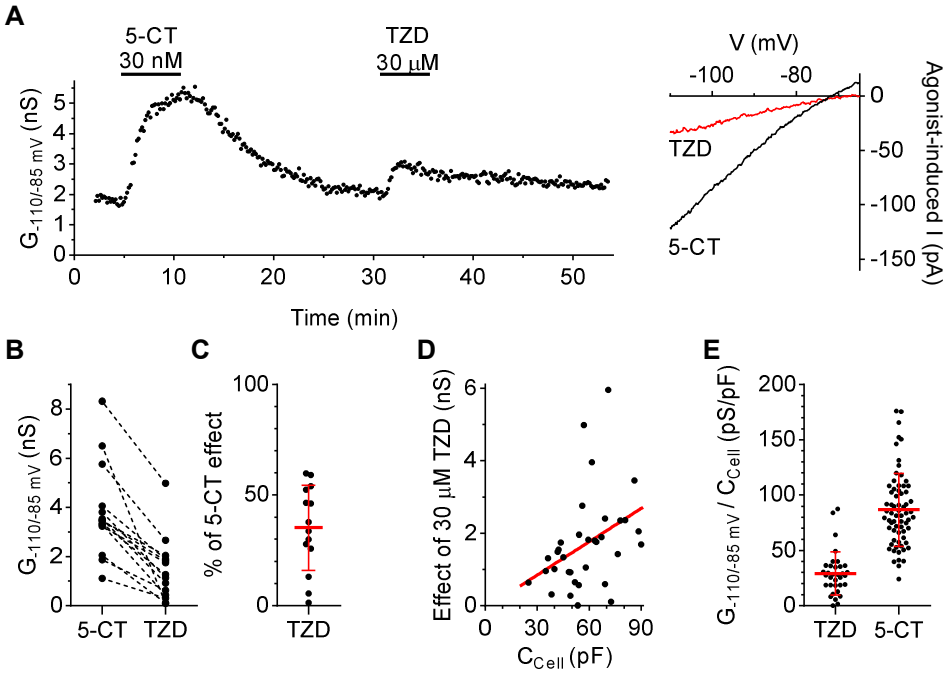

Figure 20. Trazodone is a partial agonist at 5-HT_{1A} receptors.
(A) *Left panel*: Time-course of a representative experiment performed to compare the maximal effect of TZD (30 µM) with that of the full agonist 5-CT (30 nM) on GIRK conductance ($G_{-110/-85\ mV}$) in a dorsal raphe serotonergic neuron. *Right panel*: Current-voltage plot of agonist-induced currents of the same experiment. Each trace is the difference between current in the presence of the indicated agonist (average of 7 individual ramps) and control current recorded before the agonist application (average of 7 - 13 individual ramps). **(B)** Comparison of 30 µM trazodone and 30 nM 5-CT effects in individual neurons. **(C)** Scatter plot summarizing the extent of trazodone partial agonism in individual recordings (100 x $G_{-110/-85\ mV,\ TZD}$ / $G_{-110/-85\ mV,\ 5\text{-}CT}$). Bars correspond to mean ± SD. **(D)** The correlation between the effect of 30 µM trazodone ($G_{-110/-85\ mV}$) and the cell membrane capacitance (C_{Cell}). Symbols represent single experiments (n = 34). Red line represents best least square fit. Correlation analysis revealed moderate positive correlation (Pearson r = 0.38, p = 0.026) indicating that larger neurons had a higher number of activated GIRK channels. **(E)** Comparison of 30 µM trazodone (n = 34) and 30 nM 5-CT (n = 68) effects in serotonergic neuron population. Data are normalized for cell membrane capacitance. Symbols represent the response of individual neurons to the first application of any 5-HT_{1A} receptor agonist in the experiment. Bars correspond to mean ± SD.

As the magnitude of GIRK conductance responses to trazodone appeared correlated to cell membrane capacitance (Figure 20D) which reflects the surface area of recorded

neurons, the effects of trazodone and 5-CT were normalized to the membrane capacitance to correct for differences in cell size and density of GIRK channels in different neurons. The maximal trazodone effect was 29.12 ± 19.63 (pS/pF; n = 34) and resulted significantly smaller compared to that produced by 5-CT (86.68 ± 33.12 pS/pF; n = 68, p < 0.0001, unpaired t test; Figure 20E). The resulting mean efficacy of trazodone was of 33.6 % compared to that of 5-CT, a value very similar to that found when the two compounds were applied in the same neurons.

The effect of trazodone was fully reversible since the response to 5-CT applied after wash from trazodone was similar to that produced by the first 5-CT challenge (Figure 21).

These experiments also indicate that the weaker activation of 5-HT$_{1A}$ARs by trazodone compared to 5-CT was not due to desensitization of the receptors induced by the agonist. The response to the second application of 5-CT after a brief wash from trazodone was slightly smaller than the first before trazodone, but not significantly different (90.78 ± 16.29 %; n = 4; p = 0.37; Figure 21B).

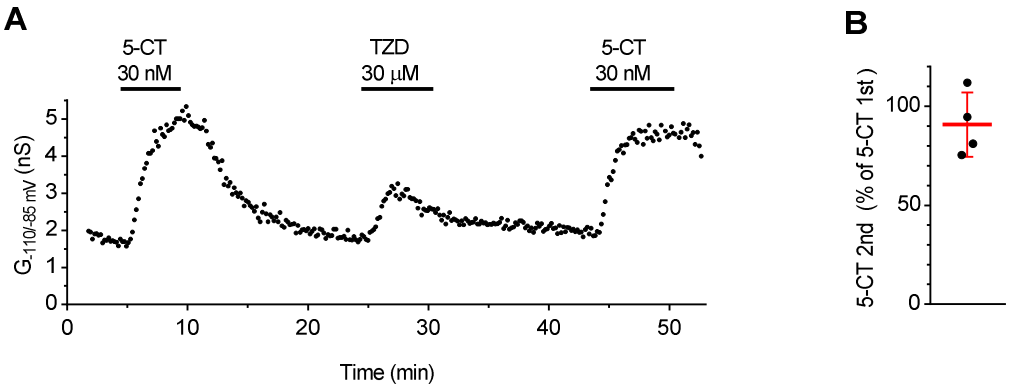

Figure 21. Trazodone is a partial agonist at 5-HT$_{1A}$ receptors.

(A) *Left panel*: A representative recording showing that the weak effect of trazodone was not due to acute desensitization of 5-HT$_{1A}$ARs. Note that the response to 30 nM 5-CT applied after 15 min of trazodone washout is similar to the first response to 5-CT. This indicates that TZD acts as a partial agonist mediating 5-HT$_{1A}$ receptor GIRK activation. **(B)** Scatter plot of the response to a second application of 5-CT (5-CT 2nd) normalized to that produced by the first application of 5-CT (5-CT 1st) in four neurons (91 ± 16 %, n = 4; p = 0.37, Wilcoxon signed rank test). Bars correspond to mean ± SD.

The weak partial agonist trazodone antagonizes 5-CT action at 5-HT$_{1A}$ autoreceptors.

The weak efficacy of trazodone suggested that the drug could exert a substantial competitive antagonism of the response to the full agonist 5-CT. We therefore compared the response to 10 nM 5-CT applied alone or in the presence of 10 µM trazodone. We have chosen submaximal concentrations of the two drugs so that eventual summation of the two effects could be revealed.

As illustrated in Figure 22, from the peak effects produced by 5-CT alone or in the presence of trazodone (4.21 ± 1.66 vs 2.42 ± 1.29 nS; $n = 5$; $p = 0.0026$, paired t test) the total activation of the GIRK conductance resulting by coapplication of 5-CT and trazodone was smaller than that measured when 5-CT was applied alone in the same neurons (54.8 ± 11.4 %, $n = 5$, Figure 22B,C).
These results show that trazodone can effectively act as an antagonist and is able to significantly decrease the activation of 5-HT_{1A}ARs by the full agonist 5-CT.

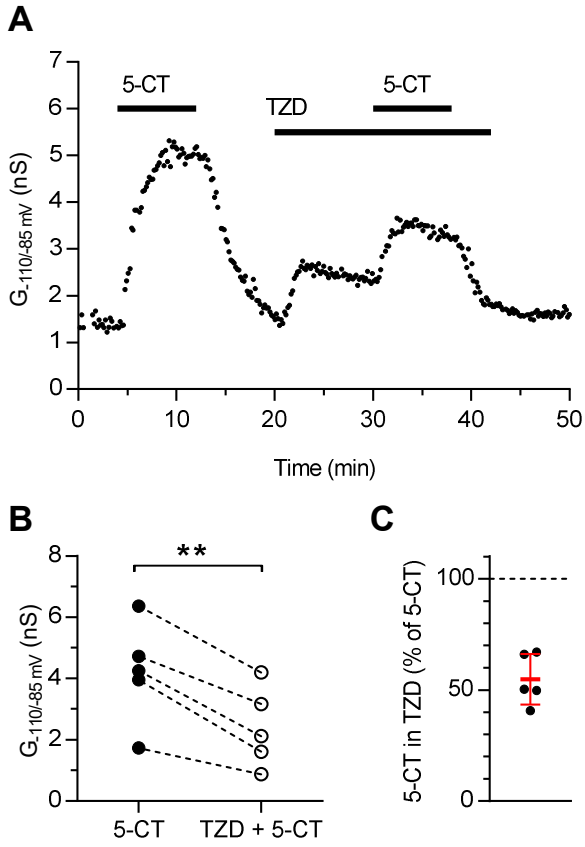

Figure 22. Quantification of partial antagonism at 5-HT_{1A}ARs by trazodone.
(A) Time-course of a representative experiment in a dorsal raphe serotonergic neuron showing that the total activation of the GIRK conductance ($G_{-110/-85\ mV}$) produced by 10 nM 5-CT in the presence of 10 µM trazodone is smaller than that measured when 5-CT is applied alone. **(B)** Comparison of 10 nM 5-CT effects in control and in the presence of 10 µM trazodone in individual neurons. ($n = 5$; $p = 0.0026$, Paired T-Test). **(C)** Scatter plot summarizing the partial antagonism of 5-CT effect exerted by trazodone at 5-HT_{1A}ARs in five experiments. Values are calculated on net 5-HT_{1A} receptor-activated GIRK conductance obtained from data shown in **(B)** after baseline conductance subtraction. Bars correspond to mean ± SD.

In order to confirm that trazodone can reversibly antagonize the action of the full agonist 5-CT we measured the effect of the addition of trazodone in the presence of 5-CT. In these experiments (n = 3) we used maximal concentrations of both drugs. The

increase in recorded serotonergic neuron GIRK slope produced by 30 nM 5-CT, was reduced during the application of 30 μM trazodone and substantially, albeit not completely, recovered upon wash of trazodone (Figure 23).

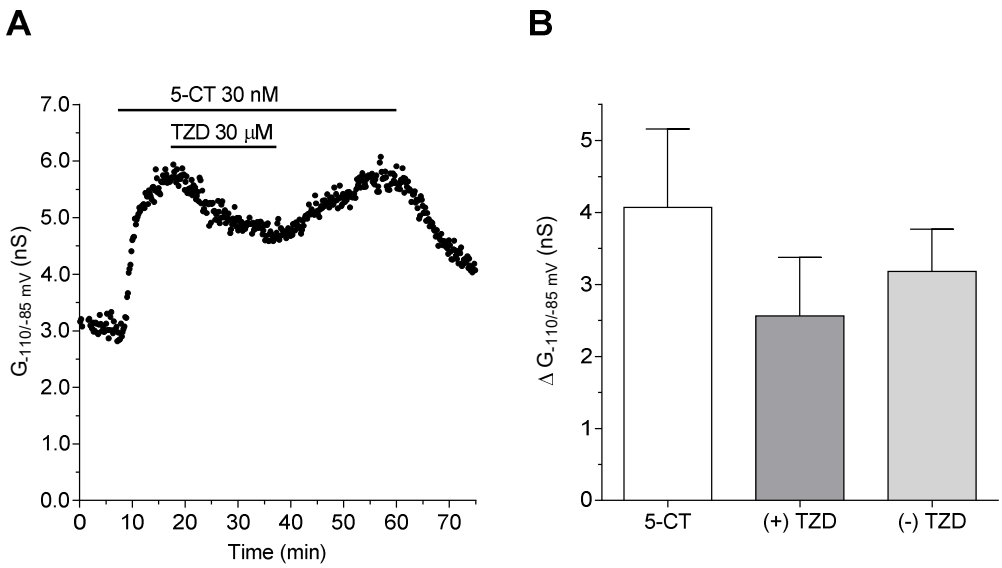

Figure 23. Trazodone is antagonist of 5-CT effect at 5-HT$_{1A}$ receptor-mediated GIRK activation. **(A)** Time-course of a representative experiment in a dorsal raphe serotonergic neuron showing that the total activation of the GIRK conductance ($G_{-110/-85\ mV}$) produced by 30 nM 5-CT. Application of TZD (30 μM) partially blocked 5-CT GIRK activation, confirming TZD as a partial agonist to 5-HT$_{1A}$ARs and antagonist of the full agonist 5-CT. **(B)** Comparison of 30 nM 5-CT effects in control and in the presence of 30 μM trazodone in individual neurons. (n = 3).

Collectively the results shown in Figures 22 and 23 confirm that, due to its weak partial agonist property at 5-HT$_{1A}$ receptors, trazodone can competitively and reversibly antagonize the action of a full agonist at 5-HT$_{1A}$ARs.

Discussion:

For more than fifty years depressed patients have been treated with medicines that decrease the symptoms of depression. However, for all the antidepressant drugs in use the mechanisms responsible for their therapeutical action remain only partially known. Nevertheless, it becomes increasingly accepted that the presence of further pharmacological actions in addition to the inhibition of serotonin and/or noradrenaline re-uptake may contribute to the safety or therapeutic profile of individual compounds that have been grouped in the class of "multimodal" antidepressant drugs (Stahl, 2009a; Sanchez et al., 2015).

Among these substances, trazodone exerts a combined action on both serotonergic and noradrenergic systems which is believed to contribute to the drug pharmacological profile of antidepressant and sleep facilitator (Stahl, 2009b; Fagiolini et al., 2012).

Trazodone binds at different receptors expressed by serotonergic neurons of DRN (Cusack et al., 1994; Owens et al., 1997), thus better knowledge of its effects through these receptors becomes important for interpreting the possible actions that concur in a therapeutic profile that encompasses sleep facilitation in addition to antidepressant effect. In particular, knowledge of the efficacy of trazodone at 5-HT_{1A}ARs becomes important because it has been proposed that co-administration of a 5-HT_{1A} receptor antagonist or partial antagonist with an SSRI may promote a faster onset of therapeutical action (Artigas et al., 2018). Moreover, trazodone shows a considerable binding affinity to α_1-adrenoceptors for which it is antagonist (Owens et al., 1997; Giannangeli et al., 1999; Krege et al., 2000; Betti et al., 2002), but the effectiveness of trazodone in antagonizing α_1-adenoceptors in the central nervous system and how this interaction could directly influence the serotonergic tone remained unresolved.

Indeed, the studies on the functional effects of trazodone on serotonergic and noradrenergic systems have been conducted *in vivo* using electrophysiological recording of neuron activity in anaesthetized rats (Scuvée-Moreau and Dresse, 1982; Ghanbari et al., 2010a, 2012). Although these studies indicated that trazodone inhibits the activity of serotonergic neurons through agonism at 5-HT_{1A} receptors, they did not clarify whether the effect involved a direct activation of 5-HT_{1A}ARs or resulted from indirect actions that can intervene *in vivo*, given the multiple effects of the drug. Notably, Ghanbari and Colleagues (2010a) observed that trazodone silenced serotonergic neuron firing and concluded that trazodone was a full agonist at 5-HT_{1A}ARs, also because they were unable to reveal any additional component of trazodone action through the antagonism at α_1-adrenoceptors at serotonergic neurons of DRN (Ghanbari et al., 2012).

Methodological considerations on the experimental approach.

It should be emphasized that the interpretation of results obtained *in vivo* may become challenging because of the complexity of local and long-loop mechanisms that regulate of serotonin neuron activity in the raphe (Figure 24).

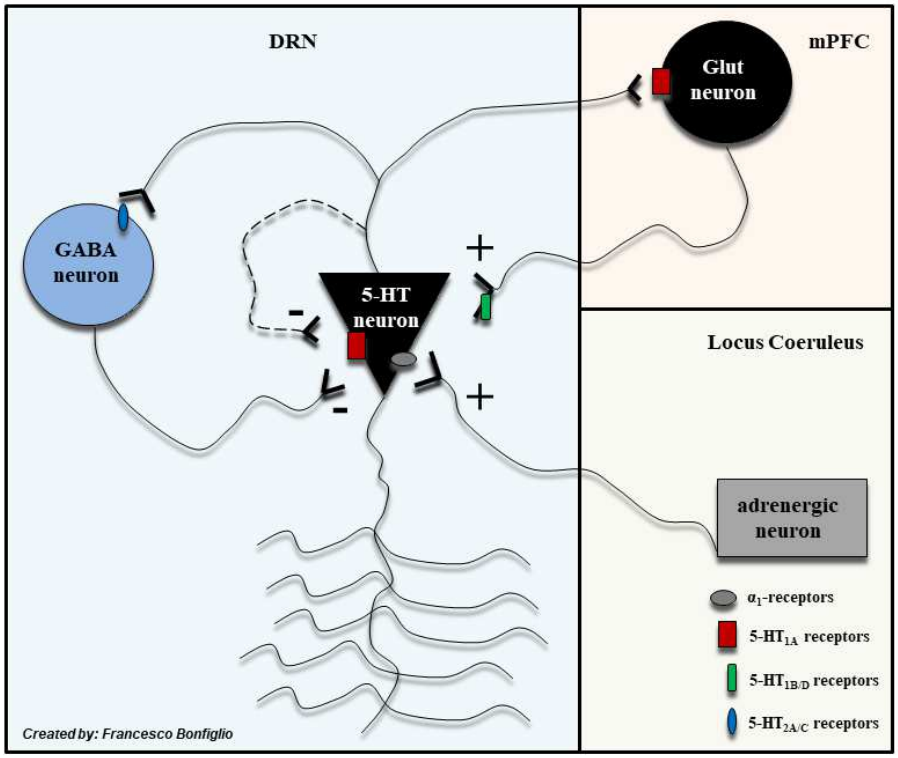

Figure 24. Schematic representation of the neural circuitry modulating the activity of serotonergic neurons *in vivo*. DRN, Dorsal Raphe Nucleus; mPFC, medial Pre-Frontal Cortex.

For instance, recording neuron activity *in vivo* does not allow to discriminate with accuracy whether the effects of trazodone are due to direct agonism at 5-HT_{1A}ARs or antagonism at α_1-adrenoceptors or to indirect effects of serotonin whose extracellular levels are increased by the inhibition of SERT produced by the drug.
Indeed, acute treatment with trazodone produces SERT inhibition and the subsequent increase in the extracellular levels of serotonin could activate a number of receptors that regulate the firing of serotonergic neurons through local or long-loop mechanisms (Figure 24).
For example, serotonergic neurons are interconnected with mPFC pyramidal neurons that send glutamatergic projections back to DRN. The release of glutamate from these terminals activates serotonergic neuron activity (Valentino et al., 2003; Soiza-Reilly and Commons 2011). However, the increased extracellular levels of serotonin produced by trazodone could activate presynaptic 5-HT_{1B} receptors of glutamatergic terminals, resulting in decrease in glutamate release onto serotonergic neurons and weakening of their activity. Similarly, serotonergic neurons in DRN are tightly

connected and tonically inhibited by local GABAergic interneurons expressing 5-$HT_{2A/C}$ receptors (Figure 24). An increase in the extracellular levels of serotonin can stimulate 5-$HT_{2A/C}$ receptors and activate GABAergic interneurons eliciting GABA release that suppress serotonergic neurons firing rate (Liu et al., 2000). Although this action would be limited by the antagonist properties of trazodone at 5-$HT_{2A/C}$ receptors (Ghanbari et al., 2012) the existence of multiple and simultaneous functional effects, including changes in noradrenergic drive produced by α_1-adrenoceptor antagonism, makes the conclusions that can be drawn from *in vivo* recordings on trazodone mechanisms of action only qualitative.

In our work, we exploited the considerable advantages offered by the *in vitro* approach for the quantitative study of trazodone actions on serotonin neurons. In fact, in slices we can visually identify serotonergic neurons from their morphology and confirm the serotonergic nature of the recorded neuron through the electrophysiological signature that can be obtained from the characteristics spike duration and firing frequency (Mlinar et al, 2016). Moreover, addition of several synaptic blockers in the bathing solution allowed us to pharmacologically isolate the recorded neurons from indirect action of the tested drugs.

As summarized below, the accurate choice of the recording technique most appropriate for the each of the objectives of our study allowed a reliable quantitative approach to the characterization of trazodone actions through α_1-adrenoceptor and 5-HT_{1A} receptors on serotonergic neurons.

The main advantage of *loose-seal cell-attached patch-clamp technique* is that neuron integrity is preserved while recording of neuron activity is performed. This avoids the generation of stretch conductances (Pellegrino et al., 1990; Nikolaev et al., 2015) thus allowing long duration recordings free from mechanically-introduced artefacts (Mlinar et al., 2016) that in conventional, sharp pipette recordings, may alter the firing rate of the recorded neuron. This permitted us to construct reliable concentration-response curves for trazodone and to test the effect of agonists and antagonists at known concentrations. Furthermore, in slices the extra-Raphe connections are severed, which contributes to decrease the possible indirect effects of the drug. Finally, it deserves to be mentioned that *in vivo* the spontaneous firing rate of serotonergic neurons is facilitated by noradrenergic inputs (Levine and Jacobs 1992) that are also severed *in vitro* and therefore the physiological facilitation of firing should be simulated by stimulation of serotonergic neurons with the selective α_1-adrenoceptor agonist phenylephrine. Although this introduces a confounding factor when studying compounds that bind to α_1-adrenoceptors adequate design of experimental protocols can be used to characterize the pharmacological properties of the compounds at these receptors.

In our study we also took advantage from the application of the *whole-cell patch-clamp* technique that allows to explore and quantify with accuracy the pharmacological characteristics of the interaction of trazodone with 5-HT_{1A}ARs in

individual serotonergic neurons. Indeed, since the amount of activated GIRK channels is proportional to the number of 5-HT_{1A} receptors stimulated, GIRK conductance reliably reports the concentration-dependent effect of the agonist and the response of serotonergic neurons to maximal 5-HT_{1A} receptors stimulation, allowing an accurate quantitative study of the potency and the intrinsic efficacy of trazodone at 5-HT_{1A}ARs. Moreover, since in whole-cell experiments α_1-adrenergic stimulation is not required for the study of 5-HT_{1A} receptor-mediated responses the recorded effect of trazodone at 5-HT_{1A}ARs is not biased by its antagonist action at α_1-adrenoceptors as it happens when recording the firing activity of serotonergic neurons.
To the best of my knowledge, this is the first work in which this technique has been applied to quantify the interaction of a therapeutic compound with 5-HT_{1A}ARs.
The important methodological advancement introduced by our work is that we provided a direct measure of the GIRK channel opening produced by the stimulation of the G protein coupled 5-HT_{1A} receptor. In fact, until now the interaction of a panel of compounds, including antidepressant drugs and anxyolitics, with 5-HT_{1A} receptors have been performed using [^{35}S]GTPγS binding (Hensler and Durgam, 2001; Shen et al., 2002; Pauwels and Colpaert, 2003; Odagaki et al., 2005; Valdizán et al., 2010; *see also in*: Hensler, 2003). Although this technique reliably measures the interaction of the drugs with the G proteins, it does not necessarily report the number of GIRK channels activated by that interaction.

A major result of our work is that we have been able to discriminate between the 5-HT_{1A} receptor-dependent and the α_1-adrenoceptor-dependent effects produced by trazodone on serotonergic neuron activity. Importantly, through our direct measure of the efficacy of trazodone at stimulating 5-HT_{1A}ARs we demonstrated that the drug is a weak partial agonist at these receptors.
Thus, the use of a panel of pharmacological tools and protocols while recording the activity of serotonergic neurons under conditions of 5-HT_{1A}AR block by Way-100635 allowed us to reveal that trazodone is an α_1-adrenoceptor competitive antagonist.
Indeed, our *in vitro* conditions allowed to manipulate the degree of α_1-adrenoceptor-dependent stimulation of serotonergic neuron firing by lowering the extracellular Ca^{2+} in the absence of PE or by applying different concentrations of PE in the presence of blocked 5-HT_{1A} receptor-mediated component by Way-100635. Moreover, the use of DRN slices from transgenic Tph2$^{-/-}$ mice lacking brain serotonin (Mössner et al., 2006; Gutknecht et al., 2012) confirmed both the presence of a serotonergic-independent inhibition of firing rate produced by trazodone and, more importantly, that all the effects of trazodone were not mediated by endogenous serotonin.
As the α_1-adrenoceptor antagonist property of trazodone was undetected *in vivo* and the drug was able to silence serotonergic neurons through the activation of 5-HT_{1A} receptors (Ghanbari et al., 2010a, 2012), the Authors concluded that trazodone is a full agonist at 5-HT_{1A}ARs. As discussed later on, to ascribe a 5-HT_{1A} receptor full agonist

property to trazodone could lead to misinterpretations on the mechanism(s) of therapeutic action of the antidepressant drug.
Our results clarify that trazodone is a competitive partial agonist at 5-HT$_{1A}$ARs, and that its efficacy at these receptors is weak. Indeed, by comparing the efficacy of trazodone with that of the full agonist 5-CT and of the prototypical 5-HT$_{1A}$ receptor partial agonist buspirone we have shown that the efficacy of trazodone is ~35 %, significantly weaker than that of buspirone (Figure 25).

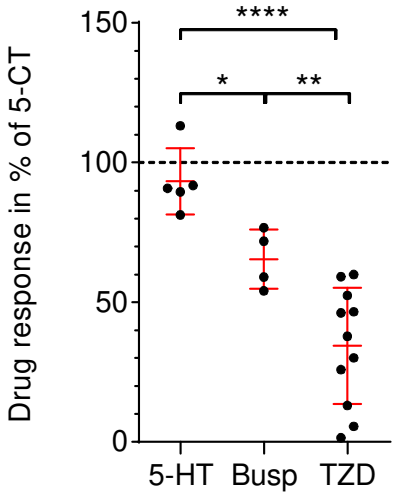

Figure 25. Efficacy of 5-HT, trazodone and buspirone at 5-HT$_{1A}$ARs compared to 5-CT. Summary scatter plot of the drug's efficacy in activating 5-HT$_{1A}$ receptor-mediated GIRK conductance compared to 5-CT. All the data are obtained by a direct comparison with 5-CT in the same neurons. The efficacy of the drug was obtained using the maximal concentration for any of the substances. Efficacies are reported as % of 5-CT response in mean ± SD (5-HT: 93.25 ± 11.85, n = 5; BUSP: 66.56 ± 9.02, n = 7; TZD: 34.36 ± 20.87, n = 11; *p< 0.05; **p< 0.01; **** p < 0.001; One-Way ANOVA followed by a Tukey *post-hoc* test).

To explain the apparent discrepancy between the results obtained *in vivo* and *in vitro*, it should be mentioned that partial agonists have beeen repeatedly shown to inhibit serotonergic neuron firing in anaesthetized rats (Vandermaelen et al., 1986; Blier and deMontigny, 1987; McMillen et al., 1987), in behaving cats (Fornal et al., 1994) and in rat DRN slices (Corradetti et al., 1996b). This is not in contrast with the low intrinsic activity of the molecule because serotonergic neurons have very high membrane resistance so that the opening of a small number of GIRK channels could effectively hyperpolarize serotonergic neurons and inhibit their firing. In agreement with this notion, the partial agonist buspirone fully suppresses the serotonergic neuron firing *in vivo* (Fornal et al., 1994), but shows partial agonist action at [^{35}S]GTPγS binding (Pauwels and Colpaert, 2003; Stark et al., 2007) and 5-HT$_{1A}$AR-activated inwardly rectifying K^+ current in serotonergic neurons (Katayama et al., 1997).

Functional consequences of the dual inhibitory mechanism of trazodone and their relevance to its therapeutical effects.

Notwithstanding the more complex effects that trazone can produce *in vivo* through its action at other receptors (e.g. 5-HT$_{2A}$) or local/long-loop feedback regulation, our data provide ground for mechanistic interpretation of the interplay between the 5-HT$_{1A}$

receptor agonist and α_1-adrenoceptor antagonist properties of trazodone in regulating serotonergic neuron firing.
The two *direct* effects of the drug on serotonergic neurons of the DRN characterized in the present work, namely α_1-adrenoceptor competitive antagonism and 5-HT_{1A}AR weak partial agonism, likely play important roles in determining the therapeutic actions that distinguish this multimodal antidepressant drug from SSRIs.

Relevance of the α_1-adrenoceptor competitive antagonism to trazodone effects on sleep.

The first important result of the present work is the demonstration that trazodone exerts a direct antagonism at α_1-adrenoceptor of serotonergic neurons. The present data also show that, consistent with the competitive nature of the antagonism, the potency of trazodone in inhibiting serotonergic neuron firing through the block of α_1-adrenoceptors is inversely proportional to the level of α_1-adrenoceptor activation.
Therefore it is conceivable that antagonism of trazodone at α_1-adrenoceptors contributes differentially to serotonergic neuron firing inhibition depending on the arousal state.

Among antidepressant drugs trazodone has a distinctive sleep regulating activity (Fagiolini et al., 2012) that favoured its off-label use in insomnia (Stahl, 2009b). The serotonergic system participates in arousal and is implicated in sleep, being active during waking and becoming progressively inactive during slow wave sleep and almost completely silent during REM sleep (McGinty and Harper, 1976; Trulson and Jacobs, 1979; Sakai and Crochet, 2000; Cespuglio, 2018). These state dependent changes in activity of serotonergic system can be ascribed, at least in part, to similar changes in noradrenergic neuron activity (*see in*: Jacobs, 1986) that facilitate the firing of serotonergic neurons via activation of α_1-adrenoceptors (Baraban and Aghajanian, 1980).
Although the relative contribution of 5-HT_{1A} and α_1-adrenoceptor effects *in vivo* cannot be fully mimicked *in vitro* as the actual degree of noradrenergic drive changes during wake-sleep cycle, we speculate that the combined 5-HT_{1A} receptor agonist and α_1-adrenoceptor antagonist effects of trazodone on these neurons could be relevant to its effects on sleep. At concentrations akin those present in human brain following administration of trazodone for sleep disorders (Settimo and Taylor, 2018), the dual action of trazodone could facilitate inhibition of serotonergic neuron firing in the phase of drowsiness when α_1-adrenoceptor stimulation is lowered (Fornal et al., 1994). In addition, antagonism at α_1-adrenoceptor is likely to dumpen the effects of noradrenergic system reactivation that occurs during sleep thereby preventing insomnia-related microarousals (*see in*: Feige et al., 2013)

Relevance of the weak partial agonism to trazodone antidepressant action.

The second important property of trazodone is the weak partial agonism at 5-HT_{1A}ARs.

The need to interrupt the 5-HT_{1A}AR-mediated inhibitory feed-back for full development of SSRI therapeutic effect, leads to an augmentation strategy using the 5-HT_{1A} receptor antagonist pindolol for blocking the inhibition of serotonergic neuron activity by the elevated serotonin (Artigas et al., 1996). Although pindolol was found to hasten the therapeutic response to SSRIs, it did not produce the expected improvement in clinical effectiveness of the treatment (Ballesteros and Callado, 2004). Nevertheless, these clinical studies provided the proof of concept that functional inactivation of 5-HT_{1A}ARs could hasten the therapeutic response to antidepressant drugs and, together with the ability of selective partial agonists to desensitize 5-HT_{1A}ARs, suggested that antidepressant drugs with 5-HT_{1A} receptor antagonist properties could produce faster and/or better clinical response to treatment (*see in*: Artigas, 2013).

Under this perspective, the weak partial agonism at 5-HT_{1A}ARs exerted by trazodone at therapeutic concentrations appears of relevance to the antidepressant effect of the drug. For example, assuming that in humans the basal extracellular concentration of serotonin in DRN is similar to that measured in the rat *in vivo* (10 nM, Crespi et al., 1988) and that trazodone produces a five-fold increase in serotonin extracellular level (Pazzagli et al. 1999), at therapeutic concentrations achievable in the brain (3 μM, Karhu et al. 2010; Kale and Agrawal, 2015) the relative occupancy at 5-HT_{1A}ARs by trazodone (K_i = ~96 nM; Cusack et al. 1994) and serotonin (3.8 nM, Sundaram et al. 1993) will be ~70% and ~30 % respectively. Under these conditions the total activation of 5-HT_{1A}ARs will be ~55 % of that produced by serotonin in the absence of the partial agonist trazodone. In other brain areas, such as hippocampus and cerebral cortex, where desensitization of 5-HT_{1A} receptors during chronic treatment does not occur (Le Poul et al, 2000), a similar level of 5-HT_{1A} receptor stimulation could be sufficient for development of the antidepressant effect. Thus, it is conceivable that at therapeutic concentrations trazodone occupies and weakly stimulates a substantial fraction of 5-HT_{1A}ARs, thereby producing a ceiling effect relative to 5-HT_{1A}AR stimulation that would occur with heightened extracellular serotonin concentration produced by the drug. Until 5-HT_{1A}ARs are desensitized, this would limit the inhibition of serotonergic neuron activity and preserve higher serotonergic system function than SSRIs while ensuring a sufficient degree of 5-HT_{1A} receptor stimulation in terminal areas.

Interestingly, Ghanbari et al. (2010a) reported that the basal firing rate *in vivo* after two days of treatment with trazodone was decreased by ~40% compared to controls. This is a relatively weaker inhibition than that observed in similar conditions with

escitalopram (~ 70 %) (Ghanbari et al., 2010b, Figure 26), although these results are from two separate experimental setting, hence not directly comparable.

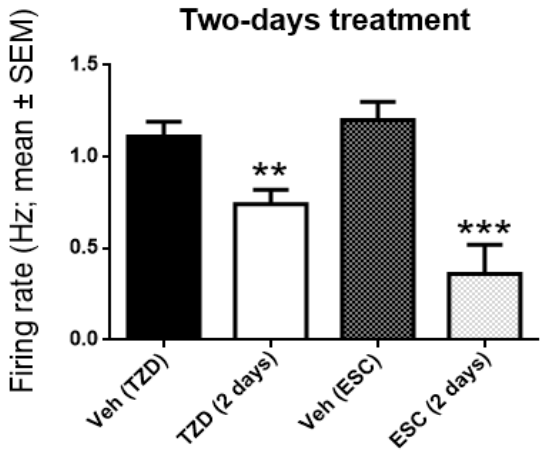

Figure 26. Inhibition of serotonergic neuron spontaneous activity during treatment with trazodone or escitalopram.
Effects of 2-days *in vivo* treatment with trazodone or escitalopram on DRN serotonergic neuron firing rate. Note that the baseline firing rate in the presence of TZD is apparently less inhibited than that recorded in the presence of the SSRI escitalopram. In both cases, the treatment did not change the sensitivity of 5-HT_{1A}ARs to 5-HT_{1A} receptor agonists. ** $p<0.01$, *** $p<0.005$ vs respective control (veh). (Adapted from Ghanbari et al., 2010a,b).

In any case, the partial antagonism exerted by trazodone does not prevent 5-HT_{1A}ARs desensitization during treatment *in vivo* (Ghanbari et al., 2010a). This is in agreement with the effect of other partial agonists (Blier and de Montigny, 1987), whereas full antagonists have been shown to prevent functional desensitization of 5-HT_{1A}ARs (e.g. Way-100635: Hervás et al., 2001).
Importantly, the antagonist effect of trazodone at 5-HT_{1A}ARs would occur starting from the first drug administration. This would limit the detrimental tonic inhibition of serotonergic neuron firing produced by the raise in extracellular serotonin starting from the beginning of the therapy, regardless the mechanism(s) involved in the recovery of neuron activity during chronic treatment with antidepressant drugs (Blier and de Montigny, 1994; Blier and Ward, 2003; Commons and Linnros, 2019).
A further consideration is relevant to the selective chronic desensitization of 5-HT_{1A}ARs produced by partial agonists *in vivo*. The reasons that confer 5-HT_{1A}ARs the ability to desensitize following prolonged agonist stimulation remain elusive, although some distinctive properties of 5-HT_{1A}ARs, such as their coupling to serotonergic neuron-specific GIRK channel subunits (Llamosas et al., 2015; Montalbano et al., 2015a) and the differential capability of full and partial agonists to couple to G protein subunits of serotonergic neurons (Valdizán et al., 2010), could be relevant to the partial efficacy and/or desensitization mechanisms activated by partial agonists. Regardless the mechanism implicated, desensitization of 5-HT_{1A}ARs by anxiolytic and antidepressant drugs with partial 5-HT_{1A} receptor agonist properties clearly indicates that full intrinsic efficacy of the agonist is not required for this effect.
Taken together these two actions, ceiling of acute autoinhibitory response of serotonergic neurons to elevated extracellular serotonin and tonic 5-HT_{1A}AR stimulation leading to desensitization during chronic antidepressant drug

administration, are expected to hasten the therapeutic response to antidepressants with partial agonist properties at 5-HT_{1A} receptors (Artigas et al, 2018).
In agreement with this hypothesis, trazodone was found to have fast onset of action in a placebo-controlled clinical trial and in an venlafaxine-controlled clinical trial in which the therapeutic effect was already present after one week of treatment (Sheehan et al., 2009; unpublished data, ACRAF, 2016: EudraCT number 2011-005878-37).
Collectively, the present results, together with the effects of chronic treatment with trazodone in laboratory animals and the clinical effectiveness of the drug, support the concept that partial agonist properties are relevant to the therapeutic action of antidepressant drugs and may contribute to hasten the clinical response.

Beyond trazodone: importance of functional determination of efficacy for inferences on the *in vivo* action of antidepressant drugs with 5-HT_{1A} receptor partial agonist activity.

The relevance of our study is not limited to the accurate description of the electrophysiological and pharmacological effects of trazodone at 5-HT_{1A}ARs, but also provides an experimental ground to establish the requirements for determining the efficacy of 5-HT_{1A} receptor partial agonist. Indeed, the methodology and accuracy in determining the efficacy of a drug becomes of crucial importance when this efficacy value is used for calculating the effect of the compound on the activity of serotonergic system during therapeutic treatment.
The comparison between the conclusions that could be drawn using efficacy values for trazodone obtained with different methodologies provides a good example for deriving potential weaknesses, methodological pitfalls and requirements for the use of the published efficacy of antidepressant drugs.
In the general discussion of the present results, I have highlighted the importance ascribed (*see* Artigas, 2013; Artigas et al., 2018) to the weak partial agonism at 5-HT_{1A}ARs exerted by an antidepressant drug in addition to SERT block (or theoretically also by a weak partial agonist in combination with an SSRI).
With antidepressant drugs that selectively inhibit SERT, i.e. SSRIs, the raised extracellular serotonin concentration will stimulate 5-HT_{1A}ARs, inhibit the activity of serotonergic neurons, and ultimately acutely decrease the serotonergic tone. This acute effect is believed to delay the therapeutic effect of most antidepressant drugs for some weeks, until homeostatic mechanisms intervene to weaken the response of 5-HT_{1A}ARs to high levels of endogenous serotonin.
In this context, it is expected that a SERT inhibitor endowed of weak partial agonist properties (e.g. trazodone) will substantially antagonize the activation of 5-HT_{1A}ARs by high levels of extracellular serotonin and therefore limit the acute decrease in activity of serotonergic neurons, an effect that is considered therapeutically favourable.

Why the accuracy in determining the efficacy parameter is it important for understanding the clinical effects of antidepressant drugs endowed of weak partial agonist properties?

Once the weak partial agonist efficacy is measured this value can be introduced in the Gaddum's equation (*see methods*) to calculate the total stimulation of 5-HT_{1A}ARs at therapeutic concentrations of the antidepressant drug in the presence of physiological and higher levels of extracellular serotonin. It should be noted that application of the Gaddum's equation requires the affinity constants (or the K_i) of the weak partial and full agonist for 5-HT_{1A} receptors, in addition to their efficacy values.

To test the applicability of the approach, as a first step we have calculated the theoretical curve for total stimulation of 5-HT_{1A}ARs at increasing concentrations of the full agonist 5-CT alone (*efficacy = 1*) and the curve for the same concentrations of 5-CT in the presence of the agonist/antagonist trazodone (*efficacy = 0.35*) at the concentration of 10 μM (Figure 27A). Calculations were performed using the published K_i values of the two compounds in rodents. This allowed a comparison of the effect of trazodone experimentally obtained using it at 10 μM in the presence of 10 nM 5-CT in rat DRN slices. In addition, because the efficacy for trazodone obtained in rat brain tissue using [^{35}S]GTPγS binding was ~0.18 (Odagaki et al., 2005) we have calculated an alternative curve for the interaction between the two compounds using the efficacy of 0.18 for trazodone. As illustrated in Figure 27A, the value for antagonism exerted by trazodone on 5-CT obtained experimentally, fairly fits with the theoretical curve obtained using an efficacy value of 0.35, but not with that constructed using the efficacy value obtained with [^{35}S]GTPγS binding.

Thus, the comparisons presented in Figure 27A raises a series of considerations and indications for the reliable methodologies to be used for obtaining the efficacy values of antidepressant drugs at 5-HT_{1A}ARs.

The first positive consideration that stems from the calculations presented in Figure 27A is that the published K_i values for trazodone and 5-CT are accurately obtained and likely represent the affinity of these compounds for 5-HT_{1A} receptors in the living brain. This was not to be taken for granted and the fact that the curve fairly fits with the measured effect of the two compounds implicitly validates the use of published K_i values for 5-HT_{1A} receptor-active compounds in this type of extrapolations.

The second consideration stems from the observation that the effect of the two agonists in combination obtained experimentally, albeit not statistically different from the calculated one, is slightly greater than expected. One possibility is that, in slices, the inhibition of SERT by trazodone produces an increase in extracellular serotonin whose full agonist action would result additive to that of 5-CT (at submaximal concentrations). Although the contribution of endogenous serotonin to the measured response could not be excluded, this was likely marginal. Indeed, brainstem slices are greatly depleted in serotonin compared to fresh tissue and their normal content can only be maintained by supplementing the serotonin synthesis with its precursor tryptophan (Mlinar et al., 2005). As a consequence, a substantial increase in

extracellular serotonin by SSRIs in slices can only be obtained in the presence of 30 μM tryptophan (Mlinar et al., 2015a), which was not present in our experiments.

Finally, the fact that the efficacy value for trazodone obtained by measuring the actual activation of GIRK channels in serotonergic neurons of the DRN results clearly different from that obtained using the [^{35}S]GTPγS binding technique is somehow intriguing. Although this discrepancy does not challenge the validity of [^{35}S]GTPγS determinations, it indicates that the crucial requirement for the application of the efficacy values to be used for the calculations applied in Figure 27A is that the efficacy should be determined on the specific neuronal population for which we want to derive the effect of the antidepressant drug.

In the case of trazodone, its efficacy in activating 5-HT$_{1A}$ receptors measured by [^{35}S]-GTPγS binding was not carried out in DRN tissue but in rat cortex and hippocampal membranes (Odagaki et al., 2005).

Considering the wealth of evidence that indicates that in serotonergic neurons 5-HT$_{1A}$ receptors and GIRK channels could have specific properties compared to those expressed in other regions of the brain (*e.g.*: Hervás et al., 2001; Shen et al., 2002; Mannoury la Cour et al., 2006), it becomes clear that the minimal requirement for making inferences on the effects of multimodal antidepressant drugs with weak partial agonism at 5-HT$_{1A}$ARs on serotonergic tone *in vivo* is that their efficacy is determined at 5-HT$_{1A}$ARs.

It should be emphasized that [^{35}S]GTPγS binding may also result a reliable technique provided that the determination of the interaction of the antidepressant drug with 5-HT$_{1A}$ receptors is carried out in raphe tissue. Indeed, in DRN the predominant neuronal population is represented by serotonergic neurons (Steinbusch et al., 1978; Steinbusch, 1981) which makes the raphe region particularly favourable for studying the activation of 5-HT$_{1A}$ARs by using [^{35}S]GTPγS binding.

Unfortunately, to the best of my knowledge, the efficacy of none of multimodal antidepressant drugs at 5-HT$_{1A}$ARs has been evaluated using either electrophysiological or [^{35}S]GTPγS binding techniques, in spite of the repeated suggestion that this parameter would be relevant for better understanding the therapeutical mechanism of action of multimodal antidepressant drugs (Artigas, 2013; Artigas et al., 2018).

The availability, for the first time of a reliable measurement of the efficacy of the multimodal antidepressant drug trazodone prompted us to calculate the theoretical curves for the interaction between therapeutic concentrations of trazodone (1 - 10 μM) and endogenous serotonin at 5-HT$_{1A}$ARs in humans (Figure 27B).

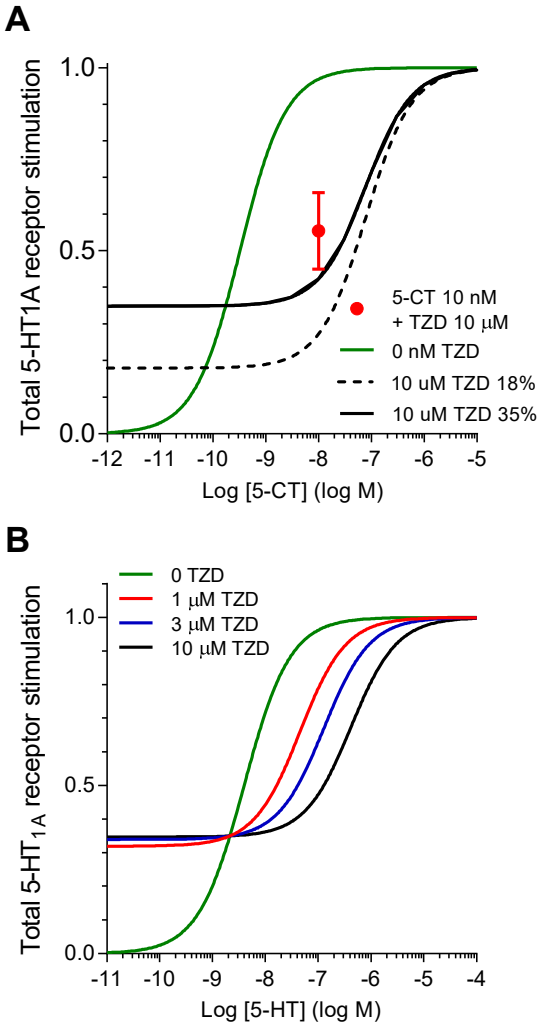

Figure 27. Calculated concentration-response relationships of 5-HT$_{1A}$AR activation by the full agonists 5-CT and 5-HT alone and in the presence of trazodone.
(A) Concentration-response relationships of 5-HT$_{1A}$ARs activation by 5-CT in the absence of trazodone and in the presence of the drug (10 µM). Curves were calculated as detailed in methods using the K_i of the two agonists for the rodent 5-HT$_{1A}$AR (5-CT: K_i = 0.325 nM; trazodone: K_i = 42 nM) and an efficacy value of 0.35 (solid line) and 0.18 (dashed line) for trazodone. Note that the response to 10 nM 5-CT in the presence of 10 µM trazodone (red dot: 54.8 ± 11.4 %, mean ± SD; n = 5) was similar (p = 0.125, Wilcoxon signed rank test) to that expected from the curve (42.2 % of maximal response produced by 5-CT) calculated using an efficacy value of 0.35 for trazodone. **(B)** Concentration-response relationships of 5-HT$_{1A}$ARs activation by 5-HT in the absence of trazodone and in the presence of various concentrations of the drug (1 - 10 µM). Curves were calculated using the K_i of the two agonists for the human 5-HT$_{1A}$AR (5-HT: K_i = 3.98 nM; trazodone: K_i = 96 nM; *see methods*) and an efficacy value of 0.35 for trazodone.

As illustrated in Figure 27B, for extracellular concentrations of endogenous 5-HT in the range of 1 - 5 nM the total activation of 5-HT$_{1A}$ARs by any concentration of trazodone and serotonin would be ~35%, that is greater than that expected with serotonin alone. However, starting at physiological concentrations (5 - 10 nM: Crespi

et al., 1988) trazodone dose dependently decreases the total activation of 5-HT_{1A}ARs and the antagonism remains substantial (40 - 60% according to trazodone concentration) up to 50 nM (which represents a 5 - 10 folds increase in extracellular serotonin concentration produced by the concomitant SERT inhibition exerted by trazodone).
Although all the above theoretical calculations of the total activation of 5-HT_{1A}ARs by endogenous serotonin in the presence of trazodone should be taken with caution, they illustrate how the weak partial agonism by trazodone could limit serotonergic neuron inhibition during treatment with the antidepressant drug. Consistent with the suggestion advanced by Artigas in recent years (Artigas, 2013; Artigas et al., 2018) that antidepressants endowed of 5-HT_{1A} receptor partial agonist property should hasten the therapeutic response, trazodone was found to have fast onset of action in a placebo-controlled clinical trial and in an active-controlled clinical trial in which the therapeutic effect was already present after one week of treatment (Sheehan et al., 2009; unpublished data, ACRAF, 2016: EudraCT number 2011- 005878-37).

Conclusions.

Our results show that trazodone directly inhibits DRN serotonergic neuron activity through weak partial agonism at 5-HT_{1A}ARs.
Our results provide, for the first time, the efficacy value of a multimodal antidepressant drug at 5-HT_{1A}ARs which is a crucial parameter for allowing a correct interpretation of the possible clinical effects of these antidepressants to be correlated with their 5-HT_{1A} receptor binding properties.
In particular, during chronic treatment with trazodone, the weak partial agonism exerted at 5-HT_{1A}ARs could be involved in hastening the appearance of the first clinical signs of antidepressant effect.
Moreover, we demonstrated that trazodone is a competitive antagonist at α_1-adrenoceptors of serotonergic neurons. These two effects are both exerted at concentration achieved in the brain with therapeutic doses of trazodone and our data may help in understanding the effectiveness and the consequent off-label use of this drug in sleep disturbances. Indeed, the overall inhibition of serotonergic neuron activity produced by the dual action of trazodone will result inversely proportional to the degree of α_1-adrenoceptor activation. Since the noradrenergic drive to serotonergic neurons changes during the sleep-wake cycle, being maximal in waking and reduced during drowsiness and sleep, trazodone given at low dose at nighttime would facilitate sleep and prevent from nocturnal awakenings.

References:

Abi-Saab, W.M., Bubser, M., Roth, R.H., Deutch, A.Y. 1999. 5-HT2 receptor regulation of extracellular GABA levels in the prefrontal cortex. Neuropsychopharmacology. Jan;20(1):92-6.

ACRAF, 2016. A randomized, double-blind study comparing the efficacy and safety of trazodone OAD and venlafaxine XR in the treatment of patients with Major Depressive Disorder. EudraCTnumber 2011-005878-37. https://www.clinicaltrialsregister.eu/ctr-search/trial/2011-005878-37/results.

Aghajanian, G.K., and Wang, R.Y., 1977. Habenular and other midbrain raphe afferents demonstrated by a modified retrograde tracing technique. Brain Res 122:229–242.

Aghajanian, G.K. 1985. Modulation of a transient outward current in serotonergic neurones by alpha 1-adrenoceptors. Nature. 1985 Jun 6-12;315(6019):501-3.

Ahlquist, R.P. 1948. A study of the adrenotropic receptors. Am J Physiol. Jun;153(3):586-600.

Albert, P.R., Zhou, Q.Y., Van Tol, H.H., Bunzow, J.R., Civelli, O. 1990. Cloning, functional expression, and mRNA tissue distribution of the rat 5-hydroxytryptamine1A receptor gene. J Biol Chem. Apr 5;265(10):5825-32.

Albert, P.R., Lembo, P., Storring, J.M., Charest, A., Saucier, C. 1996. The 5-HT1A receptor: signaling, desensitization, and gene transcription. Neuropsychopharmacology. Jan;14(1):19-25. Review

Albert, P.R., Tiberi, M. 2001. Receptor signaling and structure: insights from serotonin-1 receptors. Trends Endocrinol Metab. Dec;12(10):453-60. Review.

Albert, P.R., Lemonde, S. 2004. 5-HT1A receptors, gene repression, and depression: guilt by association. Neuroscientist. Dec;10(6):575-93. Review

Albert, P.R., Vahid-Ansari, F., Luckhart, C. 2014. Serotonin-prefrontal cortical circuitry in anxiety and depression phenotypes: pivotal role of pre- and post-synaptic 5-HT1A receptor expression. Front Behav Neurosci. Jun 6;8:199. Review.

Albert, P.R., Vahid-Ansari, F. 2019. The 5-HT1A receptor: Signaling to behavior. Biochimie. Jun;161:34-45. Oct 25. Review.

Allain, H., Lieury, A., Brunet-Bourgin, F., Mirabaud, C., Trebon, P., Le Coz, F., Gandon, J.M. 1992. Antidepressants and cognition: comparative effects of moclobemide, viloxazine and maprotiline. Psychopharmacology (Berl). 106 Suppl:S56-61.

Anderson, I.M., Tomenson, B.M. 1994. The efficacy of selective serotonin re-uptakeinhibitors in depression: a meta-analysis of studies against tricyclicantidepressants. J Psychopharmacol. Jan;8(4):238-49.

Andrade, R., Malenka, R.C., Nicoll, R.A. 1986. A G protein couples serotonin and GABAB receptors to the same channels in hippocampus. Science. Dec 5;234(4781):1261-5.

APA, 2013. (DSM-5) Diagnostic and Statistic Manual of Mental Disorders. American Psychiatric Press, Inc., Washington, DC.

Araragi, N., Mlinar, B., Baccini, G., Gutknecht, L., Lesch, K.P., Corradetti, R. 2013. Conservation of 5-HT1A receptor-mediated autoinhibition of serotonin (5-HT) neurons in mice with altered 5-HT homeostasis. Front. Pharmacol. 4 (97).

Arnt, J., Skarsfeldt, T. 1998. Do novel antipsychotics have similar pharmacological characteristics? A review of the evidence. Neuropsychopharmacology. Feb;18(2):63-101. Review.

Artigas, F., Romero, L., de Montigny, C., Blier, P. 1996. Acceleration of the effect of selected antidepressant drugs in major depression by 5-HT1A antagonists. Trends Neurosci. Sep;19(9):378-83. Review.

Artigas, F. 2013. Serotonin receptors involved in antidepressant effects. Pharmacol Ther. Jan;137(1):119-31. Review

Artigas, F., Bortolozzi, A., Celada, P., 2018. Can we increase speed and efficacy of antidepressant treatments? Part I: General aspects and monoamine-based strategies. Eur Neuropsychopharmacol. Apr;28(4):445-456.

Aston-Jones, G., Bloom, F.E. 1981. Activity of norepinephrine-containing locus coeruleus neurons in behaving rats anticipates fluctuations in the sleep-waking cycle. J Neurosci. Aug;1(8):876-86.

Aston-Jones, G., Waterhouse, B. 2016. Locus coeruleus: From global projection system toadaptive regulation of behavior. Brain Res. Aug 15;1645:75-8. Review.

Audero, E., Mlinar, B., Baccini, G., Skachokova, Z.K., Corradetti, R., Gross, C. 2013. Suppression of serotonin neuron firing increases aggression in mice. J Neurosci. May 15;33(20):8678-88.

Azmitia, E.C., Segal, M., 1978. An autoradiographic analysis of the differential ascending projections of the dorsal and median raphe nuclei in the rat. J CompNeurol. Jun 1;179(3):641-67.

Azmitia, E. and Gannon, P., 1986. The primate serotoninergic system: A review of human and animal studies and a report on Macaca fascicularis. Adv Neurol43:407–467.

Ballesteros, J., Callado, L.F. 2004. Effectiveness of pindolol plus serotonin uptake inhibitors in depression: a meta-analysis of early and late outcomes from randomised controlled trials. J Affect Disord. Apr;79(1-3):137-47.

Baraban, J.M., and Aghajanian, G.K., 1980. Suppression of firing activity of 5-HT neurons in the dorsal raphe by alpha-adrenoceptor antagonists. Neuropharmacology 19:355–363.

Baraban, J.M., and Aghajanian, G.K., 1981 Noradrenergic innervation of serotonergic neurons in the dorsal raphe: Demonstration by electron microscopic autoradiography. Brain Res 204:1–11.

Barnes, N.M., Sharp, T. 1999. A review of central 5-HT receptors and their function.Neuropharmacology. Aug;38(8):1083-152. Review.

Beckstead, R.M. 1978. Afferent connections of the entorhinal area in the rat as demonstrated by retrograde cell-labeling with horseradish peroxidase. Brain Res. Aug 25;152(2):249-64.

Berman, R.M., Cappiello, A., Anand, A., Oren, D.A., Heninger, G.R., Charney, D.S., Krystal, J.H. 2000. Antidepressant effects of ketamine in depressed patients. Biol Psychiatry. Feb 15;47(4):351-4.

Berthelsen, S., Pettinger, W.A. 1977. A functional basis for classification ofalpha-adrenergic receptors. Life Sci. Sep 1;21(5):595-606.

Betti, L., Botta, M., Corelli, F., Floridi, M., Giannaccini, G., Maccari, L., Manetti, F., Strappaghetti, G., Tafi, A., Corsano, S. 2002. Alpha(1)-adrenoceptor antagonists. 4. Pharmacophore-based design, synthesis, and biological evaluation of new imidazo-, benzimidazo-, and indoloarylpiperazine derivatives. J Med Chem. Aug 15;45(17):3603-11.

Bleumink, G.S., van Vliet, A.C., van der Tholen, A., Stricker, B.H., 2003. Fatal combination of moclobemide overdose and whisky. Neth J Med. Mar;61(3):88-90.

Blier, P., de Montigny, C. 1987. Modification of 5-HT neuron properties by sustained administration of the 5-HT1A agonist gepirone: electrophysiological studies in the rat brain. Synapse. 1(5):470-80.

Blier, P., de Montigny, C. 1994. Current advances and trends in the treatment ofdepression. Trends Pharmacol Sci. Jul;15(7):220-6.

Blier, P., Ward, N.M., 2003. Is there a role for 5-HT1A agonists in the treatment of depression? Biol. Psychiatry. 53, 193-203.

Boess, F.G., Martin, I.L, 1994. Molecular biology of 5-HT receptors. Neuropharmacology 33, 275-317.

Bonaventure, P., Schotte, A., Cras, P., Leysen, J.E. 1997. Autoradiographic mapping of 5-HT1B- and 5-HT1D receptors in human brain using [3H]alniditan, a new radioligand. Receptors Channels. 5(3-4):225-30.

Burke, W.J., Dewan, V., Wengel, S.P., Roccaforte, W.H., Nadolny, G.C., Folks, D.G. 1997. The use of selective serotonin reuptake inhibitors for depression and psychosis complicatingdementia. Int J Geriatr Psychiatry. May;12(5):519-25.

Bymaster, F.P., Hemrick-Luecke, S.K., Perry, K.W., Fuller, R.W. 1996. Neurochemical evidence for antagonism by olanzapine of dopamine, serotonin, alpha 1-adrenergic and muscarinic receptors in vivo in rats. Psychopharmacology (Berl). Mar;124(1-2):87-94.

Celada, P., Puig, M., Amargós-Bosch, M., Adell, A., Artigas, F., 2004. The therapeutic role of 5-HT_{1A} and 5-HT_{2A} receptors in depression. J Psychiatry Neurosci. Jul;29(4):252-65. Review.

Celada, P., Puig, M.V., Artigas, F. 2013. Serotonin modulation of cortical neurons and networks. Front Integr Neurosci. 2013 Apr 19;7:25.

Cespuglio, R., 2018. Serotonin: its place today in sleep preparation, triggering or maintenance. Sleep Med. 49, 31-39.

Clavier, R.M. 1979. Afferent projections to the self-stimulation regions of the dorsalpons, including the locus coeruleus, in the rat as demonstrated by thehorseradish peroxidase technique. Brain Res Bull. Jul-Aug;4(4):497-504.

Clemett, D.A., Punhani, T., Duxon, M.S., Blackburn, T.P., Fone, K.C. 2000. Immunohistochemical localisation of the 5-HT2C receptor protein in the rat CNS. Neuropharmacology. 39(1):123-32.

Commons, K.G., Linnros, S.E., 2019. Delayed Antidepressant Efficacy and the Desensitization Hypothesis. ACS Chem Neurosci. Mar 11.

Cools, R., Roberts, A.C., Robbins, T.W., 2008. Serotoninergic regulation of emotional and behavioural control processes. Trends Cogn. Sci. 12, 31-40.

Coppen, A., 1967. The biochemistry of affective disorders. Br J Psychiatry. Nov; 113(504):1237-64. Review.

Corradetti, R., Le Poul, E., Laaris, N., Hamon, M., Lanfumey, L., 1996a. Electrophysiological effects of N-(2-(4-(2-methoxyphenyl)-1-piperazinyl)ethyl)-N-(2-pyridinyl) cyclohexane carboxamide (WAY 100635) on dorsal raphe serotonergic neurons and CA1 hippocampal pyramidal cells in vitro. J. Pharmacol. Exp. Ther. 278:679-688.

Corradetti, R., Pugliese, A.M., Le Poul, E., Laaris, N., Hamon, M., Lanfumey, L. 1996b. Electrophysiological effects of WAY 100635, a new 5-HT1A receptor antagonist, on dorsal raphe nucleus serotoninergic neurones and CA1 pyramidal cells in vitro.Acta Physiol Hung. 84(4):407-9

Corradetti, R., Laaris, N., Hanoun, N., Laporte, A.M., Le Poul, E., Hamon, M., Lanfumey, L., 1998. Antagonist properties of (-)-pindolol and WAY 100635 at somatodendritic and postsynaptic 5-HT1A receptors in the rat brain. Br. J. Pharmacol. 123(3):449-62.

Cotecchia, S. 2010. The α1-adrenergic receptors: diversity of signaling networks and regulation. J Recept Signal Transduct Res. 30(6):410–419.

Cummings, K.J., Hodges, M.R. 2019. The serotonergic system and the control of breathing during development. Respir Physiol Neurobiol. Jul 27;270:103255. Review.

Cusack, B., Nelson, A., Richelson, E., 1994. Binding of antidepressants to human brain receptors: focus on newer generation compounds. Psychopharmacology (Berl). May; 114(4):559-65

Crespi, F., Martin, K.F., Marsden, C.A., 1988. Measurement of extracellular basal levels of serotonin in vivo using nafion-coated carbon fibre electrodes combined with differential pulse voltammetry. Neuroscience 27, 885-896.

Dahlstrom, A., and Fuxe K., 1964. Evidence for the existence of mono- amine-containing neurons in the central nervous system. I. Demonstration of monoamines in the cell bodies of brainstem neurons. Acta Physiol. Scand. 62(Suppl. 232):l-55.

Daszuta, A., Portalier, P. 1985. Distribution and quantification of 5-HT nerve cellbodies in the nucleus raphe dorsalis area of C57BL and BALBc mice. Relationshipbetween anatomy and biochemistry. Brain Res. Dec 23;360(1-2):58-64.

de Montigny, C., Blier, P., Chaput, Y. 1984. Electrophysiologically-identified serotonin receptors in the rat CNS. Effect of antidepressant treatment. Neuropharmacology. Dec; 23(12B):1511-20. Review.

Delille, H.K., Mezler, M., Marek, G.J. 2013. The two faces of the pharmacological interaction of mGlu2 and 5-HT2A - relevance of receptor heterocomplexes and interaction through functional brain pathways. Neuropharmacology. 2013 Jul;70:296-305. Review.

Descarries, L. , Watkins, K. C., Garcia, S. and Beaudet, A., 1982. The serotonin neurons in nucleus raphe dorsalis of adult rat: A light and electron microscope radioautographic study. J. Comp. Neurol., 207: 239-254.

Di Giovanni, G., Di Matteo, V., Pierucci, M., Benigno, A., Esposito, E. 2006. Serotonin involvement in the basal ganglia pathophysiology: could the 5-HT2C

receptor be a new target for therapeutic strategies? Curr Med Chem. 13(25):3069-81. Review.

Fagiolini, A., Comandini, A., Catena Dell'Osso, M., Kasper, S., 2012. Rediscovering trazodone for the treatment of major depressive disorder. CNS Drugs. 26, 1033-49.

Feige, B., Baglioni, C., Spiegelhalder, K., Hirscher, V., Nissen, C., Riemann, D., 2013. The microstructure of sleep in primary insomnia: an overview and extension. Int. J. Psychophysiol. 89, 171-180. Review.

Foote, S.L., Bloom, F.E., Aston-Jones, G. 1983. Nucleus locus ceruleus: new evidence of anatomical and physiological specificity. Physiol Rev. Jul;63(3):844-914. Review.

Fornal, C.A., Litto, W.J., Metzler, C.W., Marrosu, F., Tada, K., Jacobs, B.L., 1994. Single-unit responses of serotonergic dorsal raphe neurons to 5-HT1A agonist and antagonist drug administration in behaving cats. J. Pharmacol. Exp. Ther. 270, 1345-58.

Fornal, C.A., Metzler, C.W., Gallegos, R.A., Veasey, S.C., McCreary, A.C., Jacobs, B.L., 1996. WAY-100635, a potent and selective 5-hydroxytryptamine1A antagonist, increases serotonergic neuronal activity in behaving cats: comparison with (S)-WAY-100135. J. Pharmacol. Exp. Ther. 278, 752-762.

Fossati, P., Radtchenko, A., Boyer, P. 2004. Neuroplasticity: from MRI to depressive symptoms. Eur Neuropsychopharmacol. Dec;14 Suppl 5:S503-10. Review.

Fuller, R.W., 1994. Uptake inhibitors increase extracellular serotonin concentration measured by brain microdialysis. Life Sci. 55(3):163-7. Review.

Fuxe, K., 1965. Evidence for the existence of monoamine neurons in the central nervous system. iv. distribution of monoamine nerve terminals in the central nervous system. Acta physiol Scand suppl: suppl 247:37.

Gasbarri, A., Pompili, A. 2014. Serotonergic 5-HT7 receptors and cognition. Rev Neurosci. 25(3):311-23. Review.

Geddes, S.D., Assadzada, S., Sokolovski, A., Bergeron, R., Haj-Dahmane, S., Béïque, J.C. 2015. Time-dependent modulation of glutamate synapses onto 5-HT neurons by antidepressant treatment. Neuropharmacology. Aug;95:130-43.

Ghanbari, R., El Mansari, M., Blier, P. 2010a. Sustained Administration of Trazodone Enhances Serotonergic Neurotransmission: In Vivo Electrophysiological Study in the Rat Brain. J. Pharmacol. Exp. Ther. 335(1):197-206.

Ghanbari, R., El Mansari, M., Blier, P. 2010b. Electrophysiological effects of the co-administration of escitalopram and bupropion on rat serotonin and norepinephrine neurons. J Psychopharmacol. 24: 39-50.

Ghanbari, R., El Mansari, M., Blier, P., 2012. Electrophysiological impact of trazodone on the dopamine and norepinephrine systems in the rat brain. Eur. Neuropsychopharmacol. 22, 518-26.

Giannangeli, M., Cazzolla, N., Luparini, M.R., Magnani, M., Mabilia, M., Picconi, G., Tomaselli, M., Baiocchi, L. 1999. Effect of modifications of the alkylpiperazine moiety of trazodone on 5HT2A and alpha1 receptor binding affinity. J Med Chem. Feb 11;42(3):336-45.

Gobert, A., Millan, M.J. 1999. Serotonin (5-HT)2A receptor activation enhances dialysate levels of dopamine and noradrenaline, but not 5-HT, in the frontal cortex of freely-moving rats. Neuropharmacology. Feb;38(2):315-7.

Gobert, A., Rivet, J.M., Lejeune, F., Newman-Tancredi, A., Adhumeau-Auclair, A., Nicolas, J.P., Cistarelli, L., Melon, C., Millan, M.J. 2000. Serotonin(2C) receptors tonically suppress the activity of mesocortical dopaminergic and adrenergic, but not serotonergic, pathways: a combined dialysis and electrophysiological analysis in the rat. Synapse. Jun 1;36(3):205-21.

Gonda, X., Sharma, S.R., Tarazi, F.I. 2019. Vortioxetine: a novel antidepressant for the treatment of major depressive disorder. Expert Opin Drug Discov. Jan;14(1):81-89.

Govoni, S., Cuzzocrea, S., Luchelli, A., Navarra, P., Racchi, M., Scaglione, F., Spampinato, S.M. 2014. Farmacologia. Casa editrice Ambrosiana

Gutknecht, L., Araragi, N., Merker, S., Waider, J., Sommerlandt, F.M., Mlinar, B., Baccini, G., Mayer, U., Proft, F., Hamon, M., Schmitt, A.G., Corradetti, R., Lanfumey, L., Lesch, K.P. 2012. Impacts of brain serotonin deficiency following Tph2 inactivation on development and raphe neuron serotonergic specification. PLoS One. 2012;7(8):e43157.

Guyenet, P.G., Stornetta, R.L., Abbott, S.B., Depuy, S.D., Fortuna, M.G., Kanbar, R. 1985. Central CO2 chemoreception and integrated neural mechanisms of cardiovascular and respiratory control. J Appl Physiol.

Guyenet, P.G., Stornetta, R.L., Bayliss, D.A. 2010. Central respiratory chemoreception. J Comp Neurol. 2010 Oct 1;518(19):3883-906. Review.

Hagena, H., Manahan-Vaughan, D. 2017. The serotonergic 5-HT4 receptor: A unique modulator of hippocampal synaptic information processing and cognition. Neurobiol Learn Mem. Feb;138:145-153. Review.

Hajós, M., Richards, C.D., Székely, A.D., Sharp, T. 1998. An electrophysiological and neuroanatomical study of the medial prefrontal cortical projection to the midbrain raphe nuclei in the rat. Neuroscience. Nov;87(1):95-108.

Hajszan, T., MacLusky, N.J., Leranth, C. 2005. Short-term treatment with the antidepressant fluoxetine triggers pyramidal dendritic spine synapse formation inrat hippocampus. Eur J Neurosci. Mar;21(5):1299-303.

Harrington, M.A., Shaw, K., Zhong, P., Ciaranello, R.D. 1994. Agonist-induced desensitization and loss of high-affinity binding sites of stably expressed human 5-HT1A receptors. J Pharmacol Exp Ther. Mar;268(3):1098-106.

Hartig, P.R., Branchek, T.A., Weinshank, R.L. 1992. A subfamily of 5-HT1D receptor genes.Trends Pharmacol Sci. Apr;13(4):152-9. Review.

Heisler, L.K., Zhou, L., Bajwa, P., Hsu, J., Tecott, L.H. 2007. Serotonin 5-HT(2C) receptors regulate anxiety-like behavior. Genes Brain Behav. Jul;6(5):491-6.

Hensler, J., Durgam, H. 2001. Regulation of 5-HT(1A) receptor-stimulated [35S]-GtpgammaS binding as measured by quantitative autoradiography following chronic agonist administration. Br J Pharmacol. Jan;132(2):605-11.

Hensler, J.G. 2003. Regulation of 5-HT1A receptor function in brain following agonist or antidepressant administration. Life Sci. Feb 28;72(15):1665-82. Review.

Hervás, I., Vilaró, M.T., Romero, L., Scorza, M.C., Mengod, G., Artigas, F. 2001. Desensitization of 5-HT(1A) autoreceptors by a low chronic fluoxetine dose effect of the concurrent administration of WAY-100635. Neuropsychopharmacol. 24: 11-20.

Heusler, P., Pauwels, P.J., Wurch, T., Newman-Tancredi, A., Tytgat, J., Colpaert, F.C., Cussac, D. 2005. Differential ion current activation by human 5-HT(1A) receptors in Xenopus oocytes: evidence for agonist-directed trafficking of receptor signalling. Neuropharmacology. Dec;49(7):963-76.

Hodges, M.R., Richerson, G.B. 2008. Contributions of 5-HT neurons to respiratory control: neuromodulatory and trophic effects. Respir Physiol Neurobiol. Dec 10;164(1-2):222-32.

Hornung, J.P. 2003. The human raphe nuclei and the serotonergic system. J Chem Neuroanat. Dec;26(4):331-43. Review.

Hoyer, D., Clarke, D.E., Fozard, J.R., Hartig, P.R., Martin, G.R., Mylecharane, E.J., Saxena, P.R., Humphrey, P.P. 1994. International Union of Pharmacology classification of receptors for 5-hydroxytryptamine (Serotonin). Pharmacol Rev. Jun;46(2):157-203. Review.

Hyman, S.E., 2010. The diagnosis of mental disorders: the problem of reification. Annu Rev Clin Psychol. 6:155-79. Review.

Ishimura, K., Takeuchi, Y., Fujiwara, K., Tominaga, M., Yoshioka, H., Sawada, T. 1988. Quantitative analysis of the distribution of serotonin-immunoreactive cell bodiesin the mouse brain. Neurosci Lett. Sep 12;91(3):265-70.

Jacobs, B.L., Foote, S.L., and Bloom, F.E., 1978. Differential projections of neurons withinthe dorsal raphe nucleus of the rat: A horseradish peroxidase (HRP) study. BrainRes 147:149–153.

Jacobs, B.L., 1986. Single unit activity of locus coeruleus neurons in behaving animals. Prog. Neurobiol.27(2), 183-194.

Jacobs, B.L., Azmitia, E.C. 1992. Structure and function of the brain serotonin system. Physiol Rev. Jan;72(1):165-229. Review

Jacobs, B.L., and Fornal, C.A., 1993. 5-HT and motor control: A hypothesis. TrendsNeurol Sci 16:346–351

Jankowski, M.P., Sesack, S.R. 2004. Prefrontal cortical projections to the rat dorsal raphe nucleus: ultrastructural features and associations with serotonin and gamma-aminobutyric acid neurons. J Comp Neurol. Jan 19;468(4):518-29.

Jarrett, R.B., Schaffer, M., McIntire, D., Witt-Browder, A., Kraft, D., Risser, R.C., 1999. Treatment of Atypical Depression With Cognitive Therapy or Phenelzine: A Double-blind, Placebo-Controlled Trial. Arch Gen Psychiatry. 56(5):431–437.

Jentsch, M.C., Van Buel, E.M., Bosker, F.J., Gladkevich, A.V., Klein, H.C., Oude Voshaar, R.C., Ruhé, E.G., Eisel, U.L., Schoevers, R.A. 2015. Biomarker approaches in major depressive disorder evaluated in the context of current hypotheses. Biomark Med. 9(3):277-97.

Kale, P., Agrawal, Y.K. 2015. Pharmacokinetics of single oral dose trazodone: a randomized, two-period, cross-over trial in healthy, adult, human volunteers under fed condition. Front Pharmacol. Oct 2;6:224.

Karhu, D., Groenewoud, G., Potgieter, M.A., Mould, D.R., 2010. Dose proportionality of oncedaily trazodone extended-release caplets under fasting conditions. J. Clin. Pharmacol. 50, 1438-1449.

Katayama, J., Yakushiji, T., Akaike, N. 1997. Characterization of the K+ current mediated by 5-HT1A receptor in the acutely dissociated rat dorsal raphe neurons. Brain Res. Jan 16;745(1-2):283-92.

Khoury, R., Grysman, N., Gold, J., Patel, K., Grossberg, G.T. 2018. The role of 5 HT6-receptor antagonists in Alzheimer's disease: an update. Expert Opin Investig Drugs. Jun;27(6):523-533. Review.

Köhler, S., Cierpinsky, K., Kronenberg, G., Adli, M. 2016. The serotonergic system in the neurobiology of depression: Relevance for novel antidepressants. J Psychopharmacol. Jan;30(1):13-22.

Krege, S., Goepel, M., Sperling, H., Michel, M.C. 2000. Affinity of trazodone for human penile alpha1- andalpha2-adrenoceptors. BJU Int. May;85(7):959-61.

Krieger, M.S., Conrad, L.C., Pfaff, D.W. 1979. An autoradiographic study of the efferentconnections of the ventromedial nucleus of the hypothalamus. J Comp Neurol. Feb 15;183(4):785-815.

Le Poul, E., Boni, C., Hanoun, N., Laporte, A.M., Laaris, N., Chauveau, J., Hamon, M., Lanfumey, L. 2000. Differential adaptation of brain 5-HT1A and 5-HT1B receptors and 5-HT transporter in rats treated chronically with fluoxetine. Neuropharmacology. 39(1):110-22.

Lesch, K.P., Araragi, N., Waider, J., van den Hove, D., Gutknecht, L., 2012. Targeting brain serotonin synthesis: insights into neurodevelopmental disorders with long-term outcomes related to negative emotionality, aggression and antisocial behaviour. Philos. Trans. R. Soc. Lond. B Biol. Sci.67, 2426-2443.

Levine., E.S., Jacobs, B.L., 1992. Neurochemical afferents controlling the activity of serotonergic neurons in the dorsal raphe nucleus: microiontophoretic studies in the awake cat. J. Neurosci. 12, 4037-4044

Li, Y.Q., Li, H., Kaneko, T., Mizuno, N. 2001. Morphological features and electrophysiological properties of serotonergic and non-serotonergic projection neurons in the dorsal raphe nucleus. An intracellular recording and labeling study in rat brain slices. Brain Res. May 4;900(1):110-8.

Liebowitz, M.R., Quitkin, F.M., Stewart, J.W., 1984. Phenelzine v Imipramine in Atypical Depression: A Preliminary Report. Arch Gen Psychiatry. 41(7):669–677.

Liu, R.J., Jolas, T. Aghajanian, G. 2000. Serotonin 5-HT(2) receptors activate local GABA inhibitory inputs to serotonergic neurones of the dorsal raphe nucleus. Brain Res 873, 34-45.

Llamosas, N., Bruzos-Cidón, C., Rodríguez, J.J., Ugedo, L., Torrecilla, M. 2015. Deletion of GIRK2 Subunit of GIRK Channels Alters the 5-HT1A Receptor-Mediated Signaling and Results in a Depression-Resistant Behavior. Int J Neuropsychopharmacol. May 8;18(11):pyv051.

Lowell, B.B., Flier, J.S. 1997. Brown adipose tissue, beta 3-adrenergic receptors, and obesity. Annu Rev Med. 48:307-16. Review.

López-Giménez, J.F., Vilaró, M.T., Palacios, J.M., Mengod, G. 2001. Mapping of 5-HT2A receptors and their mRNA in monkey brain: [3H]MDL100,907 autoradiography and in situ hybridization studies. J Comp Neurol. Jan 22;429(4):571-89.

Malenka, R.C., Nestler, E.J., Hyman, S.E. 2009. Molecular Neuropharmacology: A Foundation for Clinical Neuroscience (2nd ed.). New York: McGraw-Hill Medical. Sydor A, Brown RY (eds.).

Mannoury la Cour, C., El Mestikawy, S., Hanoun, N., Hamon, M., Lanfumey, L. 2006. Regional differences in the coupling of 5-hydroxytryptamine-1A receptors to G proteins in the rat brain. Mol Pharmacol. Sep;70(3):1013-21. Epub 2006 Jun 13.

Meneses, A. 2014. Memory formation and memory alterations: 5-HT6 and 5-HT7 receptors, novel alternative. Rev Neurosci. 25(3):325-56. Review.

Manji, H.K., Quiroz, J.A., Sporn, J., Payne, J.L., Denicoff, K., A. Gray, N., Zarate, C.A. Jr.,Charney, D.S. 2003. Enhancing neuronal plasticity and cellular resilience to developnovel, improved therapeutics for difficult-to-treat depression. Biol Psychiatry. Apr 15;53(8):707-42. Review.

Marinelli, S., Schnell, S.A., Hack, S.P., Christie, M.J., Wessendorf, M.W., Vaughan, C.W. 2004. Serotonergic and nonserotonergic dorsal raphe neurons are pharmacologically and electrophysiologically heterogeneous. J Neurophysiol. Dec;92(6):3532-7.

McGinty, D.J., and Harper, R.M., 1976. Dorsal raphe neurons depression of firing during sleep in cats. Brain Res 101:569–575.

McMillen, B.A., Scott, S.M., Williams, H.L., Sanghera, M.K. 1987. Effects of gepirone, an aryl-piperazine anxiolytic drug, on aggressive behavior and brain monoaminergic neurotransmission. Naunyn Schmiedebergs Arch Pharmacol. Apr;335(4):454-64.

Meltzer, H.Y. 2012. Serotonergic mechanisms as targets for existing and novel antipsychotics. Handb Exp Pharmacol. (212):87-124. Review.

Mengod, G., Palacios, J.M., Cortés, R. 2015. Cartography of 5-HT1A and 5-HT2A Receptor Subtypes in Prefrontal Cortex and Its Projections. ACS Chem Neurosci. Jul 15;6(7):1089-98. Review.

Millan, M.J., Dekeyne, A., Gobert, A. 1998. Serotonin (5-HT)2C receptors tonically inhibit dopamine (DA) and noradrenaline (NA), but not 5-HT, release in the frontal cortex in vivo. Neuropharmacology. Jul;37(7):953-5.

Mitchell, P.B., Mitchell, M.S. 1994. The management of depression. Part 2. The place ofthe new antidepressants. Aust Fam Physician. Sep;23(9):1771-3, 1776-81. Review.

Mitchell, E.S., Neumaier, J.F 2005. 5-HT6 receptors: a novel target for cognitive enhancement. Pharmacol Ther. Dec;108(3):320-33. Epub 2005 Jul 7. Review.

Mlinar, B., Tatini, F., Ballini, C., Nencioni, S., Della Corte, L., Corradetti, R., 2005. Differential autoinhibition of 5-hydroxytryptamine neurons by 5-hydroxytryptamine in the dorsal raphe nucleus. Neuroreport 16, 1351-1355.

Mlinar, B., Montalbano, A., Baccini, G., Tatini, F., Berlinguer Palmini, R., Corradetti, R., 2015a. Nonexocytotic serotonin release tonically suppresses serotonergic neuron activity. J Gen Physiol.;145(3):225–251.

Mlinar, B., Montalbano, A., Piszczek, L., Gross, C., Corradetti, R., 2016. Firing Properties of Genetically Identified Dorsal Raphe Serotonergic Neurons in Brain Slices. Front Cell Neurosci. Aug 3;10:195.

Mohammad-Zadeh, L.F., Moses, L., Gwaltney-Brant, S.M. 2008. Serotonin: a review. J Vet Pharmacol Ther. 2008 Jun;31(3):187-99. Review.

Molleman, A. 2003. Patch Clamping: An Introductory Guide To Patch Clamp Electrophysiology.

Montalbano, A., Waider, J., Barbieri, M., Baytas, O., Lesch, K.P., Corradetti, R., Mlinar,B. 2015a. Cellular resilience: 5-HT neurons in Tph2(-/-) mice retain normal firing behavior despite the lack of brain 5-HT. Eur Neuropsychopharmacol. Nov;25(11):2022-35.

Montalbano, A., Corradetti, R., Mlinar, B., 2015b. Pharmacological Characterization of 5-HT1A Autoreceptor-Coupled GIRK Channels in Rat Dorsal Raphe 5-HT Neurons. PLoS One. Oct 13;10(10):e0140369.

Montalbano, A., Mlinar, B., Bonfiglio, F., Polenzani, L., Magnani, M., Corradetti, R. 2019. Dual inhibitory action of trazodone on dorsal raphe serotonergic neurons through 5-HT1A receptor partial agonism and α1-adrenoceptor antagonism. PLoS One. Sep 26;14(9):e0222855.

Morrison, J.H., Molliver, M.E., Grzanna, R., Coyle, J.T. 1981. The intra-cortical trajectoryof the coeruleo-cortical projection in the rat: a tangentially organized corticalafferent. Neuroscience.6(2):139-58.

Mosko, S.S., Haubrich, D. and Jacobs, B.L. 1977. Serotonergic afferents to the dorsalraphe nucleus: Evidence from HRP and synaptosomal uptake studies. Brain Res. 119:269–290.

Mössner, R., Freitag, C.M., Gutknecht, L., Reif, A., Tauber, R., Franke, P., Fritze, J., Wagner, G., Peikert, G., Wenda, B., Sand, P., Rietschel, M., Garritsen, H., Jacob, C., Lesch, K.P., Deckert, J. 2006. The novel brain-specific tryptophan hydroxylase-2 gene in panic disorder. J Psychopharmacol. Jul;20(4):547-52.

Nikolaev, Y.A., Dosen, P.J., Laver, D.R., van Helden, D.F., Hamill, O.P. 2015. Single mechanically-gated cation channel currents can trigger action potentials in neocortical and hippocampal pyramidal neurons. Brain Res. May 22;1608:1-13.

Odagaki, Y., Toyoshima, R., Yamauchi, T., 2005. Trazodone and its active metabolite m-chlorophenylpiperazine as partial agonists at 5-HT1A receptors assessed by [35S]GTPγS binding. J. Psychopharmacol. 19:235–241.

Owens, M.J., Morgan, W.N., Plott, S.J., Nemeroff, C.B., 1997. Neurotransmitter receptor and transporter binding profile of antidepressants and their metabolites. J. Pharmacol. Exp. Ther. 283:1305–1322.

Pauwels, P.J., Van Gompel, P., Leysen, J.E. 1993. Activity of serotonin (5-HT) receptor agonists, partial agonists and antagonists at cloned human 5-HT1A receptors that are negatively coupled to adenylate cyclase in permanently transfected HeLa cells. Biochem Pharmacol. Jan 26;45(2):375-83.

Pauwels, P.J., Colpaert, F.C. 2003. Ca2+ responses in Chinese hamster ovary-K1 cells demonstrate an atypical pattern of ligand-induced 5-HT1A receptor activation. J Pharmacol Exp Ther. Nov;307(2):608-14.

Pazzagli, M., Giovannini, M.G., Pepeu, G., 1999. Trazodone increases extracellular serotonin levels in the frontal cortex of rats. Eur. J. Pharmacol. 383, 249-257.

Pellegrino, M., Pellegrini, M., Simoni, A., Gargini, C. 1990. Stretch-activated cation channels with large unitary conductance in leech central neurons. Brain Res. Aug 20;525(2):322-6.

Penington, N.J., Kelly, J.S. 1990. Serotonin receptor activation reduces calcium current in an acutely dissociated adult central neuron. Neuron. May;4(5):751-8.

Penington, N.J., Kelly, J.S., Fox, A.P. 1993. Whole-cell recordings of inwardly rectifying K+ currents activated by 5-HT1A receptors on dorsal raphe neurones of the adult rat. J Physiol. Sep;469:387-405.

Pennanen, L., van der Hart, M., Yu, L., Tecott, L.H. 2013. Impact of serotonin (5-HT)2C receptors on executive control processes. Neuropsychopharmacology. May;38(6):957-67.

Pereira, V.S., Hiroaki-Sato, V.A. 2018. A brief history of antidepressant drug development: from tricyclics to beyond ketamine. Acta Neuropsychiatr. Dec;30(6):307-322. Review.

Peyron, C., Petit, J.M., Rampon, C., Jouvet, M., Luppi, P.H. 1998. Forebrain afferents to therat dorsal raphe nucleus demonstrated by retrograde and anterograde tracingmethods. Neuroscience. Jan;82(2):443-68.

Piñeyro, G., Blier, P., 1999. Autoregulation of serotonin neurons: role in antidepressant drug action. Pharmacol Rev. Sep;51(3):533-91. Review.

Pittenger, C., Duman, R.S. 2008. Stress, depression, and neuroplasticity: a convergence of mechanisms. Neuropsychopharmacology. Jan;33(1):88-109. Review.

Portella, M.J., de Diego-Adeliño, J., Ballesteros, J., Puigdemont, D., Oller, S., Santos, B., Álvarez, E., Artigas, F., Pérez, V. 2011. Can we really accelerate and enhance the selective serotonin reuptake inhibitor antidepressant effect? A randomized clinical trial and a meta-analysis of pindolol in nonresistant depression. J Clin Psychiatry. Jul;72(7):962-9.

Qin, K., Sethi, P.R., Lambert, N.A. 2008. Abundance and stability of complexes containinginactive G protein-coupled receptors and G proteins. FASEB J. Aug;22(8):2920-7.

Quiedeville, A., Boulouard, M., Da Silva Costa-Aze, V., Dauphin, F., Bouet, V., Freret, T. 2014. 5-HT6 receptor antagonists as treatment for age-related cognitive decline. Rev Neurosci. 25(3):417-27.

Ramirez, M.J., Lai, M.K., Tordera, R.M., Francis, P.T. 2014. Serotonergic therapies for cognitive symptoms in Alzheimer's disease: rationale and current status. Drugs. May;74(7):729-36. Review.

Raymond, J.R., Mukhin, Y.V., Gettys, T.W., Garnovskaya, M.N. 1999. The recombinant 5-HT1A receptor: G protein coupling and signalling pathways. Br J Pharmacol. Aug;127(8):1751-64. Review.

Rebholz, H., Friedman, E., Castello, J. 2018. Alterations of Expression of the Serotonin 5-HT4 Receptor in Brain Disorders. Int J Mol Sci. Nov 13;19(11). pii: E3581. Review.

Riad, M., Garcia, S., Watkins, K.C., Jodoin, N., Doucet, E., Langlois, X., el Mestikawy, S., Hamon, M., Descarries, L. 2000. Somatodendritic localization of 5-HT1A and preterminal axonal localization of 5-HT1B serotonin receptors in adult rat brain. J Comp Neurol 417:181–94.

Ruhé, H.G., Mason, N.S., Schene, A.H., 2007. Mood is indirectly related to serotonin, norepinephrine and dopamine levels in humans: a meta-analysis of monoamine depletion studies. Mol Psychiatry. 2007 Apr;12(4):331-59. Epub Jan 16. Review.

Rush, A.J., Trivedi, M.H., Wisniewski, S.R., Nierenberg, A.A., Stewart, J.W., Warden, D., Niederehe, G., Thase, M.E., Lavori, P.W., Lebowitz, B.D., McGrath, P.J., Rosenbaum, J.F., Sackeim, H.A., Kupfer, D.J., Luther, J., Fava, M. 2006. Acute and longer-term outcomes in depressed outpatients requiring one or several treatment steps: a STAR*D report. Am J Psychiatry. Nov;163(11):1905-17.

Sakai, K., Crochet, S. 2000. Serotonergic dorsal raphe neurons cease firing by disfacilitation during paradoxical sleep. Neuroreport. 11(14), 3237-41.

Sanchez, C., Asin, K.E., Artigas, F. 2015. Vortioxetine, a novel antidepressant with multimodal activity: review of preclinical and clinical data. Pharmacol Ther. Jan;145:43-57. Review.

Santana, N., Artigas, F. 2017a. Laminar and Cellular Distribution of Monoamine Receptors in Rat Medial Prefrontal Cortex. Front Neuroanat. Sep 28;11:87.

Santana, N., Artigas, F. 2017b. Expression of Serotonin2C Receptors in Pyramidal and GABAergic Neurons of Rat Prefrontal Cortex: A Comparison with Striatum. Cereb Cortex. Jun 1;27(6):3125-3139.

Saper, C.B., Swanson, L.W., Cowan, W.M. 1976. The efferent connections of the ventromedial nucleus of the hypothalamus of the rat. J Comp Neurol. Oct 15;169(4):409-42.

Saper, C.B., Fuller, P.M., Pedersen, N.P., Lu, J., Scammell, T.E., 2010. Sleep state switching. Neuron. 68,1023-1042.

Sargent, P.A., Sharpley, A.L., Williams, C., Goodall, E.M., Cowen, P.J. 1997. 5-HT2C receptor activation decreases appetite and body weight in obese subjects. Psychopharmacology (Berl). Oct;133(3):309-12.

Schildkraut, J.J. 1965. The catecholamine hypothesis of affective disorders: a review of supporting evidence. Am J Psychiatry. Nov;122(5):509-22. Review.

Schofield, S.P.M., and Everitt, B.J., 1981. The organization of indoleamine neurons in thebrain of the rhesus monkey (Macaca mulatta). J Comp Neurol 197:369–383.

Scuvée-Moreau, J., Dresse, A., 1982. Effect of trazodone on the firing rate of central monoaminergic neurons. Comparison with various antidepressants. Arch. Int. Pharmacodyn. Ther. 260:299–301.

Serrats, J., Mengod, G., Cortés, R. 2005. Expression of serotonin 5-HT2C receptors in GABAergic cells of the anterior raphe nuclei. J Chem Neuroanat. Mar;29(2):83-91.

Settimo, L., Taylor, D. 2018. Evaluating the dose-dependent mechanism of action of trazodone by estimation of occupancies for different brain neurotransmitter targets. J Psychopharmacol. 32, 96-104.

Sharp, T., Bramwell, S.R., Grahame-Smith, D.G., 1989. 5-HT1 agonists reduce 5-hydroxytryptamine release in rat hippocampus in vivo as determined by brain microdialysis. Br J Pharmacol. Feb;96(2):283-90

Sharp, T., Boothman, L., Raley, J., Quérée, P. 2007. Important messages in the 'post': recent discoveries in 5-HT neurone feedback control. Trends Pharmacol Sci. Dec;28(12):629-36. Epub Nov 9. Review.

Sharp, T. 2010. Handbook of Behavioral Neurobiology of Serotonin chapter 2.6 – Edited by Müller, C.P. and Jacobs, B. Academic Press.

Sheehan, D.V., Croft, H.A, Gossen, E.R., Levitt, R.J., Brullè, C., Bouchard, S., Rozova, A., 2009. Extended-release trazodone in major depressive disorder: a randomized, double-blind, placebo controlled study. Psychiatry 6, 20-33.

Shen, R.Y., Andrade, R. 1998. 5-Hydroxytryptamine2 receptor facilitates GABAergic neurotransmission in rat hippocampus. J Pharmacol Exp Ther. May;285(2):805-12.

Shen, C., Li, H., Meller, E. 2002. Repeated treatment with antidepressants differentially alters 5-HT1A agonist-stimulated [35S]GTP gamma S binding in rat brain regions. Neuropharmacology. Jun;42(8):1031-8.

Soiza-Reilly, M., Commons, K. G. 2011. Glutamatergic drive of the dorsal raphe nucleus. Journal of chemical neuroanatomy, 41(4), 247–255.

Sprouse, J.S., Aghajanian, G.K., 1987. Electrophysiological responses of serotoninergic dorsal raphe neurons to 5-HT1A and 5-HT1B agonists. Synapse.;1(1):3-9.

Stahl, S. M. 1998. Basic psychopharmacology of antidepressants: Part 1. Antidepressants have seven distinct mechanisms of action. The Journal of Clinical Psychiatry, 59(Suppl 4), 5-14.

Stahl, S.M., Felker, A. 2008. Monoamine oxidase inhibitors: a modern guide to an unrequited class of antidepressants. CNS Spectr. Oct;13(10):855-70. Review.

Stahl, S.M. 2009a. Stahl's Illustrated Antidepressants. Cambridge University Press.

Stahl, S.M., 2009b. Mechanism of action of trazodone: a multifunctional drug. CNS Spectr. 14, 536-346.

Stark, A.D., Jordan, S., Allers, K.A., Bertekap, R.L., Chen, R., Mistry Kannan, T., Molski, T.F., Yocca, F.D., Sharp, T., Kikuchi, T., Burris, K.D. 2007. Interaction of the novel antipsychotic aripiprazole with 5-HT1A and 5-HT 2A receptors: functional receptor-binding and in vivo electrophysiological studies. Psychopharmacology (Berl). Feb;190(3):373-82.

Steinbusch, H.W., Verhofstad, A.A., Joosten, H.W. 1978. Localization of serotonin in the central nervous system by immunohistochemistry: description of a specific andsensitive technique and some applications. Neuroscience. 3(9):811-9.

Steinbusch, H.W.M., 1981. Distribution of serotonin-immunoreactivity in the central nervous system of the rat-Cell bodies and terminals. Neuroscience 4557-618.

Stiedl, O., Pappa, E., Konradsson-Geuken, Å., Ögren, S.O. 2015. The role of the serotonin receptor subtypes 5-HT1A and 5-HT7 and its interaction in emotional learning and memory. Front Pharmacol. Aug 7;6:162. Review.

Strader, C.D., Fong, T.M., Tota, M.R., Underwood, D., Dixon, R.A. 1994. Structure and function of G protein-coupled receptors. Annu Rev Biochem. 63:101-32. Review.

Sundaram, H., Newman-Tancredi, A., Strange, P.G., 1993. Characterization of recombinant human serotonin 5HT1A receptors expressed in Chinese hamster ovary cells. [3H]spiperone discriminates between the G-protein-coupled and -uncoupled forms. Biochem. Pharmacol. 45, 1003-1009.

Swanson, L.W., Hartman, B.K. 1975. The central adrenergic system. An immunofluorescence study of the location of cell bodies and their efferent connections in the rat utilizing dopamine-beta-hydroxylase as a marker. J Comp Neurol. Oct 15;163(4):467-505

Swanson, L.W. 1976. The locus coeruleus: a cytoarchitectonic, Golgi and immunohistochemical study in the albino rat. Brain Res. Jun 25;110(1):39-56.

Theroux, T.L., Esbenshade, T.A., Peavy, R.D., Minneman, K.P. 1996. Coupling efficiencies of human alpha 1-adrenergic receptor subtypes: titration of receptor density and responsiveness with inducible and repressible expression vectors. Mol Pharmacol. Nov;50(5):1376-87.

Trulson, M.E., Jacobs, B.L., 1979. Raphe unit activity in freely moving cats: correlation with level of behavioural arousal. Brain Res. 163, 135-150

Valdizán, E.M., Castro, E., Pazos, A. 2010. Agonist-dependent modulation of G-protein coupling and transduction of 5-HT1A receptors in rat dorsal raphe nucleus. Int J Neuropsychopharmacol. Aug;13(7):835-43.

Valentino, R.J., Bey, V., Pernar, L., Commons, K.G. 2003. Substance P Acts through localcircuits within the rat dorsal raphe nucleus to alter serotonergic neuronalactivity. J Neurosci. 2003 Aug 6;23(18):7155-9.

Vandermaelen, C.P., Aghajanian, G.K., 1983. Electrophysiological and pharmacological characterization of serotonergic dorsal raphe neurons recorded extracellularlyand intracellularly in rat brain slices. Brain Res. Dec 19;289(1-2):109-19.

Vandermaelen, C.P., Matheson, G.K., Wilderman, R.C., Patterson, L.A. 1986. Inhibition of serotonergic dorsal raphe neurons by systemic and iontophoretic administration of buspirone, a non-benzodiazepine anxiolytic drug. Eur J Pharmacol. Sep 23;129(1-2):123-30.

Vertes, R.P. 2004. Differential projections of the infralimbic and prelimbic cortex inthe rat. Synapse. Jan;51(1):32-58.

Voigt, M.M., Laurie, D.J., Seeburg, P.H., Bach, A. 1991. Molecular cloning and characterization of a rat brain cDNA encoding a 5-hydroxytryptamine1B receptor. EMBO J. Dec;10(13):4017-23.

Vythilingam, M., Vermetten, E., Anderson, G.M., Luckenbaugh, D., Anderson, E.R., Snow, J., Staib, L.H., Charney, D.S., Bremner, J.D. 2004. Hippocampal volume, memory, and cortisol status in major depressive disorder: effects of treatment. Biol Psychiatry. Jul 15;56(2):101-12.

Waeber, C., Moskowitz, M.A., 1995. Autoradiographic visualisation of [3H]5-carboxamidotryptamine binding sites in the guinea pig and rat brain. Eur. J. Pharmacol. 283, 31-46.

Walker, E.P., Tadi, P. 2019. Neuroanatomy, Nucleus Raphe. Jun 16. StatPearls [Internet]. Treasure Island (FL): StatPearls Publishing; 2019 Jan-. Available from http://www.ncbi.nlm.nih.gov/books/NBK544359/.

Waterhouse, B.D., Mihailoff, G.A., Baack, J.C., and Woodward, D.J., 1986. Topographicaldistribution of dorsal and median raphe neurons projecting to motor, sensorimotorand visual cortical areas in the rat. J Comp Neurol 249:460–476.

Williams, J.T., Colmers, W.F., Pan, Z.Z. 1988. Voltage- and ligand-activated inwardly rectifying currents in dorsal raphe neurons in vitro. J Neurosci. Sep;8(9):3499-506.

World Health Organization. (2016). Depression: fact sheet. Available online at: http://www.who.int/mediacentre/factsheets/fs369/en/

Young, S.N., 2007. How to increase serotonin in the human brain without drugs. J Psychiatry Neurosci.;32(6):394–399.

Yun, H.M., Rhim, H. 2011. The serotonin-6 receptor as a novel therapeutic target. Exp Neurobiol. Dec;20(4):159-68.

Zareifopoulos, N., Papatheodoropoulos, C. 2016. Effects of 5-HT-7 receptor ligands on memory and cognition. Neurobiol Learn Mem. Dec;136:204-209. Review.

Zgombick, J.M., Borden, L.A., Cochran, T.L., Kucharewicz, S.A., Weinshank, R.L., Branchek, T.A. 1993. Dual coupling of cloned human 5-hydroxytryptamine1D alpha and 5-hydroxytryptamine1D beta receptors stably expressed in murine fibroblasts: inhibition of adenylate cyclase and elevation of intracellular calcium concentrations via pertussis toxin-sensitive G protein(s). Mol Pharmacol. Sep;44(3):575-82.

Appendix 1:

Consequences of the lack of serotonin on hippocampal synaptic plasticity in fear conditioning.

In addition to determining with accuracy the electrophysiological and pharmacological properties of trazodone on 5-HT_{1A} autoreceptors of serotonergic neurons of dorsal raphe nucleus, I partecipated in a collaboration with prof. K. P. Lesch's laboratory in Würzburg (Germany) directed to study the role of serotonergic modulation of behavioural response to fear conditioning using a transgenic mice line lacking brain serotonin.
My experimental contribution was the study of synaptic plasticity recorded *in vitro* from the *cornu ammonis* 1 (CA1) region of the hippocampus in slices taken from $Tph2^{-/-}$ mice and their littermates $Tph2^{+/-}$ and $Tph2^{+/+}$. To this purpose I used the parameter of long-term potentiation (LTP) of extracellularly recorded field excitatory postsynaptic potentials (fEPSPs) induced by theta burst stimulation (TBS) of the stratum radiatum in the CA1 region of hippocampal slices.
My experimental participation was inscribed in a complex project encompassing neurochemical and behavioural methodologies. The results of the whole research have been published (Waider et al., 2017; 2019) and therefore in this appendix I will only give an brief account of the specific results that I obtained within the collaboration reported in the article enclosed at the end of the thesis (Waider et al., 2019). Furthermore, as the technical details of the electrophysiological methodology are only succintly reported in the article, I will describe in more detail the experimental procedures that I applied for investigating synaptic plasticity in the hippocampus.

The $Tph2^{-/-}$ mouse model.

The $Tph2^{-/-}$ strain was generated in Lesch's laboratories from injections of a targeting vector into blastocysts implanted into pseudopregnant C57BL/6. The vector was designed to remove exon 5 of the *Tph2* gene with a flanking sequences (*XhoI-XhoI* deletion) by homologous recombination in wild-type genomic DNA (Gutknecht et al., 2008). The main use of this mouse strain newly generated in te frame of an EC funded collaborative project that involved our laboratory was to analyze the significance of brain serotonin in development and to understand and the differentiation and specification of the serotonergic system itself in the brain (Gutknecht et al., 2012). The main characteristic of this mouse line is that $Tph2^{-/-}$ mice are completely deprived of brain Tph2, the rate-limiting enzyme that catalyzes the hydroxylation of tryptophan to 5-hydroxytryptophan for its next transformation into serotonin. Moreover, this mouse line preserves the production of Tph1 enzyme that is instead located in the gut,

spleen, pineal gland and thymus (Walther and Bader, 2003; Walther et al., 2003; Gutknecht et al., 2009).
This mouse line is significantly different from other lines, i.e. *Nkx2.2* knockout (Briscoe et al., 1999), conditional *Lmx1b* knockout (Ding et al., 2003; Zhao et al., 2006), *Pet1*-deficient mice (Hendricks et al., 2003), *BALB/cJ* mice (Zhang et al., 2004), mutant *Tph2* mice (Beaulieu et al., 2008), because in none of these mice a total loss of brain serotonin is specifically obtained. Indeed, in most of cases the deficiency of brain serotonin is obtained by ablation, often incomplete, of serotonergic neurons (e.g. *Lmx1b* knockout and *Pet1*-deficient mice). In $Tph2^{-/-}$ mice, instead, serotonergic neurons are preserved and therefore any possible additional property of these neurons beside the synthesis of serotonin (e.g. glutamate release from serotonergic neurons: Wang et al., 2019) likely remains present *in vivo*.
The most evident developmental consequence of life-long absence of brain serotonin is body growth retardation (Alenina et al., 2009; Gutknecht et al., 2012). Indeed, $Tph2^{-/-}$ mice are considerably smaller than their $Tph2^{+/+}$ and $Thp2^{+/-}$ littermates. Nonetheless, neuron-specific serotonergic markers (except for serotonin and Tph2) are preserved and only slight upregulation in the expression of 5-HT_{1A} and 5-HT_{1B} receptors has been found (Compan et al., 1998; Gutknecht et al., 2012). Moroeover, electrophysiological properties of serotonergic neurons as firing rate and spike shape are preserved (Montalbano et al., 2015a). It should however be noted that in $Tph2^{-/-}$ mice the sensitivity of 5-HT_{1A} receptors to agonist activation is increased in comparison to that of their littermates while the density of functional receptors seems unaltered (Mlinar et al., 2017).
Even taking into account the intrinsic limits introduced by the life-long deficit of brain serotonin that could have produced adaptive consequences on higher brain functions, the $Tph2^{-/-}$ mouse line provides an useful model to investigate the possible role of the serotonergic system in regulating important brain mechanism as the regulation of panic behavour and fear responses (Mössner et al., 2006; Waider et al., 2017; 2019).

The role of serotonin in regulating synaptic plasticity in dorsal hippocampus.

In a previous paper from our collaborators, the $Tph2^{-/-}$ mouse model was used to conduct behavioural and electrophysiological experiments to study the pathophysiology of stressor- and anxiety-related disorders (Waider et al., 2017). In particular, that work highlighted the importance of brain serotonin to modulate GABAergic transmission of the basolateral amygdala. Since the hippocampus and the amygdala are tightly connected (Karst et al., 2005; Bienvenu et al., 2012; Bazelot et al., 2015) and our laboratory had previously demonstrated that, *in vitro*, endogenously released serotonin facilitates TBS-induced LTP of excitatory post-synaptic potentials in the hippocampal CA1 region (Mlinar et al., 2015b), we decided to focus on the role of serotonin in modulating synaptic plasticity in the dorsal hippocampus when an inescapable fearful stimulus occurs (Dai et al., 2008) by comparing the effects of the

foot shock protocol delivered *in vivo* on TBS-induced LTP of synaptic responses in slices taken from $Tph2^{-/-}$ mice and their littermates $Tph2^{+/-}$ and $Tph2^{+/+}$.
It is worth to remind that our recordings were conducted *ex vivo*, i.e. after the effects of serotonin on synaptic plasticity had occurred *in vivo*. Because LTP is a saturable and long-lasting phenomenon it is to be expected that the stimulation applied *in vitro* will be effective only on the synapses that were left unpotentiated during the behavioural activation of the hippocampus. Therefore, the magnitude of synaptic LTP measured under these conditions would result inversely proportional to the LTP present *in vivo* at the moment of the animal death.
As shown in Figure 1 and Figure 2, in the cohort of mice not treated with the footshock protocol (naïve mice) we did not detect any significant differences in the magnitude of TBS-induced LTP across genotypes. This indicates that the basic mechanisms underlying LTP are preserved in the lifelong absence of serotonin.

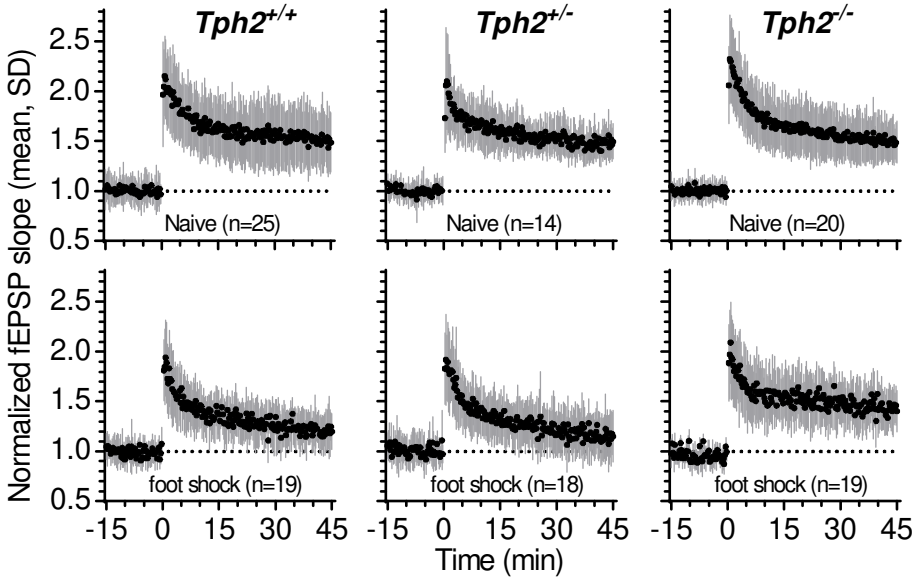

Figure 1. Summarized time-courses of theta-burst induction at hippocampal CA1 synapses in naïve and foot shock treated mice of different genotypes.
Summary of all the time-courses where long-term potentiation was induced at hippocampal CA1 apical dendrites in $Tph2^{+/+}$, $Tph2^{+/-}$ and $Tph2^{-/-}$ naïve and foot shock treated mice. Numbers (n) in graphs indicate slices tested, including replicates per mouse. Time-courses are expressed as mean ± SD.

In contrast, the fear conditioning foot shock protocol produced a significant decrease in LTP in $Tph2^{+/+}$ and $Tph2^{+/-}$ mice, but not in $Tph2^{-/-}$ mice (Figures 1 and 2). These results indicate that, *in vivo*, the presence of serotonin facilitates the induction of synaptic LTP and the development of fear memories in the hippocampus.

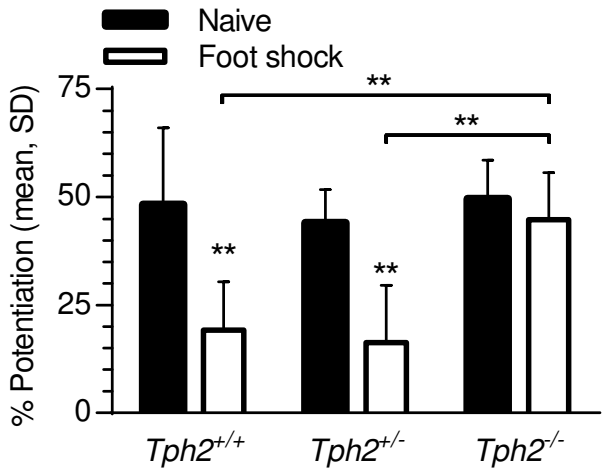

Figure 2. Lack of serotonin preents the impairment of long term potentiation in foot shock treated Tph2$^{-/-}$ mice.
Potentiation expressed as mean ± SD in naïve and foot shock-treated Tph2$^{+/+}$, Tph2$^{+/-}$, and Tph2$^{-/-}$ mice. ** $p < 0.01$. Two-way ANOVA, followed by Sidak's post hoc test.

One interpretation of the possible mechanism(s) that intervene in the CA1 hippocampus during the fear conditioning procedure implicates the increased activation of GABAergic Parvalbumin (PV) interneurons observed in Tph2$^{-/-}$ mice after fear conditioning.

In the CA1 region of the hippocampus the overall activity is regulated by neurotransmitters (including serotonin) that modulate both excitatory pyramidal neurons and different populations of GABAergic inhibitory neurons (*see in*: Klausberger and Somogyi, 2008; Somogyi et al., 2013). When the association between a fearful stimulus and the non conditioned stimulus occurs, serotonin likely mediates the inhibition of GABAergic PV-interneurons (Waider et al., 2019), which in physiological conditions dynamically change their activity during different behaviors (*see in*: Lapray et al., 2012). In the absence of serotonin, the lack of inhibition of GABAergic PV-interneurons activity during the fearful event could result in an impairment of LTP *in vivo*, which would be detected as greater LTP recorded *ex vivo*.

Fuller discussion of these data in the context of the behavioural and neurochemical changes in contextual fear conditioning produced by lack of serotonin is presented in the attached article by Waider et al. (2019).

Materials and methods applied in the electrophysiology experiments.

Animals and animal care.

Animal care and experimental procedures strictly complied with the European Communities Council Directive (2010/63/UE) and were approved by the Italian Ministry of Health (Aut: 938/2017-PR). Every effort was made to reduce the number of animals used. Tryptophan hydroxylase-2 knock-out ($Tph2^{-/-}$) mice and their littermateswere obtained from Prof. K.P. Lesch (University of Würzburg, Würzburg, Germany). Animals were housed on a 12:12h day-night cycle with food and water ad libitum.

Foot-shock protocol.

Mice of $Tph2^{+/+}$, $Tph2^{+/-}$ and $Tph2^{-/-}$ genotype were used to assess context-dependent fear memory with an unsignalated foot-shock to investigate the impact of serotonin deficiency on hippocampal plasticity. A cohort of the mice was left undisturbed in the foot shock cage and treated as naïve controls and a second cohort was tested for foot shock. Mice were placed in the cage and allowed to explore for 2 min before delivering the shocks (0.5 mA, 2s). The protocol consisted in 5 shocks with an interval time of 2 min (Dai et al., 2008). Freezing condition was evaluated with a threshold of 2 cm/s and the animal was considered immobile. After the last foot-shock, the mice were removed from the cage and the procedure for brain isolation started.

Preparation of brain slices.

Slices were prepared from animals aged 4-10 weeks. Animals were deeply anesthetized with isoflurane and decapitated. Brains were rapidly removed and dissected in ice-cold gassed (95% O_2 and 5% CO_2) artificial cerebrospinal fluid (ACSF) composed of: 124 mM NaCl, 2.75 mM KCl, 1.25 mM NaH_2PO_4, 1.3 mM $MgCl_2$, 2 mM $CaCl_2$, 26 mM $NaHCO_3$, 11 mM D-glucose. Under ice-cold ACSF the hippocampi were rapidly isolated and stored for 2 minutes. Transversal slices of 400 µm nominal thickness were cut with a McIlwan tissue chopper (Gomshall, U.K.). After discarding approximately 2 mm of the dorsal hippocampal pole, six to seven slices were transferred in an incubation chamber and left to equilibrate for 1 hour at room temperature. Subsequently, a single slice was transferred in a recording chamber on a nylon mesh submerged and superfused (2 ml/min) with oxygenated Ca^{2+} enriched ACSF (Ca^{2+} 2.5 mM, 33-34 °C) through a peristaltic pump-driven perfusion system.

Extracellular recordings.

As described previously (Mlinar et al., 2006; Morini et al. 2011), after incubation a single slice was transferred on a nylon mesh completely submerged with oxygenated and heated ACSF to a temperature of 33 ± 1 °C and continuously superfused with a flux rate of 2 ml min^{-1}. With a surgical cut, CA1 area was disconnected from the CA3

area and slice was fixed to the nylon mesh with platinum weights placed on CA3 and subiculum.

Slices were incubated for 10 min in the recording chamber before placing the electrodes and starting the stimulation with a concentric bipolar electrode (FHC, Bowdoin, ME, US) placed in the stratum radiatum after CA3/CA1 cut. Stimulating pulses (80 µs duration; 30 s interpulse interval) triggered by a PC controlled WinLTP (WinLTP Ltd, The Univerisity of Bristol), were delivered by a stimulus isolation unit (D2, Digitimer, Welwyn GardenCity, U.K.) and evoked potentials were recorded with a glass electrode filled with 150 mM NaCl placed in the distal third of the stratum radiatum at mean distance from the stimulator of 300-400 µm approximately (Figure 3A).

Signals recorded were field excitatory postsynaptic potentials (fEPSP), amplified with Neurolog NL-104 amplifiers (Digitimer, Welwyn GardenCity, U.K.), digitized with a sampling rate of 20 kHz (Digidata 1320A, Molecular Devices, Foster City, CA, US) and filtered at 5 kHz for storage in PC for off-line analysis. At the beginning of each experiment, a stimulus-response curve (SRC), obtained by gradually increasing stimulus intensity, was recorded and set to evoke a fEPSP that had an initial slope of approximately 40% of the maximum obtained in the SRC and was held constant for the whole recording (Figure 3B).

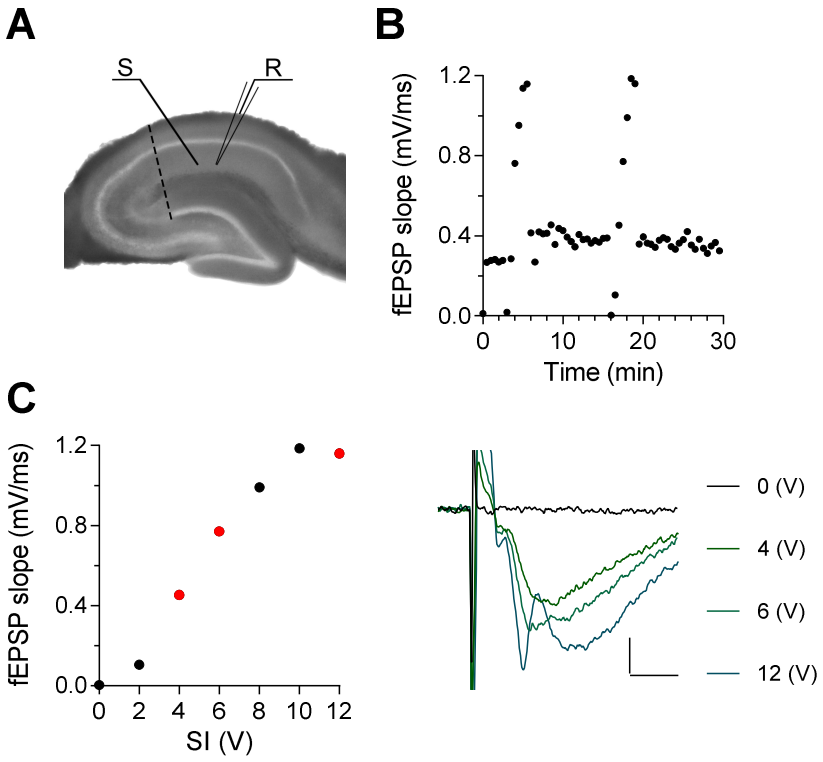

Figure 3. Exemplificative stimulus-response curve.
(A) Position of stimulating electrode (S) and recording pipette (R) on Schaffer collaterals CA1 synapses of dorsal hippocampus. Dashed line indicates the surgical cut performed to dissasociate CA1 to CA3 area and prevent recurrent propagation of action potentials. **(B)** Time-course of a stimulus-response curve (SRC) obtained with increasing stimulation of Δ2 Volts. SRC is repeated after 10 minutes to assure stability of recording before collecting baseline events. **(C)** *Left*, input-output (I/O) relationship of the SRC curve in **(B)**. Red dots are the slope values for the traces showed in the right panel. **(C)** *Right*, traces of the representative I/O points of *left*. Scale bar: 0.3 mV, 3 ms.

Long term potentiation protocol.

Long term potentiation was induced by a theta-burst stimulation (Morini et al., 2011; Mlinar et al., 2015b), consisting of a train of 5 bursts (Figure 4) of 5 stimuli (100 Hz intraburst frequency and 5 Hz burst frequency called TB5).

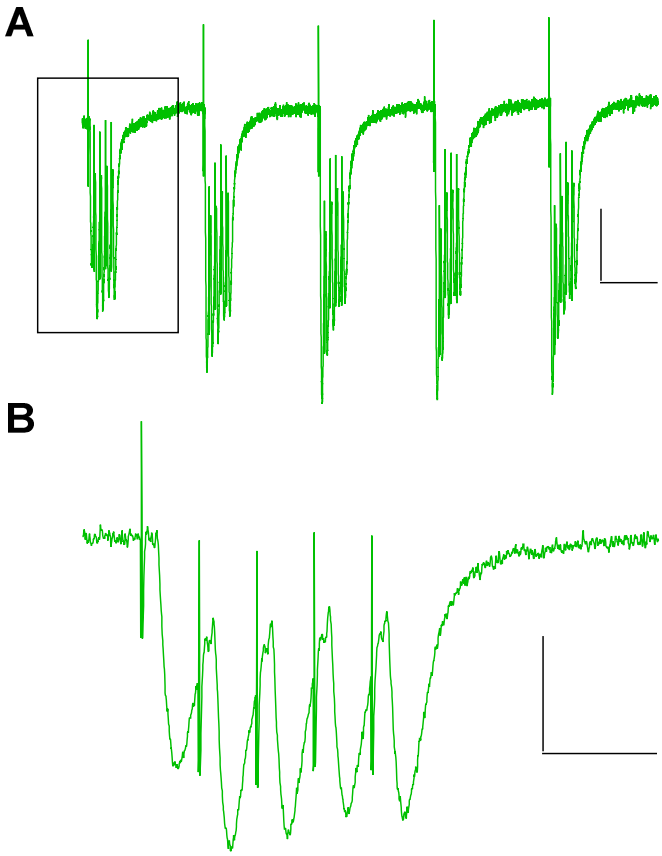

Figure 4. Example of fEPSP response to theta-burst stimulation.
(A) fEPSP response to one TB5 stimulation of the stratum radiatum in CA1. Scale bar: 0.5 mV, 100 ms. **(B)** Same fEPSP as **(A)** on expanded time scale. Scale bar: 0.5 mV, 20 ms.

TB5 was chosen among the theta rhythm-based protocols for its intermediate magnitude, thus allowing detection of modulatory effects in both facilitatory and inhibitory directions.

A SRC was performed at the end of the recording after induction of LTP, using the same voltage values as the first curve in baseline. For each experiment, the measured fEPSP slopes recorded were averaged on those in the last 5 min (-5/0 min for baseline; 40/45 min for TB5) and steady-state values and traces obtained were used for calculations and statistics (Figure 5).

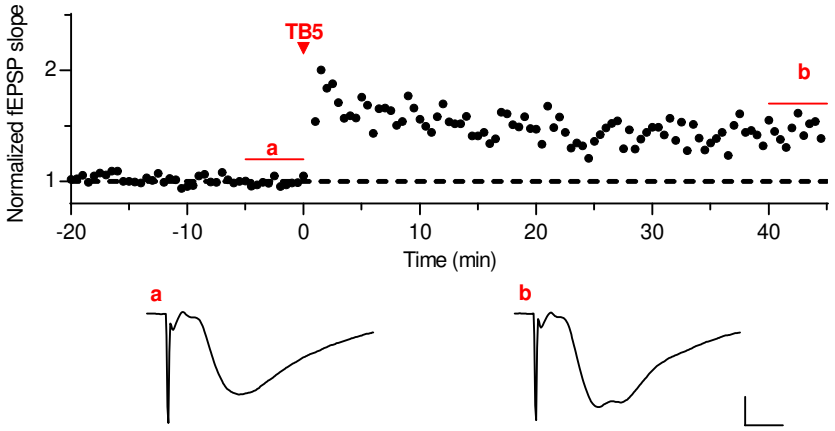

Figure 5. Steady-state traces considered for measuring synaptic changes after TB5.
Representative time-course of a long-term potentiation experiment. After at least 10 min of stable baseline, TB5 is delivered and followed for 45 min. Note the steady state values of baseline (considered at a time window of -5/0 min; a) and TB5 (considered at a time window of 40/45 min; b). Below the time-course are shown the averages of 21 traces considered in time windows a and b. Scale bar: 0.4 mV, 2 ms.

Detection of field excitatory postsynaptic potential.

Field excitatory post-synaptic potentials (fEPSPs) are measurable extracellular voltage shifts between the current measured at the pipette tip and the current measured at the ground electrode. They are generated by the interaction of glutamate released by a population of terminals simultaneously activated by the stimulus and glutamate receptors of CA1 pyramidal neuron dendrites located under the recording electrode. The inward current produced by glutamate receptor opening subtracts positive charges (Na^+ and Ca^{2+}) from the extracellular space under the electrode and this current is recorded as a negative field potential (fEPSP) proportional to the stimulus strength and number of glutamate receptors activated (e.g. see Figure 3C; Figure 6).

The hippocampus is a particularly favourable brain region for fEPSP recordings, mostly due to its highly laminated structure that allows placement of stimulating and recording electrodes in visually recognizable locations.

Normally fEPSPs are evoked by low-threshold stimulations, but by increasing the strength of the stimulus it is possible to evoke a population spike that will superimpose on the fEPSP (Figure 3C). The population spike is generated by the synchronous discharge of action potentials by the population of neurons within the detection distance of the recording the pipette. In our experiments, we recorded fEPSP signals and their slope was used for on-line and *post-hoc* analysis. The fEPSP slope was determined *on-line* as the slope of the initial downward phase of the response recorded in the stratum radiatum following the afferent volley (Johnston and Wu, 1994) and measured by linear regression in the region between 20/60 % of the fEPSP (Figure 6).

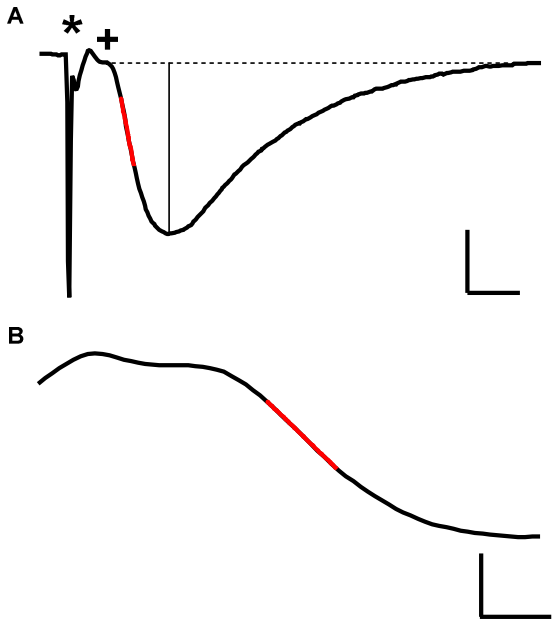

Figure 6. Description of the components of a typical field excitatory postsynaptic potential.
(A) Example of field excitatory postsynaptic potential (fEPSP) recorded in the stratum radiatum of the hippocampus from apical dendrites of CA1 pyramidal neurons. The signal is composed by a fast electrical component produced by the stimulus (*) and a biological component composed by *i)* a synaptic volley (+) representative of passive cable properties of excited fibres and *ii)* the downward deflection produced by the opening of Na^+ channels and flux of a I_{Na} inside the apical dendrites. The orizontal dashed line and the vertical solid line show the point of measure of the fEPSP amplitude. The red line represents the best linear fit of the maximal slope. Scale bar: 0.4 mV, 2 ms. **(B)** same fEPSP as **(A)** on an expanded time scale. Scale bar: 0.4 mV, 0.5 ms.

At each time point of the recorded fEPSP the electrical signal across the tissue respects the Ohm's law:

$$V = I * R$$

Where V is the voltage elicited by the stimulating electrode, I is the current produced by the opening of glutamate receptor channels and R is the resistance offered by the tissue and by the electrode. the ionic channels expressed along the stimulated fibres.
Reaching the recording pipette tip, the signal appears to be composed by a fast electrical component produced by the stimulation. This is generally mono- or bi-phasic according to the type of tip of the electrode used and according to how deep the tip is in the tissue, thus shielding the signal in a different way. The biological component of the signal is composed by the synaptic volley and the response of the dendrites to activation of glutamate receptors. The synaptic volley reports the activation of the afferent fibres and its amplitude increases proportionally to the number of fibres activated by the stimulus and located in the vicinity of the recording electrode. The dendritic response is the biological signal that accounts for the opening of Na^+ channels and flux of a I_{Na} inside the apical dendrites. The higher the number of

stimulated fibres, the greater the glutamate release from the synaptic boutons. With increasing strength of the stimuli the fEPSP increases in amplitude and the initial slope of the fEPSP becomes steeper (Figure 3C).

References:

Alenina, N., Kikic, D., Todiras, M., Mosienko, V., Qadri, F., Plehm, R., Boyé, P., Vilianovitch, L., Sohr, R., Tenner, K., Hörtnagl, H., Bader, M. 2009. Growth retardation and altered autonomic control in mice lacking brain serotonin. Proc Natl Acad Sci U S A. Jun 23;106(25):10332-7.

Bazelot, M., Bocchio, M., Kasugai, Y., Fischer, D., Dodson, P.D., Ferraguti, F., Capogna, M. 2015. Hippocampal Theta Input to the Amygdala Shapes Feedforward Inhibition to Gate Heterosynaptic Plasticity. Neuron. Sep 23;87(6):1290-1303.

Beaulieu, J.M., Zhang, X., Rodriguiz, R.M., Sotnikova, T.D., Cools, M.J., Wetsel, W.C., Gainetdinov, R.R., Caron, M.G. 2008. Role of GSK3 beta in behavioral abnormalities induced by serotonin deficiency. Proc Natl Acad Sci U S A. Jan 29;105(4):1333-8.

Bienvenu, T.C., Busti, D., Magill, P.J., Ferraguti, F., Capogna, M. 2012. Cell-type-specific recruitment of amygdala interneurons to hippocampal theta rhythm and noxious stimuli in vivo. Neuron. Jun 21;74(6):1059-74.

Briscoe, J., Sussel, L., Serup, P., Hartigan-O'Connor, D., Jessell, T.M., Rubenstein, J.L., Ericson, J. 1999. Homeobox gene Nkx2.2 and specification of neuronal identity by graded Sonic hedgehog signalling. Nature. Apr 15;398(6728):622-7.

Compan, V., Segu, L., Buhot, M.C., Daszuta, A. 1998. Differential effects of serotonin (5-HT) lesions and synthesis blockade on neuropeptide-Y immunoreactivity and 5-HT1A, 5-HT1B/1D and 5-HT2A/2C receptor binding sites in the rat cerebral cortex. Brain Res. Jun 8;795(1-2):264-76.

Dai, J.X., Han, H.L,, Tian, M., Cao, J., Xiu, J.B., Song, N.N., Huang, Y., Xu, T.L., Ding, Y.Q., Xu, L. 2008. Enhanced contextual fear memory in central serotonin-deficient mice. Proc NatlAcad Sci U S A. Aug 19;105(33):11981-6.

Ding, Y.Q., Marklund, U., Yuan, W., Yin, J., Wegman, L., Ericson, J., Deneris, E., Johnson, R.L., Chen, Z.F. 2003. Lmx1b is essential for the development of serotonergic neurons. Nat Neurosci. Sep;6(9):933-8.

Gutknecht, L., Waider, J., Kraft, S., Kriegebaum, C., Holtmann, B., Reif, A., Schmitt, A., Lesch, K.P. 2008. Deficiency of brain 5-HT synthesis but serotonergic neuron formation in Tph2 knockout mice. J Neural Transm (Vienna). Aug;115(8):1127-32.

Gutknecht, L., Kriegebaum, C., Waider, J., Schmitt, A., Lesch, K.P. 2009. Spatio-temporal expression of tryptophan hydroxylase isoforms in murine and human brain: convergent data from Tph2 knockout mice. Eur Neuropsychopharmacol. Apr;19(4):266-82.

Gutknecht, L., Araragi, N., Merker, S., Waider, J., Sommerlandt, F.M., Mlinar, B., Baccini, G., Mayer, U., Proft, F., Hamon, M., Schmitt, A.G., Corradetti, R., Lanfumey, L., Lesch, K.P. 2012. Impacts of brain serotonin deficiency following Tph2 inactivation on development and raphe neuron serotonergic specification. PLoS One. 2012;7(8):e43157.

Hendricks, T.J., Fyodorov, D.V., Wegman, L.J., Lelutiu, N.B., Pehek, E.A, Yamamoto, B., Silver, J., Weeber, E.J., Sweatt, J.D., Deneris, E.S. 2003. Pet-1 ETS gene plays a critical role in 5-HT neuron development and is required for normal anxiety-like and aggressive behavior. Neuron. Jan 23;37(2):233-47.

Johnston, D.,Wu, M.S. 1994. Foundations of cellular neurophysiology.Cambridge, MA: Bradford Books, MIT Press.

Karst, H., Berger, S., Turiault, M., Tronche, F., Schütz, G., Joëls, M. 2005. Mineralocorticoid receptors are indispensable for nongenomic modulation of hippocampal glutamate transmission by corticosterone. Proc Natl Acad Sci U S A. Dec 27;102(52):19204-7.

Klausberger, T., Somogyi, P. 2008. Neuronal diversity and temporal dynamics: the unity of hippocampal circuit operations. Science. Jul 4;321(5885):53-7. Review.

Lapray, D., Lasztoczi, B., Lagler, M., Viney, T.J., Katona, L., Valenti, O., Hartwich, K., Borhegyi, Z., Somogyi, P., Klausberger, T. 2012. Behavior-dependent specialization of identified hippocampal interneurons. Nat Neurosci. Sep;15(9):1265-71.

Mlinar, B., Mascalchi, S., Mannaioni, G., Morini, R., Corradetti, R. 2006. 5-HT4 receptor activation induces long-lasting EPSP-spike potentiation in CA1 pyramidal neurons. Eur J Neurosci. Aug;24(3):719-31.

Mlinar, B., Stocca, G., Corradetti, R. 2015b. Endogenous serotonin facilitates hippocampal long-term potentiation at CA3/CA1 synapses. J Neural Transm (Vienna). Feb;122(2):177-85.

Mlinar, B., Montalbano, A., Waider, J., Lesch, K.P., Corradetti, R. 2017. Increased functional coupling of 5-HT(1A) autoreceptors to GIRK channels in Tph2(-/-) mice. Eur Neuropsychopharmacol. Dec;27(12):1258-1267.

Montalbano, A., Waider, J., Barbieri, M., Baytas, O., Lesch, K.P., Corradetti, R., Mlinar,B. 2015a. Cellular resilience: 5-HT neurons in Tph2(-/-) mice retain normal firingbehavior despite the lack of brain 5-HT. Eur Neuropsychopharmacol. Nov;25(11):2022-35.

Morini, R., Mlinar, B., Baccini, G., Corradetti, R. 2011. Enhanced hippocampal long-termpotentiation following repeated MDMA treatment in Dark-Agouti rats. EurNeuropsychopharmacol. Jan;21(1):80-91.

Mössner, R., Freitag, C.M., Gutknecht, L., Reif, A., Tauber, R., Franke, P., Fritze, J., Wagner, G., Peikert, G., Wenda, B., Sand, P., Rietschel, M., Garritsen, H., Jacob, C., Lesch, K.P., Deckert, J. 2006. The novel brain-specific tryptophan hydroxylase-2 gene in panic disorder. J Psychopharmacol. Jul;20(4):547-52.

Somogyi, P., Katona, L., Klausberger, T., Lasztóczi, B., Viney, T.J. 2013. Temporal redistribution of inhibition over neuronal subcellular domains underlies state-dependent rhythmic change of excitability in the hippocampus. Philos Trans R Soc Lond B Biol Sci. Dec 23;369(1635):20120518.

Waider, J., Popp, S., Lange, M.D., Kern, R., Kolter, J.F., Kobler, J., Donner, N.C., Lowe, K.R., Malzbender, J.H., Brazell, C.J., Arnold, M.R., Aboagye, B., Schmitt-Böhrer, A., Lowry, C.A., Pape, H.C., Lesch, K.P. 2017. Genetically driven brain serotonin deficiency facilitates panic-like escape behavior in mice. Transl Psychiatry. Oct 3;7(10):e1246.

Waider, J., Popp, S., Mlinar, B., Montalbano, A., Bonfiglio, F., Aboagye, B., Thuy, E., Kern, R., Thiel, C., Araragi, N., Svirin, E., Schmitt-Böhrer, A.G., Corradetti, R., Lowry, C.A., Lesch, K.P. 2019. Serotonin Deficiency Increases Context-Dependent Fear Learning Through Modulation of Hippocampal Activity. Front Neurosci. Apr 24;13:245.

Walther, D.J., Bader, M. 2003. A unique central tryptophan hydroxylase isoform. Biochem Pharmacol. 2003 Nov 1;66(9):1673-80.

Walther, D.J., Peter, J.U., Bashammakh, S., Hörtnagl, H., Voits, M., Fink, H., Bader, M. 2003. Synthesis of serotonin by a second tryptophan hydroxylase isoform. Science. Jan 3;299(5603):76.

Wang, H.L., Zhang, S., Qi, J., Wang, H., Cachope, R., Mejias-Aponte, C.A., Gomez, J.A., Mateo-Semidey, G.E., Beaudoin, G.M.J., Paladini, C.A., Cheer, J.F., Morales, M. 2019. Dorsal Raphe Dual Serotonin-Glutamate Neurons Drive Reward by Establishing Excitatory Synapses on VTA Mesoaccumbens Dopamine Neurons. Cell Rep. Jan 29;26(5):1128-1142.e7.

Zhang, X., Beaulieu, J.M., Sotnikova, T.D., Gainetdinov, R.R., Caron, M.G. 2004. Tryptophan hydroxylase-2 controls brain serotonin synthesis. Science. Jul 9;305(5681):217.

Zhao, Z.Q., Scott, M., Chiechio, S., Wang, J.S., Renner, K.J., Gereau, R.W. 4th, Johnson, R.L., Deneris, E.S., Chen, Z.F. 2006. Lmx1b is required for maintenance of central serotonergic neurons and mice lacking central serotonergic system exhibit normal locomotor activity. J Neurosci. Dec 6;26(49):12781-8.

Appendix 2:

Published papers.

- *Dual inhibitory action of trazodone on dorsal raphe serotonergic neurons through 5-HT_{1A} receptor partial agonism and α_1-adrenoceptor antagonism.*
  Montalbano, A., Mlinar, B., Bonfiglio, F., Polenzani, L., Magnani, M., Corradetti, R. PLoS One. Sep 26;14(9):e0222855.

- *Serotonin Deficiency Increases Context-Dependent Fear Learning Through Modulation of Hippocampal Activity.*
  Waider, J., Popp, S., Mlinar, B., Montalbano, A., Bonfiglio, F., Aboagye, B., Thuy, E., Kern, R., Thiel, C., Araragi, N., Svirin, E., Schmitt-Böhrer, A.G., Corradetti, R., Lowry, C.A., Lesch, K.P. Front Neurosci. Apr 24;13:245.

PLOS ONE

RESEARCH ARTICLE

Dual inhibitory action of trazodone on dorsal raphe serotonergic neurons through 5-HT_{1A} receptor partial agonism and α_1-adrenoceptor antagonism

Alberto Montalbano[1], Boris Mlinar[1], Francesco Bonfiglio[1], Lorenzo Polenzani[2], Maurizio Magnani[2], Renato Corradetti[1]*

1 NEUROFARBA—Dipartimento di Neuroscienze, Psicologia, Area del Farmaco e Salute del Bambino, Università di Firenze, Firenze, Italia, **2** Angelini RR&D (Research, Regulatory & Development), Angelini S.p. A, S.Palomba-Pomezia (Roma), Italia

* renato.corradetti@unifi.it

Citation: Montalbano A, Mlinar B, Bonfiglio F, Polenzani L, Magnani M, Corradetti R (2019) Dual inhibitory action of trazodone on dorsal raphe serotonergic neurons through 5-HT_{1A} receptor partial agonism and α_1-adrenoceptor antagonism. PLoS ONE 14(9): e0222855. https://doi.org/10.1371/journal.pone.0222855

Editor: Alexander G. Obukhov, Indiana University School of Medicine, UNITED STATES

Received: June 12, 2019

Accepted: September 9, 2019

Published: September 26, 2019

Data Availability Statement: All relevant data are within the manuscript.

Funding: This study was funded by Angelini S.p.A., by grant number 039RD15382 awarded to Prof. Renato Corradetti. The funder provided support in the form of salaries for authors L.P and M.M., but did not have any additional role in the study design, data collection and analysis, decision to publish, or preparation of the manuscript. The specific roles of

Abstract

Trazodone is an antidepressant drug with considerable affinity for 5-HT_{1A} receptors and α_1-adrenoceptors for which the drug is competitive agonist and antagonist, respectively. In this study, we used cell-attached or whole-cell patch-clamp recordings to characterize the effects of trazodone at somatodendritic 5-HT_{1A} receptors (5-HT_{1A}ARs) and α_1-adrenoceptors of serotonergic neurons in rodent dorsal raphe slices. To reveal the effects of trazodone at α_1-adrenoceptors, the baseline firing of 5-HT neurons was facilitated by applying the selective α_1-adrenoceptor agonist phenylephrine at various concentrations. In the absence of phenylephrine, trazodone (1–10 μM) concentration-dependently silenced neurons through activation of 5-HT_{1A}ARs. The effect was fully antagonized by the selective 5-HT_{1A} receptor antagonist Way-100635. With 5-HT_{1A} receptors blocked by Way-100635, trazodone (1–10 μM) concentration-dependently inhibited neuron firing facilitated by 1 μM phenylephrine. Parallel rightward shift of dose-response curves for trazodone recorded in higher phenylephrine concentrations (10–100 μM) indicated competitive antagonism at α_1-adrenoceptors. Both effects of trazodone were also observed in slices from *Tph2*$^{-/-}$ mice that lack synthesis of brain serotonin, showing that the activation of 5-HT_{1A}ARs was not mediated by endogenous serotonin. In whole-cell recordings, trazodone activated 5-HT_{1A}AR-coupled G protein-activated inwardly-rectifying (GIRK) channel conductance with weak partial agonist efficacy (~35%) compared to that of the full agonist 5-CT. Collectively our data show that trazodone, at concentrations relevant to its clinical effects, exerts weak partial agonism at 5-HT_{1A}ARs and disfacilitation of firing through α_1-adrenoceptor antagonism. These two actions converge in inhibiting dorsal raphe serotonergic neuron activity, albeit with varying contribution depending on the intensity of α_1-adrenoceptor stimulation.

these authors are articulated in the 'author contributions' section.

Competing interests: I have read the journal's policy and the authors of this manuscript have the following competing interests: Drs. L. Polenzani and M. Magnani are full-time employees of Angelini S.p.A. Dr. R. Corradetti has received research grants from Angelini S.p.A. This does not alter our adherence to PLOS ONE policies on sharing data and materials. All other Authors declare no conflict of interest.

Introduction

The brain serotonin (5-HT) system modulates a variety of brain functions including mood, cognition, emotional behaviour, and sleep [1, 2, 3] and its dysregulation appears to contribute in related psychopathological states such as depression, anxiety, impulsivity and aggression [4].

Trazodone is an antidepressant drug that, in addition to its inhibitory activity at cell membrane 5-HT transporter (SERT), is a competitive ligand at 5-HT_{1A} 5-HT_{2A}, 5-HT_{2C} receptors and α_1-adrenoceptors for which it displays considerable affinity [5, 6]. Although these pharmacological properties have been suggested to contribute a favourable safety profile such as facilitation of sleep and reduced sexual dysfunction [7], the direct effects of trazodone on serotoninergic neuron activity are still not adequately known for modelling the possible pharmacological mechanisms underlying the therapeutic action(s) of the drug.

In the dorsal raphe nucleus (DRN) the spontaneous activity of serotonergic neurons is maximally facilitated during wake by noradrenergic input via α_1-adrenoceptor stimulation [8] and activation of 5-HT system contributes to arousal [9, 10]. Under these conditions, the firing of serotonergic neurons is tonically limited *via* the stimulation of somatodendritic 5-HT_{1A} autoreceptors (5-HT_{1A}ARs) exerted by the endogenous 5-HT present in the extracellular space surrounding serotonergic neurons [11, 12]. However, increased extracellular 5-HT in raphe nuclei acutely produced by block of SERT results in (auto)inhibition of serotonergic neuron activity and consequently in reduction of 5-HT release in projection brain areas. This is believed to delay the onset of antidepressant therapeutic effect until subsensitivity of 5-HT1AARs develops to weaken the autoinhibitory feedback [13, 14]. On the basis of this notion it has been proposed that the association of 5 HT_{1A} receptor antagonists could hasten the response to monoamine uptake blockers [15, 16, 17] and, more recently, that antidepressant drugs with partial agonist property at 5 HT_{1A} receptors could display faster onset of therapeutic response [18].

In vivo recording of serotonergic neuron activity in anaesthetized rats showed that acute administration of trazodone inhibits DRN serotonergic neuron firing [19] an action mediated by activation of somatodendritic 5-HT_{1A}ARs which desensitize after chronic treatment with the antidepressant drug [20]. Nevertheless, the direct functional effects of trazodone on 5-HT_{1A}ARs are still insufficiently characterized to establish whether the drug exerts full or partial agonism at 5-HT_{1A}ARs. In the rat, in a functional assay *in vitro* trazodone was found to activate [^{35}S]GTPγS binding with weak efficacy [21], while *in vivo* its action on serotonergic neuron firing appeared consistent with stronger agonism at 5-HT_{1A}ARs [22].

The interplay between the 5-HT_{1A} receptor agonist activity and α_1-adrenoceptor antagonist activity of trazodone at the level of serotonergic neurons likely plays a crucial role in regulating the firing of serotonergic neurons, hence the release of 5-HT in projection areas during acute and chronic administration of the drug. Actually, a strong noradrenergic input to the dorsal and other raphe nuclei has been identified [23, 24] which tonically activates raphe serotonergic neurons through postsynaptic α_1-adrenoceptors [25]. Therefore, the α_1-adrenoceptor antagonist properties of trazodone could participate to the inhibiton of DRN serotonergic neuron firing by reducing the noradrenergic drive, but experiments *in vivo* were unable to quantify this action in the DRN in conditions in which trazodone appeared to have α_1-adrenoceptor blocking effects in the hippocampus [22].

In the present work we designed *in vitro* experiments directed to quantify the agonist efficacy of trazodone at 5-HT_{1A}ARs of DRN serotonergic neurons and to establish the possible effect of α_1-adrenoceptor antagonism. Here we show that trazodone exerts weak partial agonist

action at 5-HT_{1A}ARs and α_1-adrenoceptor antagonism at low micromolar concentrations that are relevant to the therapeutic effects of the drugs.

Materials and methods

Animals and animal care

Animal care and experimental procedures strictly complied with the European Communities Council Directive (2010/63/UE) and were approved by the Italian Ministry of Health (Aut: 224/2017-PR and 938/2017-PR). Every effort was made to reduce the number of animals used. Male Wistar rats were purchased from Envigo Italy (Milan, Italy). Tryptophan hydroxylase-2 knock-out (*Tph2*$^{-/-}$) mice were obtained from Prof. K.P. Lesch (University of Würzburg, Würzburg, Germany). Animals were housed on a 12:12 h day-night cycle with food and water *ad libitum*.

Procedures for tissue isolation, slice superfusion and electrophysiological recording from DRN serotonergic neurons of rat and mouse have been previously described in detail [26, 27, 28].

Preparation of brain slices

Slices were prepared from animals aged 4–10 weeks (4–5 weeks for whole-cell patch-clamp recordings). Animals were deeply anesthetized with isoflurane and decapitated. Brains were rapidly removed and dissected in ice-cold gassed (95% O_2 and 5% CO_2) artificial cerebrospinal fluid (ACSF) composed of: 124 mM NaCl, 2.75 mM KCl, 1.25 mM NaH_2PO_4, 1.3 mM $MgCl_2$, 2 mM $CaCl_2$, 26 mM $NaHCO_3$, 11 mM D-glucose. The brainstem was sliced coronally into 200 μm thick slices with a vibratome (DSK, T1000, Dosaka, Japan). After recovery for at least 90 min at room temperature, the slices were individually transferred to the recording chamber and superfused continuously, at a rate of 2 ml min^{-1}, with warmed ACSF (Warner Instruments in-line heater TC324-C). Slices were allowed to equilibrate for at least 15 min before the beginning of the recording. Drugs were bath-applied through a peristaltic pump-driven perfusion system and a complete exchange of the recording chamber volume occurred in approximately 1 min. Neurons within DRN were visualized by infrared differential interference contrast (IR-DIC) video microscopy with a Newicon camera (C2400-07; Hamamatsu, Hamamatsu City, Japan) mounted on an upright microscope (Axioskop; Zeiss, Göttingen, Germany). Recordings were made using an EPC-10 amplifier (HEKA Elektronic, Lamberecht, Germany). Patch pipettes were prepared from thick-walled borosilicate glass on a P-97 Brown-Flaming electrode puller (Sutter Instruments, Novato, CA, USA). Data were analyzed using Patchmaster 2 (HEKA Elektronic), Clampfit 9.2 (Molecular Devices, Sunnyvale, CA, USA) and Prism 7 software (GraphPad Software, San Diego, CA, USA).

Electrophysiology

Action potential firing activity of serotonergic neurons was recorded by loose-seal cell-attached recordings at a temperature of 34–36˚C. To reproduce in slices the noradrenergic drive which facilitates serotonergic neuron firing during wakefulness [8]), ACSF was supplemented with the α_1-adrenoceptor agonist phenylephrine (PE, 10 μM, unless otherwise stated). In a set of experiments neuron firing was facilitated in an α_1-adrenoceptor–independent mode using a modified ACSF containing low Ca^{2+} (0.67 mM), high K^+ (5.5 mM) and no PE. When appropriate, ACSF contained a "cocktail" of glutamate GABA/glycine and adenosine A_1 receptor blockers consisting of: 10 μM NBQX (2,3-dioxo-6-nitro-1,2,3,4-tetrahydrobenzo[f]quinoxaline-7-sulfonamide disodium salt), 20 μM d-AP5 (d-(-)-2-amino-5-phosphonopentanoic

acid), 10 μM SR-95531 (6-imino-3-(4-methoxyphenyl)-1(6H)-pyridazinebutanoic acid hydrobromide), 2 μM CGP-55845 (3-N[1-(S)-(3,4-dichlorophenyl)ethyl]amino-2-(S)-hydroxypropyl-P-benzyl-phosphinic acid hydrochloride) and 10 μM strychnine hydrochloride, 0.2 μM DPCPX (8-Cyclopentyl-1,3-dipropylxanthine) to functionally isolate the recorded neuron from major synaptic input. Patch pipettes were prepared from thick-walled borosilicate glass on a P-97 Brown-Flaming electrode puller (Sutter Instruments, Novato, CA, USA) and had resistances of 3–6 MΩ when filled with solution containing (in mM): 125 NaCl, 10 HEPES, 2.75 KCl, 2 $CaCl_2$, 1.3 $MgCl_2$ (pH 7.4 with NaOH). Loose-seal cell-attached recordings (5–20 MΩ seal resistance) were acquired continuously in the voltage-clamp mode. Signals were filtered at 3 kHz and digitized at 10 kHz. The firing rate was reported using 10 s bins. Data were analysed using Clampfit 9.2 (Molecular Devices, Sunnyvale, CA, USA). Most recorded neurons were located in the dorsal and ventromedial part of the DRN. Neurons were identified according to electrophysiological criteria [12, 29]. Only neurons with a stable baseline firing rate were used.

Methods used for measuring G protein-activated inwardly-rectifying (GIRK) channel conductance have been detailed previously [12, 27]. All experiments were performed in ACSF supplemented with a cocktail of neurotransmitter blockers (*see* above). ACSF contained 5.5 mM K^+ to increase the driving force for inward potassium current (the additional 2.75 mM by Na^+ substitution). Recording pipettes had a resistance of 2–5 MΩ. The pipette solution consisted of: 120 mM K-gluconate, 15 mM KCl, 2 mM $MgCl_2$, 10 mM HEPES, 0.1 mM EGTA, 10 mM Na_2phosphocreatine, 4 mM MgATP, 0.3 mM Na_3GTP (pH 7.35 with KOH). After establishing whole-cell recording configuration, serotonergic neurons were identified on the basis of electrophysiological properties displayed in current-clamp mode (action potential half-height width $>$ 1.1 ms; absent or very small fast afterhyperpolarization; sustained repetitive firing in response to depolarizing current injection). In current-clamp recordings signals were filtered at 5 kHz and digitized at 25 kHz. To estimate inwardly-rectifying K^+ conductance, we used hyperpolarizing voltage ramps from the holding potential of -65 mV (to -125 mV, every 10 s; 100 mV s^{-1}; 3 kHz cutoff frequency low-pass filter; 10 kHz sampling frequency) and measured the conductance from the slope of inward K^+ current in the range from -110 to -85 mV ($G_{-110/-85\ mV}$). To monitor access resistance throughout the recording, hyperpolarizing pulses (10 mV; 100 ms duration; 16 kHz low-pass filter; 25 kHz sampling frequency; cell capacitance cancellation circuit switched off) were interlaced with ramps. Access resistance was not compensated and when it was higher than 25 MΩ recordings were discarded. Concentration–response curves for trazodone were obtained using a cumulative protocol in which increasing concentrations were applied in 7–10 min intervals as appropriate. Average of 7 consecutive individual ramps, corresponding to the segment with the maximal effect for the given trazodone concentration were used to obtain conductance values. To calculate net 5-HT_{1A}AR-activated GIRK current and conductance ($G_{5\text{-}HT1A}$) present during a recording, the 5-HT_{1A}AR-insensitive current was measured at the end of a recording following application of the selective 5-HT_{1A} receptor antagonist Way-100635 (20 nM; 10–15 min) and subtracted from the total current.

Calculation of concentration-response relationships

For creating cumulative concentration-response curves for trazodone, the drug was applied for 10–30 min (as appropriate for the specific experimental objective) and mean firing rates were calculated from the last one-minute segment of each experimental epoch (e.g. baseline, trazodone 0.3 μM, 1 μM, etc.). Trazodone dose-response relationship for suppression of serotonergic neuron firing was computed by fitting data to the logistic equation $b + (a—b) / (1 + (EC_{50} / [trazodone])^{n}{}_{H})$, where EC_{50} is the half-maximally effective concentration, n_H is the

Hill coefficient, a is the baseline firing rate and *b* is the fraction remaining at the maximal trazodone effect. Fitting of average dose-response relationship of normalized firing rate: for each experiment, firing rate was measured during the last 2 min of drug application for each concentration and normalized by taking the pre-drug baseline firing rate as unity. Then the relationship for suppression of serotonergic neuron firing was computed by fitting mean values (± SD) for each concentration to the logistic equation, $b + (1—b) / (1 + (EC_{50} / [trazodone])^{n}{}_{H})$, where EC_{50} is the half-maximally effective concentration, n_H is the Hill coefficient and *b* is the fraction remaining at the maximal trazodone effect.

The respective fractional occupancy of 5-HT_{1A} receptors by trazodone and the full agonist, either 5-carboxamidotryptamine (5-CT) or 5-HT, in the presence of trazodone was calculated using the Gaddum equation: $[AR]/Rt = [A]/([A]+Ka(1+[B]/Kb))$, where [AR]/Rt is the fractional occupancy by the full agonist, [A] is the concentration of the full agonist with Ka affinity constant and [B] and Kb are trazodone concentration and affinity, respectively. To allow comparison of theoretical values with the responses experimentally obtained in rat serotonergic neurons, we calculated the occupancies for 5-CT and trazodone by applying the K_i of the two agonists for the rodent 5-HT_{1A} (5-CT: K_i = 0.325 nM, [30]; trazodone: K_i = 42 nM, [5]). For the action of trazodone on 5-HT we used the K_i of the two agonists for the human 5-HT_{1A} receptor (5-HT: K_i = 3.98 nM, [31, 32]; trazodone: K_i = 96 nM, [6]) to allow inference on the effects of trazodone on responses to endogenous 5-HT *in vivo*.

In both cases, the expected total activation of GIRK conductance was calculated from the respective occupancies of the two compounds by using the measured maximal efficacy of 0.35 for trazodone and 1.0 for the full agonist.

Drugs

Trazodone was provided by A.C.R.A.F. S.p.A. (Santa Palomba, Rome). 5-HT, SR-95531, D-AP5, NBQX were purchased from Ascent Scientific Ltd. (Bristol, UK). Way-100635 maleate, CGP-55845 hydrochloride, 5-CT and DPCPX were purchased from Tocris Bioscience (Bristol, UK). L-Phenylephrine and strychnine hydrochloride from Sigma-Aldrich S.r.l. (Milan, Italy).

Statistical analysis

Data are presented as geometric mean and confidence interval (C.I.) or mean ± SD as appropriate. Statistical comparisons were performed by ANOVA followed by Tukey *post-hoc* test, paired or unpaired t-test (two tailed), as appropriate. Pearson test was used to assess for correlation between variables. All the statistical tests were performed by GraphPad Prism version 7. Throughout the analyses, statistical significance was taken as $p < 0.05$.

Results

Concentration-dependent inhibition of serotonergic neuron firing by trazodone is mediated by more than one action

Application of trazodone produced a concentration-dependent inhibition of DRN serotonergic neuron activity facilitated by 10 μM PE in standard ACSF (Fig 1A and 1B).

The effect of trazodone was partially antagonized by the selective 5-HT_{1A} receptor antagonist Way-100635. Trazodone silenced neurons with a mean of EC_{50} values = 1.78 μM (Geometric mean, GM, 95% Confidence Interval, 95% C.I.: 1.165–2.713, n = 11; Fig 1C). In a subset of experiments in which Way-100635 (20 nM) was added to 10 μM trazodone, the firing rate recovered to less of 50% relative to baseline firing rate (47.54 ± 21; 41%; n = 7; Fig 1D) suggesting that trazodone effect was only in part mediated by activation of 5-HT_{1A}ARs.

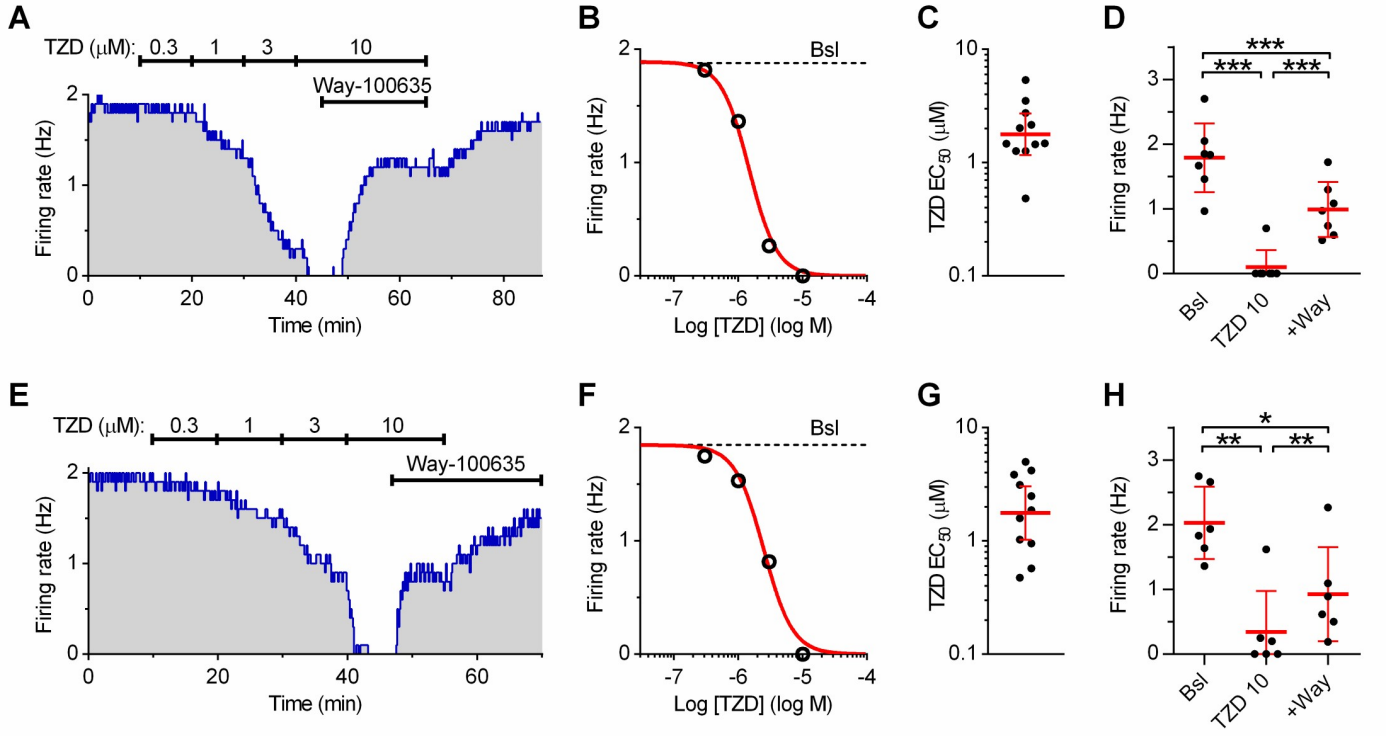

Fig 1. The inhibition of 5-HT neuron activity by trazodone. (A-D): Effect of trazodone (TZD) in control ACSF. **(A)** Representative recording illustrating the time-course of the changes in firing frequency produced by increasing concentrations of trazodone. The maximal effect was partially reversed by the selective 5-HT_{1A} receptor antagonist Way-100635 (20 nM). **(B)** Dose-response curve (DRC) resulting from the experiment shown in **(A)**. Red line is the best least-squares fit to the logistic equation. **(C)** Scatter plot of the individual EC_{50} values calculated from all experiments (n = 11). **(D)** Antagonism of trazodone (10 μM) effect by addition of Way-100635 (+Way; n = 7; One-way RM ANOVA: $F_{(2,6)} = 107.6$; $p < 0.0001$) in the subset of experiments in which Way was added at the end of the DRC, e.g. in (A). **(E-H)**: Effect of trazodone in a cocktail of antagonists (*see* methods). **(E)** Representative recording of the concentration-dependent changes in firing frequency produced by trazodone. The effect of 10 μM trazodone was partially reversed by Way-100635 (20 nM). Note the recovery of firing rate in Way-100635 after the washout of trazodone. **(F)** DRC resulting from the experiment shown in **(E)**. Red line is the best least-squares fit to the logistic equation. **(G)** Scatter plot of the individual EC_{50} values calculated from all experiments (n = 11). **(H)** Antagonism of trazodone (10 μM) effect by Way-100635 (+Way; n = 6; One-way RM ANOVA: $F_{(2,5)} = 28.68$; $p < 0.0014$) in the subset of experiments in which Way was added at the end of the DRC, e.g. in (A). In **(B)** and **(F)**, dotted line indicates the baseline (Bsl) firing rate before application of trazodone. In **(C)** and **(G)**, red line and error bars indicate the geometric mean and 95% C.I. In all experiments the activity of serotonergic neurons was facilitated by the presence of 10 μM phenylephrine. * $p < 0.05$; ** $p < 0.01$; *** $p < 0.001$ (One-way RM ANOVA, followed by a Tukey *post-hoc* test).

https://doi.org/10.1371/journal.pone.0222855.g001

The non 5-HT1AAR-mediated decrease in firing of serotonergic neurons produced by trazodone could indirectly be elicited by changes in the release of GABA, glycine or adenosine from neighbour neurons, or glutamate from terminals. We therefore carried out a set of experiments in ACSF containing a "cocktail" of receptor antagonists for major neurotransmitters (*see* methods).

Under these conditions, the inhibitory effect of trazodone was very similar to that exerted in standard ACSF (Fig 1E–1H). The average EC_{50} value was 1.77 μM (GM, 95% C.I.: 1.023–3.034, n = 11). Statistical comparison of EC_{50} values in individual neurons revealed no differences of trazodone effect in standard ACSF and cocktail ACSF (unpaired t test, two tails: $t = 0.2813$; $df = 20$; $p = 0.7814$). Similar to the previous set of experiments, in a subset of experiments in which Way-100635 (20 nM) was added to 10 μM trazodone, the firing rate recovered to 45.93 ± 30.32% (n = 6, Fig 1H) of baseline firing rate. These results demonstrate that the Way-100635-insensitive inhibitory effect trazodone was directly exerted on serotonergic neurons and not mediated by release of GABA, glycine, adenosine and glutamate from the local

network of neurons and terminals. Nevertheless, all subsequent experiments were performed in the presence of synaptic antagonists.

Trazodone directly activates 5-HT$_{1A}$ receptors in Tph2$^{-/-}$ mice

To ascertain whether the inhibition of serotonergic neuron firing by trazodone was due to direct stimulation of 5-HT$_{1A}$ARs or was indirectly mediated by a possible raise in extracellular 5-HT caused by SERT inhibition produced by the drug, we repeated these experiments in *Tph2*$^{-/-}$ mice that lack synthesis of brain 5-HT [33]). In this set of experiments 20 nM Way-100635 was added to the trazodone concentration that produced more than 90% inhibition of neuron firing (Fig 2A).

In the nine neurons tested, serotonergic neuron firing was silenced at concentrations $\leq$ 10 μM with an average EC$_{50}$ value of 0.66 μM (GM, 95% C.I.: 0.3157–1.364, n = 9; Fig 2C). As shown in Fig 2A and 2B, in four neurons in which 1 μM trazodone decreased the firing by 96.1 ± 7.3%, the effect was fully antagonized by Way-100635. When 10 μM trazodone was required to silence the recorded neurons, Way-100635 significantly, but only partially, antagonized the effect that recovered by 40.13 ± 6.74% (n = 5, Fig 2B). These results confirmed that trazodone was a direct agonist at 5-HT$_{1A}$ARs. The greater potency of trazodone in inhibiting firing (EC$_{50}$ = 0.66 μM) compared to that observed in rat (EC$_{50}$ = 1.77 μM) is likely to be ascribed to the supersensitivity of 5-HT$_{1A}$ARs in *Tph2*$^{-/-}$ mice compared to *Tph2*$^{+/+}$ mice (~2,5 folds) [34].

The non 5-HT$_{1A}$ receptor-mediated effect of trazodone depends on α$_1$-adrenoceptor activation and is competitively surmounted by the α$_1$-adrenoceptor agonist phenylephrine

The experiments reported in 3.1 and 3.2 show that trazodone inhibits the firing of serotonergic neurons by direct activation of 5-HT$_{1A}$ARs and that an additional inhibitory effect of the drug contributes in silencing firing. As trazodone is an α$_1$-adrenoceptor ligand and in our experiments the activity of serotonergic neurons was facilitated by the presence of 10 μM PE, the non 5-HT$_{1A}$ receptor-mediated inhibitory effect of trazodone could result from disfacilitation of neuron firing produced by α$_1$-adrenoceptor antagonism.

In preparations in which the neuron firing was facilitated by a low concentration of PE (1 μM) in the presence of Way-100635 (20 nM), the application of 10 μM trazodone silenced the neurons and the effect was fully reversed by the addition of 100 μM PE (Fig 3A and 3B; n = 5).

This showed that the non 5-HT$_{1A}$ receptor-mediated effect of trazodone could be surmounted by increasing PE concentration, indicating that trazodone was acting as competitive antagonist at α$_1$-adrenoceptors. Accordingly, when the firing was facilitated by low calcium/high potassium ACSF (*see* methods) in the *absence* of PE, trazodone 10 μM produced a pure 5-HT$_{1A}$ receptor-mediated inhibition of serotonergic neuron activity (Fig 3C and 3D).

To better characterize the contribution of α$_1$-adrenoceptor antagonism in the inhibition of serotonergic neuron firing by trazodone, we compared the concentration-dependent effect of trazodone in preparations where the firing was facilitated by different concentrations of PE (1, 10, 100 μM) in the presence of 20 nM Way-100635 to block the 5-HT$_{1A}$ receptor-mediated effect of trazodone (Fig 4).

In PE 1 μM, trazodone concentration-dependently suppressed neuron firing (Fig 4A and 4B) with an average EC$_{50}$ value of 1.985 μM (GM, 95% C.I.: 1.451–2.716, n = 15; Fig 4C). When neurons were activated by PE 10 μM the average EC$_{50}$ value was increased to 9.881 μM (GM, 95% C.I.: 7.284–13.40, n = 11; Fig 4D–4F). As illustrated in Fig 4G, in PE 100 μM we

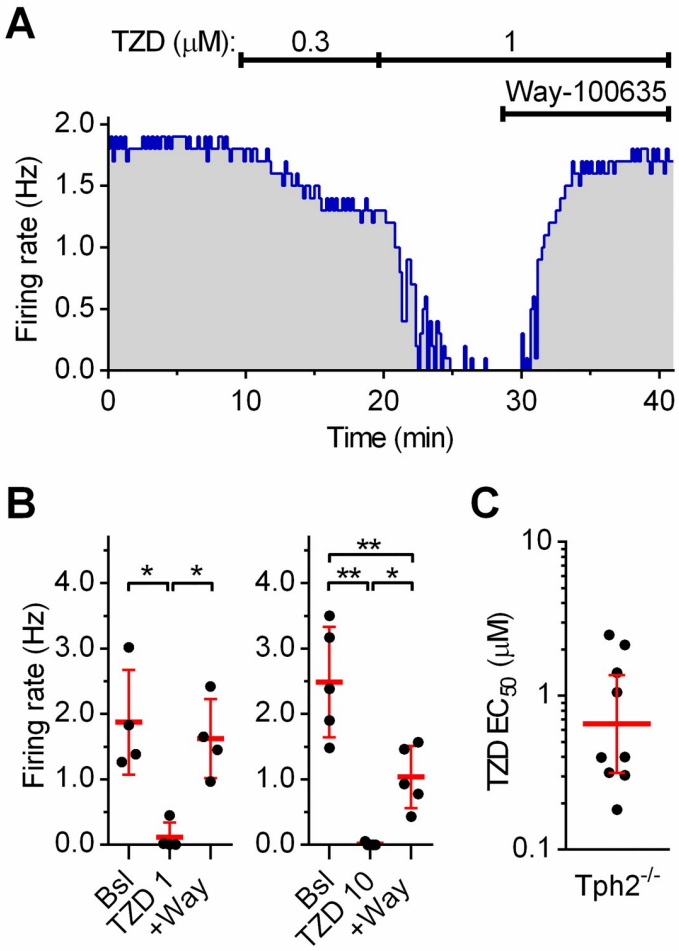

Fig 2. Effect of trazodone in *Tph2*$^{-/-}$ mice. (A) Representative recording of concentration-dependent effect of trazodone (TZD). The effect was fully antagonized by 20 nM Way-100635. **(B)** Summary of the antagonism exerted by 20 nM Way-100635 (+Way) on responses to 1 μM (n = 4; One-way RM ANOVA: $F_{(2,3)} = 36.24$; $p < 0.0045$) and 10 μM (n = 5; One-way RM ANOVA: $F_{(2,4)} = 41{,}95$; $p < 0.0028$) trazodone. Note the partial antagonism of responses to 10 μM trazodone. **(C)** Scatter plot of the individual EC_{50} values calculated from all experiments (n = 9). Red line and error bars indicate the geometric mean and 95% C.I.. The activity of serotonergic neurons was facilitated by the presence of 10 μM PE. * $p < 0.05$; ** $p < 0.01$ (One-way RM ANOVA, followed by a Tukey *post-hoc* test).

https://doi.org/10.1371/journal.pone.0222855.g002

applied only 10 and 30 μM trazodone to avoid a likely contamination of responses by aspecific effects of the drug at higher concentrations. From this set of experiments (n = 9) individual EC_{50} values could not be calculated, while the mean effects for these two drug concentrations were sufficient to obtain the EC_{50} value for trazodone effect in 100 μM PE (39.07 μM) from the calculated average concentration-response curve. Fig 4H illustrates the rightward shift of concentration-response curves for the α_1-adrenoceptor-mediated inhibitory effect of trazodone produced by increasing the concentration of PE from 1 μM to 100 μM.

Based on the experiments shown in Fig 4, in the presence of PE 100 μM the contribution of α_1-adrenoceptor antagonism in the overall inhibitory effect at concentrations of trazodone up to 10 μM was small (12 ± 8% *see* Fig 4G). We therefore sought to evaluate the potency of trazodone in suppressing serotonergic neuron firing through 5-HT1AAR stimulation in these

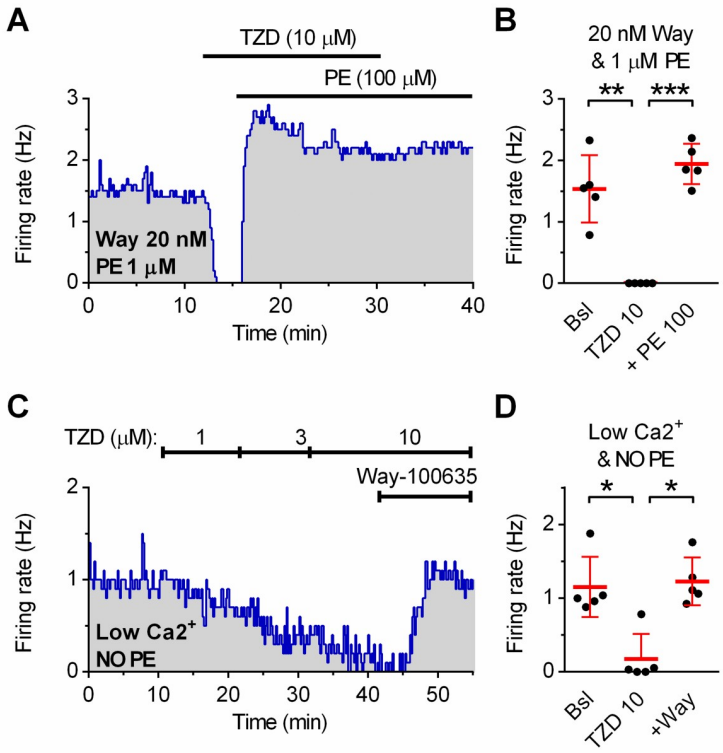

Fig 3. Antagonism at α_1-adrenoceptors by trazodone contributes in the inhibition of serotonergic neuron activity. **(A)** Representative recording of neuron activity facilitated by 1 μM phenylephrine (PE) in the presence of Way-100635 (+Way; 20 nM). The inhibitory effect of 10 μM trazodone (TZD) is surmounted by addition of 100 μM phenylephrine (PE). **(B)** Summary of five experiments (mean ± SD; One-way RM ANOVA: $F_{(2,4)} = 48.74$; $p < 0.0002$). **(C)** Representative recording of the concentration-dependent effect of trazodone on neuron activity facilitated by low calcium ACSF (*see* methods) in the absence of PE. **(D)** Summary of five experiments (mean ± SD; One-way RM ANOVA: $F_{(2,4)} = 16.21$; $p < 0.0122$) * $p < 0.05$; ** $p < 0.01$; *** $p < 0.001$ (One-Way RM ANOVA followed by Tukey *post-hoc* test).

https://doi.org/10.1371/journal.pone.0222855.g003

conditions (i.e. in PE 100 μM) in which the α_1-adrenoceptor antagonism by the drug was minimized. As shown in Fig 5A and 5B, trazodone inihibited the activity of neurons in a concentration-dependent manner and the effect was completely antagonized by the addition of Way-100635 (20 nM; Fig 5A and 5E).

The average dose-response relationship calculated on the mean response of nine experiments, is reported in Fig 5C. In eight neurons in which individual EC_{50} could be calculated the average EC_{50} value was of 4.365 μM (GM, 95% C.I.: 2.553–7.466, n = 8; Fig 5D). Notably, the curve shown in Fig 5C suggested that the agonism of trazodone at 5-HT_{1A}ARs was partial. Nevertheless, due to the residual interference of α_1-adrenoceptor antagonism by trazodone at concentrations > 10 μM the efficacy of the drug at 5-HT_{1A}ARs was impossible to be reliably quantified.

Trazodone activates 5-HT_{1A} autoreceptor-coupled GIRK channels in serotonergic neurons with weak partial agonist action

To clarify whether trazodone was a partial agonist, we investigated the potency and the functional effect of trazodone at 5-HT_{1A}ARs of rat DRN serotonergic neurons recorded in whole-cell configuration. To this purpose, we measured the changes in slope conductance of 5-HT_{1A}

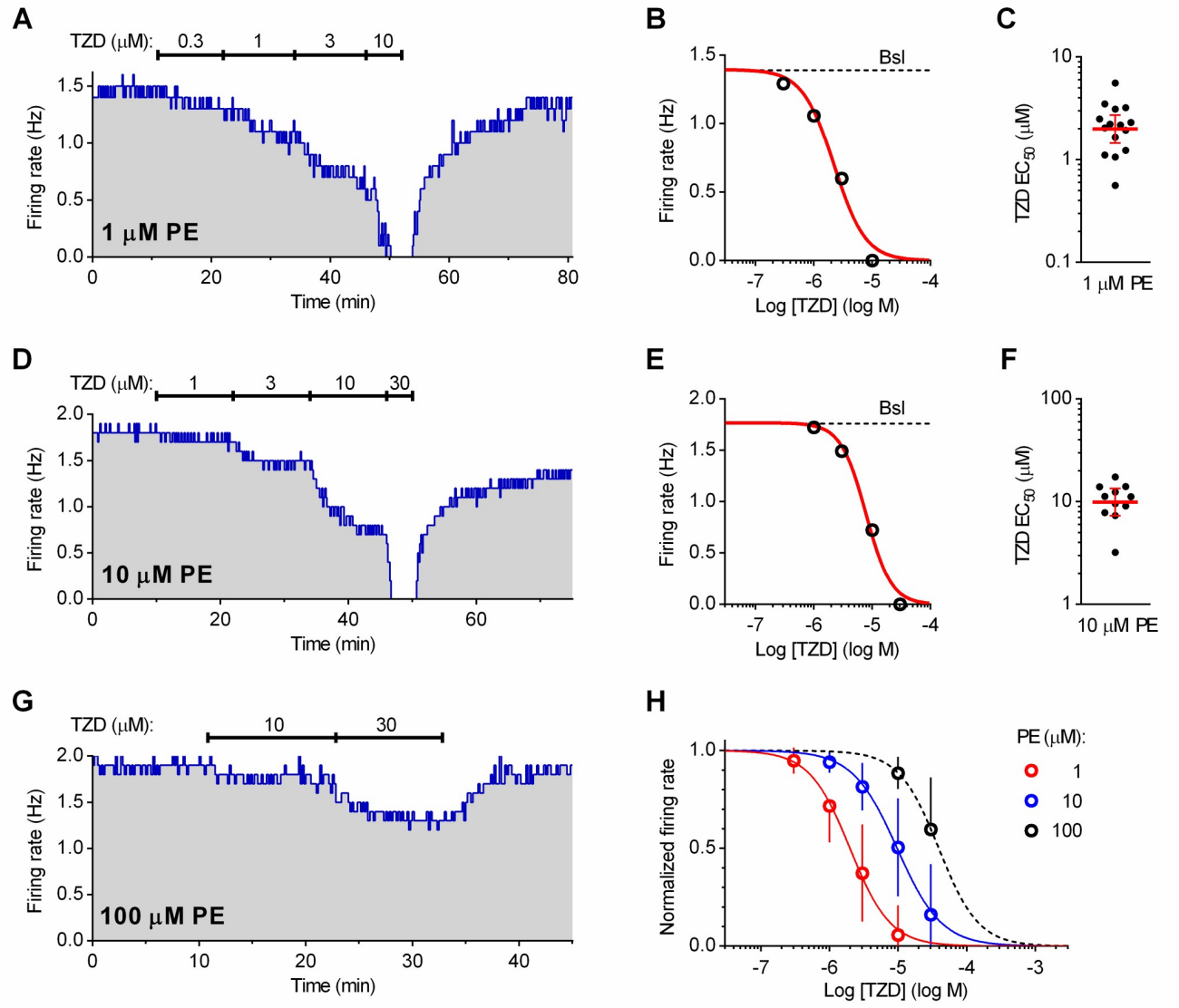

Fig 4. Block of 5-HT$_{1A}$ receptors by Way-100635 uncovers the α_1-adrenoceptor- dependent effect of trazodone. **(A)** Representative experiment showing the effect of trazodone (TZD) on neuron firing facilitated by 1 μM phenylephrine (PE) in the presence of Way-100635 (20 nM). **(B)** DRC resulting from the experiment shown in **(A)**. Red line is the best least-squares fit to the logistic equation. **(C)** Scatter plot of the individual EC_{50} values calculated from fifteen similar experiments. **(D)** Representative experiment showing the effect of trazodone on neuron firing facilitated by 10 μM PE **(E)** DRC resulting from the experiment shown in **(D)**. Red line is the best least-squares fit to the logistic equation. Note that 30 μM trazodone is required to silence the neuron. **(F)** Scatter plot of the individual EC_{50} values calculated from eleven experiments. **(G)** Representative recording from a set of experiments (n = 9) in which trazodone 10 μM and 30 μM was applied in the presence of 100 μM PE. In **(B)** and **(E)**, dotted line indicates the baseline (Bsl) firing rate before application of trazodone. In **(C)** and **(F)**, red line and error bars indicate the geometric mean and 95% C.I. **(H)** Average DRCs of trazodone effect obtained from the experiments in PE 1–100 μM. Symbols and error bars correspond to the mean values± SD obtained for each concentration in the corresponding set of experiments. Red line is the best least-squares fit to the logistic equation. Data are normalized on average baseline firing rates recorded before trazodone application. The baseline firing rates of neurons recorded in the three groups were (Hz, mean ± SD): 1.840 ± 0.5444 in PE 1μM (n = 15), 1.766 ± 0.4040 in PE 10μM (n = 11) and 1.970 ± 0.5559 in PE 100 μM (n = 9). These values were not significantly different ($F_{(2.32)} = 0.4046$; p = 0.6706; One-Way ANOVA).

https://doi.org/10.1371/journal.pone.0222855.g004

receptor-coupled GIRK channels, which provided a direct measure of 5-HT$_{1A}$ receptor activation produced by the application of trazodone. As illustrated in Fig 6, the concentration-dependent effect of trazodone (1–30 μM; n = 12) was maximal at 30 μM and was reversed by

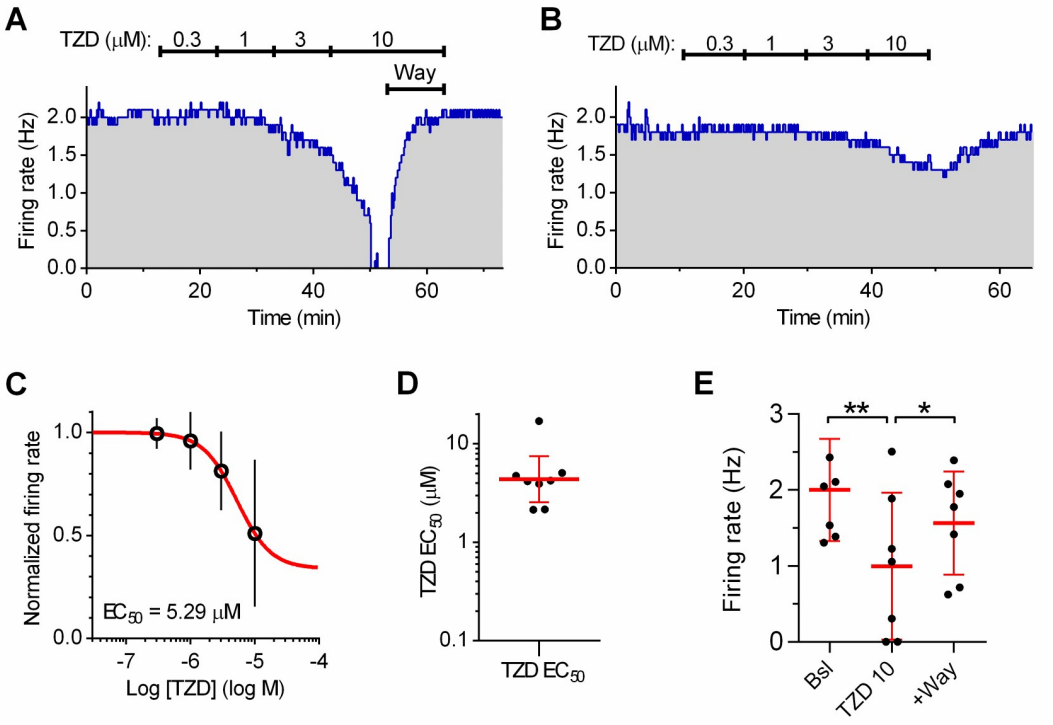

Fig 5. Activation of 5-HT$_{1A}$ receptors by trazodone in high phenylephrine. **(A, B)** Representative recordings of potent **(A)** and weak **(B)** trazodone (TZD effects on serotonergic neuron firing in the presence of 100 μM phenylephrine. Note that trazodone effect in **(A)** was fully antagonized by 20 nM Way-100635 (Way). **(C)** Average DRC obtained from all the experiments (n = 11). **(D)** Summary scatter plot of individual EC_{50} values from experiments in which complete DRC were obtained (n = 8). Data are normalized on Bsl firing rate. Red line is the best least-squares fit to the logistic equation. Symbols and error bars report the mean value ± SD. **(E)** Summary of the antagonism of Way-100635 on trazodone 10 μM (mean ± SD; n = 7; One-way RM ANOVA: $F_{(2,6)} = 11.80$; $p < 0.0015$). $^{*}p < 0.05$, $^{**}p < 0.01$ (One-Way RM ANOVA followed by a Tukey *post-hoc* test).

https://doi.org/10.1371/journal.pone.0222855.g005

the application of the selective 5-HT$_{1A}$ receptor antagonist Way-100635. In nine out twelve recorded neurons, the magnitude of the concentration-dependent increases in GIRK channel conductance permitted reliable fitting of data in individual concentration-response curves. The average EC_{50} value for GIRK channel opening by trazodone obtained from individual neurons was 3.34 μM (Geometric mean, 95% C.I.: 2.21–5.06; n = 9; Fig 6B).

To quantify the efficacy of trazodone at 5-HT$_{1A}$ARs, we compared the effect of the maximally active concentration of trazodone with that of the 5-HT$_{1A}$ receptor full agonist 5-CT in the same neurons. In all recordings in which 5-CT (30 nM) and trazodone (30 μM) were applied in the same neurons 5-CT produced an increase in GIRK channel conductance greater than that of trazodone (n = 14; Fig 6C) whose effect was occasionally very small (n = 3). From the peak effects produced by trazodone and 5-CT the calculated average efficacy of trazodone compared to 5-CT was 35.3% (Fig 6D; paired t test, two tails: t = 6.588; df = 13; $p < 0.0001$; n = 14). To confirm these findings in a larger number of neurons and to further ensure that the application of 5-CT in the same neuron did not change the sensitivity to trazodone action at 5-HT$_{1A}$ARs, we compared the response to single applications of 5-CT and trazodone in different neurons. As the magnitude of GIRK conductance responses to trazodone appeared correlated to cell membrane capacitance (Fig 6E), which reflects the surface area of recorded neurons, the effects of trazodone and 5-CT were normalized to the membrane capacitance to

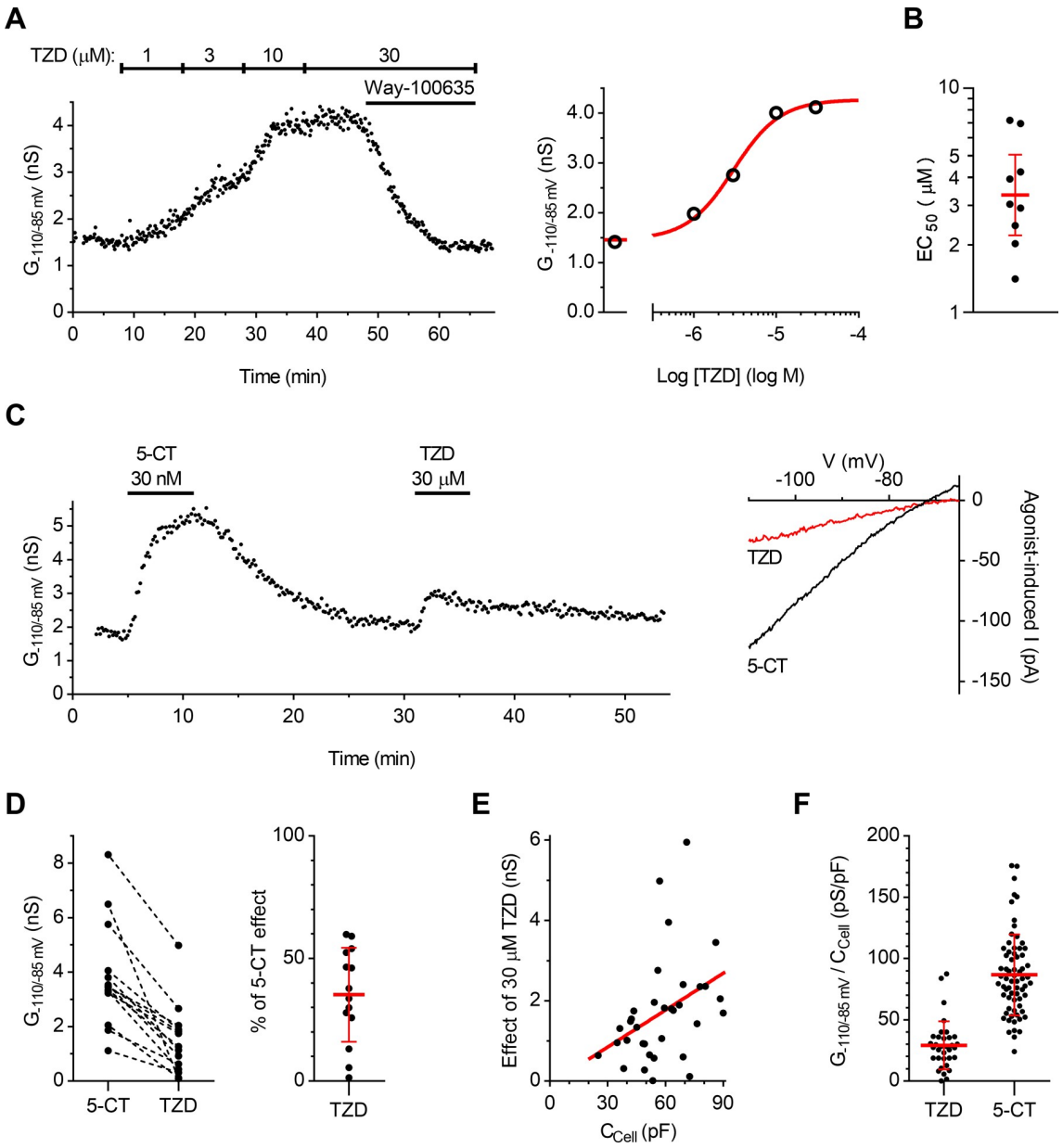

Fig 6. Trazodone partially activates 5-HT$_{1A}$ receptor-coupled GIRK channels of serotonergic neurons. **(A)** Concentration-response relationship for 5-HT1AAR-mediated activation of GIRK conductance by trazodone. *Left panel*: Time-course of a representative experiment showing the effect of increasing concentrations of bath-applied trazodone (TZD) on GIRK conductance ($G_{-110/-85\ mV}$) in a serotonergic neuron. $G_{-110/-85\ mV}$ was measured as the slope conductance activated in the range from -110 to -85 mV membrane potential by hyperpolarizing ramps under whole-cell voltage-clamp (*see* methods). Application of the selective 5-HT$_{1A}$ receptor antagonist Way-100635 (20 nM) reveals the 5-HT$_{1A}$ receptor-mediated component of the response. Time indicates duration of whole-cell configuration. *Right panel*: concentration-response relationship of the same experiment. The red line is the best least-squares fit to the logistic equation. **(B)** Scatter plot of EC_{50} values of trazodone in individual neurons (n = 9). Note the ordinate in logarithmic scale. Bars correspond to geometric mean ± 95% C.I. **(C)** *Left panel*: Time-course of a representative experiment performed to compare the maximal effect of trazodone (30 μM) with that of the full agonist 5-CT (30 nM) on GIRK conductance ($G_{-110/-85\ mV}$) in a serotonergic neuron. *Right panel*: Current-voltage plot of agonist-induced currents of the same experiment. Each trace is the difference between current in the presence of the indicated agonist and control current recorded before the agonist application. **(D)** *Left graph*: Comparison of 30 μM trazodone and 30 nM 5-CT effects in individual neurons. *Right graph*: Scatter plot summarizing the extent of trazodone partial agonism in individual recordings (100 x $G_{-110/-85\ mV,\ TZD}$ / $G_{-110/-85\ mV,\ 5\text{-}CT}$). Bars correspond to mean ± SD. **(E)** The correlation between the effect of 30 μM trazodone ($G_{-110/-85\ mV}$) and the cell membrane capacitance (C_{Cell}). Symbols represent single experiments (n = 34). Red line represents best least square fit. Correlation analysis revealed moderate positive correlation (Pearson $r = 0.38$, $p = 0.026$). **(F)** Comparison of 30 μM trazodone (n = 34) and 30 nM 5-CT (n = 68) effects in serotonergic neuron population.

Data are normalized for cell membrane capacitance. Symbols represent the response of individual neurons to single applications of 5-HT_{1A} receptor agonists. Bars correspond to mean ± SD.

https://doi.org/10.1371/journal.pone.0222855.g006

correct for differences in cell size and density of GIRK channels in different neurons. The maximal trazodone effect was 29.12 ± 19.63 (pS/pF; n = 34) and resulted significantly smaller compared to that produced by 5-CT (86.68 ± 33.12 pS/pF; n = 68; unpaired t test two tails, t = 9.333; df = 100; $p < 0.0001$; Fig 6F). The resulting mean efficacy of trazodone was of 33.6% compared to that of 5-CT, a value very similar to that found when the two compounds were applied in the same neurons.

The weak partial agonism by trazodone partially antagonizes full agonist action of 5-CT at 5-HT_{1A} autoreceptors

The weak efficacy of trazodone suggested that the drug could exert a competitive antagonism of the response to the full agonist 5-CT. We therefore compared the response to 10 nM 5-CT applied alone or in the presence of 10 μM trazodone. We have chosen submaximal concentrations of the two drugs so that eventual summation of the two effects could be revealed. As illustrated in Fig 7, comparison of peak effects produced by 5-CT alone or in the presence of trazodone (4.21 ± 1.66 vs 2.42 ± 1.29 nS; Fig 7B; n = 5; paired t test, two tails: t = 6.675; df = 4; p = 0.0026) shows that the total activation of the GIRK conductance resulting by coapplication of 5-CT and trazodone was smaller (54.8 ± 11.4%, n = 5, Fig 7C) than that measured when 5-CT was applied alone in the same neurons.

The quantification of the agonist efficacy of trazodone at 5-HT_{1A}ARs provided a measured value for a theoretical estimate of 5-HT_{1A}AR activation in the absence of trazodone and in the presence of the drug [35] (*see* methods). The calculated response to 10 nM 5 CT in the presence of 10 μM trazodone (42.2% of maximal response produced by 5 CT) was not statistically different from that reported in Fig 7C (54.8 ± 11.4%, n = 5; p = 0.125 Wilcoxon signed rank test).

These results show that trazodone is able to significantly decrease the activation of 5-HT_{1A}ARs produced by the full agonist 5-CT and confirmed the applicability of the measured efficacy value to estimate the effects of different trazodone concentrations on the total 5-HT_{1A}AR activation by a full agonist using the known affinity constants of the agonists.

Discussion

Trazodone displays relatively high affinity for several proteins involved in the direct or indirect regulation of serotonergic neuron activity, including 5-HT_{1A} receptors, α_1-adrenoceptors and SERT [5]. The present study elucidates how the binding of trazodone at these sites translates into direct changes of serotonergic neuron activity. In particular, we characterized the properties of 5-HT1AAR activation by trazodone and the relevance of α_1-adrenoceptor antagonism in the overall effect of the drug on serotonergic neuron activity. The data reported herein demonstrate that trazodone is an α_1-adrenoceptor antagonist and a weak partial agonist at 5-HT_{1A}ARs of DRN serotonergic neurons. Functionally, these two independent actions converge in inhibiting the activity of serotonergic neurons with variable contribution according to the noradrenergic drive elicited by PE in vitro and, presumably, to the arousal state *in vivo*.

The activity of serotonergic neurons is physiologically facilitated by noradrenergic tone which varies during the sleep-wake cycle, being maximal during wake [36]. At the same time the extracellular 5-HT present in the raphe tonically stimulates 5-HT_{1A}ARs thereby limiting neuron firing [37, 38, 12]. The latter action is greatly enhanced when the reuptake of 5-HT is

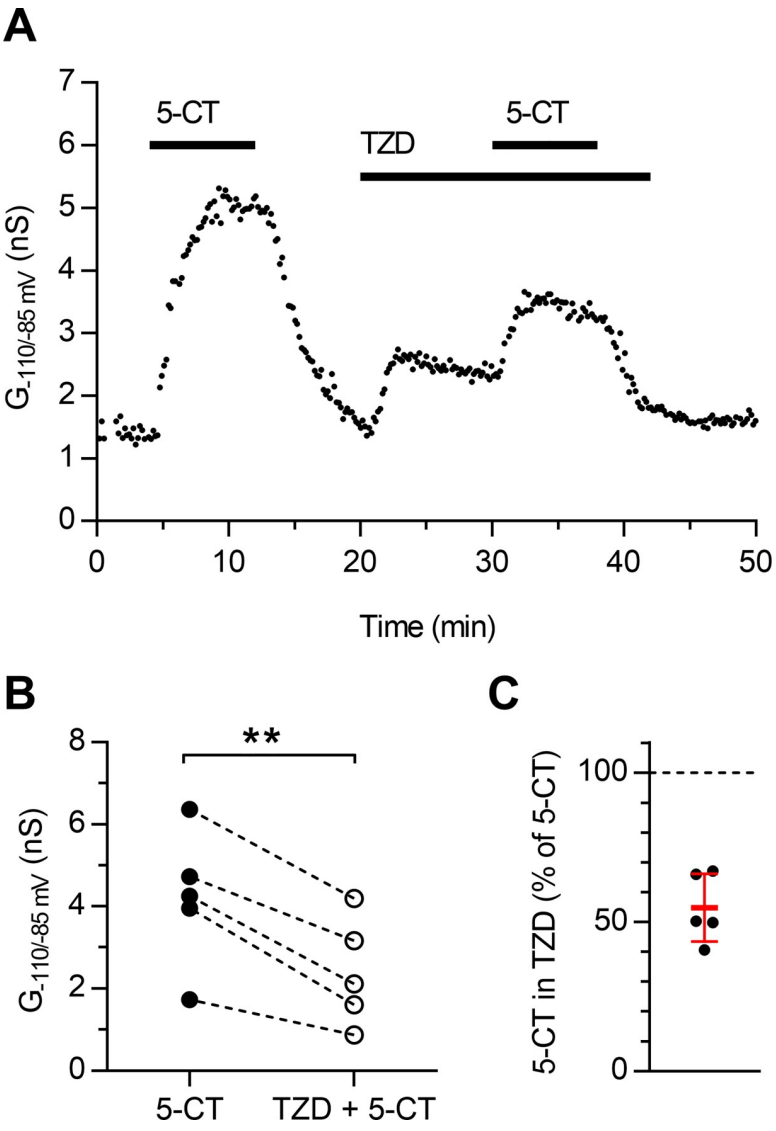

Fig 7. Antagonism at 5-HT$_{1A}$ autoreceptors by trazodone. (A) Time-course of a representative experiment in a serotonergic neuron showing that the total activation of the GIRK conductance ($G_{-110/-85\ mV}$) produced by 10 nM 5-CT in the presence of 10 μM trazodone (TZD) is smaller than that measured when 5-CT is applied alone. **(B)** Comparison of 10 nM 5-CT effects in control and in the presence of 10 μM trazodone in individual neurons (n = 5). **(C)** Scatter plot summarizing the antagonism of 5-CT effect exerted by trazodone at 5-HT$_{1A}$ARs in five experiments. Values are calculated on net 5-HT$_{1A}$ receptor-activated GIRK conductance obtained from data shown in **(B)** after baseline conductance subtraction. Bars correspond to mean ± SD. $^{**}p< 0.01$ (paired t test, two tails).

https://doi.org/10.1371/journal.pone.0222855.g007

inhibited by antidepressant drugs. This effect is believed to result in a therapeutically inappropriate limitation of serotonergic neuron activity for some weeks, until 5-HT1AAR desensitization occurs [13, 14] or other compensatory mechanisms reconduct serotonergic neuron firing to normal rate in spite of active autoinhibition [39].

Trazodone inhibits the firing of serotonergic neurons recorded from the DRN in anaesthetized rats [19] through an action involving 5-HT$_{1A}$ receptor activation [20]. However, *in vivo* studies did not fully elucidate whether the firing suppression was due to direct activation of 5-HT$_{1A}$ARs, increase in extracellular 5-HT due to SERT inhibition, α_1-adrenoceptor antagonism, or a combination of these effect. Our experiments show that trazodone directly activates

5-HT_{1A}ARs since the effect of the drug was not modified when the local action of the major neurotransmitters was prevented by selective antagonists. Furthermore, the 5-HT_{1A} receptor-mediated inhibition of firing was present in *Tph2*$^{-/-}$ mice that lack brain 5-HT indicating that this effect of trazodone was not mediated by endogenous 5-HT acting on serotonergic or neighbour neurons.

In our extracellular recordings the firing of serotonergic neurons was facilitated by the stimulation of α_1-adrenoceptors with PE to reproduce the activation of serotonergic neurons by noradrenergic drive *in vivo* [40]. Therefore, although in our *in vitro* conditions disfacilitation of firing due to α_1-adrenoceptor antagonism by trazodone resulted additive to the 5-HT_{1A} receptor-mediated inhibitory effect, these two components of trazodone action could be pharmacologically better discriminated than *in vivo* models. Thus, in the presence of the selective 5-HT_{1A} receptor antagonist Way-100635 the effect of trazodone was concentration-dependently surmounted by increasing PE, indicating that trazodone is a competitive antagonist at α_1-adrenoceptors. Consistently, when serotonergic neuron firing was facilitated by lowering Ca^{2+} content in the ACSF *in the absence of PE*, trazodone silenced serotonergic neuron firing and the effect was fully antagonized by Way-100635. Furthermore, when the effect of α_1-adrenoceptor antagonism by trazodone was minimized by the presence of high PE the 5-HT_{1A} receptor-mediated inhibition persisted, although efficacy was much weaker, suggesting that trazodone is a partial agonist at 5-HT_{1A}ARs.

The partial agonism of trazodone at 5-HT_{1A}ARs was confirmed by means of whole-cell recording in which we quantified the net increase in serotonergic neuron membrane conductance produced by the opening of GIRK channels in response to the drug in the absence of PE. The amount of activated GIRK channels is proportional to the number of receptors stimulated, thus GIRK conductance reliably reports the concentration-dependent effect of agonists allowing for quantitative evaluation of the potency and intrinsic efficacy of trazodone at 5-HT_{1A}ARs.

The efficacy of trazodone in activating 5-HT_{1A}ARs was about one third of that of the full agonist 5-CT with a potency in the low micromolar range, hence this action would occur at therapeutic concentrations of the drug [41]. The weak efficacy of trazodone in activating 5-HT_{1A}ARs is consistent with data obtained using 5-HT_{1A} receptor-stimulated [^{35}S]-GTPγS binding in rat hippocampal and cortical membrane preparations ($\leq$ 20% at 30 μM) [21]).

We also show that the weak intrinsic activity of trazodone exerts partial antagonism of the action of the full agonist 5-CT. Thus, at therapeutic concentrations the weak partial agonism of trazodone could antagonize the full activation of 5-HT_{1A}ARs of endogenous 5-HT, whose extracellular concentration is raised by the concomitant block of SERT produced by trazodone.

Notably, the partial antagonism exerted by trazodone does not prevent 5-HT1AAR desensitization during treatment *in vivo* (20). This is in agreement with the effect of other partial agonists [42], whereas full antagonists have been shown to prevent functional desensitization of 5-HT_{1A}ARs (e.g. Way-100635 [43].

Notwithstanding the more complex effects that trazodone can produce *in vivo* through its action at other receptors (e.g. 5-HT_{2A}) or local/long-loop feedback regulation, our data provide the ground for mechanistic interpretation of the interplay between the 5-HT_{1A} receptor agonist and α_1-adrenoceptor antagonist properties of trazodone in directly regulating serotonergic neuron firing.

Trazodone exerted functionally considerable effects on both 5-HT_{1A}ARs and α_1-adrenoceptors at concentrations $\leq$ 3 μM that are relevant to the clinical effects of the drug when used as antidepressant or off label hypnotic. One single oral dose of 300 mg trazodone-ER (extended release) produces stable plasma concentrations of ~3 μM for 12 h in healthy

volunteers [44]. At this concentration, trazodone would weakly activate 5-HT_{1A}ARs but, at the same time, would substantially antagonize the full activation of 5-HT1AARs by 5-HT whose level is raised by the block of SERT produced by the drug. In humans, assuming that the basal extracellular concentration of 5-HT in DRN is similar to that measured in the rat *in vivo* (~10 nM) [45] and that trazodone produces a fivefold increase in 5-HT extracellular level [46]), at therapeutic concentrations achievable in the brain (3 μM) the relative occupancy at 5-HT_{1A}ARs by trazodone and 5-HT would be ~70% and ~30% respectively (*see* methods). Under these conditions the total activation of 5-HT_{1A}ARs will be ~52% of that produced by 50 nM 5-HT in the absence of the weak partial agonist trazodone.

Interestingly, Ghanbari et al. [20] reported that the basal firing rate *in vivo* after two days of treatment with trazodone was decreased by ~40% compared to controls. This is a relatively weaker inhibition than that observed in similar conditions with escitalopram (~ 70%) [47], although results are from two separate experimental setting, hence not directly comparable.

Importantly, the antagonist effect of trazodone would occur starting from the first drug administration. This would limit the detrimental tonic inhibition of serotonergic neuron firing produced by the raise in extracellular 5-HT starting from the beginning of the therapy, regardless the mechanism(s) involved in the recovery of neuron activity during chronic treatment with antidepressant drugs [13, 14, 39]. Recently, it has been proposed that faster and/or better clinical response to treatment could be achieved with antidepressant drugs that combine SERT inhibition with 5-HT_{1A} receptor partial agonism [18]. In agreement with this hypothesis, clinical signs of antidepressant effect were detected after one week of treatment with trazodone [48]).

Among antidepressant drugs trazodone has a distinctive sleep regulating activity [49]) that favoured its off-label use in insomnia [7]. The 5-HT system participates in arousal and is implicated in sleep, being active during waking and becoming progressively inactive during slow wave sleep and almost completely silent during REM sleep [9, 50, 51, 3]. These state dependent changes in activity of 5-HT system can be ascribed, at least in part, to similar changes in noradrenergic neuron activity [52], that facilitate the firing of serotonergic neurons via activation of α_1-adrenoceptors [25].

Although the relative contribution of 5-HT_{1A} and α_1-adrenoceptor effects *in vivo* cannot be fully mimicked *in vitro* as the actual degree of noradrenergic drive changes during wake-sleep cycle, the combined 5-HT_{1A} receptor agonist and α_1-adrenoceptor antagonist effects of trazodone on these neurons could be relevant to its effects on sleep. At concentrations akin those present in human brain following administration of trazodone for sleep disorders [41], the dual action of trazodone could facilitate inhibition of serotonergic neuron firing in the phase of drowsiness when α_1-adrenoceptor stimulation is lowered [53]. In addition, antagonism at α_1-adrenoceptor is likely to dampen the effects of noradrenergic system reactivation that occurs during sleep thereby preventing insomnia-related microarousals [54].

In conclusion, our results show that trazodone directly inhibits DRN serotonergic neuron activity through 5-HT_{1A} receptor weak partial agonism and α_1-adrenoceptor antagonism. Collectively our data suggest that the overall inhibition of neuron activity produced by the dual action of trazodone will result inversely proportional to the degree of α_1-adrenoceptor activation, being maximal when α_1-adrenoceptor is low and gradually decreasing with higher α_1-adrenoceptor stimulation.

Acknowledgments

The authors wish to thank Dr. Serena Tongiani, Dr. Nicola Carucci and Dr. Beatrice Garrone for their helpful comments on the manuscript.

Author Contributions

Conceptualization: Boris Mlinar, Lorenzo Polenzani, Maurizio Magnani, Renato Corradetti.

Formal analysis: Boris Mlinar, Renato Corradetti.

Funding acquisition: Renato Corradetti.

Investigation: Alberto Montalbano, Francesco Bonfiglio.

Project administration: Renato Corradetti.

Supervision: Boris Mlinar.

Writing – original draft: Renato Corradetti.

Writing – review & editing: Boris Mlinar, Lorenzo Polenzani, Maurizio Magnani, Renato Corradetti.

References

1. Cools R, Roberts AC, Robbins TW. Serotoninergic regulation of emotional and behavioural control processes. Trends Cogn Sci. 2008; 12: 31–40. https://doi.org/10.1016/j.tics.2007.10.011 PMID: 18069045
2. Saper CB, Fuller PM, Pedersen NP, Lu J, Scammell TE. Sleep state switching. Neuron 2010; 68:1023–1042 https://doi.org/10.1016/j.neuron.2010.11.032 PMID: 21172606
3. Cespuglio R. Serotonin: its place today in sleep preparation, triggering or maintenance. Sleep Med. 2018; 49:, 31–39. https://doi.org/10.1016/j.sleep.2018.05.034 PMID: 30029993
4. Lesch KP, Araragi N, Waider J, van den Hove D, Gutknecht L. Targeting brain serotonin synthesis: insights into neurodevelopmental disorders with long-term outcomes related to negative emotionality, aggression and antisocial behaviour. Philos Trans R Soc Lond B Biol Sci. 2012; 67: 2426–2443.
5. Owens MJ., Morgan WN, Plott SJ, Nemeroff CB. Neurotransmitter receptor and transporter binding profile of antidepressants and their metabolites. J Pharmacol Exp Ther. 1997; 283: 1305–1322. PMID: 9400006
6. Cusack B, Nelson A, Richelson E. Binding of antidepressants to human brain receptors: focus on newer generation compounds. Psychopharmacology (Berl) 1994; 114: 559–565.
7. Stahl SM. Mechanism of action of trazodone: a multifunctional drug. CNS Spectr. 2009; 14: 536–346. PMID: 20095366
8. Levine ES, Jacobs BL. Neurochemical afferents controlling the activity of serotonergic neurons in the dorsal raphe nucleus: microiontophoretic studies in the awake cat. J Neurosci. 1992; 12: 4037–4044. PMID: 1357117
9. McGinty DJ, Harper RM. Dorsal raphe neurons: depression of firing during sleep in cats. Brain Res. 1976; 101: 569–575. https://doi.org/10.1016/0006-8993(76)90480-7 PMID: 1244990
10. Chazalon M, Dumas S, Bernard JF, Sahly I, Tronche F, de Kerchove d'Exaerde A, et al. The GABAergic Gudden's dorsal tegmental nucleus: A new relay for serotonergic regulation of sleep-wake behavior in the mouse. Neuropharmacology 2018; 138: 315–330. https://doi.org/10.1016/j.neuropharm.2018.06.014 PMID: 29908240
11. Fornal CA, Metzler CW, Gallegos RA, Veasey SC, McCreary AC, Jacobs BL. WAY-100635, a potent and selective 5-hydroxytryptamine1A antagonist, increases serotonergic neuronal activity in behaving cats: comparison with (S)-WAY-100135. J Pharmacol Exp Ther. 1996; 278: 752–762. PMID: 8768728
12. Mlinar B, Montalbano A, Baccini G, Tatini F, Berlinguer Palmini R, Corradetti R. Nonexocytotic serotonin release tonically suppresses serotonergic neuron activity. J Gen Physiol. 2015; 145: 225–251. https://doi.org/10.1085/jgp.201411330 PMID: 25712017
13. Blier P, de Montigny C. Current advances and trends in the treatment of depression. Trends Pharmacol Sci. 1994; 15: 220–226. https://doi.org/10.1016/0165-6147(94)90315-8 PMID: 7940983
14. Blier P, Ward NM. Is there a role for 5-HT_{1A} agonists in the treatment of depression? Biol Psychiatry 2003; 53: 193–203. https://doi.org/10.1016/s0006-3223(02)01643-8 PMID: 12559651
15. Artigas F, Romero L, De Montigny C, Blier P. Acceleration of the effect of selected antidepressant drugs in major depression by 5-HT1A antagonists. 1996; Trends Neurosci. 19: 378–383. https://doi.org/10.1016/S0166-2236(96)10037-0 PMID: 8873352

16. Piñeyro G, Blier P. Autoregulation of serotonin neurons: role in antidepressant drug action. 1999; Pharmacol Rev. 51: 533–591. PMID: 10471417

17. Portella MJ, de Diego-Adeliño J, Ballesteros J, Puigdemont D, Oller S, Santos B, et al. Can we really accelerate and enhance the selective serotonin reuptake inhibitor antidepressant effect? A randomized clinical trial and a meta-analysis of pindolol in nonresistant depression. 2011; J Clin Psychiatry 72: 962–969. https://doi.org/10.4088/JCP.09m05827blu PMID: 21034693

18. Artigas F, Bortolozzi A, Celada P. Can we increase speed and efficacy of antidepressant treatments? Part I: General aspects and monoamine-based strategies. 2018; Eur Neuropsychopharmacol. 28: 445–456. https://doi.org/10.1016/j.euroneuro.2017.10.032 PMID: 29174531

19. Scuvée-Moreau J, Dresse A. Effect of trazodone on the firing rate of central monoaminergic neurons. Comparison with various antidepressants. 1982; Arch Int Pharmacodyn Ther 260: 299–301. PMID: 7165436

20. Ghanbari R, El Mansari M, Blier P. Sustained Administration of Trazodone Enhances Serotonergic Neurotransmission: In Vivo Electrophysiological Study in the Rat Brain. 2010a; J Pharmacol Exp Ther; 335: 197–206. https://doi.org/10.1124/jpet.110.169417 PMID: 20647493

21. Odagaki Y, Toyoshima R, Yamauchi T. Trazodone and its active metabolite m-chlorophenylpiperazine as partial agonists at 5-HT1A receptors assessed by [35S]GTPγS binding. 2005; J Psychopharmacol. 19: 235–241. https://doi.org/10.1177/0269881105051526 PMID: 15888508

22. Ghanbari R, El Mansari M, Blier P. Electrophysiological impact of trazodone on the dopamine and norepinephrine systems in the rat brain. 2012; Eur Neuropsychopharmacol. 22: 518–526. https://doi.org/10.1016/j.euroneuro.2011.11.005 PMID: 22154666

23. Baraban JM, Aghajanian GK. Noradrenergic innervation of serotonergic neurons in the dorsal raphe: demonstration by electron microscopic autoradiography. 1981; Brain Res. 204: 1–11. https://doi.org/10.1016/0006-8993(81)90646-6 PMID: 6166350

24. Peyron C, Luppi PH, Fort P, Rampon C, Jouvet M. Lower brainstem catecholamine afferents to the rat dorsal raphe nucleus. 1996; J Comp Neurol. 364: 402–413. https://doi.org/10.1002/(SICI)1096-9861(19960115)364:3<402::AID-CNE2>3.0.CO;2-8 PMID: 8820873

25. Baraban JM, Aghajanian GK. Suppression of firing activity of 5-HT neurons in the dorsal raphe by alpha-adrenoceptor antagonists. 1980; Neuropharmacology 19:, 355–363. https://doi.org/10.1016/0028-3908(80)90187-2 PMID: 6104308

26. Araragi N, Mlinar B, Baccini G, Gutknecht L, Lesch KP, Corradetti R. Conservation of 5-HT1A receptor-mediated autoinhibition of serotonin (5-HT) neurons in mice with altered 5-HT homeostasis. 2013; Front Pharmacol. 4 (97). https://doi.org/10.3389/fphar.2013.00097 PMID: 23935583

27. Montalbano A, Corradetti R, Mlinar B. Pharmacological Characterization of 5-HT1A Autoreceptor-Coupled GIRK Channels in Rat Dorsal Raphe serotonergic neurons. 2015a; PLoS One 10, e0140369. https://doi.org/10.1371/journal.pone.0140369 PMID: 26460748

28. Montalbano A, Waider J, Barbieri M, Baytas O, Lesch KP, Corradetti R, et al. Cellular resilience: serotonergic neurons in Tph2-/- mice retain normal firing behavior despite the lack of brain 5-HT. 2015b; Eur Neuropsychopharmacol. 25: 2022–2035. https://doi.org/10.1016/j.euroneuro.2015.08.021 PMID: 26409296

29. Mlinar B, Montalbano A, Piszczek L, Gross C, Corradetti R. Firing Properties of Genetically Identified Dorsal Raphe Serotonergic Neurons in Brain Slices. 2016; Front Cell Neurosci 10: 195. https://doi.org/10.3389/fncel.2016.00195 PMID: 27536220

30. Waeber C, Moskowitz MA. Autoradiographic visualisation of [3H]5-carboxamidotryptamine binding sites in the guinea pig and rat brain. 1995; Eur J Pharmacol. 283: 31–46. https://doi.org/10.1016/0014-2999(95)00275-p PMID: 7498319

31. Boess FG, Martin IL Molecular biology of 5-HT receptors. 1994; Neuropharmacology 33: 275–317. https://doi.org/10.1016/0028-3908(94)90059-0 PMID: 7984267

32. Sundaram H, Newman-Tancredi A, Strange PG. Characterization of recombinant human serotonin 5HT1A receptors expressed in Chinese hamster ovary cells. [3H]spiperone discriminates between the G-protein-coupled and -uncoupled forms. 1993; Biochem Pharmacol. 45: 1003–1009. https://doi.org/10.1016/0006-2952(93)90243-p PMID: 8461029

33. Gutknecht L, Kriegebaum C, Waider J, Schmitt A, Lesch KP. Spatio-temporal expression of tryptophan hydroxylase isoforms in murine and human brain: convergent data from Tph2 knockout mice. 2009; Eur Neuropsychopharmacol. 19: 266–82. https://doi.org/10.1016/j.euroneuro.2008.12.005 PMID: 19181488

34. Mlinar B, Montalbano A, Waider J, Lesch KP, Corradetti R. Increased functional coupling of 5-HT(1A) autoreceptors to GIRK channels in Tph2(-/-) mice. 2017; Eur Neuropsychopharmacol. 27:1258–1267. https://doi.org/10.1016/j.euroneuro.2017.10.033 PMID: 29126768

35. Kenakin T, Williams M. Defining and characterizing drug/compound function. 2014; Biochem Pharmacol. 87: 40–63. https://doi.org/10.1016/j.bcp.2013.07.033 PMID: 23954707

36. Berridge CW, Schmeichel BE, España RA. Noradrenergic modulation of wakefulness/arousal. 2012; Sleep Med Rev. 16: 187–197. https://doi.org/10.1016/j.smrv.2011.12.003 PMID: 22296742

37. Andrade R, Huereca D, Lyons JG, Andrade EM, McGregor KM. 5-HT1A Receptor-Mediated Autoinhibition and the Control of Serotonergic Cell Firing. 2015; ACS Chem Neurosci 6: 1110–1115. https://doi.org/10.1021/acschemneuro.5b00034 PMID: 25913021

38. Mlinar B, Tatini F, Ballini C, Nencioni S, Della Corte L, Corradetti R. Differential autoinhibition of 5-hydroxytryptamine neurons by 5-hydroxytryptamine in the dorsal raphe nucleus. 2005; Neuroreport 16: 1351–1355. https://doi.org/10.1097/01.wnr.0000175249.25535.bf PMID: 16056138

39. Commons KG, Linnros SE. Delayed Antidepressant Efficacy and the Desensitization Hypothesis. 2019; ACS Chem Neurosci. https://doi.org/10.1021/acschemneuro.8b00698 PMID: 30807103

40. Vandermaelen CP, Aghajanian GK. Electrophysiological and pharmacological characterization of serotonergic dorsal raphe neurons recorded extracellularly and intracellularly in rat brain slices. 1983; Brain Res. 289: 109–119. https://doi.org/10.1016/0006-8993(83)90011-2 PMID: 6140982

41. Settimo L, Taylor D. Evaluating the dose-dependent mechanism of action of trazodone by estimation of occupancies for different brain neurotransmitter targets. 2018; J Psychopharmacol. 32: 96–104. https://doi.org/10.1177/0269881117742101 PMID: 29332554

42. Blier P, de Montigny C. Modification of 5-HT neuron properties by sustained administration of the 5-HT1A agonist gepirone: electrophysiological studies in the rat brain. 1987; Synapse 1: 470–480. https://doi.org/10.1002/syn.890010511 PMID: 2905533

43. Hervás I, Vilaró MT, Romero L, Scorza MC, Mengod G, Artigas F. Desensitization of 5-HT(1A) autoreceptors by a low chronic fluoxetine dose effect of the concurrent administration of WAY-100635. 2001; Neuropsychopharmacol. 24: 11–20.

44. Karhu D, Groenewoud G, Potgieter MA, Mould DR. Dose proportionality of oncedaily trazodone extended-release caplets under fasting conditions. 2010; J Clin Pharmacol. 50: 1438–1449. https://doi.org/10.1177/0091270009360979 PMID: 20173086

45. Crespi F, Martin KF, Marsden CA. Measurement of extracellular basal levels of serotonin in vivo using nafion-coated carbon fibre electrodes combined with differential pulse voltammetry. 1988; Neuroscience 27: 885–896. https://doi.org/10.1016/0306-4522(88)90191-1 PMID: 3252175

46. Pazzagli M, Giovannini MG, Pepeu G. Trazodone increases extracellular serotonin levels in the frontal cortex of rats. 1999; Eur J Pharmacol. 383: 249–257. https://doi.org/10.1016/s0014-2999(99)00644-5 PMID: 10594316

47. Ghanbari R, El Mansari M, Blier P. Electrophysiological effects of the co-administration of escitalopram and bupropion on rat serotonin and norepinephrine neurons. 2010b; J Psychopharmacol. 24: 39–50. https://doi.org/10.1177/0269881108095714 PMID: 18719044

48. Sheehan DV, Croft HA, Gossen ER, Levitt RJ, Brullè C, Bouchard S, et al. Extended-release trazodone in major depressive disorder: a randomized, double-blind, placebo controlled study. 2009; Psychiatry 6: 20–33. PMID: 19724732

49. Fagiolini A, Comandini A, Catena Dell'Osso M, Kasper S. Rediscovering trazodone for the treatment of major depressive disorder. 2012; CNS Drugs. 26: 1033–49. https://doi.org/10.1007/s40263-012-0010-5 PMID: 23192413

50. Trulson ME, Jacobs BL. Raphe unit activity in freely moving cats: correlation with level of behavioural arousal. 1979; Brain Res. 163: 135–150. https://doi.org/10.1016/0006-8993(79)90157-4 PMID: 218676

51. Sakai K, Crochet S. Serotonergic dorsal raphe neurons cease firing by disfacilitation during paradoxical sleep. 2000; Neuroreport. 11: 3237–3241. https://doi.org/10.1097/00001756-200009280-00037 PMID: 11043555

52. Jacobs BL. Single unit activity of locus coeruleus neurons in behaving animals. 1986; Prog Neurobiol. 27: 183–194. PMID: 3529238

53. Fornal CA, Litto WJ, Metzler CW, Marrosu F, Tada K, Jacobs BL. Single-unit responses of serotonergic dorsal raphe neurons to 5-HT1A agonist and antagonist drug administration in behaving cats. 1994; J Pharmacol Exp Ther 270: 1345–1358. PMID: 7932189

54. Feige B, Baglioni C, Spiegelhalder K, Hirscher V, Nissen C, Riemann D. The microstructure of sleep in primary insomnia: an overview and extension. 2013; Int J Psychophysiol. 89: 171–180. https://doi.org/10.1016/j.ijpsycho.2013.04.002 PMID: 23583625

frontiers in Neuroscience

ORIGINAL RESEARCH
published: 24 April 2019
doi: 10.3389/fnins.2019.00245

Serotonin Deficiency Increases Context-Dependent Fear Learning Through Modulation of Hippocampal Activity

Jonas Waider[1], Sandy Popp[1], Boris Mlinar[2], Alberto Montalbano[2], Francesco Bonfiglio[2], Benjamin Aboagye[1], Elisabeth Thuy[1], Raphael Kern[1], Christopher Thiel[1], Naozumi Araragi[3,4], Evgeniy Svirin[1,5], Angelika G. Schmitt-Böhrer[6], Renato Corradetti[2], Christopher A. Lowry[7] and Klaus-Peter Lesch[1,5,8]*

[1] Division of Molecular Psychiatry, Center of Mental Health, University of Würzburg, Würzburg, Germany, [2] Department of Neuroscience, Psychology, Drug Research, and Child Health, University of Florence, Florence, Italy, [3] Max Delbrück Center for Molecular Medicine in the Helmholtz Association, Berlin, Germany, [4] Charité – Universitätsmedizin Berlin, Berlin, Germany, [5] Laboratory of Psychiatric Neurobiology, Institute of Molecular Medicine, I.M. Sechenov First Moscow State Medical University, Moscow, Russia, [6] Department of Psychiatry, Psychosomatics, and Psychotherapy, Center of Mental Health, University of Würzburg, Würzburg, Germany, [7] Department of Integrative Physiology and Center for Neuroscience, University of Colorado Boulder, Boulder, CO, United States, [8] Department of Translational Psychiatry, School for Mental Health and Neuroscience, Maastricht University, Maastricht, Netherlands

OPEN ACCESS

Edited by:
Guillaume Lucas, INSERM U1215 Neurocentre Magendie, France

Reviewed by:
Luc Maroteaux, INSERM U839 Institut du Fer à Moulin, France
Bettina Bert, Freie Universität Berlin, Germany
Stefano Comai, Vita-Salute San Raffaele University, Italy

***Correspondence:**
Jonas Waider
Waider_J@ukw.de

Specialty section:
This article was submitted to Neuropharmacology, a section of the journal Frontiers in Neuroscience

Received: *29 September 2018*
Accepted: *01 March 2019*
Published: *24 April 2019*

Citation:
Waider J, Popp S, Mlinar B, Montalbano A, Bonfiglio F, Aboagye B, Thuy E, Kern R, Thiel C, Araragi N, Svirin E, Schmitt-Böhrer AG, Corradetti R, Lowry CA and Lesch K-P (2019) Serotonin Deficiency Increases Context-Dependent Fear Learning Through Modulation of Hippocampal Activity. Front. Neurosci. 13:245. doi: 10.3389/fnins.2019.00245

Brain serotonin (5-hydroxytryptamine, 5-HT) system dysfunction is implicated in exaggerated fear responses triggering various anxiety-, stress-, and trauma-related disorders. However, the underlying mechanisms are not well understood. Here, we investigated the impact of constitutively inactivated 5-HT synthesis on context-dependent fear learning and extinction using tryptophan hydroxylase 2 (*Tph2*) knockout mice. Fear conditioning and context-dependent fear memory extinction paradigms were combined with c-Fos imaging and electrophysiological recordings in the dorsal hippocampus (dHip). *Tph2* mutant mice, completely devoid of 5-HT synthesis in brain, displayed accelerated fear memory formation and increased locomotor responses to foot shock. Furthermore, recall of context-dependent fear memory was increased. The behavioral responses were associated with increased c-Fos expression in the dHip and resistance to foot shock-induced impairment of hippocampal long-term potentiation (LTP). In conclusion, increased context-dependent fear memory resulting from brain 5-HT deficiency involves dysfunction of the hippocampal circuitry controlling contextual representation of fear-related behavioral responses.

Keywords: tryptophan hydroxylase 2, knockout, fear learning, extinction, long-term potentiation, hippocampus, immediate-early gene, serotonin deficiency

INTRODUCTION

Anxiety disorders are common and result in substantial economic costs to individuals and society (Bereza et al., 2009). The current global prevalence of anxiety disorders is approximately 7.3%, ranging from 5.4 to 10.4% (Baxter et al., 2013). Many individuals meet diagnostic criteria for multiple anxiety disorders and comorbidity with other psychiatric disorders (Kessler et al., 2005;

Miyazaki et al., 2011). A hallmark of anxiety disorders is dysfunctional acquisition and extinction of conditioned fear memories (Grillon, 2002; Milad et al., 2008).

Evidence suggests that serotonin plays an important role in control of anxiety and fear responses (Lesch et al., 1996; Lowry et al., 2005; Maier and Watkins, 2005; Maier et al., 2006; Baratta et al., 2016; Bocchio et al., 2016). Mice with a targeted inactivation of *Tph2* have provided insights into the role of 5-HT in the modulation of anxiety-like behaviors. Previous studies of lifelong deficiency of brain 5-HT synthesis are consistent with the hypothesis that the brain serotonergic system plays an important role in control of anxiety-like behaviors (Mosienko et al., 2015), fear learning, and behavioral responses to stress (Gutknecht et al., 2015), effects that might be due to alterations in GABAergic transmission (Jorgensen et al., 2013; Waider et al., 2013). Furthermore, mice with defects in 5-HT system development leading to reduction of 5-HT neurons showed differential anxiety-like behaviors and fear memory (Hendricks et al., 2003; Dai et al., 2008; Schaefer et al., 2009; Kiyasova et al., 2011; Song et al., 2011; Brooks et al., 2014). Indeed, the 5-HT system is thought to play an essential role in the regulation of fear memory in rodents (Graeff and Zangrossi, 2010; Bocchio et al., 2016). Studies in animals demonstrate a direct anatomical connection between the main sources of serotonin in the brain, the brainstem dorsal and median raphe nuclei as well as forebrain limbic structures, such as the medial prefrontal cortex, hippocampus, and amygdala, that control anxiety and fear responses (Maier et al., 2006; Hale and Lowry, 2011; Fernandez et al., 2016; Muzerelle et al., 2016). Of particular interest to contextual fear conditioning is the dorsal hippocampus (dHip; Bauer, 2015), which receives serotonergic projections primarily from the median raphe nucleus (Azmitia and Whitaker-Azmitia, 1995; McQuade and Sharp, 1997; Lowry, 2002).

Consistent with this hypothesis, acute administration of selective 5-HT reuptake inhibitors (SSRIs) 60 min before testing results in a decrease in contextual fear expression (Hashimoto et al., 1996; Li et al., 2001; Gravius et al., 2006), while it increases conditioned fear expression in auditory fear conditioning setting (Burghardt et al., 2007). Furthermore, peripheral administration of SSRIs decreases neuronal activity, immediate-early gene expression, and plasticity in the hippocampus (Staubli and Otaky, 1994; Igelstrom and Heyward, 2012; Ravinder et al., 2013). In addition to these effects of serotonergic signaling on fear expression, other studies provide support for a role for multiple 5-HT receptor types in the dHip in conditioned fear memory consolidation (Schmidt et al., 2017).

We previously showed that *Tph2* mutant ($Tph2^{-/-}$) mice display enhanced acquisition of conditioned fear and escape-oriented behavior in response to aversive foot shock, in association with altered basolateral amygdala function (Waider et al., 2017). Here, we investigated the impact of a lifelong abscence of brain 5-HT synthesis on the contextual domain of fear learning, using fear conditioning combined with an extinction paradigm, functional immunohistochemistry, and electrophysiological recordings within the hippocampal formation.

MATERIALS AND METHODS

Animals

Adult male $Tph2^{+/+}$, $Tph2^{+/-}$, and $Tph2^{-/-}$ mice on a mixed Sv129/C57BL/6N genetic background (Gutknecht et al., 2012), 2–5 months of age, were housed individually in a controlled environment (12 h/12 h light/dark cycle, light phase 7 am–7 pm, 21 ± 0.5°C room temperature, 50 ± 5% humidity) with food and water *ad libitum*. Mice were allowed to acclimate for 1 week before being subjected to fear conditioning experiments. Tests were performed during the light phase between 10:00 and 15:00. All experiments were performed in accordance with the European Parliament and Council Directive (2010/63/EU) and were approved by local authorities (55.2-2531.01-57/12) and (IT: 938/2017-PR).

Fear Conditioning and Contextual Fear Extinction Training

In order to assess context-dependent fear memory and extinction, $Tph2^{-/-}$, $Tph2^{+/-}$, and $Tph2^{+/+}$ mice (n = 8–9/genotype) were exposed to a fear conditioning protocol as previously described (Waider et al., 2017) and subsequently subjected to a context-dependent extinction protocol (EXT; **Figure 1**). Briefly, on day 0, mice were placed by a blinded operator in randomized order into the fear conditioning test box (TSE Systems, Homburg, Germany), which was comprised of a transparent Perspex arena (23 cm × 23 cm × 35 cm) on a stainless steel foot shock grid (floor bars 4 mm diameter, distance rod center to rod center 8.9 mm) that was connected to a shocker-scrambler unit for delivering foot shocks of defined duration and intensity (Raab et al., 2018). The arena was placed inside in a square-shaped base frame (outer size: 31 cm × 31 cm) with integrated animal detection sensors (XY and Z axes featuring 16 sensors mounted 14 mm apart). All sensors were scanned with a sampling rate of up to 100 Hz to monitor the animal's position and movement at high spatial and temporal resolution. The test box was operated in a sound-attenuating housing (52 cm × 52 cm × 65 cm) featuring a loudspeaker and two lamps in the ceiling for software-controlled application of acoustic stimuli and continuous house-light illumination (set to 100 lux in all testing phases), respectively.

Mice were allowed to freely explore for 2 min the test box before receiving three pairings of a 20 s tone cue (80 dB, 4 kHz), co-terminating with a 2 s foot shock (FS, 0.6 mA) at an inter-trial interval (ITI) of 1 min. Mice were removed from the chamber 2 min after the last tone-shock pairing. Starting 24 h after conditioning, mice were tested for recall and extinction of context-dependent fear on two consecutive days (day 1 and 2). Each extinction session consisted of re-exposing the animals to the conditioning context for 800 s without negative reinforcement.

Freezing was defined as no light-beam interruption for at least 2 s and expressed as percentage of time relative to total session duration (Rivero et al., 2015; Raab et al., 2018). Additionally, other indices of locomotor activity and exploratory behavior (i.e., distance moved, mean and maximum velocity, activity vs.

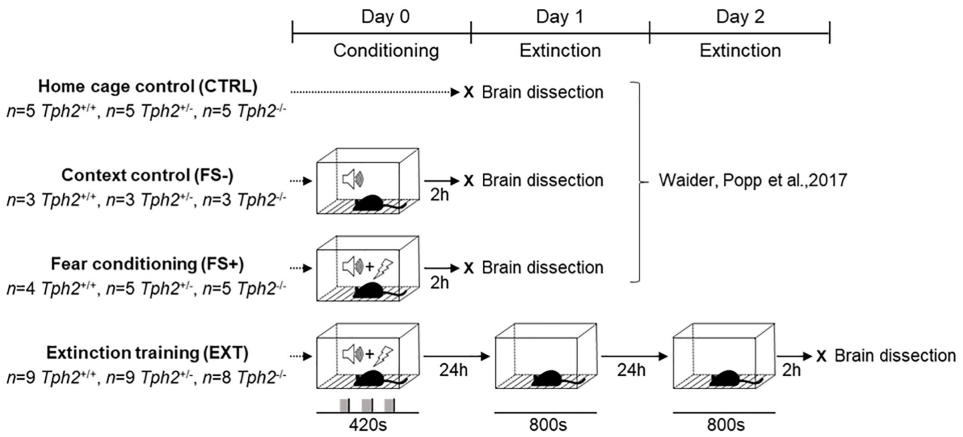

FIGURE 1 | Experimental design for c-Fos immunoreactivity after fear conditioning and context-dependent extinction. *Tph2*$^{+/+}$, *Tph2*$^{+/-}$, and *Tph2*$^{-/-}$ mice were exposed to a fear conditioning (FC) protocol and subsequently subjected to a context-dependent extinction protocol. On day 0 mice were placed in the conditioning chamber receiving three pairings of a 20 s tone cue co-terminating with a 2 s foot shock. On day 1 and again on day 2, mice were tested for recall and extinction of context-dependent fear memory using an extinction session consisting of re-exposing the animals to the conditioning context for 800 s without negative reinforcement. Two hours after extinction on day 2, brains were dissected for hippocampal c-Fos expression analysis (EXT) and compared to controls that were left undisturbed in the home cage (CTRL), controls that were exposed to the FC context and tone cue without foot shocks (FS–), and mice that underwent FC with tone-signaled foot shocks (FS+) with brain dissection 2 h after the test (Waider et al., 2017).

inactivity, rearing) were measured continuously by the light-beam detection system. Inactivity was defined as the percentage of time the animal's speed fell below a threshold of 2 cm/s. Using the same fear conditioning system (TSE FCS 303410 series), Misane et al. (2005) have shown that there is a close linear correlation between operator-scored freezing (using a time-sampling procedure in which the animal was instantly scored as either freezing or active every 10 s) and computer-derived inactivity (activity threshold 1 cm/s) both in context- and tone-dependent memory tests. Moreover, Toth et al. (2012) have shown that there is no difference between hand-scored freezing, TSE-determined freezing (defined as no light-beam interruption for at least 3 s), and Noldus Ethovision-determined inactivity.

To determine acquisition of the conditioned fear response, freezing was measured continuously throughout the training session. The maximum movement velocity was taken as an indicator of the animal's unconditioned reactivity to foot shock (Waider et al., 2017). During extinction training, freezing was continuously recorded in 20 s time-bins and, except for the first 20 s, averaged into blocks of 1 min to assess recall and extinction of contextual fear memory.

C-Fos and Parvalbumin Immunostaining in the Dorsal Hippocampus

Two hours after extinction on day 2, the brains of the mice that underwent context-dependent extinction training (EXT) were prepared for immunostaining of parvalbumin (PV) and c-Fos as previously described (Waider et al., 2017). The brain sections were analyzed and compared with the brains of mice that were either left undisturbed in the home cage (CTRL), exposed to the fear conditioning context and tone without foot shocks (FS-), or underwent fear conditioning with tone-signaled foot shocks (FS+) as previously described (Waider et al., 2017; **Figure 1**). In brief, serially cut 30 μm-thick cryostat sections were used for immunofluorescent stainings. Primary antibodies used were mouse anti-PV (1:200; Swant, Marly, Switzerland) and rabbit anti-c-Fos (1:400; Santa Cruz Biotechnology, Dallas, TX, United States). Sections were incubated in 1:400 diluted secondary antibodies, goat anti-mouse 488 and goat anti-rabbit 555 (Invitrogen, Carlsbad, CA, United States). Pictures were acquired with a motorized inverted system epifluorescence microscope IX81 (Olympus, Tokyo, Japan). Pictures were taken with 20× objective in x-y directions. Images were then processed using CellSense (Olympus, Tokyo, Japan), and corrected for contrast and brightness using ImageJ v2.0.0 (Schindelin et al., 2012). Three to five sections from −1.06 mm bregma to −2.06 mm bregma of the dHip, spaced 180 μm apart, were delineated with contours according to a stereotactic atlas of the mouse brain (Franklin and Paxinos, 1997). Immunoreactive (ir) cells were counted as c-Fos-ir only when the nucleus, according to DAPI (4′, 6-diamidino-2-phenylindole) counterstaining, showed complete fluorescent signal. When the PV signal superimposed or surrounded the cell nucleus, it was counted as c-Fos/PV-ir. The sum of counted cells of all sections per mouse were divided by the total contour area to calculate the cell densities per region of interest.

Electrophysiology

To investigate the impact of 5-HT deficiency on hippocampal plasticity under basal conditions and after contextual fear conditioning with unsignaled foot shocks, an independent cohort of mice was either left undisturbed (naïve controls) or subjected to a foot shock procedure according to Dai et al. (2008). Mice were placed in the box and allowed to freely explore for 2 min before receiving five foot shocks (0.5 mA, 2 s) with ITI of 2 min. Two minutes after the last foot shock, mice were

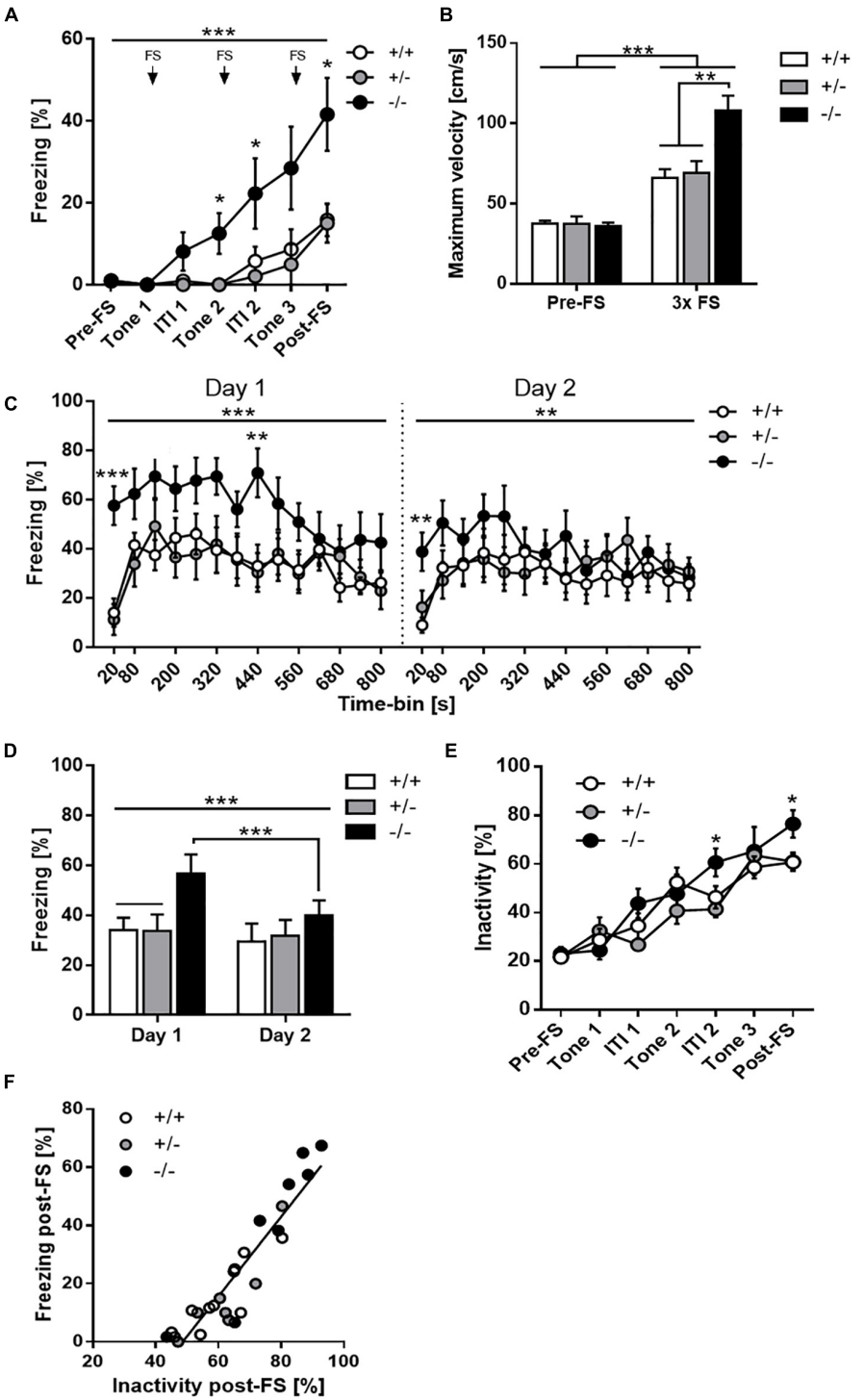

FIGURE 2 | Increased context-dependent fear memory recall but effective contextual extinction learning due to 5-HT deficiency. **(A)** Time-course analysis of the conditioned fear response of *Tph2*$^{+/+}$, *Tph2*$^{+/-}$, and *Tph2*$^{-/-}$ mice during acquisition training showing relative freezing levels before the first pairing of a tone cue with a foot shock (pre-FS), during tone presentations and inter-trial intervals (ITI), and after the last foot shock (post-FS). **(B)** Unconditioned foot shock reactivity, measured as maximum movement velocity before the first pairing of a tone cue with a foot shock (pre-FS) and following the foot shock (3 × FS). **(C)** Time-course analysis of the freezing response during contextual fear memory recall and extinction training on day 1 and 2 after conditioning. **(D)** Average freezing scores in the two extinction sessions. **(E)** Time-course analysis of the inactivity level during acquisition training showing relative inactivity levels. **(F)** Positive relationship between freezing scores obtained after the last foot shock (post-FS) in the conditioning session and inactivity scores. Data are shown as means + or ± SEM. *$p < 0.05$, **$p < 0.01$ and ***$p < 0.001$.

removed from the chamber and slices were prepared. Field excitatory postsynaptic potentials (fEPSPs) in the CA1 region of the dHip were recorded in transversal slices as previously described (Morini et al., 2011; Mlinar et al., 2015). LTP was induced by theta burst stimulation (TBS) comprised of a single train of 5 bursts of 5 stimuli (100 Hz intra-burst frequency, 5 Hz burst frequency). Stimulation intensity for baseline measurement and LTP induction was set to evoke fEPSP corresponding to 35–40% of the maximal response. Typically, more than one slice was used per mouse and the results of all determinations per genotype and treatment are shown and analyzed in order to account for the overall variability of LTP responses in the different genotypes. Mean values from replicates (2–4) in the same animal were used for genotype x treatment statistical analysis reported in results.

Statistical Analyses

Data were analyzed using IBM SPSS Statistics 21 (IBM Corp., Armonk, NY, United States) or GraphPad Prism version 6.00 (GraphPad Software, San Diego, CA, United States). Behavioral data were analyzed by two- or three-way mixed analysis of variance (ANOVA) with genotype as the between-subjects factor and with time and day as within-subjects factors. When appropriate, degrees of freedom were corrected using Greenhouse-Geisser estimates of sphericity.

An ANCOVA was performed in addition to the regular ANOVA to adjust for the effect of post-shock freezing (=covariate) on subsequent freezing during extinction sessions. Immunohistochemical and electrophysiological data were analyzed by two-way ANOVA with group and genotype as between-subjects factors. Unless otherwise indicated, Bonferroni *post hoc* tests were performed to evaluate significant main effects or simple effects following a significant interaction. Correlations between behavioral parameters and c-Fos expression were calculated using the Pearson correlation coefficient.

Results are presented as mean ± SEM unless stated otherwise. The significance level was set at $p < 0.05$ and $p < 0.1$ was highlighted as approaching statistical significance.

RESULTS

Increased Acquisition of Fear Conditioning in *Tph2*$^{-/-}$ Mice

Two-way mixed ANOVA for freezing during fear acquisition training (**Figure 2A**) revealed a significant main effect of time [$F_{(2.8,64.4)} = 17.54$, $p < 0.001$] and genotype [$F_{(2,23)} = 7.70$, $p = 0.003$], as well as a time × genotype interaction [$F_{(5.6,64.4)} = 2.73$, $p = 0.023$]. *Post hoc* tests showed that freezing levels were very low before the first tone-shock pairing and gradually increased thereafter over the course of training. However, *Tph2*$^{-/-}$ mice acquired the conditioned fear response more rapidly than *Tph2*$^{+/-}$ and *Tph2*$^{+/+}$ mice, as evidenced by significantly elevated freezing levels *Tph2*$^{-/-}$ mice from the second tone presentation onward. Furthermore, the reactivity to foot shock, as measured by the maximum movement velocity (Vmax), was significantly increased in *Tph2*$^{-/-}$ compared to *Tph2*$^{+/-}$ and *Tph2*$^{+/+}$ mice [genotype effect: $F_{(2,23)} = 9.63$, $p < 0.001$; **Figure 2B**].

Moreover, comparison of baseline (pre-FS) Vmax and foot shock-induced Vmax revealed a significant increase in all three genotypes (*Tph2*$^{+/+}$: $p < 0.01$, *Tph2*$^{+/-}$: $p < 0.001$ and *Tph2*$^{-/-}$: $p < 0.0001$), thereby demonstrating that *Tph2*$^{+/+}$ and *Tph2*$^{+/-}$ mice showed a clear response to FS, which was further exaggerated in *Tph2*$^{-/-}$ mice [phase x genotype interaction: $F_{(2,23)} = 8.223$, $p = 0.002$].

Besides freezing, we analyzed inactivity using an activity threshold of 2 cm/s. Baseline (pre-FS) inactivity (immobility/resting: ∼20–25%) did not significantly differ between genotypes ($p = 0.861$; **Figure 2E**). Inactivity increased linearly across tone-FS trials in all three genotypes [main effect of phase: $F_{(4.2,96.2)} = 55.73$, $p < 0.0001$] and reached maximum levels after three tone-FS pairings (∼61% in *Tph2*$^{+/+}$ and *Tph2*$^{+/-}$, ∼76% in *Tph2*$^{-/-}$ mice). Similar to freezing, *Tph2*$^{-/-}$ mice were significantly less active than *Tph2*$^{+/-}$ and *Tph*$^{+/+}$ mice after the 2nd and 3rd tone-FS pairing [phase x genotype interaction: $F_{(8.4,96.2)} = 2.27$, $p = 0.026$]. Moreover, there was a close linear correlation between post-shock freezing and post-shock inactivity ($r = 0.926$, $p < 0.0001$) with similar steepness of regression slopes in *Tph2*$^{+/+}$, *Tph2*$^{+/-}$ and *Tph2*$^{-/-}$ mice (**Figure 2F**).

Increased Recall but Effective Extinction of Contextual Fear Memory in *Tph2*$^{-/-}$ Mice

Analysis of freezing during extinction training on day 1 and 2 after fear conditioning revealed a significant time-bin x genotype [$F_{(9.5,149.5)} = 2.02$, $p = 0.041$, **Figure 2C**] and day × genotype [$F_{(2,299)} = 5.29$, $p = 0.013$, **Figure 2D**] interaction, but no genotype main effect [$F_{(2,23)} = 2.09$, $p = 0.147$]. *Post hoc* tests showed that, within sessions, *Tph2*$^{-/-}$ mice promptly froze upon placement into the conditioned context, while freezing onset was slightly delayed in *Tph2*$^{+/-}$ and *Tph2*$^{+/+}$ mice. Moreover, freezing levels of *Tph2*$^{-/-}$ mice remained elevated during the first minutes of testing but were indistinguishable from the other genotypes at the end of the session due to a steeper decline of the freezing response in *Tph2*$^{-/-}$ compared to *Tph2*$^{+/-}$ and *Tph2*$^{+/+}$ mice (**Figure 2C**). Accordingly, *Tph2*$^{-/-}$ mice showed a significantly stronger decrease of freezing than *Tph2*$^{+/-}$ and *Tph2*$^{+/+}$ mice across the two extinction sessions (**Figure 2D**).

Since *Tph2*$^{-/-}$ mice displayed significantly enhanced acquisition of conditioned fear and post-shock freezing levels in the conditioning session, we performed an analysis of covariance to control for differences in post-shock freezing levels. Three-way mixed ANCOVA confirmed a significant effect of post-shock freezing [$F_{(1,22)} = 12.56$, $p = 0.002$] as well as a time-bin x genotype [$F_{(9.9,138.6)} = 2.46$, $p = 0.011$] and day x genotype [$F_{(2,286)} = 2.73$, $p = 0.087$] interaction on the freezing scores obtained during extinction training. *Post hoc* tests again showed that *Tph2*$^{-/-}$ mice froze significantly more than *Tph2*$^{+/-}$ and *Tph2*$^{+/+}$ mice during the first 20 s of context re-exposure. However, freezing levels were indistinguishable among genotypes thereafter. Furthermore, *Tph2*$^{-/-}$ mice

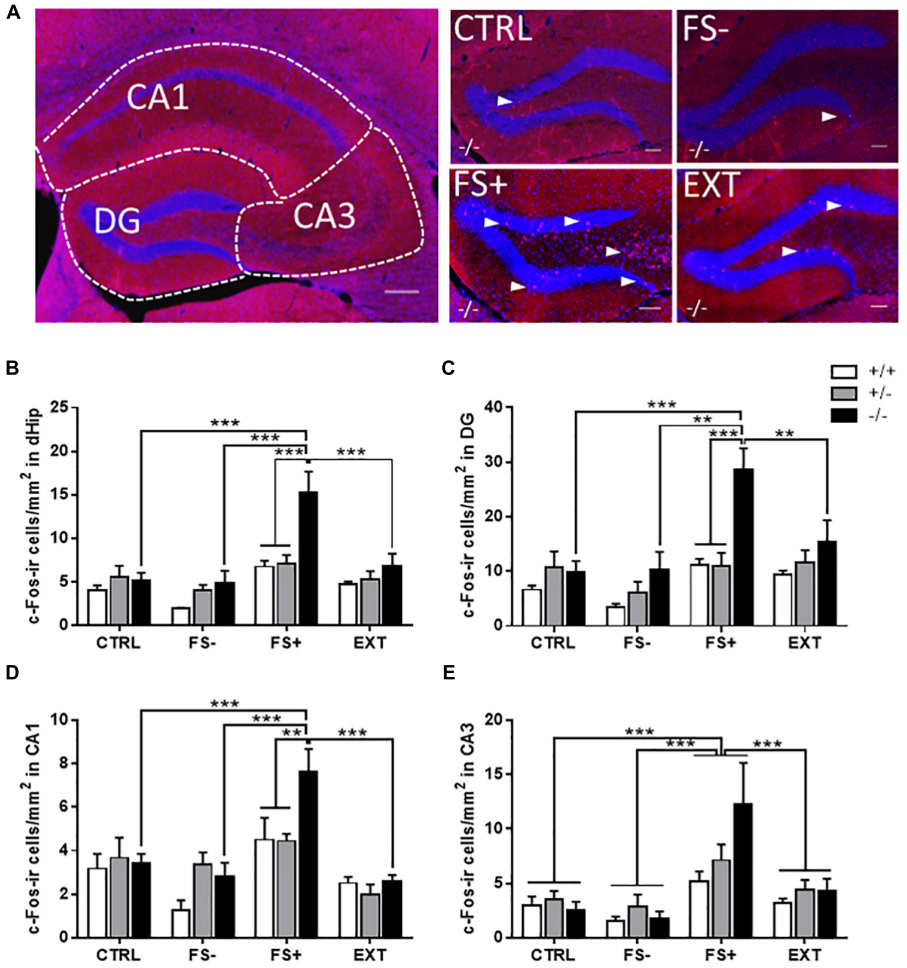

FIGURE 3 | Increased c-Fos activity in the dorsal hippocampus (dHip) of *Tph2*$^{-/-}$ mice following fear conditioning. (**A**, left panel) Overview of the dHip indicating the subregions dentate gyrus (DG), cornu ammonis area 1 (CA1), and cornu ammonis area 3 (CA3) and (**A**, right panel) higher magnification images depicting the DG of representative *Tph2*$^{-/-}$ mice for the different groups: home cage controls (CTRL), context controls subjected to the conditioning procedure without foot shocks (FS–), fear-conditioned mice receiving three tone-signaled foot shocks (FS+), fear-conditioned mice that underwent two extinction training sessions (EXT). Quantification of c-Fos-ir cell densities in **(B)** the total dHip, **(C)** DG, **(D)** CA1, and **(E)** CA3 of *Tph2*$^{+/+}$, *Tph2*$^{+/-}$, and *Tph2*$^{-/-}$ mice of the four different groups. Arrowheads in **(A)** indicate c-Fos-ir cells (red), DAPI-stained cell nuclei (blue). Scale bars in **(A)**: 200 μm (left panel) and 100 μm (right panel). Data are shown as means + SEM. $^{**}p < 0.01$; $^{***}p < 0.001$.

were able to extinguish the conditioned fear more efficiently than *Tph2*$^{+/-}$ and *Tph2*$^{+/+}$ mice, as evidenced by a stronger decline of the freezing response both within and across the two extinction sessions.

Taken together, these results indicate that 5-HT deficiency due to *Tph2* inactivation augmented context-dependent fear memory recall and facilitated both intra- and intersession extinction learning.

Increased c-Fos Activation Due to Fear Conditioning in *Tph2*$^{-/-}$ Mice

Because of the strong effect of 5-HT deficiency on post-shock freezing, an indicator of short-term memory for contextual fear (Fanselow, 1980), we analyzed c-Fos activation in the dHip and its subregions, dentate gyrus (DG), cornu ammonis area 1 (CA1), and 3 (CA3) of *Tph2*$^{-/-}$, *Tph2*$^{+/-}$ and *Tph2*$^{+/+}$ mice that were either left undisturbed in the home cage (CTRL), exposed to the fear conditioning procedure without foot shocks (FS−) or with foot shocks (FS+), or subjected to fear conditioning and subsequent extinction training (EXT) (**Figure 3**).

An increased density of c-Fos-ir cells was found in the dHip, especially in the granule cell layer and hilus of the DG (**Figure 3A**) of FS+ *Tph2*$^{-/-}$ mice. Quantification confirmed a significant genotype x group interaction for the density of c-Fos-ir cells in the total dHip [$F_{(6,51)} = 3.05$, $p = 0.0126$; **Figure 3B**], in the DG [$F_{(6,51)} = 2.31$, $p = 0.0477$; **Figure 3C**], and in the CA1 area [$F_{(6,51)} = 2.59$, $p = 0.0288$; **Figure 3D**]. *Post hoc* analyses showed that the number of c-Fos-ir cells was increased in the total dHip, DG and CA1 of *Tph2*$^{-/-}$ after fear conditioning relative to respective *Tph2*$^{+/-}$ and *Tph2*$^{+/+}$ FS+ controls as well as to CTRL, FS−, and EXT *Tph2*$^{-/-}$ mice ($p < 0.01$). A similar activation

pattern was observed in the CA3 region, although only a group main effect was detected [$F_{(3,51)}$ = 9.59, $p < 0.0001$; **Figure 3E**], with a significantly increased density of c-Fos-ir cells in FS+ animals compared to CTRL, FS−, and EXT mice (all $p < 0.001$).

Correlation analysis of the conditioned fear response (post-shock freezing) with the c-Fos-ir cell density in FS− and FS+ animals detected a strong positive relationship specifically in *Tph2*$^{-/-}$ mice ($r \geq 0.7501$, $p \leq 0.0321$; **Table 1**). A similar but less exclusive correlation pattern was observed for the density of c-Fos-ir cells with the unconditional response to FS (shock reactivity). Taken together, these data indicate that fear conditioning in *Tph2*$^{-/-}$ mice increased hippocampal activity, while context-dependent extinction training of fear memory normalized hippocampal c-Fos expression within the dHip of *Tph2*$^{-/-}$ mice.

Foot Shock Reduces C-Fos Activation of PV-ir Cells in 5-HT-Deficient Mice

Since PV-ir neurons in the hippocampus were previously shown to be involved in contextual memory (Donato et al., 2013), we analyzed c-Fos-ir neurons in the dHip by double-immunofluorescent staining with PV, a marker of a subset of inhibitory GABAergic interneurons (Gulyas et al., 1999). Because c-Fos-ir densities did not differ between CTRL and FS− animals but were highly increased in fear-conditioned FS+ *Tph2*$^{-/-}$ mice, we focused our further analyses on the FS+ group compared to the CTRL group (**Figure 4**). PV-ir cells were predominantly found in the CA3 and CA1 regions of the dHip, specifically in the stratum lacunosum, pyramidal layer, and stratum oriens with a high density of c-Fos/PV double-ir neurons in the CA1 region (**Figures 4B,E**). In the total dHip, ANOVA detected an almost significant genotype x group interaction for the density of c-Fos/PV double-ir neurons [$F_{(2,24)}$ = 3.14, p = 0.06; **Figure 4C**]. PV-ir neurons in FS+ *Tph2*$^{-/-}$ mice showed reduced c-Fos-ir cells relative to CTRL *Tph2*$^{-/-}$ mice (p = 0.053), while FS+ *Tph2*$^{+/+}$ and *Tph2*$^{+/-}$ mice displayed no alterations compared to respective CTRL mice. Within the FS+ group, *Tph2*$^{+/-}$ mice showed the highest c-Fos/PV-ir density compared to *Tph2*$^{+/+}$ (p = 0.05) and *Tph2*$^{-/-}$ (p = 0.009) mice.

In CA1, a similar but significant genotype x group interaction was detected for the density of c-Fos/PV double-ir neurons [$F_{(2,24)}$ = 4.77, p = 0.018; **Figure 4E**]. *Post hoc* tests revealed that CTRL *Tph2*$^{-/-}$ mice showed increased c-Fos/PV double-ir cell densities relative to CTRL *Tph2*$^{+/+}$ (p = 0.047). However, FS+ *Tph2*$^{-/-}$ mice showed reduced c-Fos/PV double-ir cell densities relative to CTRL *Tph2*$^{-/-}$ as well as FS+ *Tph2*$^{+/-}$ ($p < 0.05$) and FS+ *Tph2*$^{+/+}$ ($p < 0.1$) mice. Neither differences among genotypes nor among CTRL and FS+ groups were found for the density of PV-ir neurons in dHip (**Figure 4D**) and CA1 (**Figure 4F**). Altogether these data indicate increased recruitment of PV neurons in the dorsal CA1 region of CTRL *Tph2*$^{-/-}$ mice, which is absent after fear conditioning.

LTP Impairment by Inescapable Foot Shock Is Absent in *Tph2*-Deficient Mice

In the CA1 region, plasticity is modulated by endogenous 5-HT (Mlinar et al., 2015). Here, we investigated the impact of 5-HT deficiency on TBS-induced LTP of fEPSP in the hippocampal CA1 region of *Tph2*-deficient mice (**Figure 5C**). Similar LTP of fEPSP responses were found across genotypes in naïve mice (**Figure 5A**, upper panels), indicating that basic mechanisms underlying LTP are preserved in the life-long absence of 5-HT. Since the 5-HT system has been implicated in foot shock-induced impairment of LTP (Dai et al., 2008), we compared LTP in slices obtained from animals exposed to repeated foot shock stress (**Figure 5A**, lower panels, **B,D**). Two-way ANOVA revealed a significant genotype x group interaction [$F_{(2,30)}$ = 9.37 p = 0.0484; **Figure 5D**]. *Post hoc* analysis confirmed decreased LTP in *Tph2*$^{+/+}$ (p = 0.0011) and *Tph2*$^{+/-}$ (p = 0.002) mice after foot shock relative to naïve controls, an effect that was absent in *Tph2*$^{-/-}$ mice (**Figures 5A,B,D**) indicating that presence of 5-HT during foot shock is required for the stress-induced impairment of LTP.

DISCUSSION

We previously showed that lifelong absence in brain 5-HT synthesis following constitutive *Tph2* inactivation in mice enhanced acquisition of conditioned fear and promoted unconditioned escape responses to electric foot shock (Waider et al., 2017). Here, we were able to replicate and extend these findings, which indicate that

TABLE 1 | Pearson's correlation of shock reactivity and post-shock freezing with c-Fos density in the dorsal hippocampus and its subregions of FS− and FS+ animals.

		Shock reactivity				Post-shock freezing			
		Total	**+/+**	**+/−**	**−/−**	**Total**	**+/+**	**+/−**	**−/−**
dHip	*r*	0.6636	0.7071	0.5517	0.7493	0.6193	0.2035	0.2821	0.8590
	p	0.0006	0.0756	0.1563	0.0324	0.0016	0.6616	0.4985	0.0063
DG	*r*	0.6592	0.7065	0.3972	0.8409	0.6083	0.2151	0.1633	0.9279
	p	0.0006	0.0759	0.3298	0.0089	0.0021	0.6432	0.6992	0.0009
CA1	*r*	0.6453	0.4586	0.8015	0.7217	0.5401	−0.0100	0.6363	0.7501
	p	0.0009	0.3006	0.0168	0.0433	0.0078	0.9830	0.0898	0.0321
CA3	*r*	0.5561	0.7337	0.4562	0.5655	0.5950	0.3135	0.2460	0.7541
	p	0.0059	0.0605	0.2558	0.1441	0.0027	0.4936	0.5570	0.0307

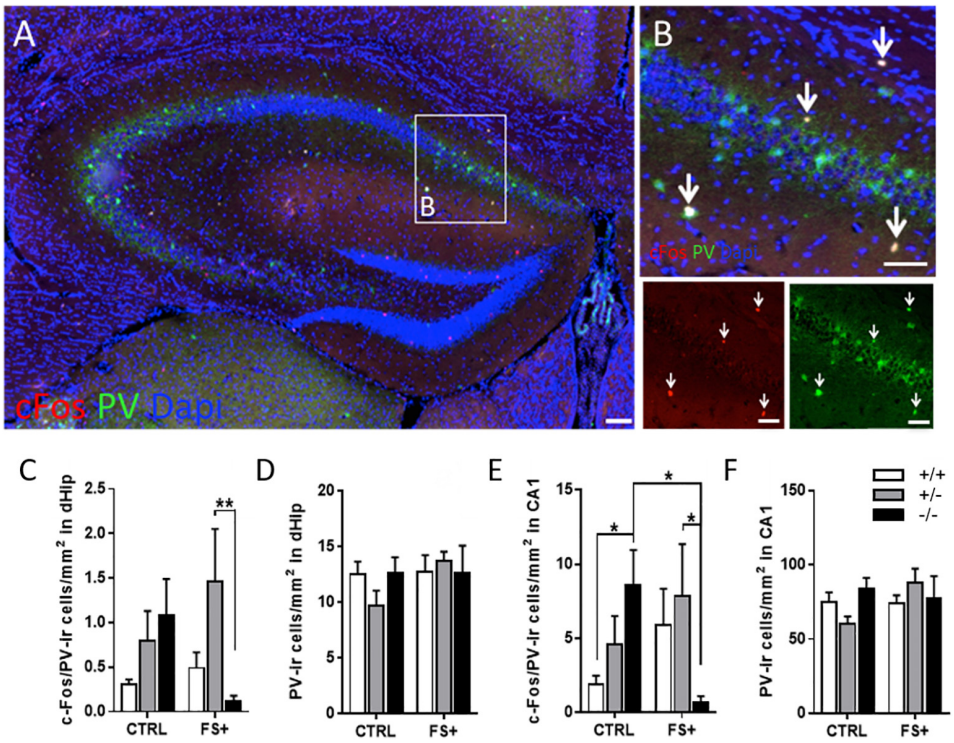

FIGURE 4 | Lifelong brain 5-HT synthesis deficiency prevents activation of parvalbumin-ir neurons in fear conditioning. **(A)** Anti-parvalbumin (PV) (green) and c-Fos (red) immunofluorescent staining with DAPI in the dorsal hippocampus (dHip) of a fear conditioned *Tph2*$^{+/-}$ mouse. **(B)** Magnified with magnified area of cornu ammonis area 1 (CA1). Density of c-Fos/PV-ir cells of home cage control (CTRL) and fear-conditioned (FS+) *Tph2*$^{+/+}$, *Tph2*$^{+/-}$, and *Tph2*$^{-/-}$ mice in **(C)** dHip and **(E)** CA1. PV-ir cell density of CTRL and FS+ *Tph2*$^{+/+}$, *Tph2*$^{+/-}$, and *Tph2*$^{-/-}$ mice in **(D)** dHip and **(F)** CA1. Data are shown as means + SEM. *$p < 0.05$; **$p < 0.01$. Two-way ANOVA followed by Fisher's LSD *post hoc* test. Scale bar: 100 μm.

constitutive *Tph2* inactivation results in faster acquisition of conditioned fear and increased escape-like behavior in response to foot shock, as well as enhanced contextual representation of the fear memory, but functional extinction of the context. By combining fear conditioning with immediate-early gene expression, our data emphasize that lifelong 5-HT deficiency renders the dHip hyperexcitable in fear conditioning.

The dHip encodes the contextual component of fear learning during early acquisition phases (Fanselow and Dong, 2010; Maren et al., 2013). Furthermore, direct glutamatergic projections from the BLA to the dHip have been shown to be both necessary and sufficient for repeated long-term foot shock-mediated memory impairments (Rei et al., 2015), while neurons in the BLA become activated during hippocampal theta network activity or optogenetic stimulation of CA1 pyramidal neurons (Bienvenu et al., 2012; Bazelot et al., 2015).

Because compensation through a 5-HT-dependent mechanism are absent in *Tph2*$^{-/-}$ mice (Gutknecht et al., 2012; Waider et al., 2017), resilience to foot shock-mediated memory impairments may be derived directly from absence of 5-HT signaling in the dHip. Indeed, inescapable foot shock and novel aversive contexts were reported to impair contextual memory and the induction of LTP in the hippocampal CA1 region (Foy et al., 1987; Sacchetti et al., 2002; Dai et al., 2008).

Moreover, it has long been suggested that 5-HT counteracts the consolidation of stressful memories, presumably mediated by 5-HT1A receptors in the dHip, which then may lead to tolerance with chronic aversive events (Graeff et al., 1996). In contrast to *Lmx1b* cKO mice, which lack raphe 5-HT neurons (Dai et al., 2008), 5-HT neurons in *Tph2*$^{-/-}$ mice are unable to synthesize 5-HT, but are functionally preserved (Gutknecht et al., 2012; Montalbano et al., 2015).

Here, we chose a consolidated foot shock protocol (Dai et al., 2008) to investigate whether the absence of 5-HT influences hippocampal LTP formation to allow direct comparison of our data with those obtained using a different animal model of 5-HT system impairment. Although the protocol applied for the LTP and the behavioral experiments differed and, therefore, quantitative correlation of plasticity impairment with the behavioral effects was not possible, our results demonstrate that 5-HT is required for foot shock-induced impairment of LTP. Indeed, 5-HT has been shown to shift hippocampal activity along the longitudinal axis toward the ventral part (Mlinar and Corradetti, 2018). Thus, an absence of this mechanism in *Tph2*$^{-/-}$ mice may result in an overactivation of the hippocampal circuitry, manifested as enhanced c-Fos immunostaining and overrepresentation of the contextual

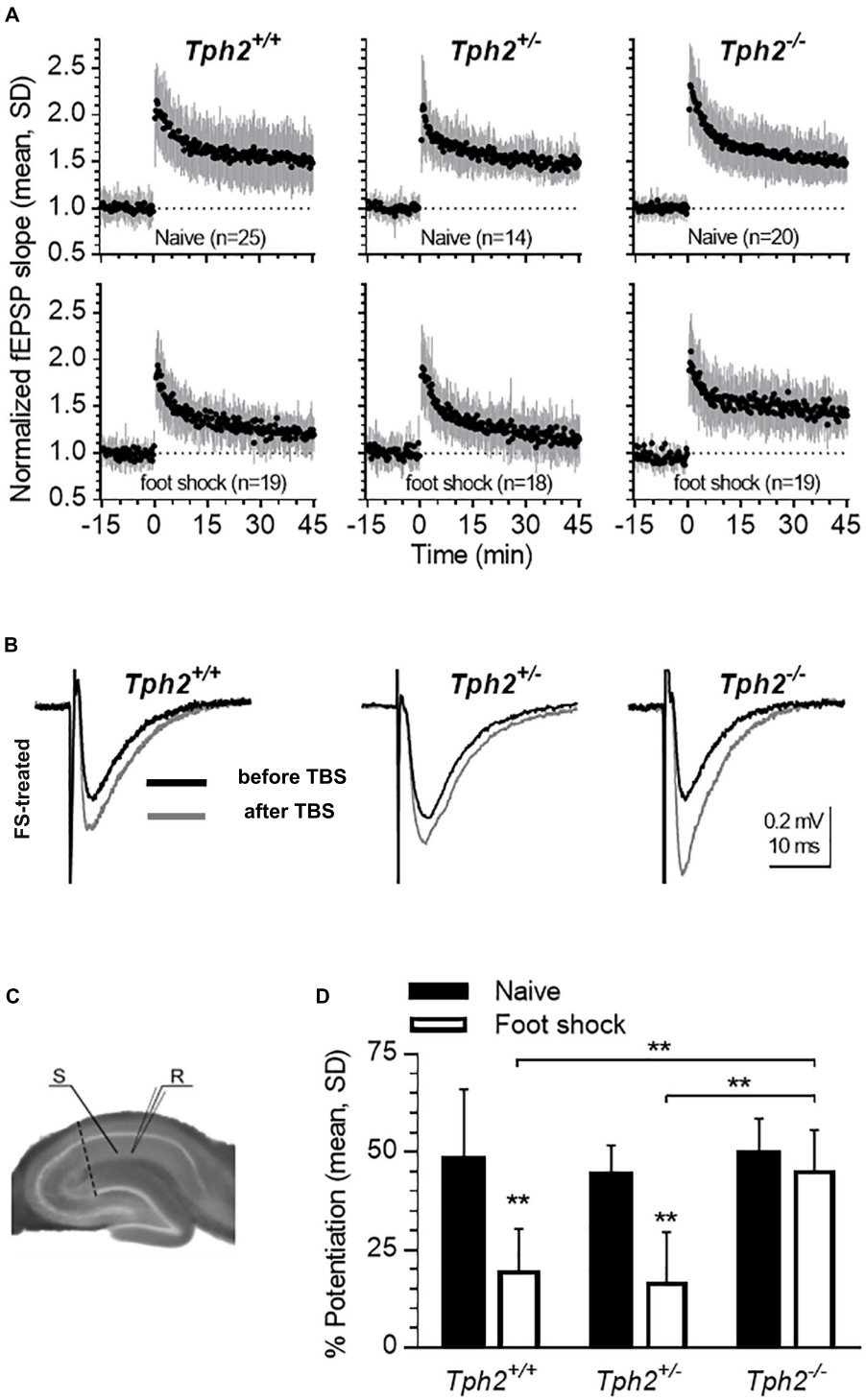

FIGURE 5 | Lack of 5-HT impedes foot shock-induced reduction in hippocampal long-term potentiation (LTP). **(A)** Time-course of LTP in slices obtained from naïve and foot shock-treated mice (*Tph2*$^{+/+}$, *Tph2*$^{+/-}$, and *Tph2*$^{-/-}$ mice; naïve: n = 8,6,5; foot shock: n = 5,6,6). Mean ± SD of fEPSP slope values normalized to the baseline mean from 5 to 0 min before theta burst stimulation (TBS). Numbers (n) in graphs indicate slices tested, including replicates per mouse. **(B)** Representative traces of recordings foot shock-treated *Tph2*$^{+/+}$, *Tph2*$^{+/-}$, and *Tph2*$^{-/-}$ mice before and after TBS. **(C)** Positioning of stimulation electrode (S) on Schaffer collaterals and recording electrode (R) in CA1. The dashed line indicates a cut made between cornu ammonis area 1 (CA1) and cornu ammonis area 3 (CA3) to prevent recurrent propagation of action potentials. **(D)** LTP is expressed as the percent change measured 40–45 min after TBS in respect to baseline between naïve and foot shock-treated *Tph2*$^{+/+}$, *Tph2*$^{+/-}$, and *Tph2*$^{-/-}$ mice. $^{**}p < 0.01$. Two-way ANOVA, followed by Sidak's *post hoc* test.

component in fear learning. In line with this, a mouse model lacking hippocampal serotonergic input showed alterations in contextual fear memory with no differences in LTP formation under baseline conditions (Fernandez et al., 2017).

However, recall of context-dependent aversive memory is exaggerated in *Tph2*$^{-/-}$ mice, supporting the view that 5-HT mediates inhibition of context-dependent aversive memories through inhibition of LTP, while under non-aversive conditions, increased endogenous 5-HT release facilitated LTP induction in the CA1 region, and may underlie the *in vivo* positive effects of augmented 5-HT tone on cognitive performance (Mlinar et al., 2015).

In this respect, it may be of interest in a follow up study to analyze the response of the ventral hippocampus, which is involved in emotional fear processing (Fanselow and Dong, 2010), and is modulated differentially by 5-HT along its longitudinal axis (Mlinar and Corradetti, 2018).

Formation of context-dependent memories requires changes in the expression of calcium-binding proteins of GABAergic interneurons, including hippocampal PV-ir cells (Bienvenu et al., 2012; Donato et al., 2013, 2015). In line with previous studies, 5-HT has been shown to modulate PV-specific neurons in the hippocampus (Gulyas et al., 1999). Our results hint toward an involvement of CA1 PV-ir neurons in context-dependent fear conditioning, which is prevented in *Tph2*$^{-/-}$ mice, although activity of the hippocampus is generally increased. Especially in *Tph2*$^{+/-}$ mice, fear conditioning recruited the highest number of PV-ir neurons. Thus, it seems that 5-HT-dependent activation of PV neurons may protect the dHip from overactivation. Furthermore, the increased hippocampal activity in *Tph2*$^{-/-}$ mice due to fear conditioning may prevent an increased response of the BLA, as observed in *Tph2*$^{+/-}$ mice, to inhibit flight or panic responses (Waider et al., 2017). Thus, further studies are required to investigate the differential role of 5-HT on PV neuron-dependent theta synchronization in Hip and BLA (Amilhon et al., 2015).

Increased active coping in novel, aversive, and inescapable situations is mediated through an amygdala-ventrolateral periaqueductal gray (vlPAG) circuit, mediated through the dorsolateral PAG (Hale et al., 2012; Tovote et al., 2016). 5-HT neurons of the vlPAG inhibit panic-like responses mediated by dorsolateral PAG neurons (Pobbe et al., 2011; Spannuth et al., 2011). Indeed, *Tph2*$^{-/-}$ mice show increased post-shock freezing and increased flight responses, although the BLA did not respond to foot shock with an altered activity compared to *Tph2*$^{+/+}$ mice (Waider et al., 2017). Thus, the increased hippocampal response in mice completely devoid of 5-HT-mediated regulatory mechanisms may influence the PAG in its role to translate inputs from the amygdala into an appropriate behavioral response, resulting in increased freezing and flight behaviors.

In conclusion, exaggerated context-dependent fear memory and shock reactivity resulting from brain 5-HT deficiency likely involves dysfunction of the raphe-hippocampal innervation controlling fear-related behavioral responses and is presumably due to the failure of 5-HT receptor-mediated inhibition of hippocampal circuitries. Furthermore, our data indicate largely effective extinction learning, during repetitive context exposure without negative reinforcement and without 5-HT functioning. Thus, context-dependent extinction training may represent a strategy to adapt behavioral therapy for patients suffering from 5-HT system dysfunction associated with anxiety-, stress-, and trauma-related disorders.

AUTHOR CONTRIBUTIONS

JW, RC, ASB, and KPL designed and supervised the study. JW, SP, BM, AM, FB, BA, ET, RK, CT, NA, ES, and ASB performed and analyzed the experiments. JW, SP, BM, RC, CL, and KPL interpreted the results and wrote the manuscript.

FUNDING

This study was supported by the German Research Foundation (DFG: SFB TRR58-A05 to KPL and WA 3446/2-1 to JW), the European Union's Seventh Framework Program (FP7/2007–2013) under Grant No. 602805 (Aggressotype), the Horizon 2020 Research and Innovation Program under Grant No. 728018 (Eat2beNICE), the 5-100 Russian Academic Excellence Project (to KPL) and the University of Florence (ex60% to RC).

ACKNOWLEDGMENTS

We thank P. Gaspar for helpful discussion as well as N. Schraud for technical assistance. We are grateful to Zachary D. Barger for proofreading the manuscript.

REFERENCES

Amilhon, B., Huh, C. Y., Manseau, F., Ducharme, G., Nichol, H., Adamantidis, A., et al. (2015). Parvalbumin interneurons of hippocampus tune population activity at theta frequency. *Neuron* 86, 1277–1289. doi: 10.1016/j.neuron.2015.05.027

Azmitia, E., and Whitaker-Azmitia, P. (1995). "Anatomy, cell biology, and plasticity of the serotonergic system. Neuropsychopharmacological implications for the actions of psychotropic drugs," in *Psychopharmacology: the Fourth Generation of Progress*, eds F. E. Bloom and D. J. Kupfer (New York, NY: Raven Press), 443–449.

Baratta, M. V., Kodandaramaiah, S. B., Monahan, P. E., Yao, J., Weber, M. D., Lin, P. A., et al. (2016). Stress enables reinforcement-elicited serotonergic consolidation of fear memory. *Biol. Psychiatry* 79, 814–822. doi: 10.1016/j.biopsych.2015.06.025

Bauer, E. P. (2015). Serotonin in fear conditioning processes. *Behav. Brain Res.* 277, 68–77. doi: 10.1016/j.bbr.2014.07.028

Baxter, A. J., Scott, K. M., Vos, T., and Whiteford, H. A. (2013). Global prevalence of anxiety disorders: a systematic review and meta-regression. *Psychol. Med.* 43, 897–910. doi: 10.1017/S003329171200147X

Bazelot, M., Bocchio, M., Kasugai, Y., Fischer, D., Dodson, P. D., Ferraguti, F., et al. (2015). Hippocampal theta input to the amygdala shapes feedforward inhibition to gate heterosynaptic plasticity. *Neuron* 87, 1290–1303. doi: 10.1016/j.neuron.2015.08.024

Bereza, B. G., Machado, M., and Einarson, T. R. (2009). Systematic review and quality assessment of economic evaluations and quality-of-life studies related to

generalized anxiety disorder. *Clin. Ther.* 31, 1279–1308. doi: 10.1016/j.clinthera.2009.06.004

Bienvenu, T. C., Busti, D., Magill, P. J., Ferraguti, F., and Capogna, M. (2012). Cell-type-specific recruitment of amygdala interneurons to hippocampal theta rhythm and noxious stimuli in vivo. *Neuron* 74, 1059–1074. doi: 10.1016/j.neuron.2012.04.022

Bocchio, M., McHugh, S. B., Bannerman, D. M., Sharp, T., and Capogna, M. (2016). Serotonin, amygdala and fear: assembling the puzzle. *Front. Neural Circuits* 10:24. doi: 10.3389/fncir.2016.00024

Brooks, L. R., Enix, C. L., Rich, S. C., Magno, J. A., Lowry, C. A., and Tsai, P. S. (2014). Fibroblast growth factor deficiencies impact anxiety-like behavior and the serotonergic system. *Behav. Brain Res.* 264, 74–81. doi: 10.1016/j.bbr.2014.01.053

Burghardt, N. S., Bush, D. E. A., McEwen, B. S., and LeDoux, J. E. (2007). Acute selective serotonin reuptake inhibitors increase conditioned fear expression: blockade with a 5-HT(2C) receptor antagonist. *Biol. Psychiatry* 62, 1111–1118. doi: 10.1016/j.biopsych.2006.11.023

Dai, J. X., Han, H. L., Tian, M., Cao, J., Xiu, J. B., Song, N. N., et al. (2008). Enhanced contextual fear memory in central serotonin-deficient mice. *Proc. Natl. Acad. Sci. U.S.A.* 105, 11981–11986. doi: 10.1073/pnas.0801329105

Donato, F., Chowdhury, A., Lahr, M., and Caroni, P. (2015). Early- and late-born parvalbumin basket cell subpopulations exhibiting distinct regulation and roles in learning. *Neuron* 85, 770–786. doi: 10.1016/j.neuron.2015.01.011

Donato, F., Rompani, S. B., and Caroni, P. (2013). Parvalbumin-expressing basket-cell network plasticity induced by experience regulates adult learning. *Nature* 504, 272–276. doi: 10.1038/nature12866

Fanselow, M. S. (1980). Conditioned and unconditional components of post-shock freezing. *Pavlov. J. Biol. Sci.* 15, 177–182.

Fanselow, M. S., and Dong, H. W. (2010). Are the dorsal and ventral hippocampus functionally distinct structures? *Neuron* 65, 7–19. doi: 10.1016/j.neuron.2009.11.031

Fernandez, S. P., Cauli, B., Cabezas, C., Muzerelle, A., Poncer, J. C., and Gaspar, P. (2016). Multiscale single-cell analysis reveals unique phenotypes of raphe 5-HT neurons projecting to the forebrain. *Brain Struct. Funct.* 221, 4007–4025. doi: 10.1007/s00429-015-1142-4

Fernandez, S. P., Muzerelle, A., Scotto-Lomassese, S., Barik, J., Gruart, A., Delgado-Garcia, J. M., et al. (2017). Constitutive and acquired serotonin deficiency alters memory and hippocampal synaptic plasticity. *Neuropsychopharmacology* 42, 512–523. doi: 10.1038/npp.2016.134

Foy, M. R., Stanton, M. E., Levine, S., and Thompson, R. F. (1987). Behavioral stress impairs long-term potentiation in rodent hippocampus. *Behav. Neural Biol.* 48, 138–149. doi: 10.1016/S0163-1047(87)90664-9

Franklin, K. B. J., and Paxinos, G. (1997). *The Mouse Brain in Stereotaxic Coordinates*. San Diego: Academic Press.

Graeff, F. G., Guimarães, F. S., De Andrade, T. G. C. S., and Deakin, J. F. (1996). Role of 5-HT in stress, anxiety, and depression. *Pharmacol. Biochem. Behav.* 54, 129–141. doi: 10.10160091-3057(95)02135-3

Graeff, F. G., and Zangrossi, H. Jr. (2010). The dual role of serotonin in defense and the mode of action of antidepressants on generalized anxiety and panic disorders. *Cent. Nerv. Syst. Agents Med. Chem.* 10, 207–217. doi: 10.2174/187152491100603020 7

Gravius, A., Barberi, C., Schafer, D., Schmidt, W. J., and Danysz, W. (2006). The role of group I metabotropic glutamate receptors in acquisition and expression of contextual and auditory fear conditioning in rats - a comparison. *Neuropharmacology* 51, 1146–1155. doi: 10.1016/j.neuropharm.2006.07.008

Grillon, C. (2002). Startle reactivity and anxiety disorders: aversive conditioning, context, and neurobiology. *Biol. Psychiatry* 52, 958–975. doi: 10.1016/S0006-3223(02)01665-7

Gulyas, A. I., Acsady, L., and Freund, T. F. (1999). Structural basis of the cholinergic and serotonergic modulation of GABAergic neurons in the hippocampus. *Neurochem. Int.* 34, 359–372. doi: 10.1016/S0197-0186(99)00041-8

Gutknecht, L., Araragi, N., Merker, S., Waider, J., Sommerlandt, F. M., Mlinar, B., et al. (2012). Impacts of brain serotonin deficiency following Tph2 inactivation on development and raphe neuron serotonergic specification. *PLoS One* 7:e43157. doi: 10.1371/journal.pone.0043157

Gutknecht, L., Popp, S., Waider, J., Sommerlandt, F. M., Goppner, C., Post, A., et al. (2015). Interaction of brain 5-HT synthesis deficiency, chronic stress and sex differentially impact emotional behavior in Tph2 knockout mice. *Psychopharmacology* 232, 2429–2441. doi: 10.1007/s00213-015-3879-0

Hale, M. W., and Lowry, C. A. (2011). Functional topography of midbrain and pontine serotonergic systems: implications for synaptic regulation of serotonergic circuits. *Psychopharmacology* 213, 243–264. doi: 10.1007/s00213-010-2089-z

Hale, M. W., Shekhar, A., and Lowry, C. A. (2012). Stress-related serotonergic systems: implications for symptomatology of anxiety and affective disorders. *Cell. Mol. Neurobiol.* 32, 695–708. doi: 10.1007/s10571-012-9827-1

Hashimoto, S., Inoue, T., and Koyama, T. (1996). Serotonin reuptake inhibitors reduce conditioned fear stress-induced freezing behavior in rats. *Psychopharmacology* 123, 182–186. doi: 10.1007/BF02246175

Hendricks, T. J., Fyodorov, D. V., Wegman, L. J., Lelutiu, N. B., Pehek, E. A., Yamamoto, B., et al. (2003). Pet-1 ETS gene plays a critical role in 5-HT neuron development and is required for normal anxiety-like and aggressive behavior. *Neuron* 37, 233–247. doi: 10.1016/S0896-6273(02)01167-4

Igelstrom, K. M., and Heyward, P. M. (2012). Inhibition of hippocampal excitability by citalopram. *Epilepsia* 53, 2034–2042. doi: 10.1111/j.1528-1167.2012.03660.x

Jorgensen, C. V., Jacobsen, J. P., Caron, M. G., Klein, A. B., Knudsen, G. M., and Mikkelsen, J. D. (2013). Cerebral 5-HT2A receptor binding, but not mGluR2, is increased in tryptophan hydroxylase 2 decrease-of-function mice. *Neurosci. Lett.* 555, 118–122. doi: 10.1016/j.neulet.2013.08.073

Kessler, R. C., Chiu, W. T., Demler, O., Merikangas, K. R., and Walters, E. E. (2005). Prevalence, severity, and comorbidity of 12-month DSM-IV disorders in the National Comorbidity Survey Replication. *Arch. Gen. Psychiatry* 62, 617–627. doi: 10.1001/archpsyc.62.6.617

Kiyasova, V., Fernandez, S. P., Laine, J., Stankovski, L., Muzerelle, A., Doly, S., et al. (2011). A genetically defined morphologically and functionally unique subset of 5-HT neurons in the mouse raphe nuclei. *J. Neurosci.* 31, 2756–2768. doi: 10.1523/JNEUROSCI.4080-10.2011

Lesch, K. P., Bengel, D., Heils, A., Sabol, S. Z., Greenberg, B. D., Petri, S., et al. (1996). Association of anxiety-related traits with a polymorphism in the serotonin transporter gene regulatory region. *Science* 274, 1527–1531. doi: 10.1126/science.274.5292.1527

Li, X. B., Inoue, T., Hashimoto, S., and Koyama, T. (2001). Effect of chronic administration of flesinoxan and fluvoxamine on freezing behavior induced by conditioned fear. *Eur. J. Pharmacol.* 425, 43–50. doi: 10.1016/S0014-2999(01)01159-1

Lowry, C. A. (2002). Functional subsets of serotonergic neurones: implications for control of the hypothalamic-pituitary-adrenal axis. *J. Neuroendocrinol.* 14, 911–923. doi: 10.1046/j.1365-2826.2002.00861.x

Lowry, C. A., Johnson, P. L., Hay-Schmidt, A., Mikkelsen, J., and Shekhar, A. (2005). Modulation of anxiety circuits by serotonergic systems. *Stress* 8, 233–246. doi: 10.1080/10253890500492787

Maier, S. F., Amat, J., Baratta, M. V., Paul, E., and Watkins, L. R. (2006). Behavioral control, the medial prefrontal cortex, and resilience. *Dialogues Clin. Neurosci.* 8, 397–406.

Maier, S. F., and Watkins, L. R. (2005). Stressor controllability and learned helplessness: the roles of the dorsal raphe nucleus, serotonin, and corticotropin-releasing factor. *Neurosci. Biobehav. Rev.* 29, 829–841. doi: 10.1016/j.neubiorev.2005.03.021

Maren, S., Phan, K. L., and Liberzon, I. (2013). The contextual brain: implications for fear conditioning, extinction and psychopathology. *Nat. Rev. Neurosci.* 14, 417–428. doi: 10.1038/nrn3492

McQuade, R., and Sharp, T. (1997). Functional mapping of dorsal and median raphe 5-hydroxytryptamine pathways in forebrain of the rat using microdialysis. *J. Neurochem.* 69, 791–796. doi: 10.1046/j.1471-4159.1997.69020791.x

Milad, M. R., Orr, S. P., Lasko, N. B., Chang, Y., Rauch, S. L., and Pitman, R. K. (2008). Presence and acquired origin of reduced recall for fear extinction in PTSD: results of a twin study. *J. Psychiatr. Res.* 42, 515–520. doi: 10.1016/j.jpsychires.2008.01.017

Misane, I., Tovote, P., Meyer, M., Spiess, J., Ogren, S. O., and Stiedl, O. (2005). Time-dependent involvement of the dorsal hippocampus in trace fear conditioning in mice. *Hippocampus* 15, 418–426. doi: 10.1002/hipo.20067

Miyazaki, M., Yoshino, A., and Nomura, S. (2011). Relationships between anxiety severity, diagnosis of multiple anxiety disorders, and comorbid major

depressive disorder. *Asian J. Psychiatry* 4, 293–296. doi: 10.1016/j.ajp.2011.10.003

Mlinar, B., and Corradetti, R. (2018). Differential modulation of CA1 impulse flow by endogenous serotonin along the hippocampal longitudinal axis. *Hippocampus* 28, 217–225. doi: 10.1002/hipo.22825

Mlinar, B., Stocca, G., and Corradetti, R. (2015). Endogenous serotonin facilitates hippocampal long-term potentiation at CA3/CA1 synapses. *J. Neural Transm.* 122, 177–185. doi: 10.1007/s00702-014-1246-7

Montalbano, A., Waider, J., Barbieri, M., Baytas, O., Lesch, K.-P., Corradetti, R., et al. (2015). Cellular resilience: 5-HT neurons in Tph2$^{-/-}$ mice retain normal firing behavior despite the lack of brain 5-HT. *Eur. Neuropsychopharmacol.* 25, 2022–2035. doi: 10.1016/j.euroneuro.2015.08.021

Morini, R., Mlinar, B., Baccini, G., and Corradetti, R. (2011). Enhanced hippocampal long-term potentiation following repeated MDMA treatment in Dark-Agouti rats. *Eur. Neuropsychopharmacol.* 21, 80–91. doi: 10.1016/j.euroneuro.2010.07.007

Mosienko, V., Beis, D., Pasqualetti, M., Waider, J., Matthes, S., Qadri, F., et al. (2015). Life without brain serotonin: reevaluation of serotonin function with mice deficient in brain serotonin synthesis. *Behav. Brain Res.* 277, 78–88. doi: 10.1016/j.bbr.2014.06.005

Muzerelle, A., Scotto-Lomassese, S., Bernard, J. F., Soiza-Reilly, M., and Gaspar, P. (2016). Conditional anterograde tracing reveals distinct targeting of individual serotonin cell groups (B5-B9) to the forebrain and brainstem. *Brain Struct. Funct.* 221, 535–561. doi: 10.1007/s00429-014-0924-4

Pobbe, R. L., Zangrossi, H. Jr., Blanchard, D. C., and Blanchard, R. J. (2011). Involvement of dorsal raphe nucleus and dorsal periaqueductal gray 5-HT receptors in the modulation of mouse defensive behaviors. *Eur. Neuropsychopharmacol.* 21, 306–315. doi: 10.1016/j.euroneuro.2010.05.004

Raab, A., Popp, S., Lesch, K. P., Lohse, M. J., Fischer, M., Deckert, J., et al. (2018). Increased fear learning, spatial learning as well as neophobia in Rgs2(-/-) mice. *Genes Brain Behav.* 17:e12420. doi: 10.1111/gbb.12420

Ravinder, S., Burghardt, N. S., Brodsky, R., Bauer, E. P., and Chattarji, S. (2013). A role for the extended amygdala in the fear-enhancing effects of acute selective serotonin reuptake inhibitor treatment. *Transl. Psychiatry* 3:e209. doi: 10.1038/tp.2012.137

Rei, D., Mason, X., Seo, J., Graff, J., Rudenko, A., Wang, J., et al. (2015). Basolateral amygdala bidirectionally modulates stress-induced hippocampal learning and memory deficits through a p25/Cdk5-dependent pathway. *Proc. Natl. Acad. Sci. U.S.A.* 112, 7291–7296. doi: 10.1073/pnas.1415845112

Rivero, O., Selten, M. M., Sich, S., Popp, S., Bacmeister, L., Amendola, E., et al. (2015). Cadherin-13, a risk gene for ADHD and comorbid disorders, impacts GABAergic function in hippocampus and cognition. *Transl. Psychiatry* 5:e655. doi: 10.1038/tp.2015.152

Sacchetti, B., Lorenzini, C. A., Baldi, E., Bucherelli, C., Roberto, M., Tassoni, G., et al. (2002). Time-dependent inhibition of hippocampal LTP in vitro following contextual fear conditioning in the rat. *Eur. J. Neurosci.* 15, 143–150. doi: 10.1046/j.0953-816x.2001.01844.x

Schaefer, T. L., Vorhees, C. V., and Williams, M. T. (2009). Mouse plasmacytoma-expressed transcript 1 knock out induced 5-HT disruption results in a lack of cognitive deficits and an anxiety phenotype complicated by hypoactivity and defensiveness. *Neuroscience* 164, 1431–1443. doi: 10.1016/j.neuroscience.2009.09.059

Schindelin, J., Arganda-Carreras, I., Frise, E., Kaynig, V., Longair, M., Pietzsch, T., et al. (2012). Fiji: an open-source platform for biological-image analysis. *Nat. Methods* 9, 676–682. doi: 10.1038/nmeth.2019

Schmidt, S. D., Furini, C. R. G., Zinn, C. G., Cavalcante, L. E., Ferreira, F. F., Behling, J. A. K., et al. (2017). Modulation of the consolidation and reconsolidation of fear memory by three different serotonin receptors in hippocampus. *Neurobiol. Learn. Mem.* 142(Pt A), 48–54. doi: 10.1016/j.nlm.2016.12.017

Song, N. N., Xiu, J. B., Huang, Y., Chen, J. Y., Zhang, L., Gutknecht, L., et al. (2011). Adult raphe-specific deletion of LMX1B leads to central serotonin deficiency. *PLoS One* 6:e15998. doi: 10.1371/journal.pone.0015998

Spannuth, B. M., Hale, M. W., Evans, A. K., Lukkes, J. L., Campeau, S., and Lowry, C. A. (2011). Investigation of a central nucleus of the amygdala/dorsal raphe nucleus serotonergic circuit implicated in fear-potentiated startle. *Neuroscience* 179, 104–119. doi: 10.1016/j.neuroscience.2011.01.042

Staubli, U., and Otaky, N. (1994). Serotonin controls the magnitude of LTP induced by theta bursts via an action on NMDA-receptor-mediated responses. *Brain Res.* 643, 10–16. doi: 10.1016/0006-8993(94)90003-5

Toth, I., Dietz, M., Peterlik, D., Huber, S. E., Fendt, M., Neumann, I. D., et al. (2012). Pharmacological interference with metabotropic glutamate receptor subtype 7 but not subtype 5 differentially affects within- and between-session extinction of Pavlovian conditioned fear. *Neuropharmacology* 62, 1619–1626. doi: 10.1016/j.neuropharm.2011.10.021

Tovote, P., Esposito, M. S., Botta, P., Chaudun, F., Fadok, J. P., Markovic, M., et al. (2016). Midbrain circuits for defensive behaviour. *Nature* 534, 206–212. doi: 10.1038/nature17996

Waider, J., Popp, S., Lange, M. D., Kern, R., Kolter, J. F., Kobler, J., et al. (2017). Genetically driven brain serotonin deficiency facilitates panic-like escape behavior in mice. *Transl. Psychiatry* 7:e1246. doi: 10.1038/tp.2017.209

Waider, J., Proft, F., Langlhofer, G., Asan, E., Lesch, K. P., and Gutknecht, L. (2013). GABA concentration and GABAergic neuron populations in limbic areas are differentially altered by brain serotonin deficiency in Tph2 knockout mice. *Histochem. Cell Biol.* 139, 267–281. doi: 10.1007/s00418-012-1029-x

Conflict of Interest Statement: The authors declare that the research was conducted in the absence of any commercial or financial relationships that could be construed as a potential conflict of interest.